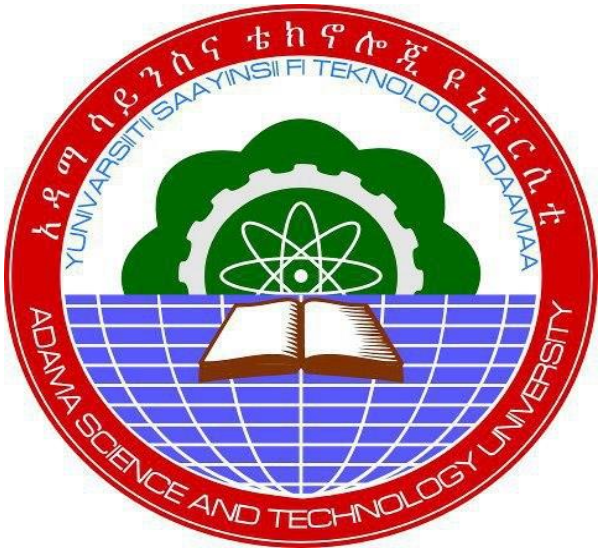

School of Mechanical, Chemical and Materials Engineering

Designing and Prototyping of Multi-Crop Solar Powered Harvester

By

Principal Researcher: Getaw Ayay

Co-Researcher: Haileyesus Kebere

April 6, 2020

Contents

List of Figures

Lists of Photo

Lists of Part Drawings

List of Tables

Acknowledgement

We would like to thank Adama Science and Technology University for supporting us financially to make this research. We greatly thank Mr. Yilkal Dinkayehu for his unreserved and positive all-time support during making the prototype.

Abbreviations and Symbols

A----------Area	MPa----------Mega Pascal
Ah----------Ampere hour	m----------mass, meter, module
a----------acceleration	mm----------millimeter
B----------width	m/s----------meter per second
BHN ----------Brinell hardness number	mm/s----------millimeter per second
b----------base	m/s^2----------meter per square second
C----------center distance	N----------Newton, Normal force
CAD----------Computer Aided Design	Nm----------Newton meter
ca----------cutter bar assembly	Nmm----------Newton millimeter
cb----------cutter bar	n----------numbers, factor of safety
d----------diameter	P----------power, pitch
D----------diameter	P_p----------peak power
DC----------direct current	R----------radius
D_p ----------pitch diameter	RPM----------revolution per minute
E----------modulus of elasticity	r----------radial, radius
E_d----------daily energy	rad/s----------radian per second
F----------force	rpm---------- revolution per minute
f----------follower, friction	S----------displacement, second, side
G----------modulus of rigidity	T----------Torque, number of teeth
GPa ----------Giga Pascal	t----------width, spacing of knife section, time
g----------gravity	t_o---------- spacing of the guard lip
H----------stroke length, hoop	V ---------- speed, velocity, volt
HP----------horse power	W----------watt
h----------hour, height	Wh----------watt hour
h/ha----------hour per hectare	Z----------section modulus
ha/----------hectare per hour	β----------angle of outstroke or return stroke
hp----------horse power	θ----------angle of rotation
I----------second moment of area	ϑ----------poison ratio
IC----------Internal combustion	μ---------coefficient of friction, included angle
K----------velocity ratio	ρ----------density
KPa----------Kilo Pascal	τ----------shear stress or strength
KWh----------kilo watt hour	σ----------Normal stress
L----------length or longer side of cam	ω- ----------rotational speed
M----------bending moment	

Abstract

The demands on the grains have been being increased radically in Ethiopia. The existing ways of harvesting grains are not differed from the ancient methods. In order to satisfy the needs our ancestors have been being applied their full money, power and times which leads financial and physical weakness and health problems especially on their backbones. No one was hearing and trying to minimize and eradicate this problem. Hence, a simple to operate and cheap in cost harvester is designed and prototyped which is driven by solar power. The machine harvest grains that have grass physical nature such as wheat, barley, Teff, rice even the grass itself for animal feed.

The design and prototype were achieved by following a method of reviewing literatures, collecting data, synthesizing and analyzing the mechanism and structure at a preliminary and detail design stage (using manual and CATIA software), making drawings, manufacturing a prototype and testing.

The designed harvester has two solar panel 200 watt each, 1.5 hp DC Motor, divider, cutter system, lugged belt conveyor system, two stage power transmission system and two wheels vehicle system. The harvester is 1614.5 mm width, 1602 mm length, 1862.92 mm height and 93.03 Kg mass. It can harvest 609.6 mm width of grain at a speed of 500 mm/s i.e., it can harvest 0.110 ha/hr. The prototype of the solar grain harvester has one hp DC motor, 2.4 m^2 solar panel, three-wheels vehicle and cutter assembly. The test shows that the solar energy supplied into the harvester was capable enough to drive the whole system. Therefore, small-scale solar grain harvester will become preferable means of harvester because it is none pollutant and freely available.

Chapter 1 Introduction

Agriculture in Ethiopia is the foundation of the country's economy, accounting for half of gross domestic product (GDP), 83.9% of exports, and 80% of total employment. Grains are the most important field crops and the chief element in the diet of most Ethiopians. The principal grains are Teff, wheat, barley, corn, sorghum, and millet. Ethiopia's demand for grain continued to increase because of population pressures.

The mechanization of agriculture not only reduces the overall cost of production but also increases the total agricultural yield. Through mechanized farming, many countries in the world are reaching the upper limits of their cultivable land. The increasing use of agricultural machinery, equipment and fertilizers coupled with better irrigation facilities, together revolutionizes the agricultural sector.

It is obvious that different types and levels of harvesting tools and machines are applicable in different countries. However, the current harvesting systems are not different from the ancient styles in Ethiopia because the level of economy is very poor. We couldn't afford to buy any of them. Due to this reason, the farmers have been being forced to use the traditional and the time and power consuming way of harvesting. Since the pressures on demand of the grains are increasing drastically, it will be difficult to supply the future needs. Therefore, a simple and cheap system should be implemented which can fill the gap between the traditional and high-level modern ways of harvesting.

The harvester that we are going to designed and prototyped is a small-scale harvester that is driven by solar power. The machine is operated only by a single person. There are different types of grains that could be harvested using this machine. These grains have a physical appearance of grassed such as wheat, barley, Teff, rice grass, etc.

Statement of the problem

The current harvesting system in Ethiopia is traditional. This is due to the low-level economy of the farmer, the awareness of the people and the high taxation system of the government. The harvesting times, of the grains, have been being elongated for months to cover small pieces of lands. This has adverse effect both on the farms and on the country productivity. The farmers have been killing more time that maximizes the cost of production and they will not think for further value-added processes and more production systems. In addition, the amount of seeds collected will be reduced since it falls into the ground and eaten by animals. This leads to an abrupt time-to

time increasing on the price of the grains and the demand will not be satisfied. Beside this, the country will not prepare the grains on time both for the people and for foreign countries, which makes the country uncompetitive and lags behind others in supplying the foods.

Objectives

The main aim of this research is to design a harvester operated by solar energy and to manufacture the prototype locally using our manpower and workshop. Specifically, the mechanism that transfers input power to output will be designed and the necessary parameters of the source of power will be analyzed. Hence, the frames, motors, connecting mechanisms, cutters, collectors, couplings, joints, and solar panels will be synthesized and analyzed.

Significance of the study

The harvester has very great role to maximize the harvesting rate of grains. It collects more grains than a person can do. Since the time required to harvest grains reduced, the farmers will gain additional time in order to have further farming time. That means they can farm more than once per year. The productivity will be increased because the grains will be harvested at the critical stages. In addition, there will be a chance for the producers to add values on their seeds. The burden on the workers reduced which will increase their life span.

There will be an opportunity to a job for the young sisters and brothers in manufacturing, operation and maintenance stages. They will get a stimulation of "yes we can", yes, we do by our own and yes, we can stand by our own. This in turn reduces not only the flooding out of foreign currency but also the flooding out of our believes.

Scope of the research

The researchers have the obligation to carry out the detail activities that are the mechanical design parts, the prototype, and the overall analysis of the solar panel and the motor. There will not be detail study on the solar panel and motor parts of the harvester. After successful completion of the project, there will be further detail analysis and synthesis on the solar panel and motor parts if it is needed which is out of this research.

Research Gap

The previous harvesting systems are either manual or mechanical. The mechanical harvesters are operated using fuel energy. Fuel energy is efficient in driving the system however, it is expensive and pollutant. To overcome these a solar powered harvester is proposed. Since the efficiency of solar power is low, it is necessary to think over the mechanism of existing harvesters. The current

harvesters have a mechanism that has sliding cutter bar. It is obvious that sliding friction is higher than rolling friction. So that by changing the sliding to rolling cutter bar it is possible to minimize the energy needed to overcome frictional resistance. Therefore, an efficient solar harvester can be achieved using cutter bar that oscillates on rolling support.

Chapter 2 Literature Review

This literature will review only about harvesting of grains that can be classified into two broad categories, i.e., hand harvesting and mechanical harvesting. **Hand/Manual harvesting is** also termed as hand reaping; it includes plucking the ears of grain directly by hand, cutting the grain stalks with a sickle, cutting them with a scythe, or with a later type of scythe called a cradle whereas, **mechanical harvesting is** done by employing a mechanical reaper or reaping machine.

Hand/Manual harvesting

In traditional method of harvesting, harvesting is done manual methods. Harvesting of major cereals, pulse and oilseed crops are done by using sickle whereas tuber crops are harvested by country plough or spade. All these traditional methods involve drudgery and consume long time.

Serrated blade sickle: It has a serrated curved blade and a wooden handle. The handle of improved sickle has a bend at the rear for better grip and for avoiding hand injury during operation. Serrated blade sickles cut the crop by principle of friction cutting like in saw blade. The crop is held in one hand and the sickle is pulled along an arc for cutting. Cutting of crop close to the ground is possible with modified handle. Energy requirement is 80-110 **man-h/ha**. It can be used effectively for harvesting of wheat, rice and grasses [1].

[61]


[59]


[59]

Figure 2-1 Manual Harvesting Tools

Mechanical harvesting equipment

The use of machines can help to harvest at proper stage of crop maturity and reduce drudgery and

operation time and facilitates extra days for land preparation and earlier planting of the next crop. Considering these, improved harvesting tools, equipment, combines are being accepted by the farmers.

Reapers: are used for harvesting of crops mostly at ground level. It consists of crop-row divider, cutter bar assembly, feeding and conveying devices. Reapers are classified based on conveying of crops as given below:

i. **Vertical conveying reaper windrower:** It consists of crop row divider, star wheel, cutter bar, and a pair of lugged canvas conveyor belts. This type of machines cut the crops and then conveys vertically to one end and windrows the crops on the ground uniformly. Collection of crops for making bundles is easy and it is done manually.

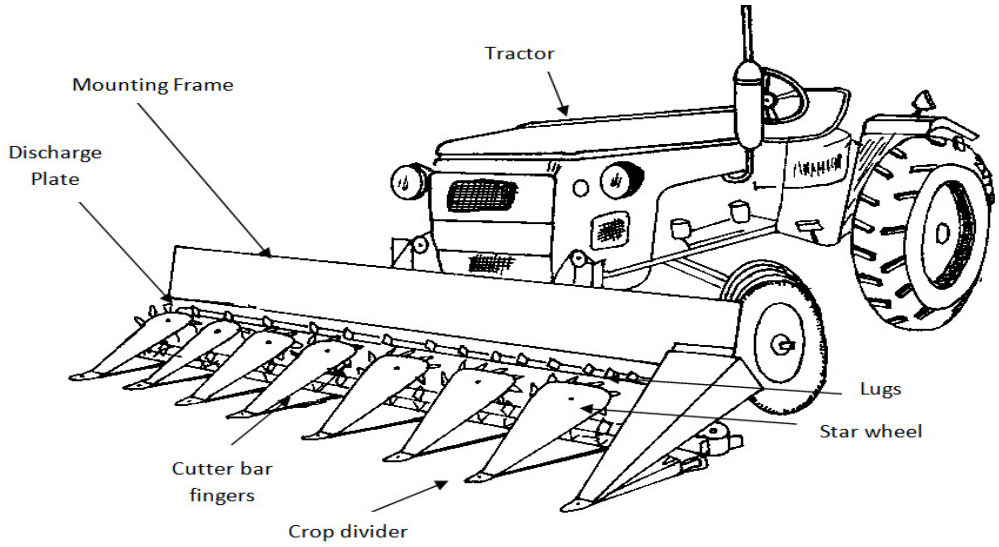

Figure 2-2 Tractor Front Mounted Conveyer Reaper Windrower [47]

Self-propelled walking type, self-propelled riding type and tractor mounted 186 type reaper-windrowers is available. These types of reapers are suitable for crops like wheat and rice. The field capacities of these machines vary from 0.20-0.40 ha/h [1].

ii. **Horizontal conveying reapers:** This type of reapers is provided with crop dividers at the end, crop gathering reel, cutter bar and horizontal conveyor belt. They cut the crop, convey the crop horizontally to one end and drop it to the ground in head-tail fashion. Collection of crops for making bundles is difficult. This type of reapers is tractor mounted and suitable for wheat, rice, soybean, and gram. Performance of reapers with narrow-pitch cutter bar is better for soybean and gram crops.

iii. **Bunch conveying reapers**: This type of reapers is similar to horizontal conveying reapers

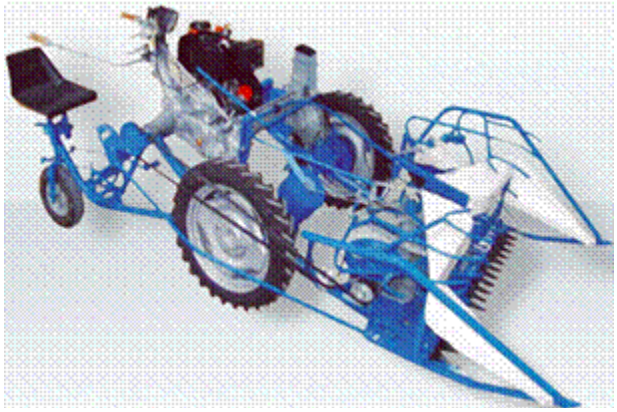

Figure 2-3 Horizontal Conveying Reaper [62]

except that the cut crop is collected on a platform and is being released occasionally to the ground in the form of a bunch by actuating a hand lever. Here, collection of crops for making bundles is difficult. Bullock drawn and tractor-operated models are available and they are suitable for harvesting wheat, rice and soybean crops. Reaper binders the cutting unit of this type of reapers may be disc type or cutter bar type. After cutting, the crop is conveyed vertically to the binding mechanism and released to the ground in the form of bundles.

Strippers: The design of a tractor front mounted stripper is available for collection of matured grass seeds from the seed crops. It consists of a reel having helical rubber bats that beat the grass over a sweeping surface where the ripened seeds are detached and the seeds are collected in the seed box.

Combine Harvesters: Various designs of combine harvester having 2 to 6 m long cutter bar are commercially available. However, the need of a small whole crop combine harvester is felt. The

Figure 2-4 Combine Harvester [63]

function of a combine harvester is to cut, thresh, winnow and clean grain/seed. It consists of header unit, threshing unit, separation unit, cleaning unit and grain collection unit. The function of the

header is to cut and gather the crop and deliver it to the threshing cylinder. The reel pushes the straw back on to the platform while the cutter bar cuts it. The crops are threshed between cylinder and concave due to impact and rubbing action. The threshed material is shaken and tossed back by the straw rack so that the grain moves and falls through the openings in the rack onto the cleaning shoe while the straw is discharged at the rear. The cleaning mechanism consists of two sieves and a fan. The grain is conveyed with a conveyor and collected in a grain tank.

Self-propelled walking type reaper: it consists of crop row divider, star wheel, cutter bar, and a pair of lugged canvas conveyor belts and a handle fitted with clutch and brakes. This type of machines cut the crops, conveys it vertically to one end, and windrows the crops on the ground uniformly. Collection of crops for making bundles is easy and it is done manually. Self-propelled walking type, self-propelled riding type and tractor mounted type vertical conveyor reaper are also available. These types of reapers are suitable for crops like wheat and rice. In this reaper there is no shattering of the crop

Figure 2-5 Self Propelled Walking Type Reaper [64]

Modern gas powered and electric powered lawn mowers cut grass with a single blade revolving at a high-speed parallel to the ground. The blade is slightly raised along its rear edge to create draft that lifts the cutting blades before its cutting operation. Mulching mowers suspends clippings and other debris near the blade shredding them before blowing them straight down in the lawn where they serve as manure for future lawn growth. Okoro (2010) designed a locally operated engine powered lawn mower. The mower is fitted with horizontal cutting blade attached to a vertical shaft. The mower was tested and the average effective field capacity and efficiency were 0.127 ha/hr. and 88.4% respectively. Jeremy (2005) designed and fabricated solar charged lawn mower.

The machine was dependent on weather since the battery would be charged using photovoltaic

panel (i.e. solar panel). The common disadvantage was that the engine runs down easily and the cost of production was high for an average individual to purchase.

Gasoline-powered rotary mover: The story of one experiment in the design of rotary moving equipment is that of C-Stacy, a farmer in the Midwest region of the United States. His concept was the use of a toothed circular saw blade mounted horizontally on a vertical shaft, which would be suspended at a height of approximately 2 inches (50 mm) and moved across a lawn to cut grass and other lawn vegetation at a uniform height. The power for his experimental mower was an electric motor. The success of Stacy's design was limited by two factors: the relatively small diameter of the saw blades he used for his experiments, which were about 8 inches (200 mm); and the fact that toothed circular saw blades are not an ideal tool for cutting free- standing grass and other plants. Stacy did not come up with any idea for a cutter similar to modern rotary mower straight blades, and soon dropped his experiments with rotary mowing. The string trimmer was invented in the early 1970s by George Ballads of Houston, Texas, who conceived the idea while watching the revolving action of the cleaning brushes in an automatic car wash. His first trimmer was made by attaching pieces of heavy-duty fishing line to a popcorn can bolted to an edger. Ballads developed this into what he called the "Weed Eater", since it chewed up the grass and weeds around trees. Victor and Vern's, (2003) designed and developed a power operated rotary weedier for wet land paddy. The complex nature of the machine makes its maintenance and operation difficult for the peasant farmers. Generally, in areas like ours, the conventional methods of grass cutting involved the use of cutlasses whichever met the maximum satisfaction. More so, it is strenuous, time and labor intensive.

Moheb M. A. El-Sharabasy (July 2006) constructed and manufactured a self-propelled machine suits for cutting some grain crops to minimize losses and maximize efficiency. The machine consists of four main devices names: cutter bar, crop reel, conveyor belt, and transmission system. The new constructed machine was operated in rice and wheat fields at four kinematic parameters and four grain moisture contents to determine the proper operating parameters for cutting both rice and wheat crop. Results indicated that the maximum field capacity and the lowest operating cost of (0.452, 0.621 fed/h), (37.50, 37.26 L.E/fed) were obtained at low kinematic parameters of (1.8, 1.45) and low grain moisture content of (21.45, 19.11 %); maximum both field efficiency and cutting efficiency of (69.17, 82.15 %), (86.88, 91.41 %) were obtained at high kinematic parameters of (4.67, 3.20) and low grain moisture content of (21.45, 19.11 %); minimum fuel and

energy consumed of (1.51, 0.47 l/h), (2.97, 1.53 KWh/fed) were obtained at kinematic parameters of (2.33, 1.78) and grain moisture content of (22.20, 20.10 %) and minimum grain losses and criterion cost of (1.03, 0.76 %), (72.18, 64.82 L.E/fed) were obtained at kinematic parameters of (2.33, 1.78) and grain moisture content of (22.20, 20.10 %) for both rice and wheat crop, respectively.

Prof. P.B. Chavan, Prof. D.K. Patil and Prof. D.S. Dhondge (2015) Designed and Developed a manually Operated Reaper. When machine is pushed by the operator at the designed speed in the field, rear wheel rotation leads to reciprocate cutter bar with the help of sprocket and chain. The crop lifter guides the crop to the cutter bar and the crop is cut by the cutter. The cut crop is conveyed with the help of star wheel at one side by the lugged belt conveyer for easy collection and bundling. Based on analysis of results, it has drawbacks like unsuitable for non-uniform land and high-power requirement due to its weight.

Ganesh C. Bora and Gunner K. Hansen (2007) developed a small engine-powered harvesting aid for small area farmers. The machine was a modified brush cutter. The original cutter blade was replaced by a 25 cm diameter circular saw blade. A metal plate and rubber guard assembly were fitted behind the blade on the handle to guide the cut stalk to the left side. The machine performed well in the field conditions with a field capacity of 0.51 ha per day consuming 0.25L of fuel in an hour. It was 7.8 times faster than manual harvesting though the field loss was around 2.3% as against 1% in manual harvesting. The break-even area was 1 ha and payback period of for the investment was one year. The machine should be affordable to low income farmers in developing countries and women would also be able to taste the fruits of mechanization.

Figure 2-6 Low Cost Mechanical Aid for Rice Harvesting [14]

Muhammad Nadeem and et al (2015) did a research work on designing of self-propelled reaper and evaluating its performance for harvesting of rice, brassica and wheat crops. Fields of rice,

wheat and brassica were selected University of Agriculture Faisalabad, Pakistan. Factorial experiments (3 x 3) were conducted at each site with three levels of moisture content i.e.27%, 22% and 19 % for rice, 16.7%, 14.5% and 13% for wheat, and 18.32%, 16.05% and 15.7% for brassica were selected. The levels of machine's ground speed were1.94, 2.54 and 3.18km/h. Twenty-seven plots (1.524 x 3m) were selected randomly in each field to collect data for average percentage (%) slippage, shatter losses and field efficiency. The machine was operated at selected levels of ground speeds and moisture contents for each crop. Factorial analysis of variance (ANOVA) showed that the selected levels of ground speed and moisture contents have significant (p=0.05) effect on % slippage and field efficiency and non-significant on shatter losses for rice and wheat crops, whereas significant effect in brassica. Results indicated that in early harvesting at high moisture content, the shatter losses were significantly lower with the higher % slippage. Results reported that the shatter losses, field efficiency and % slippage were influenced by selected levels of ground speed and moisture contents. A suitable combination of ground speed and moisture content can minimize the grain losses and increase the yield and profitability of the farmer's community.

Figure 2-7 Improved design of self-propelled reaper for tall crops [15]

A. Celik (2006) design a push type cutter bar mower shown in **Figure** 2-8. It has a total width 862 mm, maximum engine speed 7000 rpm, maximum crank speed 700 rpm, engine power 1.47 kW, sharpness of knife 22°, hardness of knife (HRC) 57, effective working width 802 mm, knife stroke 56 mm, cutting height 64 mm, knife speed 1.12 m/s, forward speed 0.45 m/s, effective field capacity 0.11 ha/h and field efficiency (decimal) 0.875.

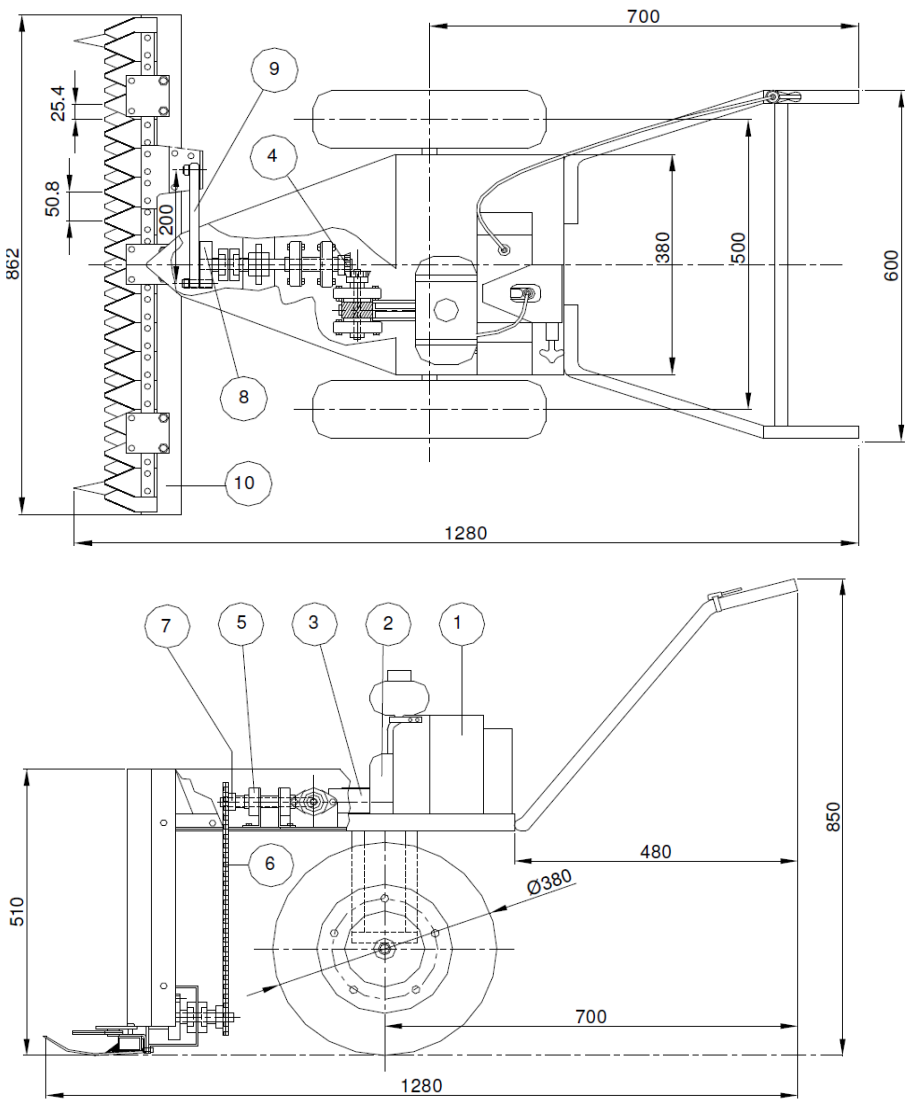

Figure 2-8 Push Type Cutter Bar Mower (Dimensions in millimeters) [17]

Summary on mechanical Harvesting Equipment

All the existing mechanical harvester i.e., low cost mechanical aid for rice harvesting, vertical conveying reaper windrower, horizontal conveying reapers, bunch conveying reapers, combine harvesters, self-propelled walking type reaper and gasoline-powered rotary mover are driven using fuel energy. As it is obvious, fuel energy is available in specific place, expensive and pollutant. This research was proposed to check the feasibility of driving mechanical harvesters using one of the renewable energies (Solar). Solar energy is clean and available freely in almost all places.

Physical and mechanical properties of Crops Straw

M.J. O'Dogherty, J.A. Huber, J. Dyson and C.J. Marshall (2002) conducted a series of experiments

to measure the physical properties, tensile and shear strengths and elastic moduli of stem between nodes of wheat straw (var Mercia) at stem moisture in the range 8 to 22% w.b. Tensile strength was in the range 21.2 to 31.2MPa and shear strength in the range 4.91 to 7.26MPa. Young's modulus was between 4.76 and 6.58 GPa and the rigidity modulus in the range 267 to 547 MPa.

Hamed Tavakoli, Seyed Saeid Mohtasebi and A. Jafari (2009) conducted a research on determining physical and mechanical properties of wheat straw as influenced by moisture content. The objective of this research was to determine the effects of moisture content and internode position on some physical and mechanical properties of wheat straw. The experiments were conducted at four moisture contents of 10.2, 14.3, 18.4, and 22.6% w.b. and at three internode positions down from the ear. Based on the results obtained, the values of the physical properties increased with increasing moisture content. The physical properties also increased towards the third internode position. For all the physical properties studied, the values of the first internode position had significant differences with those of the other two internode positions. Moreover, for the moisture contents studied in this research, the values of shear strength were within the ranges 6.81-10.78, 7.02-11.49, and 7.12-11.78 MPa for the first, second and third internode positions, respectively. The maximum specific shearing energy was 36.26 MJ mm -2, which occurred at the third internode position with the moisture content of 22.6% w.b. The bending strength and Young's modulus decreased with increase in the moisture content. Their values also decreased towards the third internode position.

The amount of force on cutter bar depends on average cross-sectional area of grain, moisture contents, sharpness of blade, and shear strength of grain. (R.L. Kushwaha, A.S. Vaishnav, and G.C. Koerb, 1983) found that the average cross-sectional area of wheat is 2.32 mm^2 and the optimum value of moisture content is between 8% and 10%. The optimum moisture is needed for efficient shearing of straw, lower cutting energy required with increased sharpness of the blade. The variations in shear velocity do not affect the shear strength of the straw and the shear strength of straw is 7-11MPa (N/mm^2).

A research was carried out by Hamed Tavakoli (2009) to determine the effects of moisture content and internode position on physical and mechanical properties of barley straw. The experiments were conducted at four moisture contents of 10.8%, 14.3%, 18.5%, and 22.5% w.b. and at three internode positions down from the ear. Based on the results obtained, the moisture content did not have significant effect on physical properties of barley straw. There was a significant increase in

the stem's major and minor diameters, thickness, wall cross-sectional area, second moment of area, and mass per unit length towards the third internode position. At the different moisture contents studied, the values of the shear strength were within the ranges of 3.90 to 5.27 MPa, 4.31 to 5.96 MPa, and 4.49 to 6.18 MPa for the first, second, and third internode positions, respectively. The maximum specific shearing energy was 32.53 MJ mm-2, occurred at the third internode position with the moisture content of 22.5% w.b. The bending stress and Young's Modulus decreased with an increase in moisture content. Their values also decreased towards the third internode position.

Another study was conducted by H. Tavakoli and et al (2009) with the aim to evaluate the effects of the moisture content, internode position, and loading rate on the bending characteristics of barley straw including bending stress and Young's modulus. In the study, 9 treatments were performed as randomized complete block design with 5 replications. The characteristics were determined at three moisture levels: 10%, 15%, and 20% wet basis, three loading rates: 5, 10, and 15 mm/min, and three internodes: the first, second, and third internodes. The results showed that both the bending stress and Young's modulus decreased with an increase in the moisture content and towards the third internode position. The average bending stress was obtained as 8.41 MPa varying from 6.32 to 12.41 MPa, while the average Young's modulus was calculated as 473.88 MPa ranging from 330.94 to 618.91 MPa.

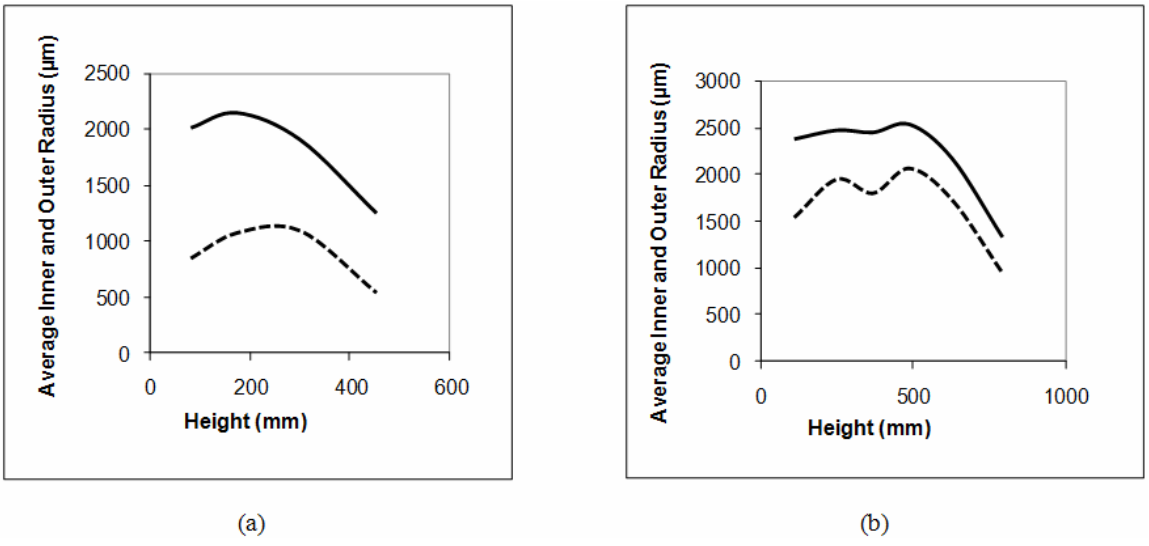

Figure 2-9 Outer and inner radii vs. height (a) Wheat (Triticum sativum L.) Stems (b) Barley (Hordeum vulgare L.) Stems (Solid outer radius, dashed inner radius) [16]

Gozde Değer and et al (2010) studied on strength of wheat and barley stems. In this study, physical and mechanical properties of wheat and barley stems are examined on moisture content of 28-23%

w.b. Transverse sections of the stems are magnified by a microscope and the material structure in the transverse sections are analyzed with image processing programs. Geometric properties such as inner, outer radius, stem wall thickness and density variation of the material along the radius are measured and density variations are approximated by a mathematical model. The result of inner and outer radius is shown in **Figure** 2-9.

The outer and inner radii can be approximated for the height of 100 mm from **Figure** 2-9. The outer and inner radii for wheat are 2.1 mm and 0.875 mm, and for barley are 2.375 mm and 1.550 mm respectively. The average cross sectional of wheat and barley becomes 11.44 mm^2 and 10.17 mm^2 respectively.

Tom Leblicq et al (2014) studied about mechanical analysis of the bending behavior of plant stems. The aim of this study was to model the processes which lead to failure of plant stems due to bending and to gain insight into the phenomena. The measured diameter (x) and estimated diameter (y) were correlated by y = 0.9985x for Germany (wheat), Spain (barley) and Belgium (wheat). In the same way the measured wall thickness (x) and estimated wall thickness (y) were correlated by y = 0.7298x for Germany (wheat), Spain (barley) and Belgium (wheat). The estimated mean diameter and wall thickness is shown in **Table** 2-1.

Table 2-1 Estimated Mean Diameter and Wall Thickness [18]

		Germany (Wheat)		Belgium (Wheat)		Spain(Barley)	
N		60		60		60	
		μ	σ	μ	σ	μ	σ
$F_y^{(m)}$	[N]	3.12	1.43	4.42	1.59	6.67	2.26
$H_y^{(m)}$	[mm]	1.94	0.53	1.45	0.32	1.90	0.29
$r^{(e)}$	[mm]	1.19	0.17	1.93	0.32	1.56	0.25
$t^{(e)}$	[mm]	0.39	0.11	0.37	0.061	0.36	0.048
$E^{(e)}$	[GPa]	3.59	1.28	1.94	0.93	3.58	1.39
R^2		0.98	0.001	0.98	0.03	0.98	0.001

Where μ-mean, σ-standard deviation, Fy-force at buckling, Hy-deflection at buckling, r-stem radius, t-stem wall thickness, E-Young's modulus, m-measured and e-estimated by least squares fitting.

Table 2-2 Measured Mean Diameter and Wall Thickness

	Germany (wheat)	Belgium (wheat)	Spain (barley)

Mean radius (mm)	1.192	1.933	1.562
Mean Stem wall thickness (mm)	0.53	0.51	0.49
Mean cross sectional area mm^2	3.087	5.377	4.055

The measured mean diameter and wall thickness can be determined and shown in **Table** 2-2.

M. Tavakoli (2010) compared the mechanical properties between two varieties of rice straw (Hashemi and Alikazemi). The experiments were conducted at moisture contents of 71.6 and 70.8% w.b. for Hashemi and A likazemi varieties, respectively and three internode positions down from the ear. The mean values for shear strength of rice straw at different internode positions varied from 8.81 to 20.22 and 7.12 to 11.16 MPa for Hashemi and Alikazemi varieties, respectively. The shearing energy of Hashemi and Alikazemi varieties increased from 122.76 to 236.06 and 86.89 to 191.31 MJ, respectively, towards the third internode position. The bending strength and Young's Modulus of Hashemi variety were significantly higher ($p<0.05$) than those of Alikazemi variety. The results showed that the energy requirement for shearing of Hashemi variety is more than Alikazemi variety.

R. Tabatabaee Koloo and A. Borgheie (2006) conducted a study to measuring the static and dynamic cutting force of stems for Iranian rice varieties. The static and dynamic shearing strength was different among the varieties. The maximum and minimum shearing strengths were related to the varieties Khazar and Hashemi, with an average of 1629 and 1429 kPa for static test and values of 187.4 and 144 kPa for the dynamic test, respectively. The shearing strength decreased from 234.4 kPa to 137.4 KPa with an increase in blade cutting speed from 0.6 to 1.5 m/s. Blade bevel angle and blade type had no significant effect on the shearing strength of rice stem.

Chapter 3 Research methodology

The main activities on this research are designing and making the prototype of the harvester. Therefore, these had achieved by walking according to following the ways:

a. **Literature Review**: innovators had carried out different types and levels of harvester. In addition, materials related solar panels and motors had brushed up.
b. **Data collection**: the physical appearance and the strength of the grain that will be harvested are the main input for our design analysis. Hence, these and other true data that are important to our success should be collect from trusted sources.
c. **Preliminary Design:** A best Concept was selected after generating different possible systems of harvesters that was designed further. The best concept should be selected using appropriate principles.
d. **Detail Design:** After refining the best concept and using appropriate data and principles, the geometrical synthesis and analysis and the strength analysis had carried out at this stage. These had done by using manual and CAD software like CATIA and ANSYS.
e. **Drawings:** Part, assembly and detailed drawings had prepared according to the need for clarity, explanation, manufacturing, assembly, operation and maintenance.
f. **Prototyping:** After buying parts, each part had manufactured and assembled to test and evaluate the performance of the harvester.

Chapter 4 Results and discussions

Preliminary Design

The harvester is driven by using solar power. Hence, it should have solar panel, battery, motor, power transmission between motor shaft and cutter bar shaft. There is always movement during harvesting, i.e., the harvester should have at least two wheels. One of the basic activities in this research is synthesizing the mechanisms between the motor and cutter. In addition, there is analysis of solar panel size, motor capacity, and structure development and strength analysis. The latter provide strength and make the system together by supporting and driving the cutting mechanisms. Therefore, the mechanism synthesis should be done first.

Development of Alternative Cutting Mechanism

The cutting mechanism always moves in straight line in reciprocating motion. The reciprocation of the cutter can be done by using either slider crank mechanism or cam and follower.

Among the above alternatives, one of the best mechanisms should be selected using appropriate design and manufacturing criteria. These criteria are like possibility to design and manufacture the system using the current available knowledge and technologies, ease of operation, structure simplicity, easy to implement, efficiency, wear rate and Compactness see **Table** 4-1. It is possible to select one of the best acceptable mechanism of the harvester using weightage method. The values are 1, 2, 3, 4 and 5. Maximum value is 5 and minimum value is 1.

Table 4-1 Comparison of Alternative Working Mechanism

S. No	Criteria	Weight	Slider crank mechanism		cam and follower	
			Rating	Weighted score	Rating	Weighted score
1	Structure simplicity	12%	4	0.48	4	0.48
2	Easy to implement	12%	4	0.48	4	0.48
3	Efficiency	20%	2	0.4	4	0.8
4	wear rate	15%	3	0.45	2	0.3
5	Compactness	5%	3	0.15	5	0.25
6	Easy to manufacture	10%	4	0.4	3	0.3
7	Easy to design	10%	4	0.4	3	0.3
8	Easy to Operate	8%	5	0.4	5	0.4

9	Availabilities of technology	8%	4	0.32	4	0.32
	Total Score			3.48		3.63
	Continue?			No		Yes

Basic Structure of Cutting Mechanism

The cutter oscillates using cam and follower mechanism as shown in **Figure** 4-1. This type of cam does not require a return spring.

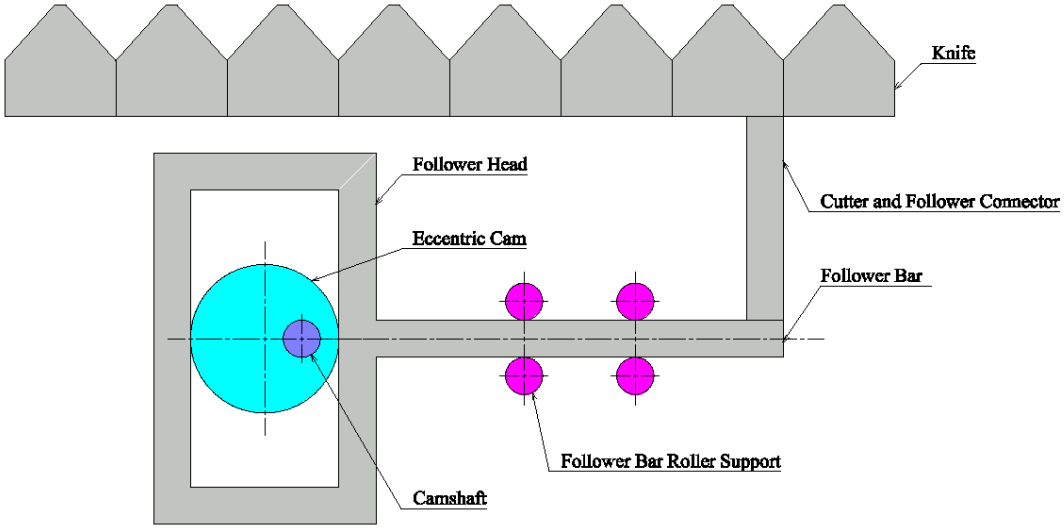

Figure 4-1 Basic Structure of Cutting Mechanism

Functional Analysis

The harvester composed of power system, driving system, frames, cutter system and conveyor system. Its means tree is shown in **Table** 4-2.

Table 4-2 Functional Analysis of Solar Harvester

Harvester					
Power System	Driving System	Cutter System	Conveyor system	Guide System	Vehicle System
Solar panel	DC motor	Cutter bar	Pulley	Crop lifter	Tire
Battery	Coupling	Guide lip	Roller	Divider	Handle
Charge control	Gear Box	Joints	Belt	Star Wheel	Shock absorber
Supports & frames	Supports & frames	Supports & frames	Supports & frames	Supports & frames	Supports & frames
Joints	Joints	Cutter	Joints	Joints	Joints

Working Principles

A DC motor drives the system. The power is supplied into the DC Motor either from DC batteries or direct solar panels. As the DC motor starts, the power is transmitted to intermediate shaft through the belt pulley mechanism see **Figure 4-2**. This power is again transmitted to the camshaft through bevel gear assembly. When camshaft rotates, the positive return follower reciprocates back and forth using eccentric cam see **Figure** 4-3. At the same time, the cutter bar reciprocates back and forth together with follower since the attachment is rigid. When the cutter bar reciprocates, it cuts the grain. At the same time, the camshaft drives the lugged conveyor system through the pulley in order to collect the grains to one side.

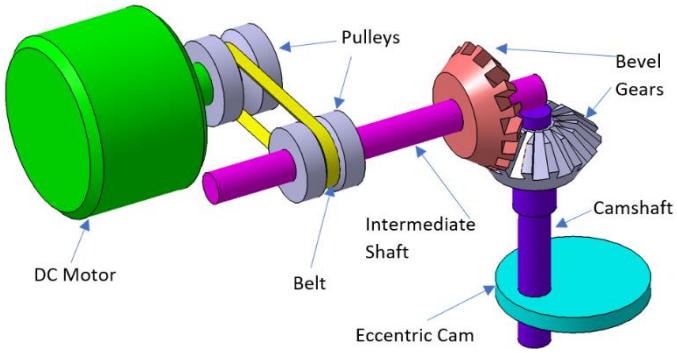

Figure 4-2 Power Transmission System

Geometry Synthesis and analysis

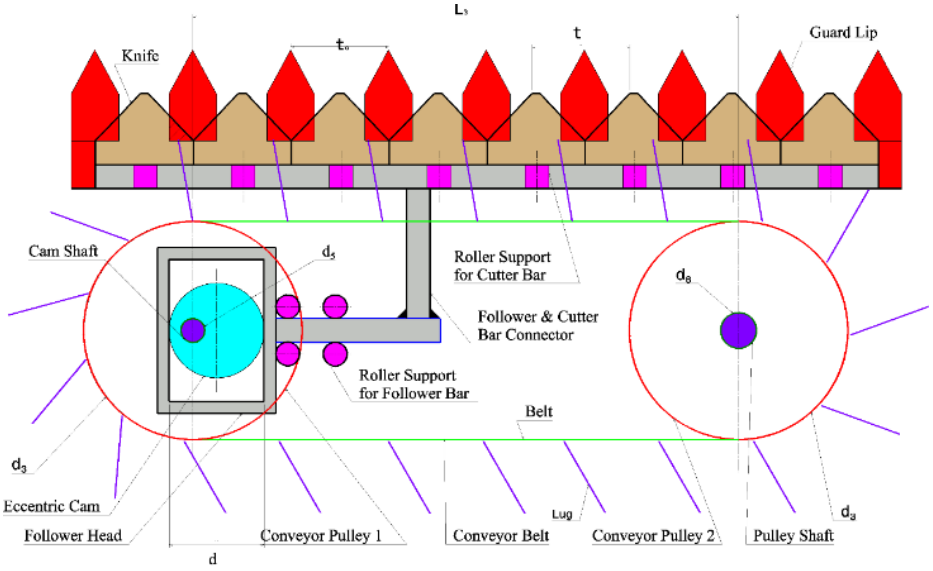

Figure 4-3 Basic Structure of Cutting and Conveying Mechanism

The basic geometrical synthesis and analysis carried for the speed of DC motor, speed of pulley

on the DC motor shaft, speed of camshaft, length of cam tip, stroke length of the follower, speed of lugged conveyor, pitch of lugs and pitch of star wheels.

Analysis of Cutting Force of Straws

The cutting force of a straw can be modelled from shearing strength of grain. The knife cut the straw between the edge of the guard lip. This shows that the grain is harvested due to shearing. Hence, the shearing stress (τ_s) of the straw has direct and indirect relation with the shearing force (F_s) and cross-sectional area (A_s) of a straw respectively.

$$\tau_s = \frac{F_s}{A_s} - - \rightarrow F_s = \tau_s A_s \text{ ----------4-1}$$

The shearing force (F_s) can be determined from the Physical and mechanical properties of crops. These properties are studied by different researchers. The studies have been carried in different countries, different values of moisture contents and different species of grains. The results show that their values differ in different magnitudes of shearing strength and cross-sectional area. It is advisable to consider the worst things in order to make the harvester universal i.e., applicable throughout the world. This means that the capacity of the harvester can be analyzed by using maximum values of shearing strength and cross-sectional area which are taken from different literatures see **Table** 4-3. Hence, the machine can harvest efficiently all types of grains in all countries.

The shearing strength and cross-sectional area of wheat is the highest value. So that the geometry, force and strength analysis should be based on wheat which 36.365 N shearing force.

Table 4-3 Physical and Mechanical Properties of Grains (See Literature Review)

Straw	**Wheat**	**Barley**	**Rice**
Minimum cross-sectional area A mm^2	2.32	nf	nf
Maximum cross-sectional area A mm^2	3.087	5.377	4.055
Minimum shearing strength τ MPa	4.91	3.90	1.429
Maximum shearing strength τ MPa	11.78	6.18	1.629
Maximum shearing force F N	36.365	33.23	6.606

Note: nf is for not found

$$F_s = \tau_s A_s = 11.78 * 3.087\ N = 36.365\ N$$

The total cutting force (F_{ca})becomes the product of total numbers of straws (n) that is cut at a time and shearing force (F_s) for single straw.

$F_{ca} = nF_s = 36.365n\ N$ ---------- *4-2*

The total number of straws (n) cuts at a time is equal to the total numbers of knives (n). The numbers of knives depend on width of cut (L) and the spacing of knife section (t).

$n = \frac{L}{t}$ ---------- *4-3*

The total cutting force (F_{ca}) can be defined using **equations** 4-2 and 4-3.

$F_{ca} = 36.365\frac{L}{t}\ N$ ---------- *4-4*

The spacing of knife section (t) is recommended by (D.N. Sharma and S. Mukesh, 2010) to 76.2 mm. The total cutting force (F_{ca}) can be redefined and has a direct relation with the width of cut (L in mm).

$$F_{ca} = 36.365\frac{L}{76.2\ mm}\ N = 0.477L\ \frac{N}{mm}$$

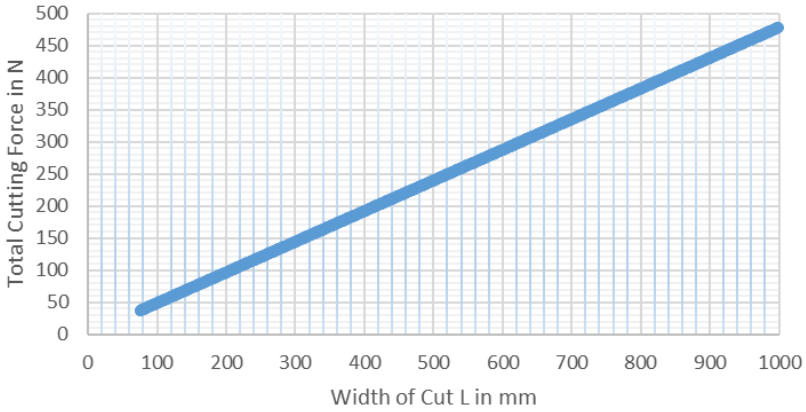

Figure 4-4 Relation of Width of Cut and Cutting Force

The length of the cutter bar is preferable to make very small value. Because the source of power is solar, that is to make lightweight and compact in size. The aim of reducing the cutter bar length is to reduce the energy requirement or to have lightweight and compact size harvester. It is decided to select 610.000 mm cutter bar length (L). The corresponding total cutting force becomes 290.97 N as shown in **Figure** 4-4.

Kinematic Analysis of Eccentric Cam and Flat Face Follower

The contact between cam and follower is tangency at A. The cam rotates about point B. The cam center is at point C (G). The radius of the cam is (AC'=DC-S=R). The radius of the base circle is equal to radius of cam minus BC. When the camshaft rotates by θ, the follower displaces S amount. This displacement can be defined mathematically by considering $\Delta ABC'$ and ΔADB. The radial distance (r) between point A and B depends on the position of the cam see **Figure** 4-5. Hence, the

displacement (s) of the follower depends on the eccentric distance (e) between point B and C, and the radial distance (r) from axis of rotation to the contact point between cam and follower.

$$s = r\cos\beta - (R - e) \quad \text{---------- 4-5}$$

The radial distance r can be defined by applying sine and cosine laws on $\Delta ABC'$.

$$r^2 = R^2 + e^2 - 2Re\cos\theta \quad \text{---------- 4-6}$$

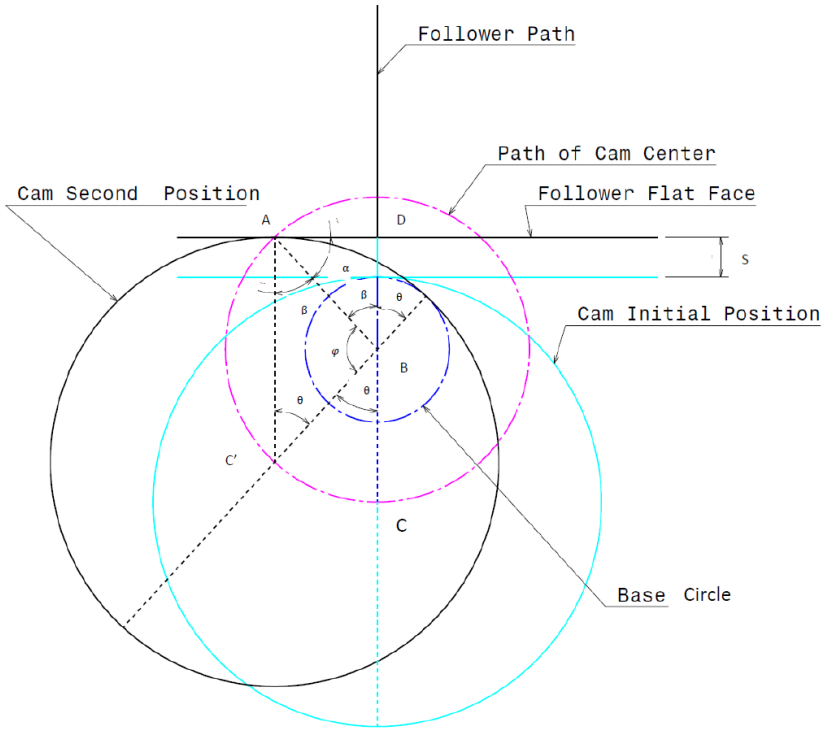

Figure 4-5 Schematic Diagram of Eccentric Cam and Flat Face Follower

$$r = \frac{\sin\theta}{\sin\beta}e = \frac{\sin\theta}{\sqrt{1-\cos^2\beta}}e \quad \text{---------- 4-7}$$

After rearranging and simplifying **equations** 4-5, 4-6 and 4-7, the follower displacement becomes;

$$s = \sqrt{R^2 + e^2 - 2Re\cos\theta - e^2\sin^2\theta} - R + e \quad \text{---------- 4-8}$$

The displacement of the follower becomes minimum and maximum when cam angle is 0^o and 180^o respectively. The maximum displacement is equal to the stroke of the cutter bar which is 76.2 mm (D.N. Sharma and S. Mukesh, 2010). The eccentric distance (e) becomes 38.1 mm.

The angular velocity (ω_3) of camshaft is constant. Hence, the velocity (V_f) and acceleration (a_f) of the follower becomes as follows;

$$V_f = \frac{dS}{dt} = \frac{2Re\sin\theta - e^2\sin 2\theta}{2\sqrt{R^2+e^2-2Re\cos\theta-e^2\sin^2\theta}}\omega_3 \quad \text{---------- 4-9}$$

$$a_f = a_k = \frac{dV}{dt} = \left[\frac{Re\cos\theta - e^2\cos 2\theta}{\sqrt{R^2+e^2-2Re\cos\theta - e^2\sin^2\theta}} - \frac{(2Re\sin\theta - e^2\sin 2\theta)^2}{4(R^2+e^2-2Re\cos\theta - e^2\sin^2\theta)^{1.5}}\right]\omega_3{}^2 \quad \text{---------- 4-10}$$

The velocity and acceleration of the follower is in a range of $[-e\omega_3, e\omega_3]$ *and* $[-e\omega_3{}^2, e\omega_3{}^2]$ *respectively. The minimum forward speed of the machine (*V_m*) is 0.5 m/s. The average knife or follower speed (*V_k *or* V_f*) can be found using the velocity ratio formula (D.N. Sharma and S. Mukesh, 2010).*

$$K = \frac{V_k}{V_m} = \frac{V_f}{V_m} = 1.3\ to\ 1.4 \quad \text{---------- 4-11}$$

Since the velocity of the machine is slow, the ratio should be maximum (K=1.4). Hence, the minimum velocity of the knife or follower which able to harvest becomes:

$$V_k = V_f = K \times V_m = 1.4 \times 0.5 = 0.7 m/s$$

The smallest angular speed of the camshaft to which able to harvest the straws can be determined from the minimum velocity of the knife or follower when the position of the cam is at 90°.

$$V_f = e\omega_3 \longrightarrow \omega_3 = V_f/e = 700/38.1 = 18.373\ rad/s$$

The minimum angular speed of the cam (ω_3) that fulfils the minimum speed of the knife (0.7 m/s) is 18.373 rad/s correspondingly the minimum acceleration of the follower or knife (a_k) becomes 12.861 m/s.

Kinetic Analysis of Eccentric Cam and Flat Face Follower

Kinetic analysis shall be carried in order to determine input parameters for the capacity of the DC motor and dimensions of the cross section of the different components of the harvester. The main components of cutting system is shown in **Figure** 4-6.

The driving force (F) applied on the follower by the cam can be defined by using friction force between cam and flat face follower (f_3), normal forces by the roller supports on the follower bar (N_2 and N_1), total grain cutting force applied by the knives (F_{ca}), friction force between cutter bar and roller supports (f_5), friction forces between the follower bar and roller supports on the bottom, left and right sides (f_4, f_2 and f_1 *respectively*), mass of cutter bar and follower assemblies (m), acceleration of follower (a), coefficient of friction between follower and cutter assembly and roller supports ($\mu_5=\mu_4=\mu_2=\mu_1=\mu$), mass of cutter bar ($m_{cb}$), mass of follower ($m_f$), gravitational acceleration (m_f), moment about z-axis (M_z), width of cutter (b), coefficient of friction between cam and follower (μ_3).

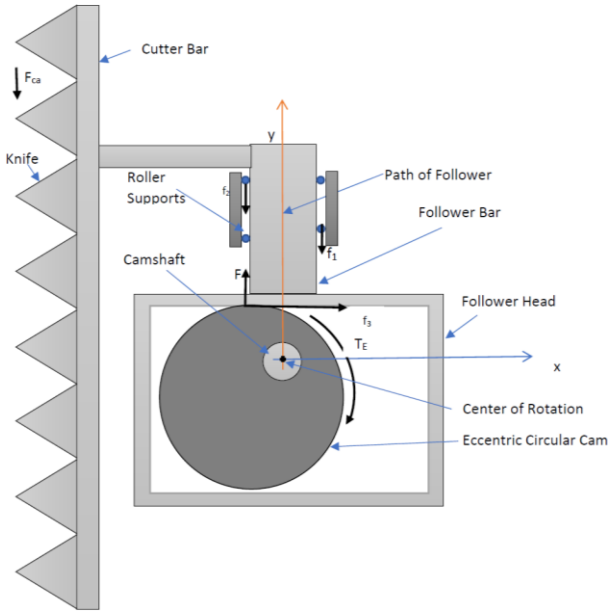

Figure 4-6 2D Representation of Cutting System

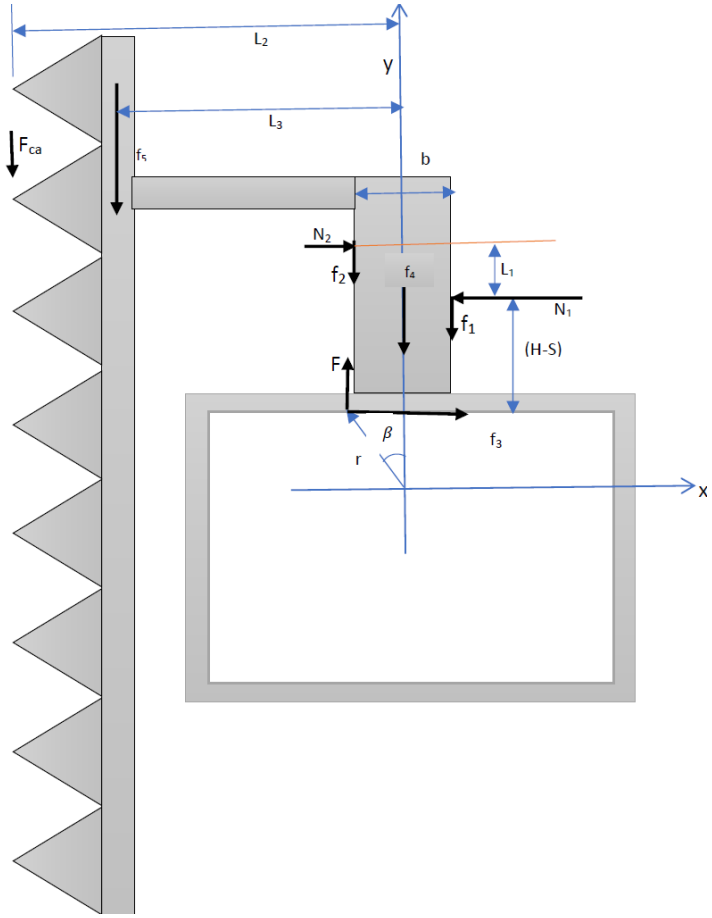

Figure 4-7 Free Body Diagram of Follower and Cutter Bar

The driving force (F) applied on the follower by the cam can be defined by applying equation of

motion for the follower.

$$\sum F_x = 0 \rightarrow f_3 + N_2 - N_1 = 0 \text{ ---------- 4-12}$$

$$\sum \mathrm{F_y} = \mathrm{ma} \rightarrow \mathrm{F} - \mathrm{F_{ca}} - \mathrm{f_5} - \mathrm{f_4} - \mathrm{f_2} - \mathrm{f_1} = \mathrm{ma}$$

$$ma = F - F_{ca} - \mu_5 m_{cb} g - \mu_4 m_f g - \mu_2 N_2 - \mu_1 N_1 \text{ ---------- 4-13}$$

$$\sum \mathrm{M_z} = 0$$

$$-r\cos\beta\, f_3 - r\sin\beta\, F - (L_1 + R + e)N_2 + (R + e)N_1 + \frac{b}{2} f_2 - \frac{b}{2} f_1 + L_2 F_{ca} + L_3 f_5 = 0 \text{- 4-14}$$

$$F = \frac{F_{ca}\left(\frac{L_1}{2\mu} + L_2\right) + \frac{mL_1(\mu g + a_f)}{2\mu} + \mu L_3 m_{cb} g}{e\sin\theta + \mu_3\sqrt{R^2 + e^2 - 2Re\cos\theta - e^2\sin^2\theta} + \frac{\mu\mu_3 b}{2} - \mu_3 R - \mu_3 e + \frac{(1-\mu\mu_3)L_1}{2\mu}} \text{ ---------- 4-15}$$

The coefficient of friction (μ_5=μ_4=μ_2=μ_1= μ) between follower and roller supports, cutter assembly and roller supports are 0.0011 for cylindrical roller bearing (**Michael M. Khonsari and E. Richard Booser, 2017**). The coefficient of friction (μ_3) between cam and follower is 0.029 for greasy hard steel on hard steel sliding friction (**Dudley D. Fuller**). The driving force (F) applied on the follower by the cam can be redefined by substituting values of e, a_f, $\mathrm{F_{ca}}$, μ and μ_3 i.e., 38.1 mm, 12.861 m/s, 290.97 N, 0.0011 and 0.029 respectively.

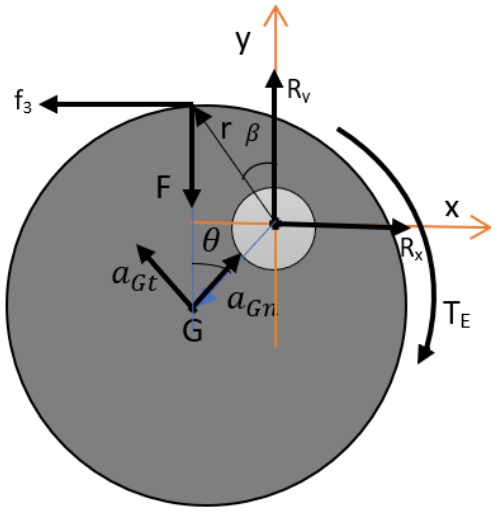

Figure 4-8 Free Body Diagram of Eccentric Cam

The torque $\mathrm{T_E}$ applied by the eccentric cam on the camshaft can be analyzed by using equation 17-15 of (R. C. Hibbeler, 2010) equation of motion of rotating mass about a fixed axis.

$$\sum \mathrm{M_o} = r_G m_c a_{Gt} + I_G \alpha = e m_c e\alpha + I_G \alpha = 0$$

$$r\cos\beta\, f_3 + r\sin\beta\, F = \mathrm{T}_E$$

$$T_E = F(\mu_3\sqrt{R^2 + e^2 - 2Re\cos\theta - e^2\sin^2\theta} + e\sin\theta) \text{ ---------- 4-16}$$

Where F is defined in **equation** 4-15.

The resultant force (R) applied on the eccentric cam by the camshaft can be analyzed by applying equation of motion as follows

$$\sum \mathrm{F_x} = m_c a_{Gnx}$$

$$R_x - f_3 = m_c e\omega^2 \sin\theta \text{ ---------- 4-17}$$

$$\sum \mathrm{F}_y = m_c a_{Gny}$$

$$R_y - F = m_c e\omega^2 \cos\theta \text{ ---------- 4-18}$$

$$R = \sqrt{F^2(1+\mu^2) + 2Fm_c e\omega^2(\mu\sin\theta + \cos\theta) + {m_c}^2 e^2 \omega^4} \text{ ---------- 4-19}$$

Where $\mathrm{M_o}$ is moment about rotating axis, r_G is position mass center with respect to rotating axis, m_c is mass cam, a_{Gt} and $m_c a_{Gn}$ is tangential and normal acceleration of cam mass center about rotating axis respectively, I_G is mass moment of inertia of cam about its mass center, α is angular acceleration of cam which is zero,, Rx and Ry are reactions force in the x and y axes.

Kinematics and Kinetics Analysis of Conveyor Pulley

The camshaft is subjected a torque (T) which comes from eccentric cam (T_E) and conveyor pulley (T_C).

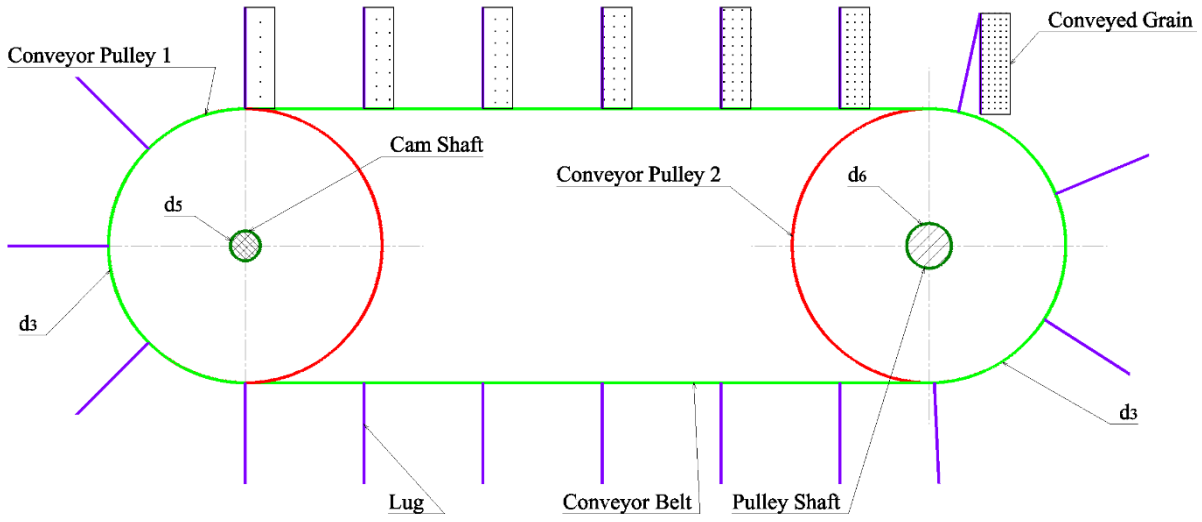

Figure 4-9 2D Representation of Conveyor System

The cut straw of the grain is conveyed to one side by the lug from left to right shown in **Figure** 4-9. The magnitude of conveying force F_c applied by the lugs depends on the weight of straw, frictional force between the straw and cutter bar surface, forward speed of the harvester, speed of

the lug, pitch of lug and diameter of straw. The kinematics relations of straw and lug shall be first defined in order to get the force F_c applied by the lugs. The kinematic analysis can be analyzed by assuming that the straws feed into the harvester in rows by the star wheel. This kinematics can also be analyzed by assuming that that these rows of straws are close to each other about their diameter. Hence, the time t_s required to feed a straw into the knife is the ratio of diameter of straw (d_s) and forward speed of the harvester V_m.

$$t_s = \frac{d_s}{V_m} \text{ ---------- 4-20}$$

The first cutter feeds straw into the conveyor with a feed rate of;

$$feed\ rate = \frac{1\ straw}{t_s} = \frac{V_m}{d_s} \text{ ---------- 4-21}$$

The time required for the lug to cover the pitch is determined by using speed of belt (V_b) and pitch of lug (p).

$$t_p = \frac{p}{V_b} = \frac{2p}{\omega_3 d_3} \text{ ---------- 4-22}$$

The conveying rate of the lug is defined by the time required for the lug to cover a pitch

$$conveying\ rate = \frac{1\ cycle\ of\ lug}{t_p} = \frac{V_b}{p} = \frac{\omega_3 d_3}{2p} \text{ ---------- 4-23}$$

The numbers of straws (n_1) feed into the conveyor from the first cutter becomes the ratio of feeding and conveying rates.

$$n_1 = \frac{feeding\ rate}{conveying\ rate} = \frac{2V_m p}{\omega_3 d_3 d_s} \text{ ---------- 4-24}$$

Hence, the numbers of straws n_2 conveyed in front of the second cutter becomes the sum of the numbers of straws n_s cut by the first and second cutter. In general, the total numbers of straws conveyed in front of any of the cutter can be defined as;

$$n_i = in_1 = i\frac{2V_m p}{\omega_3 d_3 d_s} \text{ ---------- 4-25}$$

Where i-natural number from one up to final numbers of cutter or blade.

Therefore, the total numbers of straws n_s conveyed through the lugs becomes the sum of straws in between the first and last cutter or blade, mathematically;

$$n_s = \sum_{i\to 1}^{n_k} i\frac{2V_m p}{\omega_3 d_3 d_s} \text{ ---------- 4-26}$$

Where n_k-total numbers of cutter or blade

The total weight of the straws W_{sT} conveyed at a time becomes the product of weight of a straw W_s and total numbers of straws n_s, i.e.,

$W_{sT} = n_s W_s = n_s m_s g = m_s g \sum_{i\to 1}^{n_k} i \frac{2V_m p}{\omega_3 d_3 d_s}$ ---------- *4-27*

Where m_s-mass of a straw

The speed of lugged belt (V_b) must be greater than the speed of the knife ($V_k = 0.7$ m/s) or follower (V_f=0.7 m/s) in order to convey quickly the cut crop.

$$V_b = \omega_3 \frac{d_3}{2} > 0.7 \frac{m}{s} \rightarrow d_3 > \frac{2 \times 0.7}{18.373} = 0.0762\, m = 76.2\, mm$$

The speed of lugged belt (V_b) is recommended between 1.33 and 1.5 m/s by (D.N. Sharma and S. Mukesh, 2010). Since the harvester has slow speed, it is preferable to use the smallest value of lugged belt (V_b=1.33 m/s). The corresponding diameter of the conveyor pulley becomes;

$$d_3 = \frac{2 \times 1.33}{18.373} = 0.145m = 145\, mm$$

The pitch of the lug (p) depends on the diameter of the star wheel. The speed of star wheel (V_s) is same as the speed of lugged belt ($V_b = 1.33\, m/s$) which is determined by considering diameter of star wheel arm (D_s) and angular speed (ω_4) of star wheel.

$$V_s = \omega_4 D_s/2 = 1.33\, m/s$$

The diameter of the star wheel (D_s) has a relation with pitch (p) of lug, numbers of arms (Na) on star wheel and width of cut (L). According to Devnani (1985), the pitch of lugs (P) on flat belt of conveyor is given by;

$\pi \times D_s = P \times N_a \rightarrow P = \pi \times D_s/N_a$ ---------- *4-28*

The cut width (L) is covered by the rows of star wheels. The cut width (L) and diameter of star wheel (D_s) can be related by considering the numbers of star wheels (N_s).

$L = N_s D_s = 610\, mm$ ---------- *4-29*

Equation 4-29 shows that there is inverse relation between diameter of star wheel (D_s) and the numbers of star wheels (N_s). When the numbers of star wheels are too many, the star wheel center of rotation becomes closer to the conveyor belt and it needs a lot of supports which makes complex structure. If the numbers of star wheels are too few, the center of rotation of star wheel becomes too far from conveyor belt which feeds uncut straws into the conveyor. Hence, it is recommended to choose 4 numbers of star wheels (N_s) and correspondingly the diameter of star wheel (D_s) becomes 152.5 mm.

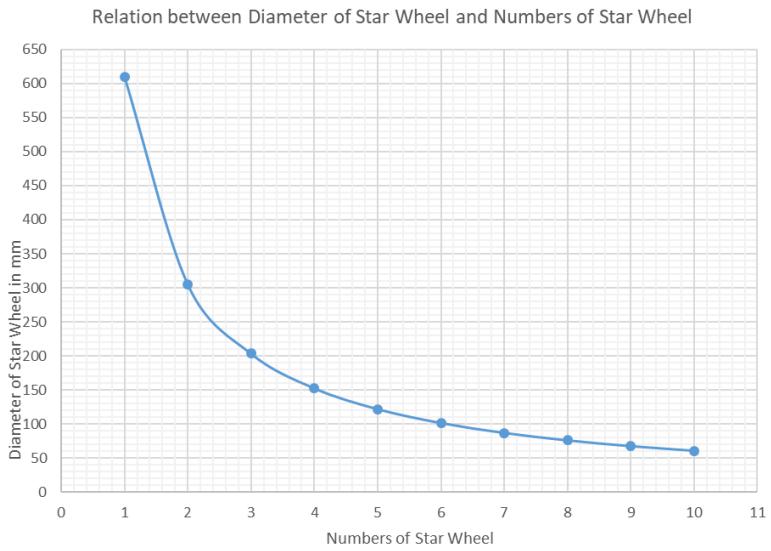

Figure 4-10 Relation of Star Wheel Diameter and Number of Star Wheel

The pitch (p) of lug has also inverse relation with the numbers of arms (Na) on star wheel.

$$P = \pi \times 152.5/N_a = 479.093/N_a$$

It is recommended to choose 5 numbers of arms on the star wheel and correspondingly 95.819 mm pitch of lug.

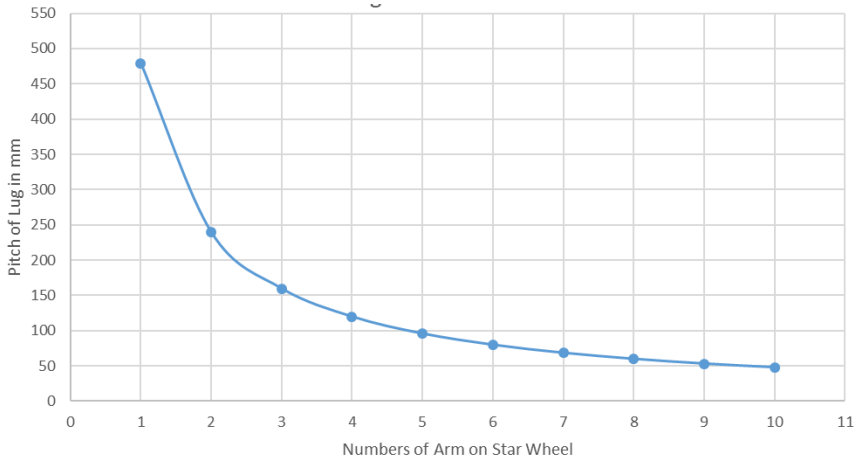

Figure 4-11 Relation of Pitch of Lug and Number of Arms on Star Wheel

The cutting force was analyzed for wheat straw due to its relatively higher strength among barley and rice. There is no information which directly measures the whole mass of mature wheat plant. Hence, it can be determined by considering the mass of shoot (leaf and stem) and spike (kernel) of a wheat. According to (**Yuncai Hu, et al, 2006**) the mass of the shoot is approximately 2.7 gram. According to (**H. M. AUSTENSON and P. D. WALTON, 1970**) the mean mass of the 1000 spike (kernel) is 32.0 gram for Thatcher wheat. Therefore, the total mass of mature wheat (m_s) becomes

an average of 34.7 grams.

The diameter of the wheat straw (d_s) can be estimated from **Table** 4-3 using maximum cross-sectional area of wheat i.e., 3.087 mm^2. Hence, it (d_s) becomes 1.983 mm.

The total weight of the straws W_{sT} conveyed at a time can be determined by substituting the above values into **equation** 4-27**.**

$$W_{sT} = m_s g \frac{2V_m p}{\omega_3 d_3 d_s} \sum_{i\to 1}^{8} i = 34.7 \times 10^{-3} \times 9.81 \times \frac{2 \times 500 \times 95.819}{18.373 \times 145 \times 1.983} \times 36 = 222.612N$$

The magnitude of the conveying force F_c applied by the lugs to convey the whole straws at a time can be analyzed by applying equation of motion in the direction of motion of the conveyor see **Figure** 4-12.

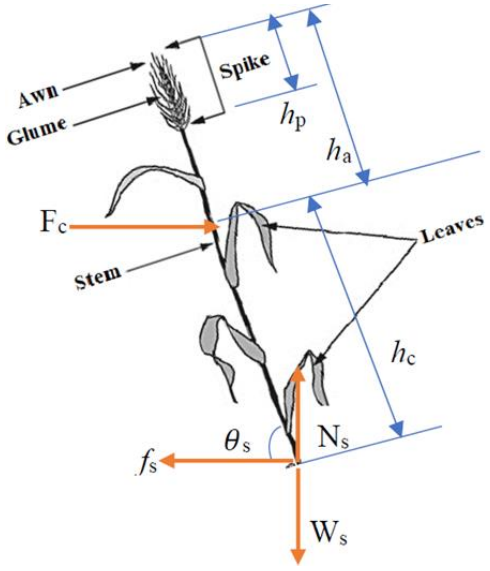

Figure 4-12 Free Body Diagram of Whole Conveyed Grain

$$\sum \mathrm{F} = m_S a_G = 0$$

$$F_c = f_s = \mu_4 W_{sT} = \mu_4 m_s g \sum_{i\to 1}^{n_k} i \frac{2V_m p}{\omega_3 d_3 d_s} \text{ ---------- } 4\text{-}30$$

The static coefficient of friction (μ_4) between the cut straw of wheat at 10% moisture content and polished steel is 0.13 (**S. Afzalinia1 and M. Roberge, 2007)**.

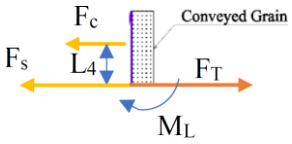

Figure 4-13 Free Body Diagram of Lug

The initial tightness of the conveyor belt F_s should be equal to or greater than the force F_c to convey the whole straws at instant of time.

$$\sum \mathrm{F} = 0$$

$$F_c = F_T - F_S \text{ ---------- 4-31}$$

The applied force on lug F_c should be corelated with the torque of the conveyor pulley installed into the camshaft using equation of motion in a rotating mass about a fixed axis G (Hibbeler, 2010).

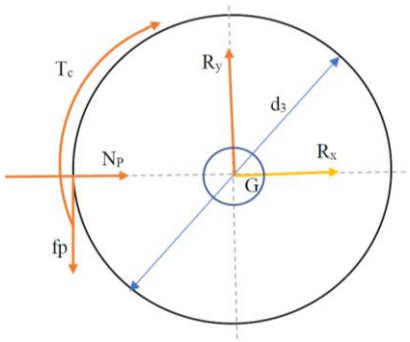

Figure 4-14 Free Body Diagram of Pulley

$$\sum T_G = r_G m_c a_{Gt} + I_G \alpha = 0$$

$$\frac{d_3}{2} f_p = T_c = \frac{d_3}{2} \mu_5 N_p \text{ ---------- 4-32}$$

$$\sum F_n = 0$$

$$N_P + R_x = 0 \longrightarrow R_x = -N_P = -\frac{2T_c}{d_3 \mu_5} \text{ ---------- 4-33}$$

$$\sum F_t = m_p a_t = 0$$

$$R_y = f_p = \mu_5 N_p = \frac{2T_c}{d_3} \text{ ---------- 4-34}$$

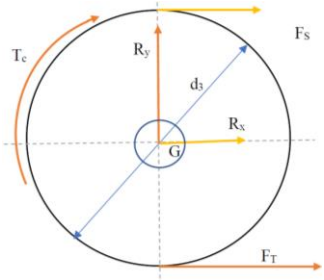

Figure 4-15 Free Body Diagram of Flat Belt and Pulley

The torque (T_C) in the pulley and force on the tight (F_T) and slack (F_S) side of belt can be related by taking summation of torque about center of mass (G).

$$\sum T_G = r_G m_c a_{Gt} + I_G \alpha = 0 \longrightarrow T_C = (F_T - F_S)\frac{d_3}{2} = F_C \frac{d_3}{2}$$ ---------- *4-35*

The normal force in the above three equation can be redefined by applying equation of motion for the flat belt and lug assembly, i.e.;

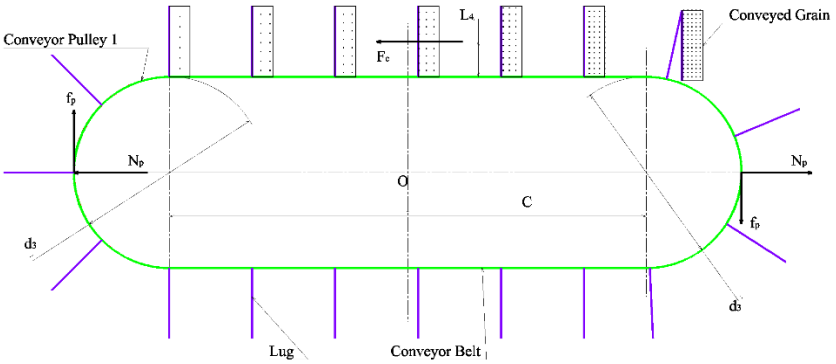

Figure 4-16 Free Body Diagram of Flat Belt and Lug Assembly

$$\sum \mathrm{M}_o = 0$$

$$(\frac{d_3}{2} + L_4)F_c - 2(\frac{d_3 + C}{2})f_p \leq 0$$

$$N_p = \frac{(\frac{d_3}{2}+L_4)}{\mu_5(d_3+C)}F_c = \frac{(d_3+2L_4)T_c}{\mu_5(d_3+C)d_3}$$ ---------- *4-36*

Half of the length of lug can be defined by using **equations** 4-33 and 4-36 as follows.

$$L_4 \leq 0.5d_3 + C$$ ---------- *4-37*

The torque in the camshaft by the conveyor pulley is defined by substituting **equation** 4-30 into 4-35, i.e.;

$$T_c = \frac{d_3}{2}(F_c) = \mu_4 m_s g \sum_{i\to 1}^{n_k} i \frac{V_m p}{\omega_3 d_s}$$ ---------- *4-38*

The cut straw is expected to be conveyed in upright position ($\theta = 90^o$). However, it will be conveyed practically in a range of angles between 0^o and 180^o due to different reasons like permanent bending of the stem during growth, variation in height, scarcity of feed straw, etc. The lose becomes high when the straws are conveyed at smaller or higher angles. Hence, there should be optimum height (h_c) between cutter bar and lug positions in order to keep this optimum height. The center of mass (G) of the plant for **Figure** 4-17 can be determined by applying equation 9-2 of Hibbeler (2010).

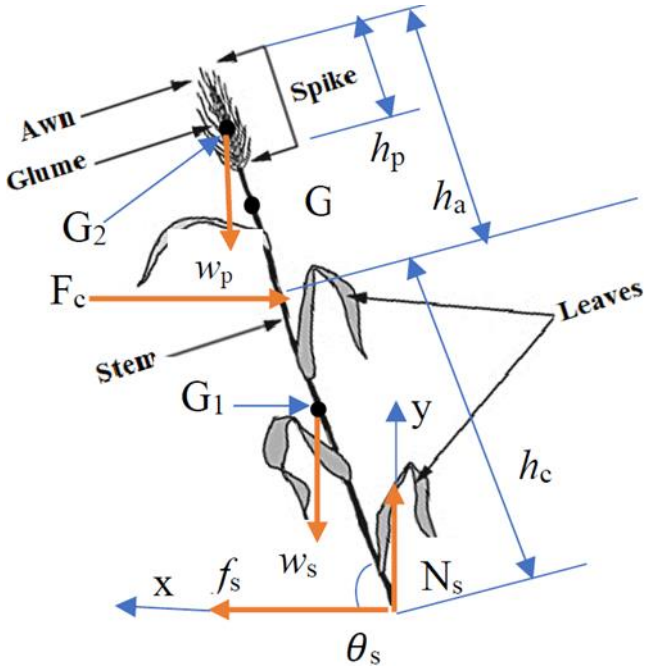

Figure 4-17 Free Body Diagram for Single straw

$$\bar{x} = \frac{\sum \bar{x}_i m_i}{\sum m_i} = \frac{\bar{x}_{G1} m_s + \bar{x}_{G2} m_p}{m_s + m_p}$$

$$\bar{x} = \frac{{}^{(h_c+h_a-h_p)}/_{2}\cos\theta_s m_s + (h_c+h_a-{}^{h_p}/_{2})\cos\theta_s m_p}{m_s+m_p} \text{ ---------- 4-39}$$

$$\bar{y} = \frac{\sum \bar{y}_i m_i}{\sum m_i} = \frac{\bar{y}_{G1} m_s + \bar{y}_{G2} m_p}{m_s + m_p}$$

$$\bar{y} = \frac{{}^{(h_c+h_a-h_p)}/_{2}*\sin\theta_s m_s + (h_c+h_a-{}^{h_p}/_{2})\sin\theta_s m_p}{m_s+m_p} \text{ ---------- 4-40}$$

The distance (d) from bottom end of cut grain up to center of mass (G) becomes;

$$\bar{d} = \sqrt{\bar{x}^2 + \bar{x}^2} = \frac{{}^{(h_c+h_a-h_p)}/_{2} m_s + (h_c+h_a-{}^{h_p}/_{2}) m_p}{m_s+m_p} \text{ ---------- 4-41}$$

The sum of moments about G must be zero otherwise the cut plant will not be stable during conveying that is;

$$w_p(\bar{x}_{G2} - \bar{x}) + F_c(\bar{y} - y_c) - w_s(\bar{x} - \bar{x}_{G1}) - f_s\bar{y} + N_s\bar{x} = 0 \text{ ---------- 4-42}$$

The sum of force in the y-axis is;

$$\sum F_y = 0 \rightarrow N_s = (w_s + w_p) = (m_s + m_p)g \text{ ---------- 4-43}$$

The sum of force in the x-axis is;

$\sum F_x = 0 - - \rightarrow F_c = f_s = \mu_4 N_s = \mu_4(m_s + m_p)g$ ---------- *4-44*

Equation 4-42 **c**an be simplified by substituting **equation** 4-44 into 4-42;

$m_p(\bar{x}_{G2}) - \mu_4(m_s + m_p)y_c + m_s(\bar{x}_{G1}) = 0$ ---------- *4-45*

The vertical height (y_c) between lug center and cutter bar can be defined as follows in terms of each centroidal distances.

$y_c = \frac{m_p(\bar{x}_{G2}) + m_s(\bar{x}_{G1})}{\mu_4(m_s + m_p)}$ ---------- *4-46*

The length of straw (h_c) between lug center and cutter bar can be defined as follows in terms of ratio of spike (h_p) and plant (h) height ($k = h_p/h$).

$$h_c \sin\theta_s = \frac{m_p\left(h_c + h_a - {h_p}/{2}\right) + m_s\left(h_c + h_a - h_p\right)/2}{\mu_4(m_s + m_p)}\cos\theta_s$$

$h_c = \frac{m_p(2-k) + m_s(1-k)}{2\mu_4(m_s + m_p)\tan\theta_s - m_p(2-k) - m_s(1-k)} h_a = \frac{m_p(2-k) + m_s(1-k)}{2\mu_4(m_s + m_p)\tan\theta_s} h$ ---------- 4-47

The height (h_c) depends on the relative height and weight of shoot and spike (kernel) of straws. According to Caihong Bai, Yinli Liang and Malcolm J. Hawkesford (2013) the total height of wheat plant has a wide range between (~500-1400 mm). It is recommended to consider the average (950 mm) because the shorter and longer straws will be supported by the medium straws. The wheat plant and its spike length have been studied by (Fa Cui and et al, 2011) by considering the phenotypic values for plant height of three parents and two recombinant inbred lines populations in four growing environments and its components in wheat. According to (Fa Cui and et al, 2011) the average value of the plant height above cutter bar and spike length is 827.32 mm and 100.82 mm respectively. This shows that there is a relation between plant height and spike length which is an average ratio of k=0.122.

The height (h_c) can be determined by taking moments about the mass center (G) of the wheat plant. The shoot and spike (kernel) have a mass of 2.7 and 32 grams respectively. **Equation** 4-47 becomes simplified by substituting masses and ratio (k).

$h_c = \frac{32(2-0.122) + 2.7(1-0.878)}{2\times0.13(34.7)\tan\theta_s - 32(2-0.122) - 2.7(1-0.122)} h_a = \frac{6.924}{\tan\theta_s - 6.924} h_a = \frac{32(2-0.122) + 2.7(1-0.878)}{2\times0.13(34.7)\tan\theta_s} h = \frac{6.924}{\tan\theta_s} h$ ---------- 4-48

The above two equation indicate that the angle (θ_s) must be in a range of 0^o and 90^o otherwise the heights (h_c or h_a) should be negative. The coefficient of the height (h_a) must be less than one in

order to convey the cut straw in stable condition.

$$\frac{6.924}{tan\,\theta_s - 6.924} < 1 \quad \text{---------- 4-49}$$

This implies that the angle (θ_s) becomes greater than 85.87°. The heights (h_c) should be less than 500 mm in order to convey the shortest wheat plants. Hence, the optimum heights (h_c) and angle (θ_s) of conveying can be decided to 400 mm and 86.52° respectively by considering average height of wheat plant 950 mm.

The vertical height (y_c) between lug center and cutter bar can be defined as follows in terms of each centroidal distances.

$$y_c = h_c \sin\theta_s = 400 \sin 86.52 = 399.262\ mm$$

Mathematical Modeling of the Geometry of Conveyor and Star Wheel

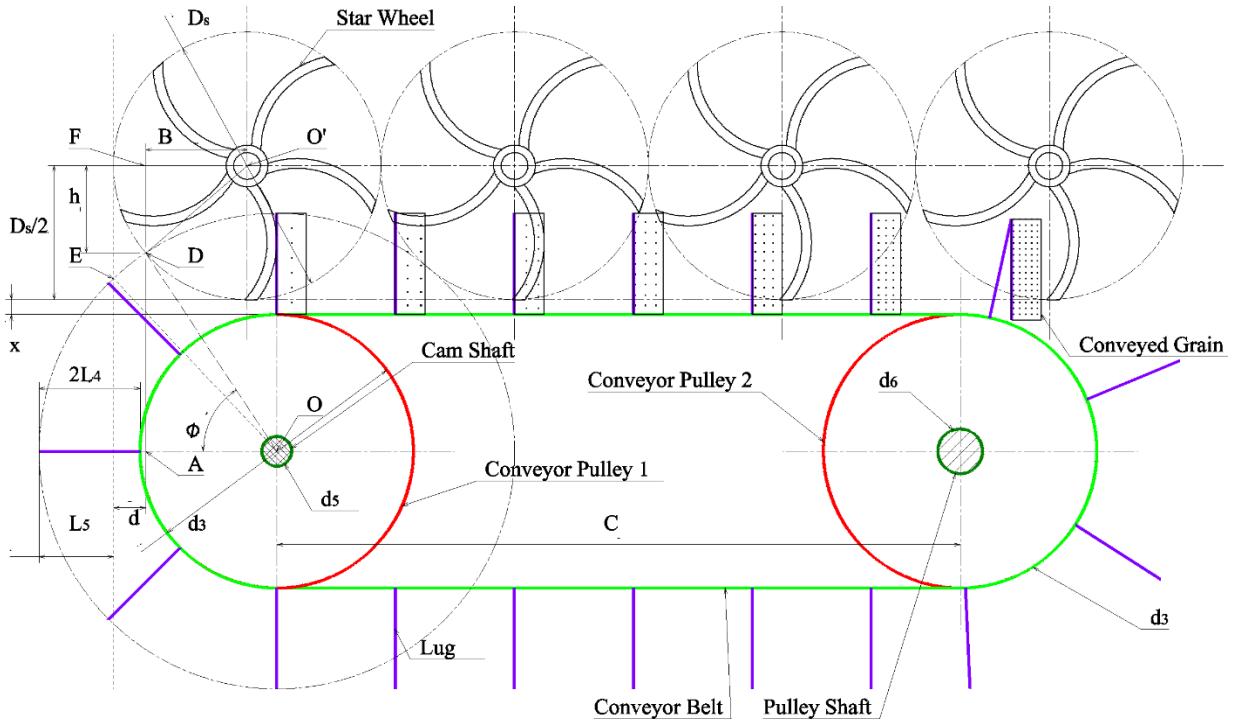

Figure 4-18 Schematic Diagram of Conveyor and Star Wheel System

The center distance (C) between the conveyor pulleys can be determined after analyzing L_4, L_5, X, Ø and h. The height (h) can be determined by applying Pythagoras theorem for ΔO'BD.

$$h = \sqrt{(D_s/2)^2 - B^2} = \sqrt{(D_s/2)^2 - (D_s/2 - d)^2} = \sqrt{D_s d - d^2} \quad \text{---------- 4-50}$$

The distance (d) must be less than the diameter of wheat straw (d_s=1.983 mm) in order to convey all the cut straws. Otherwise, few straws will be out of the intersecting point of lug and arm of star wheel.

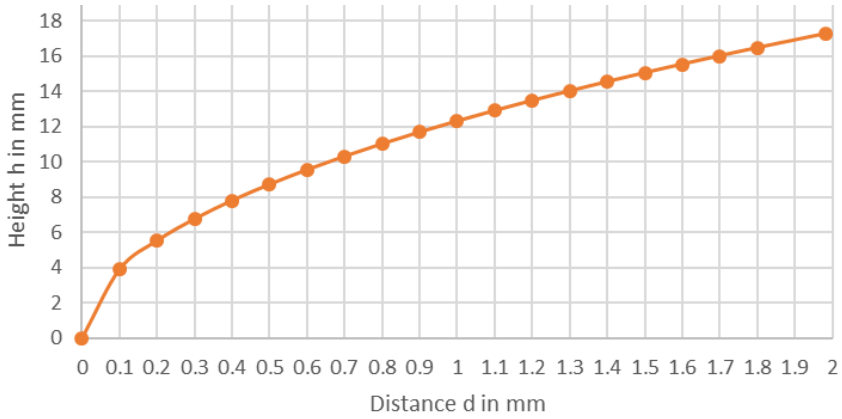

Figure 4-19 Relation of Height (h) and Distance (d)

The length (L_5) is part of lug which lies on the uncut part of the crop. Mathematically, it can be defined as follows;

$$L_5 = 2L_4 - \left(d - \left(\frac{d_3}{2} - \left(2L_4 + \frac{d_3}{2}\right) cos\,\emptyset\right)\right) = (2L_4 + \frac{d_3}{2})(1 - cos\,\emptyset) - d \quad \text{---------- 4-51}$$

The distance (AD) is the difference of distance h from AB.

$$AD = AB - h = D_s/2 + x + d_3/2 - \sqrt{D_s d - d^2} \quad \text{---------- 4-52}$$

The angle (∅) can be related with distance (AD) using sine value of angle (∅) for ΔOAD.

$$sin\,\emptyset = \frac{AD}{OD} = \frac{D_s/2+x+d_3/2-\sqrt{D_s d-d^2}}{2L_4+d_3/2} \leq 1 \quad \text{---------- 4-53}$$

The clearance (x) between the tip of star wheel arm and the conveyor belt is in a range of 10-15 mm (D.N. Sharma and S. Mukesh, 2010). The clearance (x) shall be smallest to increase the clearance between tip of lug and center of rotation of star wheel, i.e., x=10 mm. It is preferable to choose smallest value of distance (d) but the length of lug becomes highest. Hence, the value of distance (d=1.8 mm) is recommended to choose highest value which is less than the straw diameter (d_s=1.983 mm). The distance (h) becomes 16.456 mm.

The highest value of L_4 must be less than half of the diameter of star wheel ($D_s/2 = 76.125\,mm$).

$$\sin\emptyset = \frac{AD}{OD} = \frac{76.125+10+72.5-\sqrt{152.25\times1.8-1.8^2}}{2L_4+72.5} = \frac{142.155}{2L_4+72.5} \leq 1 \rightarrow L_4 \geq 34.828\,mm$$

The value of L_4 becomes in a range of [34.828, 76.125] mm. The optimum value of $2L_4$ is recommended to choose 69.828 mm and the corresponding values of ∅ and L_5 is 87.437° and 60.899 mm respectively.

The center distance between the conveyor pulleys depends on width of cut (L), diameter of conveyor pulleys and intersecting distance (d).

$$C = L - \frac{d_3}{2} - \left[2L_4 + \frac{d_3}{2}\right) cos\,\emptyset = 610 - 72.5 - 192.5\,cos\,49.793 = 413.231\,mm$$ -------- *4-54*

The parameters of the conveyor flat belt pulleys and belts can be determined as follows (R.S. KHURMI and J.K. GUPTA, 2005). The flat belt is balata belt due its water proof property. The density of balata belt is 1110 kg/m^3. The coefficient of friction (μ_5) of balata belt on cast iron pulley is 0.32. The inside length of the flat belt (L_b) can be determined by;

$$L_b = 2C + 2 \times \pi \frac{d_3}{2} = 2 \times 413.231 + 2 \times \pi \times 72.5 = 1281.993\,mm$$ ---------- *4-55*

Total Torque: The total torque (T) needed to drive the camshaft becomes the sum of torques in the eccentric cam (T_E) and conveyor pulley (T_c), i.e.;

$$T = T_E + T_c = F\left(\mu_3\sqrt{R^2 + e^2 - 2Re\,cos\,\theta - e^2 sin^2\theta} + e\,sin\,\theta\right) + F_c\frac{d_3}{2}$$----------*4-56*

Where F and F_c are defined in **equation** 4-15 and 4-30 respectively.

Mathematical Modeling of Power Transmission System

The power is transmitted in two stages. The torque and speed of the DC Motor and camshaft are the main parameters that should be fulfilled for the functionality of the harvester.

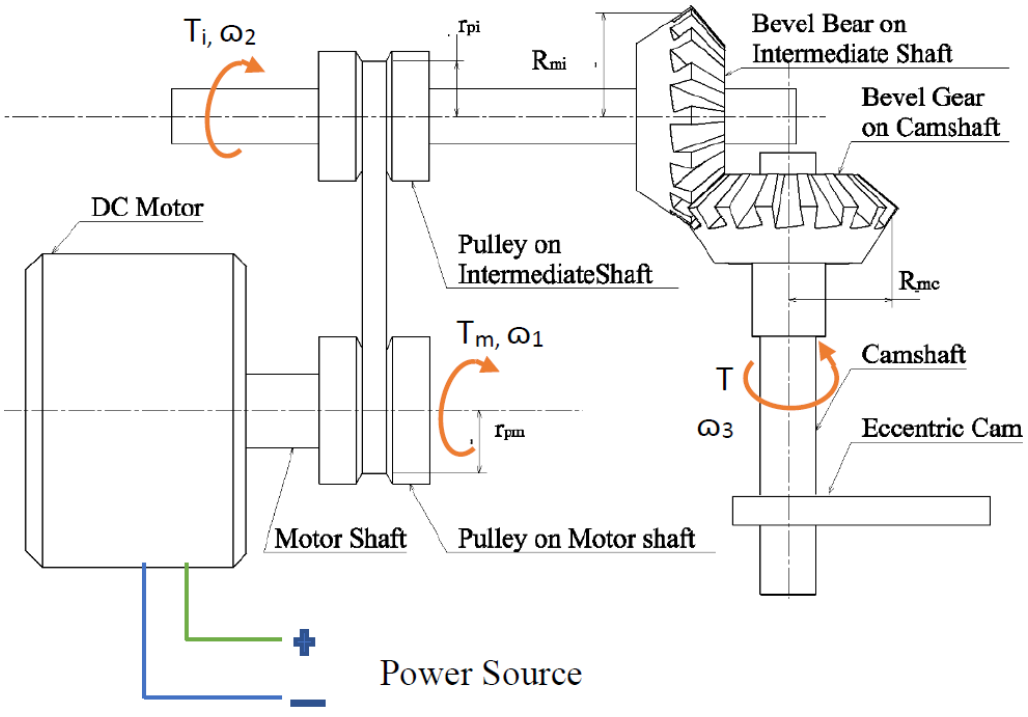

Figure 4-20 Geometry of Power Transmission System

Hence, it is necessary to corelate these parameters mathematically. The total torque T_E that shall be reached into the camshaft is defined in **equation** 4-56. This toque come from the intermediate shaft through a bevel gear combination. The tangential force (F_{Tm}) between the

bevel gears of the intermediate and camshaft is the same.

$$F_{Tm} = \frac{T_i}{R_{mi}} = \frac{T}{R_{mc}} \rightarrow T = \frac{R_{mc}T_i}{R_{mi}} \text{ ---------- } 4\text{-}57$$

The tangential force (F_{Tp}) between the pulleys of intermediate and motor shaft is the same.

$$F_{Tp} = \frac{T_i}{r_{pi}} = \frac{T_m}{r_{pm}} \rightarrow T_i = \frac{r_{pi}T_m}{r_{pm}} \text{ ---------- } 4\text{-}58$$

The torques in the motor shaft and camshaft can be related as

$$T = \frac{R_{mc}T_i}{R_{mi}} = \frac{R_{mc}}{R_{mi}}\frac{r_{pi}T_m}{r_{pm}} \; or \; T_m = \frac{R_{mi}}{R_{mc}}\frac{r_{pm}}{r_{pi}}T \text{ ---------- } 4\text{-}59$$

The tangential speed of the bevel gears about mean radius between the camshaft and intermediate shaft is same.

$$\omega_2 R_{mi} = \omega_3 R_{mc} \text{ ---------- } 4\text{-}60$$

The tangential speed of the pulleys between the motor shaft and intermediate shaft is same.

$$\omega_1 r_{pm} = \omega_2 r_{pi} \text{ ---------- } 4\text{-}61$$

Substituting ω_2 from **equation** 4-60 into **equation** 4-61 and rearranging**;**

$$\frac{\omega_1}{\omega_3} = \frac{R_{mc}r_{pi}}{R_{mi}r_{pm}} \text{ ---------- } 4\text{-}62$$

The torques in the motor shaft and camshaft can be corelated by substituting **equation** 4-62 into **equation** 4-59**.**

$$T_m = \frac{\omega_3}{\omega_1}T \text{ ---------- } 4\text{-}63$$

Where $\frac{\omega_3}{\omega_1}$ is the overall speed ratio of the power transmission system

The speed reduction ratios can be same for the first and second in order to have a compact speed reduction system i.e.,

$$\frac{r_{pi}}{r_{pm}} = \frac{R_{mc}}{R_{mi}} \text{ ---------- } 4\text{-}64$$

Mathematical Modeling of Power Requirement for the Harvester

The power that is needed to drive the harvester can be modeled by considering the relations of the supply voltage (V), torque (T_m) and angular speed (ω_1)of the motor shaft. According to DR. P.S. Bimbhra (2009)**,** the power rating (P) of a motor can be related with load torque (T_m in Nm) and operating speed (ω_1 in rad/s) of the motor as follows for loads remaining substantially constant with time.

$$P = \frac{T_m\omega_1}{1000\eta}KW = \frac{T_m\omega_1}{\eta}W \text{ ---------- } 4\text{-}65$$

Where η is overall efficiency of power transmission system

The overall efficiency of power transmission system is the product of the efficiency of v-belt cemented at shop (η_b=0.9) from (R.S. KHURMI and J.K. GUPTA, 2005) and bevel gear (η_g = 0.98) from (Robert L. Mott, 2004) power transmission.

$$\eta = \eta_b \eta_g = 0.9 \times 0.98 = 0.882$$

The amount of electrical power (P_e) supplied into the DC motor can be related with the supply voltage (V) and current (I) of DC power source as follows;

$$P_e = VI \quad \text{---------- 4-66}$$

The input electrical power (P_e) and output DC motor shaft power (P) can be related by considering electrical and mechanical power loss in the DC motor i.e., overall efficiency η_m of the DC motor.

$$\eta_m = \frac{\frac{T_m \omega_1}{\eta}}{VI} \longrightarrow T_m = \frac{\eta_m \eta VI}{\omega_1} \quad \text{---------- 4-67}$$

The supply voltage and current can be related with the torque needed at the camshaft as follows.

$$T_m = \frac{\omega_3}{\omega_1} T = \frac{\eta_m \eta VI}{\omega_1} \longrightarrow T = \frac{\eta_m \eta VI}{\omega_3} \quad \text{---------- 4-68}$$

The required parameters can be determined by selecting DC motor otherwise it is impossible to solve the parameters defined in kinematics, kinetics and power analysis of the whole harvester. Hence, NEMA 56C is selected. It has a specification of 1.5 hp, 24 V, 1800 rpm, 62.5 Amps Armature Full Load, 25 kg weight and 5.934 Nm torque. It is OMPM-DC Series permanent magnet DC motors which are designed for long motor life with permanently lubricated ball bearings and are TEFC (totally enclosed fan cooled) [41].

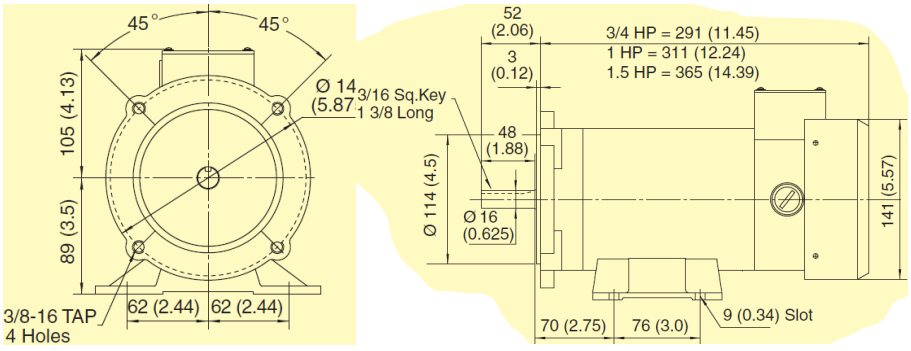

Figure 4-21 Standard Dimension of NEMA 56C DC Motor

Dimensions: mm (in) and φ= diameter [41]**.**

All OMPM-DC motors are constructed from heavy duty gauge steel including frames, end bells, mounting bases, junction boxes and covers. These DC motors are specifically designed for use

with SCR controllers where applications require torque throughout the application and speed range, as well as adjustable speeds. The required dimensions of the DC motor are shown in **Figure** 4-21 **[41].**

The amount of electrical power (P_e) supplied into the DC motor can be determined as follows;

$$P_e = VI = 24 \times 62.5 = 1500\ w$$

The amount of mechanical output power (P_m) from the DC motor becomes

$$P_m = {}^{T_m\omega_1}/_{\eta} = {}^{5.934 \times 188.496}/_{0.882} = 1268.181\ w$$

The efficiency of the DC motor is the ratio of output mechanical (P_m) and input electrical (P_e) power.

$$\eta_{\ m} = \frac{P_m}{P_e} = \frac{1268.181}{1500} = 0.85 = 84.545\%$$

The torque needed at the camshaft can be determined from **equation** 4-68 by using the voltage and current supplied into the DC motor.

$$T = \frac{\eta_{\ m}\eta VI}{\omega_3} = \frac{0.882 \times 0.85 \times 24 \times 62.5}{\omega_3} = \frac{1124.55}{\omega_3} Nm \text{ ---------- } 4\text{-}69$$

The minimum angular speed of the camshaft is 18.373 rad/s which is determined in kinematics analysis of the cam and follower. Hence, the maximum torque needed on the camshaft becomes 61.207 Nm.

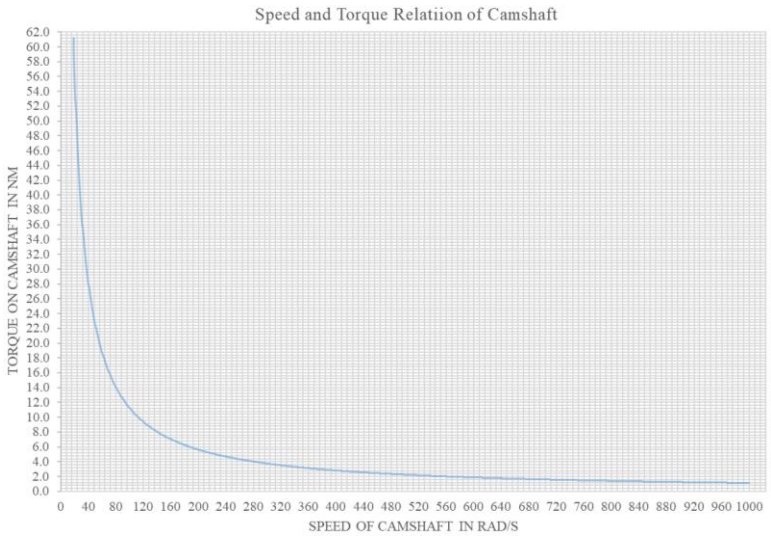

Figure 4-22 Speed and Torque Relation of Camshaft

This torque is shared by conveyor pulley (T_c) and eccentric cam (T_E). The torque on the conveyor pulley (T_c) can be determined by using **equation** 4-38.

$$T_c = \mu_4 m_s g \sum_{i\to 1}^{n_k} i \frac{V_m p}{\omega_3 d_s}$$

$$= 0.13 \times 0.0347 \times 9.81 \times \sum_{i\to 1}^{8} i \frac{0.5 \times 0.096}{18.373 \times 1.983 \times 10^{-3}} = 2.099 Nm$$

The remaining torque will be applied on the eccentric cam. Its magnitude becomes

$$T_E = T - T_C = 61.207 - 2.099 = 59.108\ Nm$$

Since the speed reduction ratio is same both for the pulleys and bevel gears system, the mean radiuses of bevel gears and pulleys can be determined as follows using **equation** 4-70.

The applied torque on pulleys and bevel gears is small which is less than or equal to $T = 61.207\ Nm$. So that it is recommended to have smaller pulleys and gears. Hence, it is decided to have $r_{pi} = R_{mc} = 48.045\ mm$ and $r_{pm} = R_{mi} = 15\ mm$. Correspondingly, the angular speed ω_2 and torque T_i of intermediate shaft becomes 58.849 rad/s and 19.109 Nm by using **equation** 4-60 and 4-58 respectively. The tangential force of the pulleys (F_{Tp}) on the motor and intermediate shafts, and bevel gears (F_{Tm}) on the intermediate and cam shafts becomes 298.298 N and 1273.952 N by using **equation** 4-58 and 4-57 respectively.

N.B: Among the parameters included in the kinematics and kinetics modelling; L_1, L_2, L_3, m_{cb}, m and R should be determined from strength analysis.

The bevel gear parameters can be determined as follows (R.S. KHURMI and J.K. GUPTA, 2005). According to (R.S. KHURMI and J.K. GUPTA, 2005), for satisfactory operations of the bevel gears

1. The face width should be from 6.3m to 9.5m, where m is the module.
2. The ratio L/b should not exceed 3 where L is cone distance and b is face width.
3. The number of teeth in pinion must not less than $\frac{48}{\sqrt{1+V.R^2}}$, where V.R is velocity ratio.

Therefore, the minimum number of teeth (T) becomes;

$$T \geq \frac{48}{\sqrt{1+V.R^2}} = \frac{48}{\sqrt{1+3.203^2}} = 14.305 \text{ ---------- } \textit{4-70}$$

Fifteen (15) number of teeth (T) is selected for the pinion in order to have compact gear box. Correspondingly, the number of teeth (T) in gear becomes 48.

The pitch diameter (D) of bevel gear is greater than its mean diameter (D_m).

The module (m) and pitch diameter (D) analyzed as follows using either small (D_p) or larger bevel (D_G) gear;

$T = \frac{D}{m}$ ---------- *4-71*

Using T_p=15, the module m decided to 3 mm by iteration in order to have compact size of gear box. Correspondingly, the pitch diameter of pinion (D_p) becomes 45 mm, addendum a=1*m=3mm, dedendum d=1.2*m=3.6mm, clearance=0.2*m=0.6 mm, working depth=2*m=6 mm and thickness of tooth=1.5708*m=4.7124 mm. In the same way, the pitch diameter of the gear (D_G) becomes 144 mm.

The angle between the shafts is perpendicular. Hence, the pitch angle (θ_{p1}) for the pinion becomes;

$$\theta_{p1} = \tan^{-1}\left(\frac{1}{V.R}\right) = \tan^{-1}\left(\frac{1}{3.203}\right) = 17.339^0$$

In the same manner, the pitch angle (θ_{p2}) for the gear becomes;

$$\theta_{p2} = \tan^{-1}(V.R) = \tan^{-1}(3.203) = 72.661^0$$

Using the above known parameters, outside or addendum cone diameter (D_{OG}) of gear and (D_{OP}) pinion becomes;

$$D_{OG} = D_G + 2a\cos\theta_{p2} = 144 + 2 \times 3 \times \cos(72.661^0) = 145.788\ mm$$

$$D_{OP} = D_P + 2a\cos\theta_{p1} = 45 + 2 \times 3 \times \cos(17.339^0) = 50.728\ mm$$

Using the above known parameters, inside or dedendum cone diameter D_{Gd} of gear and D_{pd} pinion becomes;

$$D_{Gd} = D_G - 2d\cos\theta_{p2} = 144 - 2 \times 3.6 \times \cos(72.661^0) = 141.854\ mm$$

$$D_{Pd} = D_P - 2d\cos\theta_{p1} = 45 - 2 \times 3.6 \times \cos(17.339^0) = 38.127\ mm$$

$$Cone\ distance\ (L) = \frac{D_p}{2\sin(\theta_{p1})} = \frac{45}{2\sin(17.339^0)} = 75.497\ mm$$

$$Addendum\ angle\ (\alpha) = \tan^{-1}\left(\frac{a}{Cd}\right) = \tan^{-1}\left(\frac{3}{75.497}\right) = 2.276^0$$

$$Dedendum\ angle\ (\beta) = \tan^{-1}\left(\frac{d}{Cd}\right) = \tan^{-1}\left(\frac{3.6}{75.497}\right) = 2.730^0$$

The first stage of speed reducer is pulley drive. It has diametr of pulleys on intermediate shaft (d_i=96.09) mm and motor shaft (d_m=30 mm). The pulleys and belt parameters are determined as follows.

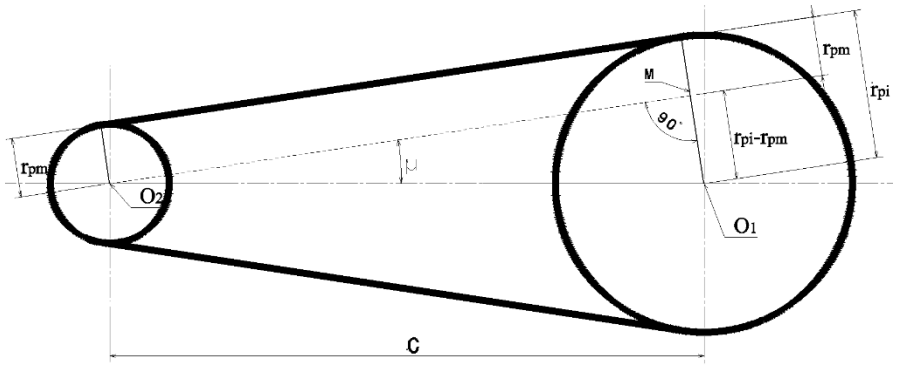

Figure 4-23 First Stage Speed Reducer (Pulley Drive Assembly)

The included angle can be related with center distance (C) by considering $\Delta O_1 O_2 M$.

$sin\,\mu = O_1M/O_2O_1 = (r_{pi} - r_{pm})/C = (48.045 - 15)/C = 33.045/C$ ---------- *4-72*

The included angle (2μ) has a range between 30^0-40^0 (R.S. KHURMI and J.K. GUPTA, 2005). Using the triangle sides C (center distance), $(r_{pi} - r_{pm})$ and angle μ; the range of center distance becomes between 127.676 mm to 96.617 mm respectively. The length of the belt is given by

$L = 2\sqrt{C^2 - \left(r_{pi} - r_{pm}\right)^2} + (\pi - 2\mu)r_{pm} + (\pi + 2\mu)r_{pi}$ ---------- *4-73*

The minimum and maximum possible inside length of v-belt is 402.712mm and 462.015 mm respectively. The maximum inside length of v-belt is smaller than the minimum available standard inside length of v-belts (610 mm). The diametr of pulleys on intermediate shaft (d_i) and motor shaft (d_m) must be increased proportionally to meet the minimum inside length of v-belt . Hence, the radius of pulley on motor shaft (r_{pm}) can be related with inside belt length by considering speed ratio, **equation** 4-73 and 4-74 as follows at the minimum included angle (μ=15º).

$L = 30.802 r_{pm}$ ---------- *4-74*

For the minimum available standard inside length of v-belts (610 mm), the radius of pulley on motor shaft (r_{pm}) becomes approximately 20 mm. Correspondingly, radius of pulley on intermediate shaft (r_{pi}) is 64.06 mm. The center distance becomes 170.235 mm.

The type of belt is V since the two pulleys are very near to each other. It is made of rubber material that has 1140 kg/m^3 density. The belt width (b) is 13 mm, thickness (t) of 8 mm, minimum pitch diameter of pulley of 75 mm and 1.06 N/m weight for A-type of belt for power ranges of 0.7-3.5 KW. The coefficient of friction between dry cast iron pulley and the belt is 0.3 (R.S. KHURMI and J.K. GUPTA, 2005).

Design Analysis of Components

Bevel Gears: There are two bevel gears in the second speed reduction stage. The pinion is in the intermediate shaft whereas the gear is in camshaft. The possible tooth profile of the gears is either 14.5^o or 20^o full depth involute due to the minimum number of teeth (18) on the pinion. According to (R.S. KHURMI and J.K. GUPTA (2005), the tooth profile should be 20^o full depth involute because 14.5^o full depth involute is used for spur and helical gears. So that the pressure angle (∅) is 20^o. The axial (W_a) and radial (W_r) forces can be determined from tangential force (W_t=1273.952 N).

The radial and axial forces in bevel gear is defined and determined as follows for the pinion. The pinion is under a torque of 19.109 Nm.

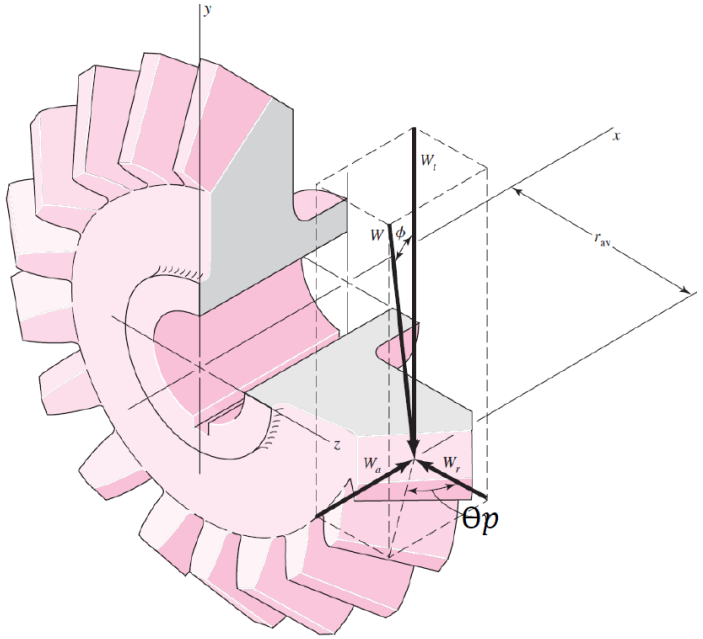

Figure 4-24 Bevel-Gear Tooth Forces [Budynas Nisbett, 2008]

$$W_r = W_t \tan \emptyset \cos \theta_p = 1273.952 \tan 20^o \cos 17.339^o = 442.610\ N$$

$$W_a = W_t \tan \emptyset \sin \theta_p = 1273.952 \tan 20^o \sin 17.339^o = 138.188\ N$$

The radial force (W_r), axial force (W_a) and torque (T) in the bevel gear is 138.188 N, 442.610 N and 61.207 Nm respectively for the gear.

Strength Analysis of Bevel Gears: The pinion and gear are made of same material; Heat-treated cast iron Grade 35, BHN 300 min, minimum tensile strength 350 MPa from Indian standard. Since the system is used in the outdoor, its safety factor (n) is four. Hence, the allowable stress becomes;

$$\sigma_{all} = \sigma_o = \frac{\sigma_y}{n} = \frac{350}{4}\frac{N}{mm^2} = 87.5\ MPa$$

The tangential tooth load (W_T) of the pinion is determine using the modified form of the Lewis equation;

$W_T = \pi(\sigma_o \times C_V)bmy'(\frac{L-b}{L})$ ---------- *4-75*

Where $\sigma_o\ is\ allowable\ static\ stress = \sigma_{all}$, $C_V\ is\ velocity\ factor$ b is face width, V peripherial speed in m/s, m is module 4, $y'\ is\ tooth\ form\ factor$, L is slant height of pitch cone or cone distance, T_E is tooth form factor, D_P is pitch diameter of pinion 30 mm and D_G is pitch diameter of gear 144 mm.

$$C_V = \frac{3}{3+v} \rightarrow v = \omega_2 \times \frac{D_P}{2} = 58.045 \times 22.5 = 1.306\frac{m}{s} \rightarrow C_V = \frac{3}{3+1.306} = 0.697$$

$$L = \sqrt{\left(\frac{D_G}{2}\right)^2 + \left(\frac{D_P}{2}\right)^2} = \sqrt{(72)^2 + (22.5)^2} = 75.434\ mm \text{ and } \frac{L}{b} \leq 3 \rightarrow b \geq 25.145\ mm$$

$$y' = 0.124 - \frac{0.686}{T_{EP}} \rightarrow T_{EP} = T_P \sec\theta_{p1} = 15 \times \sec 17.339 = 15.714 \rightarrow y' = 0.080$$

The face width b is between [6.3m=18.9 mm, 9.5m=28.5 mm] where m is module and mm millimeter. The face width is recommended to 28 mm.

$$W_T = \pi(87.5 \times 0.697) \times 28 \times 3 \times 0.080\left(\frac{75.434 - 28}{75.434}\right) = 809.623\ N$$

The maximum tangential tooth load (W_T) carrying capacity of the pinion is less than the applied tangential tool load (1273.952 N). The strength of material should be changed to a higher value in order to make safe the gear at any operation condition. The minimum possible yield strength ($\sigma_y = n\sigma_o$) of the material can be analyzed by substituting applied tangential tool load (1273.952 N) into **equation** $W_T = \pi(\sigma_o \times C_V)bmy'(\ L-bL)$ ---------- 4-75**.**

$$1273.952 = \pi(\sigma_o \times 0.697) \times 28 \times 3 \times 0.08\left(\frac{75.434 - 28}{75.434}\right)$$

$$\sigma_o = 137.682\ MPa = \frac{\sigma_y}{n} = \frac{\sigma_y}{4} - - \rightarrow \sigma_y = 550.73\ MPa$$

The next stronger material is surface hardened steel with 0.4% carbon composition, 145 (core) BHN and 551 MPa minimum tensile strength in Indian standard. Hence, the allowable stress becomes;

$$\sigma_{all} = \sigma_o = \frac{\sigma_y}{n} = \frac{551}{4}\frac{N}{mm^2} = 137.75\ MPa$$

The tangential tooth load (W_T) of the gear is determine using the modified form of the Lewis equation;

$$W_T = \pi(\sigma_o \times C_V)bmy'(\frac{L-b}{L})$$

$$C_V = \frac{3}{3+v} \rightarrow v = \omega_3 \times \frac{D_G}{2} = 18.373 \times 72 = 1.323\frac{m}{s} \rightarrow C_V = \frac{3}{3+1.323} = 0.694$$

$$L = \sqrt{\left(\frac{D_G}{2}\right)^2 + \left(\frac{D_P}{2}\right)^2} = \sqrt{(72)^2 + (22.5)^2} = 75.434\ mm \text{ and } b = 28\ mm$$

$$y' = 0.124 - \frac{0.686}{T_{EG}} \rightarrow T_{EG} = T_G \sec\theta_p = 48 \times \sec 72.661 = 161.061 \rightarrow y' = 0.12$$

$$W_T = \pi(137.75 \times 0.694) \times 28 \times 3 \times 0.12\left(\frac{75.434 - 28}{75.434}\right) = 1903.637\ N$$

Since the applied tangential load is much less than the tangential teeth load, it is a safe design.

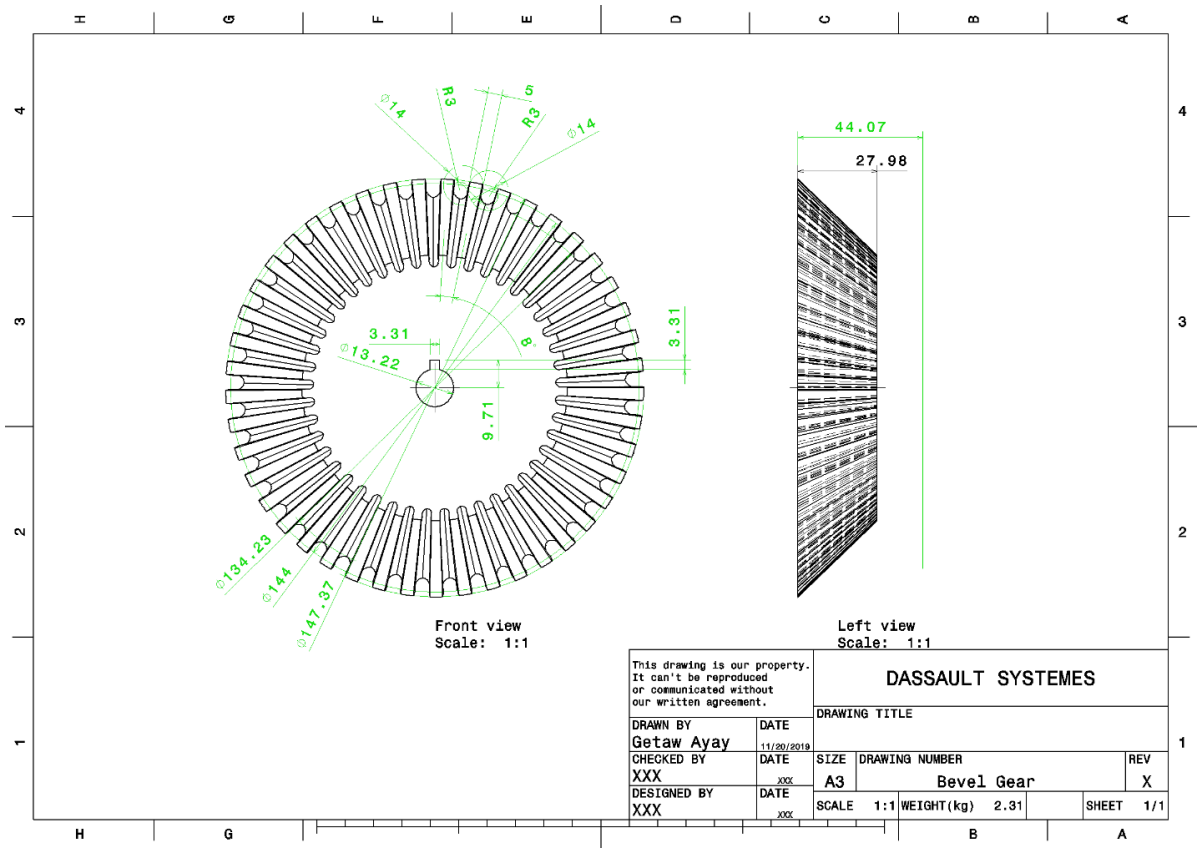

Part Drawing 4-1 Bevel Gear

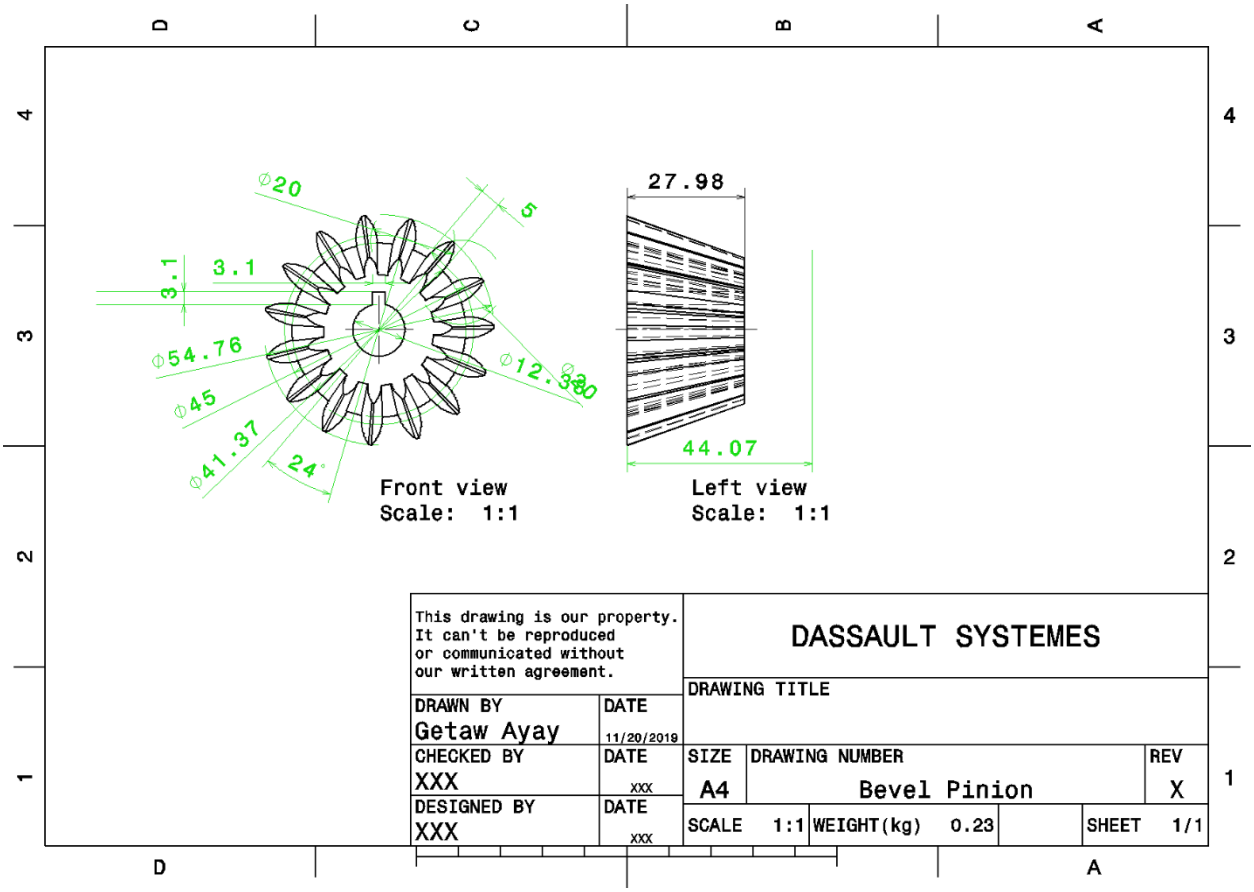

Part Drawing 4-2 Bevel Pinion Gear

Conveyor Pulleys on Idler and Cam Shaft: There are two identical flat belt pulleys except their internal diameters which are used to convey the cut straws. These are installed on the camshaft and Idler Shaft. The free body diagram of the pulleys is shown in **Figure** 4-14, **Figure** 4-15 and **Figure** 4-16. The known parameters are coefficient of friction (μ_5) between flat belt and pulley (0.32), outside diameter ($d_3 = 145\ mm$) and angular speed of camshaft ($\omega_3 = 18.373\ rad/s$). The force (F_C) required to convey the whole cut straw becomes;

$$F_c = \mu_4 m_s g \sum_{i\to 1}^{n_k} i\frac{2V_m p}{\omega_3 d_3 d_s} = 0.13 \times 0.0347 \times 9.81 \sum_{i\to 1}^{8} i\frac{2 \times 0.5 \times 95.819}{18.373 \times 0.145 \times 1.983} = 28.895\ N$$

The torque (T_C) can be determined using **equation** 4-35 or 4-38 which is 2.095 Nm.

According to Daniel Kitaw, the relation between the force of belt in the slack (F_S) and tight (F_T) side is defined by the wrap angle (α=π radian);

$$\frac{F_T}{F_S} = e^{\mu_5 \alpha} \text{ ---------- } 4\text{-}76$$

Hence, the force of belt in the slack (F_S) and tight (F_T) side can be determined by substituting

equation 4-76 into 4-31.

$$F_c = F_T - F_S = F_S(e^{\mu_5 \alpha} - 1)$$

The force of belt in the slack side (F_S) becomes 16.676 N. However, the minimum tightness of the belt in the slack side (F_S) should be equal to the effective (conveying) force ($F_C = 28.895\ N$). Hence, the minimum value of force in the belt tight side becomes 78.963 N using **equation** 4-31. The normal (N_P) and frictional (f_P) forces on the pulley can be determined using **equation** 4-32 which are 90.297 N and 28.895 N respectively.

The reaction force (R_x) in the x-axis can be determined using **equation** 4-33 which is 90.297 N. The reaction force (R_y) in the y-axis can be determined using **equation** 4-34 which is 28.895 N. Hence, the bearing force (R_b) becomes the resultant of (R_x) and (R_y).

$R_b = \sqrt{(R_x)^2 + (R_y)^2} = \sqrt{90.297^2 + 28.895^2} = 94.808\ N$

Materials for Conveyor Pulley: It is made of white heart malleable **cast iron** (WM400) and it has density of 7400 Kg/m^3, 175 GPa modulus of elasticity, 70.3 GPa modulus of rigidity, 0.26 poison's ratio, 220 BHN and 400 MPa tensile strength (V B Bhandari, 2014). The conveyor pulley is under small amount of force but it works always in outdoor. It is recommended to have 3 factor of safety (n). The allowable normal stress (σ_{all}) becomes;

$$\sigma_{all} = \frac{\sigma_y}{n} = \frac{400MPa}{3} = 133.333MPa$$

Strength Analysis of Conveyor Pulley: The pulley is subjected to both bearing and centrifugal forces which create normal stresses.

The bearing stress (σ_b) in the pulley due to camshaft is determined by;

$$\sigma_{all} = \frac{R_b}{A_b} \longrightarrow A_b = d_{5p} \times t = \frac{F_C}{\sigma_{all}} = \frac{94.808}{133.333} mm^2 = 0.711\ mm^2$$

According to (R.S. KHURMI and J.K. GUPTA, 2005) the standard width of pulley (t) is equal to width of belt (b=25 mm from flat belt design) plus 13 mm for a belt width less than 125 mm. The width of pulley (t) becomes 38 mm. Hence, the minimum safe diameter of hole of pulley (camshaft, d_{5p}) becomes 0.006 mm.

The pulley is also subjected to centrifugal stress due to ($\omega_3 = 18.373\ rad/s$). There are radial σ_r and hoop σ_H stresses developed in the pulley. The maximum radial σ_r stress of pulley on camshaft at $r = \sqrt{R_3 R_{5p}}$ is determined by:

$$\sigma_r = (3+\vartheta)\frac{\rho{\omega_3}^2}{8}(R_3 - R_{5p})^2 = (3.26)\frac{7400 \times 18.373^2}{8}(0.0725 - 0.00775)^2 = 4.268\ KPa$$

The maximum hoop stress σ_H on the internal surface is determined by:

$$\sigma_H = \frac{\rho{\omega_3}^2}{4}\left[(3+\vartheta)\left({R_3}^2\right) + (1-\vartheta){R_{5p}}^2\right]$$

$$= \frac{7400 \times 18.373^2}{4}[(3.26)(0.0725^2) + (0.74)0.00775^2] = 10.729\ KPa$$

Both maximum radial and hoop stresses are less than allowable stress i.e., the pulley is safe.

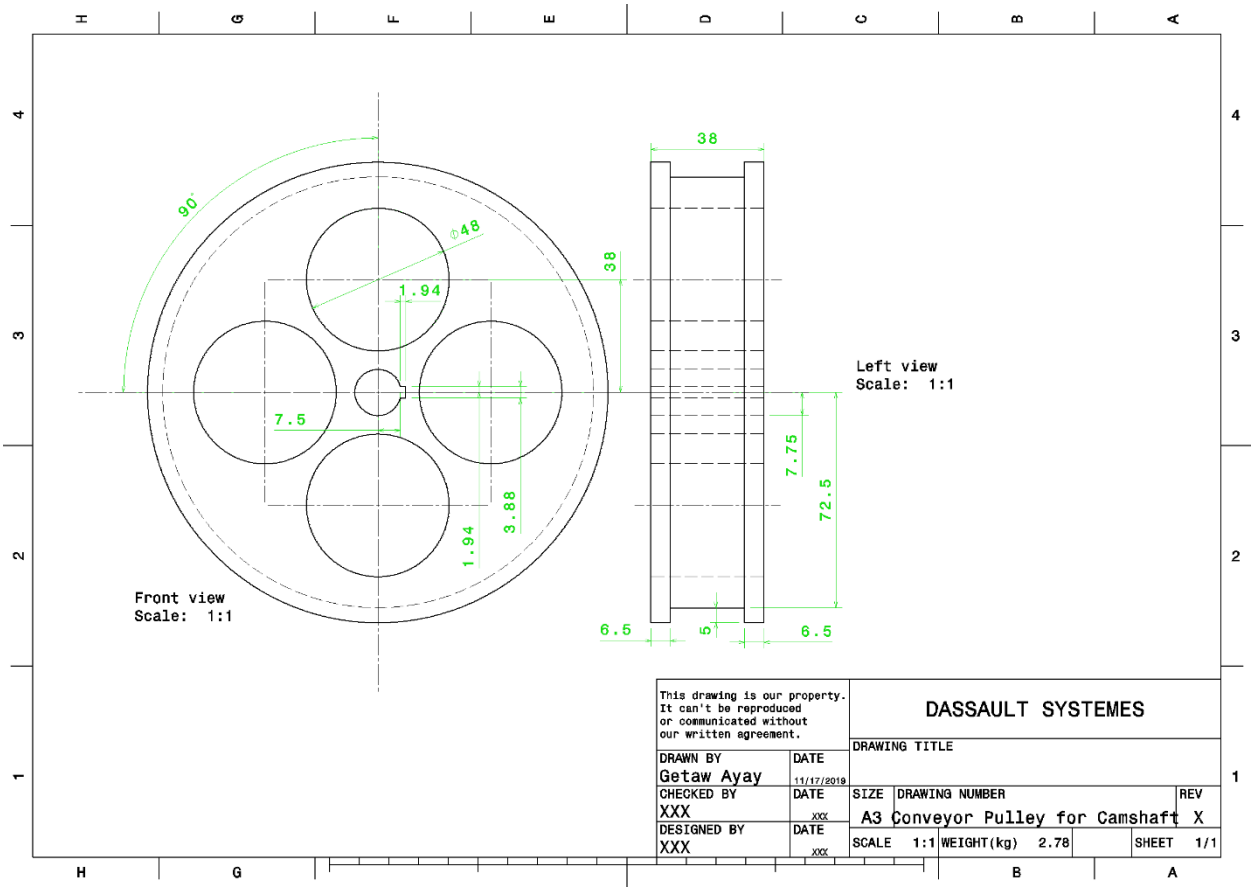

Part Drawing 4-3 Conveyor Pulley on Camshaft

Conveyor Pulley on Idler Shaft: The bearing stress (σ_b) in the pulley due to Idler Shaft is determined by;

$$\sigma_{all} = \frac{R_b}{A_b} \longrightarrow A_b = d_2 \times t = \frac{F_C}{\sigma_{all}} = \frac{94.808}{133.333}mm^2 = 0.711\ mm^2$$

According to (R.S. KHURMI and J.K. GUPTA, 2005) the standard width of pulley (t) is equal to width of belt (b=25 mm from flat belt design) plus 13 mm for a belt width less than 125 mm. The width of pulley (t) becomes 38 mm. Hence, the minimum safe diameter of idler shaft (d_2) becomes

0.019 mm.

The pulley is also subjected to centrifugal stress due to ($\omega_3 = 18.373\ rad/s$). There are radial σ_r and hoop σ_H stresses developed in the pulley. The maximum radial σ_r stress of pulley on Idler shaft at $r = \sqrt{R_3 R_2}$ is determined by:

$$\sigma_r = (3+\vartheta)\frac{\rho {\omega_3}^2}{8}(R_3 - R_2)^2 = (3.26)\frac{7400 \times 18.373^2}{8}(0.0725 - 0.0035)^2 = 5.338\ KPa$$

The maximum hoop stress σ_H on the internal surface is determined by:

$$\sigma_H = \frac{\rho {\omega_3}^2}{4}\left[(3+\vartheta)\left({R_3}^2\right) + (1-\vartheta){R_2}^2\right]$$

$$= \frac{7400 \times 18.373^2}{4}[(3.26)(0.0725^2) - (0.74)0.0035^2] = 10.695\ KPa$$

Both the maximum hoop and radial stresses are less than the allowable i.e., the pulley is safe.

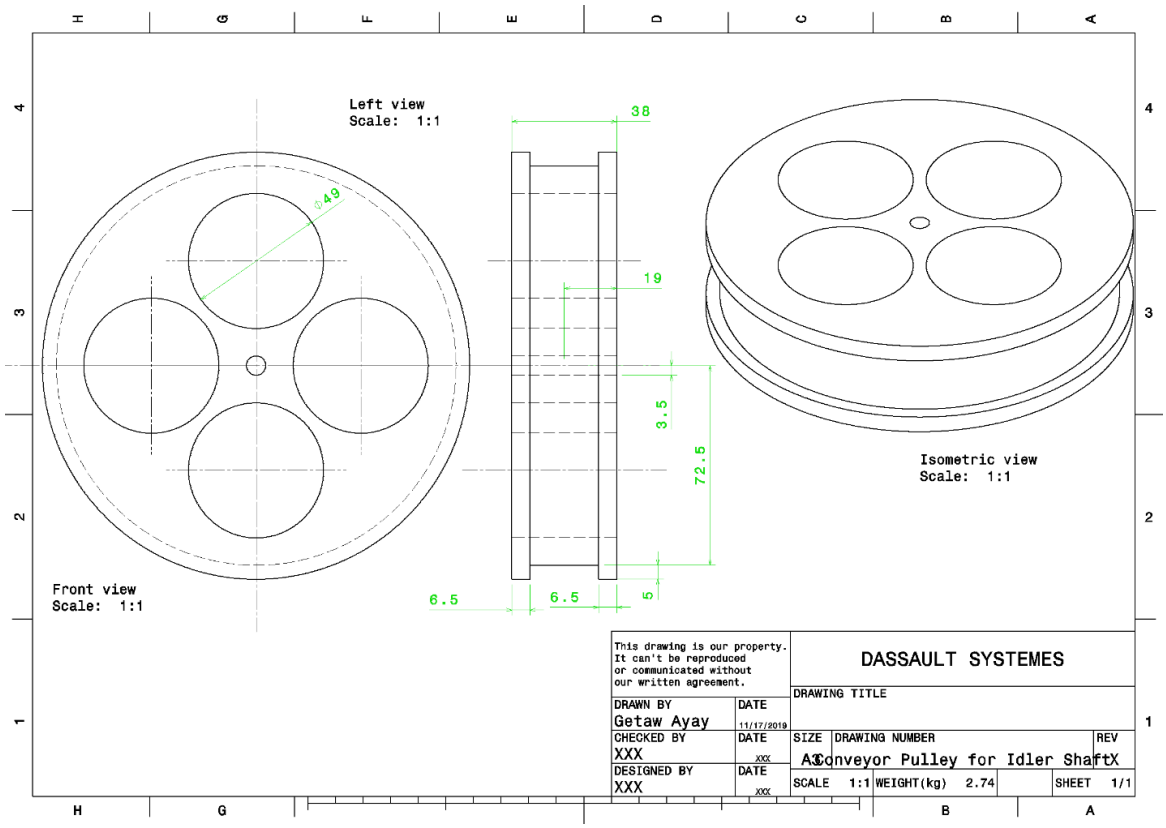

Part Drawing 4-4 Conveyor Pulley on Idler Shaft

Flat Belt: It is used to transfer power from conveyor pulley into lug. Its free body diagram is shown in **Figure** 4-15 and **Figure** 4-16. The length of flat belt (L_b), forces in the tight (F_T) and slack (F_S) side of belt are 1281.993 mm, 78.963 N and 28.895 N respectively.

It is made of balata. Balata has 1110 Kg/m^3 density, 1.5 GPa modulus of elasticity, 10 MPa ultimate tensile strength and 0.32 coefficient of friction on cast iron pulley (S Bhattacharya, et al, 2004). The safety is decided to be eight because the known tensile strength is ultimate. Hence, the allowable stress becomes;

$$\sigma_{all} = \frac{\sigma_U}{n} = \frac{10\ MPa}{8} = 1.25\ MPa$$

The flat balata belt is designed for a maximum of the tight (F_T) side of belt. Hence, the belt width (b) and thickness (t) can be determined as;

$$\sigma_{all} = \frac{F_T}{bt} \rightarrow bt = \frac{F_T}{\sigma_{all}} = \frac{78.963}{1.25} mm^2 = 63.170\ mm^2$$

According to (R.S. KHURMI and J.K. GUPTA, 2005) the standard widths of flat belt are 25, 32, 40,50, 63, 71, 80, 90, 100, 112, 125, 140, 160, 180, 200, 224, 250, 280, 315, 355, 400, 450, 500, 560 and 600 mm and also the standard flat belt thicknesses (t) are 5, 6.5, 8, 10 and 12 mm. If the smallest flat belt thickness (t=5mm) is considered the width of the belt (b) becomes 12.634 mm which is less than the minimum available standard size. Hence, the dimension of the flat balata belt is preferred to 5 mm thickness and 25 mm width.

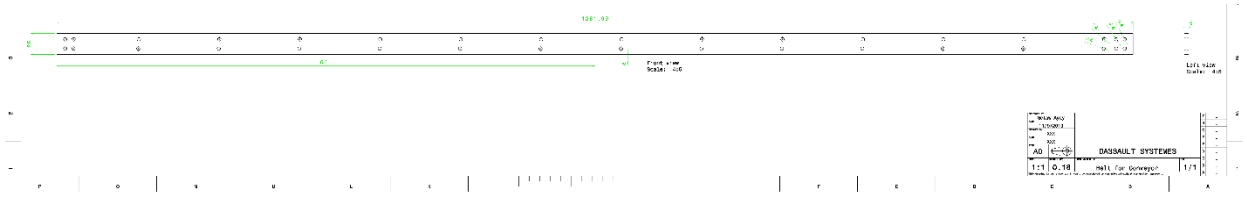

Part Drawing 4-5 Flat Belt

Lug: The lug is attached on the flat belt conveyor and its purpose is to push the cut straw during conveying into right side. The free body diagram of the lug is shown in **Figure** 4-13. The conveying force ($F_C = 28.895\ N$) is determined in the design of conveyor pulley. As it is shown in **Figure** 4-13, the lug is a cantilever beam. The length (L_4=60.899 mm) of lug is determined on mathematical modeling of the geometry of conveyor and star wheel. The unknown is its cross section. It is good use to metal plate in order to convey the cut straw in stable and upright position. The maximum bending moment occurs at the attachment of lug on the flat belt and its magnitude is equal to the product of conveying force (F_c) and lug length (L_4).

$M_L = F_C L_4$The maximum conveying force (F_C) on a single lug can be determined by modifying **equation** 4-30.

$$F_C == \mu_4 m_s g i \frac{2V_m p}{\omega_3 d_3 d_s} = 0.13 \times 34.7 \times 9.81 \times 8 \times \frac{2 \times 0.5 \times 95.819}{18.373 \times 145 \times 1.983} = 6.421\ N$$

Hence, the maximum bending moment on lug becomes;

$$M_L = F_C L_4 = 6.421\ N \times 60.899\ mm = 391.032\ Nmm = 0.391\ Nm$$

The lug should be designed for bending stress and deflection.

Material for Lug: It is made of low carbon steel i.e., Fe E220 designation, 220 MPa yield strength, 210 GPa modulus of elasticity and 7870 Kg/m^3 density. It is recommended to use 3 safety factor. The normal working stress becomes;

$$\sigma_{all} = \frac{\sigma_y}{n} = \frac{220\ MPa}{4} = 55\ MPa$$

The maximum applied bending stress is determined by using

$$\sigma_b = \sigma_{all} = \frac{MC}{I} = \frac{M}{Z} \longrightarrow Z = \frac{M}{\sigma_b} = \frac{385.269}{55} = 7\ mm^3$$

The section modulus (Z) for rectangular cross section is determined by using width of belt (b=25 mm) and thickness of lug (t);

$$Z = \frac{I}{C} = \frac{{}^{bt^3}/_{12}}{{}^{t}/_{2}} = \frac{bt^2}{6} = 7\ mm^3 \rightarrow t = 1.296\ mm$$

The nearest higher value is 1.5 mm thickness.

The maximum deflection (y_{max}) occurs at the free end of the lug.

$$y_{max} = \frac{PL^3}{3EI} = \frac{12PL^3}{3Ebt^3} = \frac{12 \times 6.421 \times 60^3}{3 \times 210 \times 10^3 \times 25 \times 1.5^3} = 0.313\ mm$$

However, the maximum allowable deflection of beam is L/360 (60/360=0.167 mm) which is less the actual deflection of lug (0.313 mm). This implies that, the lug should be decided by considering the deflection.

$$y_{max} = 0.167 == \frac{12PL^3}{3Ebt^3} = \frac{12 \times 6.421 \times 60^3}{3 \times 210 \times 10^3 \times 25 \times t^3} \rightarrow t = 1.85 \cong 2\ mm$$

The maximum deflection (y_{max}) become;

$$y_{max} = \frac{12PL^3}{3Ebt^3} = \frac{12 \times 6.421 \times 60^3}{3 \times 210 \times 10^3 \times 25 \times 2^3} = 0.132\ mm$$

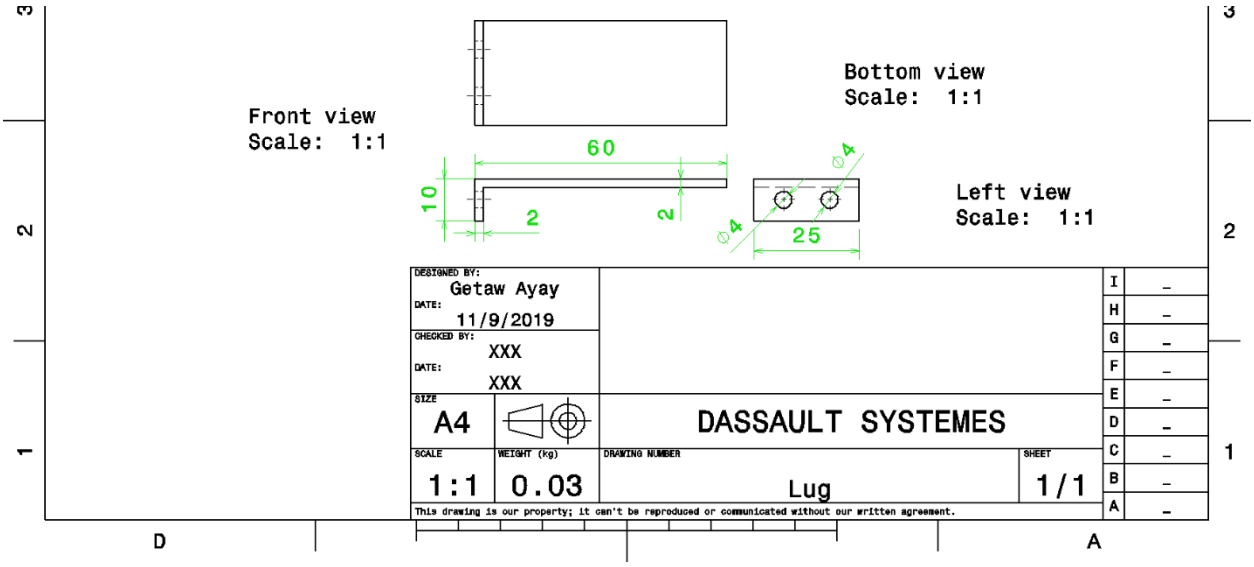

Part Drawing 4-6 Lug

Rivet: This rivet is used to fix the lug on to the flat conveyor belt. The lug is lapped on the flat belt conveyor. The conveying force ($F_C = 6.421\ N$) on the lug is transmitted to a pair of rivets i.e., each rivet shares 3.215 N shearing force. The rivet has flat head and its parameters are designed according to (R.S. KHURMI and J.K. GUPTA, 2005) figure 9.3 (h).

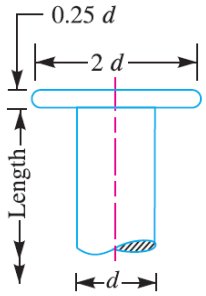

(*h*) Flat head.

Figure 4-25 Flat Head Rivet [R.S. KHURMI and J.K. GUPTA, 2005]

It is made of Aluminium with density 2700 Kg/m^3 and a tensile strength of 100 MPa. It is recommended to have 4 factor of safety. The normal and shearing working stress becomes;

$$\sigma_{all} = \frac{\sigma_y}{n} = \frac{100\ MPa}{4} = 25\ MPa$$

$$\tau_{all} = \frac{\sigma_{all}}{2} = \frac{25\ MPa}{2} = 12.5\ MPa$$

The shearing stress on the rivet becomes;

$$\tau_{all} = \frac{F_C}{A} = -\!\!\rightarrow d = \sqrt{\frac{4F_C}{\pi\tau_{all}}} = \sqrt{\frac{4 \times 3.215}{\pi \times 12.5}} = 0.572\ mm$$

The diameter of the rivet is very small. Hence, it is recommended to increase its diameter to 4 mm. Correspondingly, the head diameter, thickness, and length become 8 mm, 1 mm and 7 mm respectively (R.S. KHURMI and J.K. GUPTA,2005).

Bolt and Nut for Cutter or Blade: It is used to attach cutter or blade on the cutter bar. There are two bolts on a single blade. The bolts are the American National Standard Thread (ANST) cap screws. i.e., shank at one end and flat head at the other end. The various proportions are shown in **Figure** 4-26. A maximum of 290.97 N shearing force can be applied on the two bolts i.e., 145.485 N shearing force in each bolt. The bolts are under single shearing action.

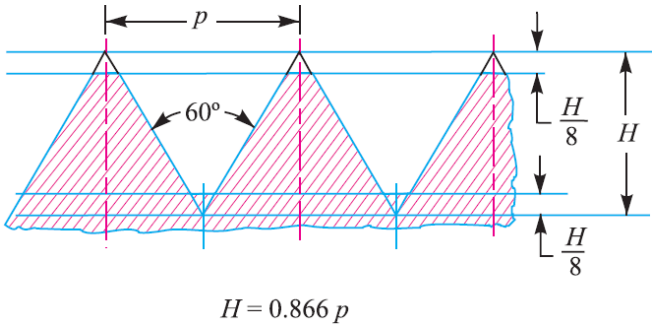

Figure 4-26 Proportions of ANST [R.S. KHURMI and J.K. GUPTA, 2005]

Materials for Bolt: It is made of Fe E 400 Indian standard, 540 MPa tensile strength and 400 MPa yield strength. It is recommended to use a factor of safety of four. The normal and shearing working stress becomes;

$$\sigma_{all} = \frac{\sigma_y}{n} = \frac{400\ MPa}{4} = 100\ MPa$$

$$\tau_{all} = \frac{\sigma_{all}}{2} = \frac{100\ MPa}{2} = 50\ MPa$$

The shearing stress on a single bolt is the ratio of half of cutting force (F_{ca}) and area (A_c) of core diameter of the bolt.

$$\tau_{all} = \frac{F_{ca}}{A_c} = -\!\!\rightarrow d_c = \sqrt{\frac{4F_{ca}}{\pi\tau_{all}}} = \sqrt{\frac{4 \times 145.485}{\pi \times 50}} = 1.925\ mm$$

The next available core diameter (d_c) and major diameter is 1.948 mm and 2.5 mm respectively (R.S. KHURMI and J.K. GUPTA, 2005). However, it will be difficult to drill 2.5 mm in our shop. Hence, it is optimized to use 3.141 mm core diameter (d_c). Correspondingly, 0.7 mm pitch, 4 mm

major diameter, 3.545 mm pitch diameter, 0.429 mm depth of thread, 8.78 mm^2 stress area, 11.5 mm length and M4 designation. In the same way, the core diameter of nut is 3.242 mm.

Note: The core diameter of the nut is already known (3.242 mm). It is made of same material as the bolt. Since the cutter bar is under dynamic condition, there should be two equal nuts in order to lock the possibility of the losing of the nut. According to (R.S. KHURMI and J.K. GUPTA (2005), the thickness (H) of the nut is proportional with the pitch diameter of the bolt (3.545 mm) see **Figure** 4-27.

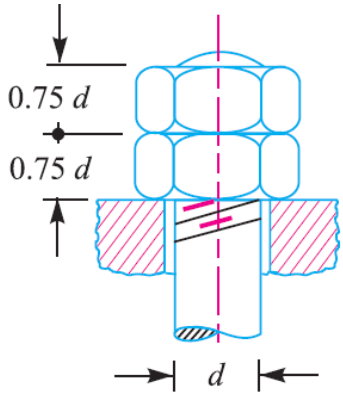

Figure 4-27 Thickness of Luck Nut

The thickness becomes;

$$H = 0.75d = 0.75 \times 3.545 = 2.659\ mm$$

Cutter or Blade: This is one of the important elements which cuts the grains. A maximum of 290.97 N force will be applied on a single blade. The total length of the cutter bar is 609.60 mm. The number of blades is eight (8). Hence, its width (s) becomes 76.2 mm. It has rectangular section. The shape of the blade is shown in **Figure** 4-28.

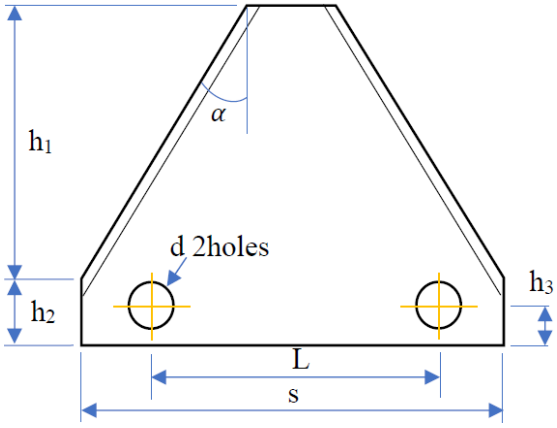

Figure 4-28 Shape of Cutter or Blade

The height (h_2) is equal to the width (b=10 mm) of cutter bar. The diameter of hole (d) is equal to diameter of bolt for cutter or blade (4 mm). the bevel angle α is 26^o for forward speed of 0.5 m/s (D.N. Sharma and S. Mukesh, 2010).

The height (h_1) can be determined by using bevel angle α and considering the width of the nose of cutter or blade.

The maximum possible value of the height (h_1) is;

$$\tan\alpha = \frac{s/2}{h_1} = \frac{s}{2h_1} \rightarrow h_1 = 78.117\ mm$$

Discussion of Dimension of Cutter or Blade: The nose of the cutter or blade is limited by the star wheel vertical support because the star wheel vertical support will be installed at a distance of 158.625 mm from the center of camshaft which is the sum of radius of star wheel (76.125 mm), clearance between conveyor pulley and end of star wheel arm (10 mm) and diameter of conveyor pulley (72.5 mm). The tail of the cutter or blade is limited by the nose of the eccentric cam (88.7 mm) plus clearance (1.3 mm) between nose of cam and tail of cutter or blade. This shows that the maximum length of the cutter or blade is equal to the difference between 158.625 mm and 90 mm which is 68.625 mm. The height (h_1) can be determined when the height (h_2=10 mm) is subtracted from 68.625 mm it will become 58.625 mm. The width of the nose of the cutter or blade becomes 19.013 mm which is determined using the geometry shown in **Figure** 4-28. The other thing is the center of holes. The center of holes on the cutter bar is at the center of its width i.e., 10 mm. Correspondingly, the center of holes on the cutter or blade is at h_3=7 mm from tail and 10 mm from sides.

Materials for Cutter or Blade: It is made of high carbon steel of Fe870 Indian standard designation and 870 N/mm^2 tensile strength and 520 N/mm^2 yield stress (σ_y). Since the system is used in the outdoor, its safety factor (n) is four. Hence, the allowable stress becomes:

$$\sigma_{all} = \sigma_w = \frac{\sigma_y}{n} = \frac{520}{4}\frac{N}{mm^2} = 130\ MPa$$

The cutter is under bending and bearing stresses.

The bearing stress due to the bolts is the ratio of half of the cutting force (F_{ca}) and bearing area (A_b=bd).

$$\sigma_{all} = \sigma_b = \frac{F_{ca}}{A_b} = \frac{F_{ca}}{A_b} = 130\ MPa = \frac{290.97}{4\text{b}} \rightarrow b = 0.560\ mm$$

The induced bending stress can be related with allowable stress;

$$\sigma_{all} = \sigma_b = \frac{My}{I} = \frac{M}{Z} = \frac{FL}{Z} \longrightarrow Z = \frac{bh^2}{6} = \frac{FL}{\sigma_{all}} = \frac{290.97 \times 63.625}{130} = 142.407\ mm^3$$

Where F is transverse force, Z is section modulus of rectangular cutter or blade, L (63.625 mm) is length of cutter or blade from tip to center of hole, b is base (shorter side) and h (76.2 mm) is height (longer side) of the rectangular cross section.

$$b = \frac{6FL}{\sigma_{all} h^2} = \frac{6 \times 290.97 \times 63.625}{130 \times 76.2^2} = 0.147\ mm$$

The thickness of blade becomes 0.560 mm due to bearing stress and 0.147 mm due to bending stress. However, there are unexpected obstacles from the lower part of the cut straw. Hence, it is recommended to increase the thickness to 1 mm.

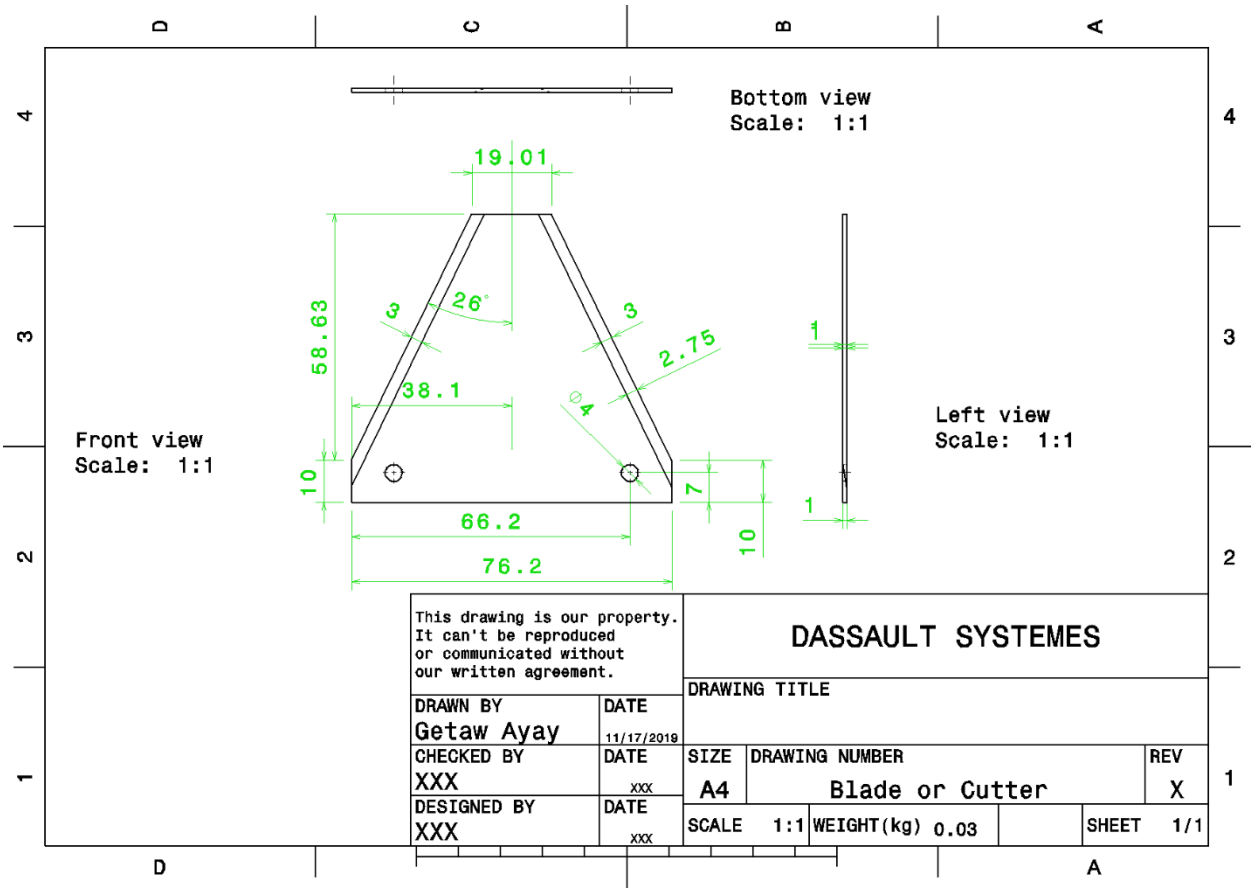

Part Drawing 4-7 Blade or Cutter

Cutter bar: It is used to transfer power from follower bar to cutter and to hold the cutters fixedly on itself. A total compressive force of 290.97 N is expected to apply on it and total length of 609.6 mm in 76.2 mm fixed supports. The cross section is solid rectangular in order to have rigid and straight reciprocation of the blades. It is made of high carbon steel of Fe870 Indian standard

designation and 870 N/mm^2 tensile strength, 520 N/mm^2 yield stress (σ_y) and 210 GPa modulus of elasticity. Since the system is used in the outdoor, its safety factor (n) is four. Hence, the allowable stress becomes:

$$\sigma_{all} = \sigma_w = \frac{\sigma_y}{n} = \frac{520}{4}\frac{N}{mm^2} = 130\ MPa$$

The applied compressive stress is equated with the allowable stress as follows.

$$\sigma_{all} = \frac{F_{ca}}{A} = -\!\!\rightarrow A = (b-D)h = \frac{F}{\sigma_{all}} = \frac{290.97}{130} = 2.238\ mm^2 \text{ ---------- } 4\text{-}77$$

Where F_{ca} is compressive force, A is cross sectional area of solid rectangular cutter bar

The area A becomes very small and D is diameter of hole of the cutter bar for bolt joint (4 mm). The dimensions (thickness h and width b) are better to determine by considering buckling of the bar.

The cross-sectional area can be determined by using buckling of the bar. The cutter bar can be considered as one fixed end and one free end column.

$$P_c = \frac{\pi^2 EI}{4L^2} -\!\!\rightarrow I = \frac{(b-D)h^3}{12} = \frac{4F_{ca\times}L^2}{\pi^2 E} \text{ ----------} 4\text{-}78$$

Note: Buckling occurs about the minimum second moment of area (I_{min}). The width b should be greater than the thickness h. It can be appropriate to choose 10 mm width which is equal to h_2 of blade. Correspondingly, the thickness h, critical load and compressive stress becomes 5 mm, 5592.033 N for 290.97 N and 87.376 N for 36.365 N, and 9.699 MPa which is an indication for safe design.

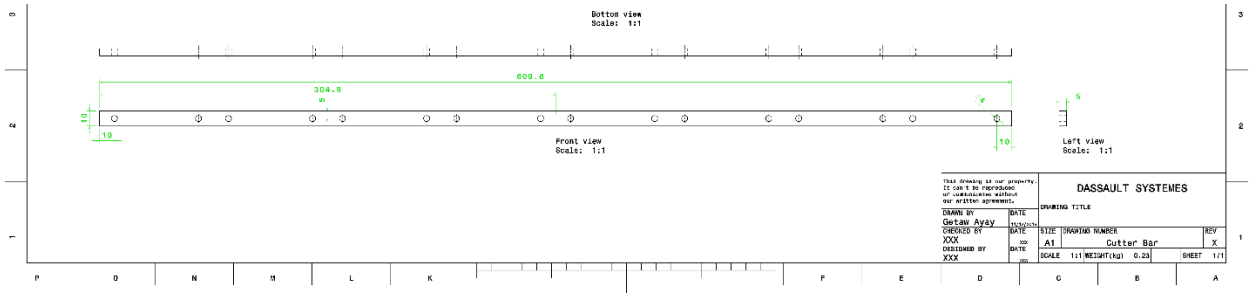

Part Drawing 4-8 Cutter Bar

Finger or Guard Lip: This is one of the important elements which is used to shear the stalk during cutting of the grains. A maximum of 290.97 N force will be applied on a single finger. It has rectangular section. The shape of the guard lip is shown in **Figure** 4-29.

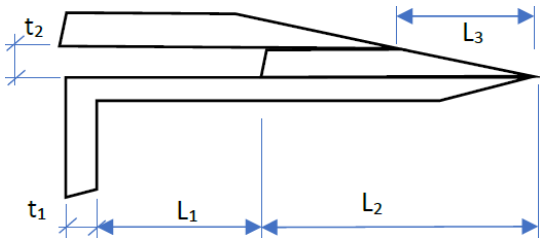

Figure 4-29 Guard Lip or Finger

Discussion on geometry of Guard Lip or Finger: The thickness t_2 is greater than the thickness of the cutter or blade (b=1mm). According to D.N. Sharma and S. Mukesh (2010), 0.5 mm clearance is required between the guard lip and cutter i.e., the thickness t_2 becomes 2 mm. The length L_1 is equal to the height h_1=58.625 mm of the blade or cutter.

Materials for Guard Lip or Finger: It is made of high carbon steel of Fe870 Indian standard designation and 870 N/mm^2 tensile strength and 520 N/mm^2 yield stress (σ_y). Since the system is used in the outdoor, its safety factor (n) is four. Hence, the allowable stress becomes:

$$\sigma_{all} = \sigma_w = \frac{\sigma_y}{n} = \frac{520}{4}\frac{N}{mm^2} = 130\ MPa$$

Bending stress is induced on it. Hence, it can be related with allowable stress;

$$\sigma_{all} = \sigma_b = \frac{My}{I} = \frac{M}{Z} = \frac{FL}{Z} \longrightarrow Z = \frac{t_1 h^2}{6} = \frac{FL}{\sigma_{all}} = \frac{290.97 \times 62}{130}$$

Where F is transverse force, Z is section modulus of rectangular guard lip, L_1 (58.625 mm) is length of guard lip on cutter part, t_1 is base (shorter side) and h is height (longer side) of the rectangular cross section. The three parts of the guard lip or finger is joined together by welding. Hence, the thickness t_1 is recommended to 4 mm.

$$h = \sqrt{\frac{6FL_1}{\sigma_{all} t_1}} = \sqrt{\frac{6 \times 290.97 \times 57.625}{130 \times 5}} = 12.441\ mm$$

The longer side h should be increased to a standard available plate width of 15 mm and thickness 4 mm [54].

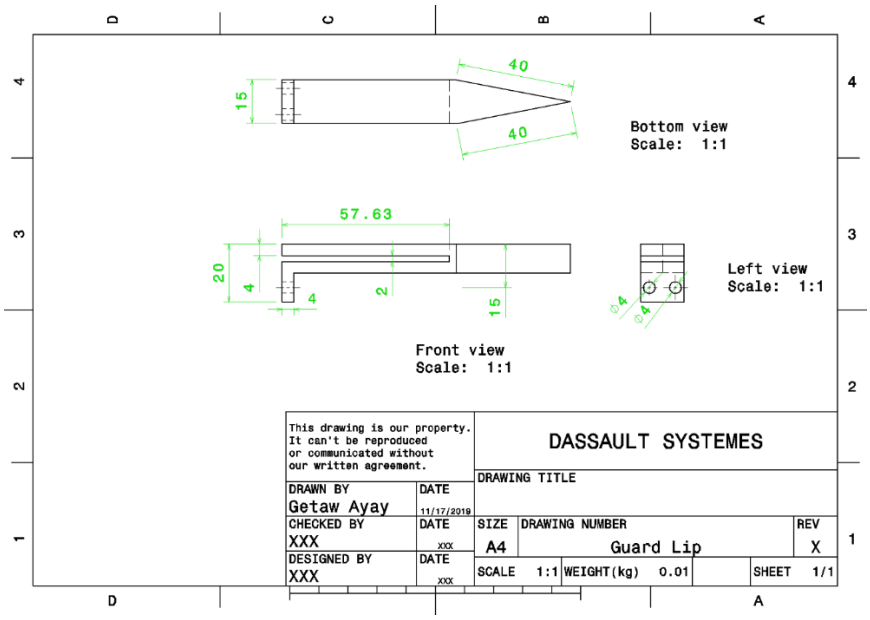

Part Drawing 4-9 Guard Lip

Bolt and Nut for Guard Lip: It is used to fix the guard lip with the guard lip bar. There are at least two bolts to fix a single guard lip which share equally 290.97 N force. The bolts are the American National Standard Thread (ANST) through hexagonal bolts i.e., shank at one end and hexagonal head at the other end. The various proportions are shown in **Figure** 4-26. A maximum of 290.97 N shearing force can be applied on the two bolts i.e., 145.485 N shearing force in each bolt. The bolts are under single shearing action.

Materials for Bolt: It is made of Fe E 400 Indian standard, 540 MPa tensile strength and 400 MPa yield strength. It is recommended to use a factor of safety of four. The normal and shearing working stress becomes;

$$\sigma_{all} = \frac{\sigma_y}{n} = \frac{400\ MPa}{4} = 100\ MPa$$

$$\tau_{all} = \frac{\sigma_{all}}{2} = \frac{100\ MPa}{2} = 50\ MPa$$

The shearing stress on a single bolt is the ratio of half of cutting force (F_{ca}) and area (A_c) of core diameter of the bolt.

$$\tau_{all} = \frac{F_{ca}}{A_c} = -\!\!\rightarrow d_c = \sqrt{\frac{4F_{ca}}{\pi\tau_{all}}} = \sqrt{\frac{4 \times 145.485}{\pi \times 50}} = 1.925\ mm$$

The next available core diameter (d_c) and major diameter is 1.948 mm and 2.5 mm respectively (R.S. KHURMI and J.K. GUPTA, 2005). However, it will be difficult to drill 2.5 mm in our shop.

Hence, it is optimized to use 3.141 mm core diameter (d_c. Correspondingly, 0.7 mm pitch, 4 mm major diameter, 3.545 mm pitch diameter, 0.429 mm depth of thread, 8.78 mm2 stress area and M4 designation. In the same way, the core diameter of nut is 3.242 mm.

Note: The core diameter of the nut is already known (3.242 mm). It is made of same material as the bolt. Since the cutter bar is under dynamic condition, there should be two equal nuts in order to lock the possibility of the losing of the nut. According to (R.S. KHURMI and J.K. GUPTA (2005), the thickness (H) of the nut is proportional with the pitch diameter of the bolt (3.545 mm) see **Figure** 4-27.

The thickness becomes;

$$H = 0.75d = 0.75 \times 3.545 = 2.659\ mm$$

Guard Lip Bar: It is used to hold the guard lip or fingers and rollers for cutter bar support in a fixed position by bolts and nuts. A 209.97 N compressive force is applied from the cutter or blade. The cross section is rectangular. It is made of high carbon steel of Fe870 Indian standard designation and 870 N/mm^2 tensile strength and 520 N/mm^2 yield stress (σ_y). Since the system is used in the outdoor, its safety factor (n) is four. Hence, the allowable stress becomes:

$$\sigma_{all} = \sigma_w = \frac{\sigma_y}{n} = \frac{520}{4}\frac{N}{mm^2} = 130MPa$$

The applied compressive stress is equated with the allowable stress as follows.

$$\sigma_{all} = \frac{F}{A} = -\!\!\rightarrow A = bh = \frac{F}{\sigma_{all}} = \frac{290.97}{130} = 2.238\ mm^2$$

Where F is compressive force, A is cross sectional area of hollow rectangular guard lip bar

The area A becomes very small. The dimensions (thickness b and height h) are better to determine by considering buckling of the bar. The guard lip bar is fixed at both ends. The maximum allowable deflection of columns is L/360, where L is length of the guard lip bar. The length of the guard lip bar should be 609.6 mm.

The cross section can be determined by using buckling of the bar.

$$F_c = \frac{4\pi^2 EI}{L^2} -\!\!\rightarrow I = \frac{bh^3}{12} = \frac{F_{c\times L^2}}{4\pi^2 E} = \frac{290.97 \times 609.6^2}{4\pi^2 \times 210000} mm^4 = 13.042\ mm^4$$

The sides b and h can be determine by using the above two equations and their values becomes 0.268 mm and 8.362 mm respectively. These values are not available on standard. Hence, it is advisable to increase the dimension. From standard, solid rectangular cross section of 10X3 mm is selected [50]. Its weight is 0.24 Kg/m.

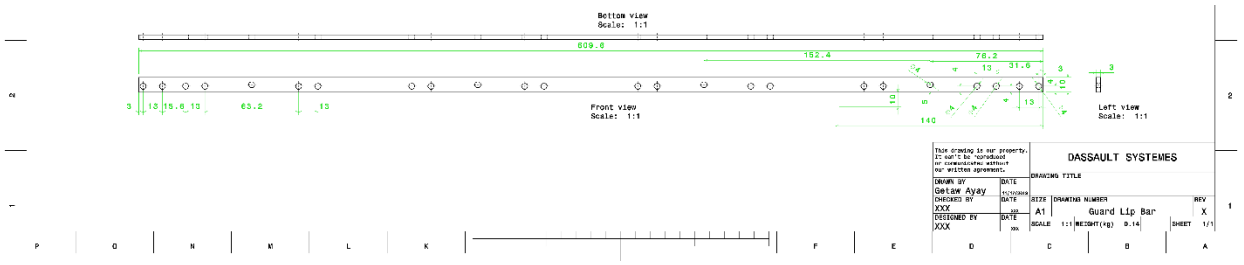

Part Drawing 4-10 Guard Lip Bar

Selection of Bearings for Cutter bar Supports: It is used to support and reduce the frictional loses between cutter bar and guard lip. The width of the guard lip bar is 10 mm. It is advisable to use single row deep groove ball bearing. The bore of bearing is 4 mm.

According to bearing catalogue [51], the specification of the single row deep groove 4 mm bore balling bearing is 16 mm outside diameter, 5 mm thickness, 1.11 KN dynamic basic load ratings, 0.38 KN static basic load ratings, 0.016 KN fatigue load limit, 95 000 rpm reference speed ratings, 60 000 rpm limiting speed ratings, 0.0054 Kg mass and 634 designation.

Bolt and Nut for Bearings on Guard Lip Bar: It is used to fix the rollers on the guard lip bar. The bolts hold the weight of cutter bar assembly which is equal to the sum of one cutter bar (0.23 Kg), eight cutters or blades (0.03 Kg each), sixteen bolts (0.007 Kg each) and nuts (0.004 Kg each) i.e., 0.646 Kg total mass. This weight is shared by four bolts i.e., 0.16 Kg each. The bolts are the American National Standard Thread (ANST) through hexagonal bolts i.e., shank at one end and hexagonal head at the other end. The various proportions are shown in **Figure** 4-26.

A maximum of 1.57 N shearing force can be applied on the bolt. The bolts are under single shearing action.

Materials for Bolt: It is made of Fe E 400 Indian standard, 540 MPa tensile strength and 400 MPa yield strength. It is recommended to use a factor of safety of four. The normal and shearing working stress becomes;

$$\sigma_{all} = \frac{\sigma_y}{n} = \frac{400\ MPa}{4} = 100\ MPa$$

$$\tau_{all} = \frac{\sigma_{all}}{2} = \frac{100\ MPa}{2} = 50\ MPa$$

The shearing stress on a single bolt is the ratio of weight) and area (A_c) of core diameter of the bolt.

$$\tau_{all} = \frac{W}{A_c} = -\!\!\rightarrow d_c = \sqrt{\frac{4W}{\pi\tau_{all}}} = \sqrt{\frac{4 \times 1.57}{\pi \times 50}} = 0.2\ mm\ mm$$

The next available core diameter (d_c) and major diameter is 1.948 mm and 2.5 mm respectively (R.S. KHURMI and J.K. GUPTA, 2005). However, the bore of the bearing for the bolt is 4 mm. Hence, the core diameter of the bolt becomes 3.141 mm core diameter (d_c). Correspondingly, 0.7 mm pitch, 4 mm major diameter, 3.545 mm pitch diameter, 0.429 mm depth of thread, 8.78 mm2 stress area and M4 designation. In the same way, the core diameter of nut is 3.242 mm.

Note: The core diameter of the nut is already known (3.242 mm). It is made of same material as the bolt. Since the cutter bar is under dynamic condition, there should be two equal nuts in order to lock the possibility of the losing of the nut. According to (R.S. KHURMI and J.K. GUPTA (2005), the thickness (H) of the nut is proportional with the pitch diameter of the bolt (3.545 mm) see **Figure** 4-27.

The thickness becomes;

$$H = 0.75d = 0.75 \times 3.545 = 2.659\ mm$$

Follower Bar: The follower bar is a part of the follower attached to the rectangular part which transfers power to the cutter bar. A 209.97 N compressive force is applied from the follower head. The cross section is hollow square in order to have light weight and rigid bar. It is made of high carbon steel of Fe870 Indian standard designation and 870 N/mm^2 tensile strength and 520 N/mm^2 yield stress (σ_y). Since the system is used in the outdoor, its safety factor (n) is four. Hence, the allowable stress becomes:

$$\sigma_{all} = \sigma_w = \frac{\sigma_y}{n} = \frac{520}{4}\frac{N}{mm^2} = 130MPa$$

The applied compressive stress is equated with the allowable stress as follows.

$$\sigma_{all} = \frac{F}{A} = -\!\!\rightarrow A = {S_o}^2 - {S_i}^2 = \frac{F}{\sigma_{all}} = \frac{290.97}{130} = 2.238\ mm^2$$

Where F is compressive force, A is cross sectional area of hollow rectangular follower bar

The area A becomes very small. The dimensions (thickness and width) are better to determine by considering buckling of the bar. The follower bar is fixed at both ends. The maximum allowable deflection of columns is L/360, where L is length of the follower bar. The minimum length of the follower bar should be 136.2 mm by considering stroke length (76.2 mm), clearances on both sides (5+5=10 mm), roller holder (40 mm) and space for joining the follower bar with cutter bar (10

mm).

The length can be determined by using buckling of the bar.

$$F_c = \frac{4\pi^2 EI}{L^2} \longrightarrow I = \frac{{S_o}^4 - {S_i}^4}{12} = \frac{F_{c\times L^2}}{4\pi^2 E} = \frac{290.97 \times 136.2^2}{4\pi^2 \times 210000} mm^4 = 0.651\ mm^4$$

The sides S_o and S_i can be determine by using the above two equations and their values becomes 2.646 mm and 2.182 mm respectively. These values are not available on standard and also their dimensions are very difficult for weld joint. Hence, it is advisable to increase the dimension. From standard, the next cross-sectional area is solid square cross section with a minimum of (S_o) 8X8 mm is selected [50]. Its weight is 0.5 Kg/m.

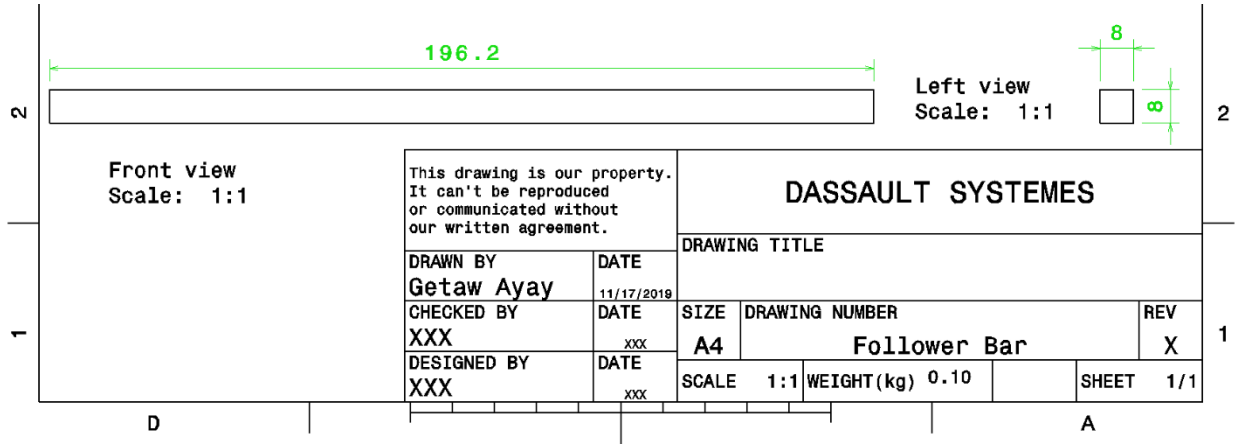

Part Drawing 4-11 Follower Bar

Support for Follower Bar: The follower bar is supported by rollers. The purpose of rollers is to reduce frictional losses. The follower is supported by the rollers at eight points i.e., there are eight rollers and eight pins in a single square box. The rollers are supported by pins which are fixed on the square box shown in **Figure** 4-30. The roller support prevents misaligning of the follower from neutral position to left, right, top or bottom direction.

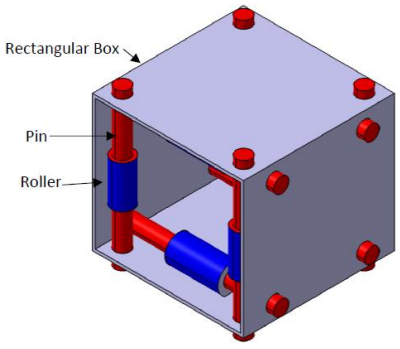

Figure 4-30 Support for Follower Bar

The dimension of the rollers, pins and rectangular box depends on the size of the follower bar (8X8 mm). The rollers are single row deep groove 4 mm bore balling bearing.

Rollers for Follower Bar: According to bearing catalogue [51], the specification of the single row deep groove 4 mm bore balling bearing is 9 mm outside diameter, 2.5 mm thickness, 0.54 KN dynamic basic load ratings, 0.18 KN static basic load ratings, 0.0007 KN fatigue load limit, 140 rpm reference speed ratings, 85 000 rpm limiting speed ratings, 0.0039 Kg mass and 618/4 designation.

Rectangular Box for Follower Bar: The dimension of the square box can be estimated by using dimension of follower bar and roller outside dimeter. The internal side of the square box (S_i) becomes the sum of the side of follower bar and dimeter of roller i.e., $S_i = 9 + 8 + 9 = 26\ mm$. The external side of the square box becomes 30 mm [52]**.** Its weight and thickness are 1.74 Kg/m and 2 mm respectively.

The diameter of the pin (d=4 mm) is equal to the bore of the single row deep groove 4 mm bore ball bearing. The head of the pin is equal to 0.5d=2 mm and its tail is equal to 0.75d=3 mm (R.S. KHURMI and J.K. GUPTA, 2005). The total length of the pin becomes 2+30+3=35 mm.

Pin for Follower Support: It is used to keep straight reciprocation of the follower bar. It has fixed supports i.e., fixed beam. Its length and diameter are 35 mm and 4 mm respectively. It is subjected to f_6=0.32 N force in the y-axis and f_3=8.438 N force in x-axis over a length of 2.5 mm. The cross section of the pin is solid circular.

The forces and bending moments on the pin can be determined from the free body diagram shown in **Figure** 4-31. Since the two forces (f_6 and f_3) are applied at the mid span of the pin and the support of pin is same at its ends, the reaction forces and moments should be equal in the respected axes. This implies that R_{Ax}= R_{Bx}, R_{Ay}= R_{By}, M_{Ax}= M_{Bx} and M_{Ay}= M_{By}.

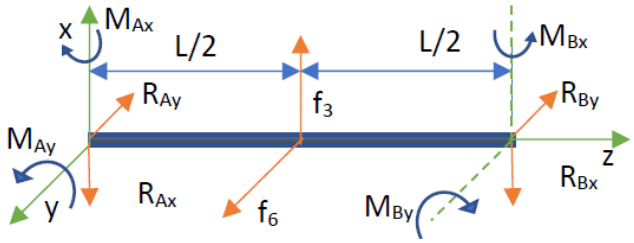

Figure 4-31 FBD of Pin

$$\sum F_x = 0$$

$$f_3 - R_{Ax} - R_{Bx} = 0 = f_3 - 2R_{Ax} \rightarrow R_{Ax} = R_{Bx} = \frac{f_3}{2} = 4.219\ N$$

$$\sum F_y = 0$$

$$f_6 - R_{Ay} - R_{By} = 0 = f_6 - 2R_{Ay} \rightarrow R_{Ay} = R_{By} = \frac{f_6}{2} = 0.16\ N$$

$$\sum M_x = 0$$

$$-M_{Ax} - \frac{L}{2}f_6 + M_{Bx} + LR_{By} = 0 \rightarrow -M_{Ax} + M_{Bx} = \frac{L}{2}f_6 - LR_{By} = 13 \times 0.32 - 26 \times 0.16 = 0$$

$$\rightarrow M_{Ax} = M_{Bx}$$

$$\sum M_y = 0$$

$$M_{Ay} + \frac{L}{2}f_3 - M_{By} - LR_{By} = 0 \rightarrow M_{Ay} - M_{By} = -\frac{L}{2}f_3 + LR_{Bx} = 13 \times 8.438 - 26 \times 4.219$$

$$\rightarrow M_{Ay} = M_{By}$$

Note: The pin is statically indeterminate because there are four unknowns and two equations. Therefore, the unknowns can be determined by considering deflection (both transverse and slope) either at point A or B using elastic curve equations.

$$\frac{d^2x}{dy^2} = \frac{M_y}{EI}$$

The deflection equation in x-axis can be derived from the free body diagram shown in **Figure** 4-32

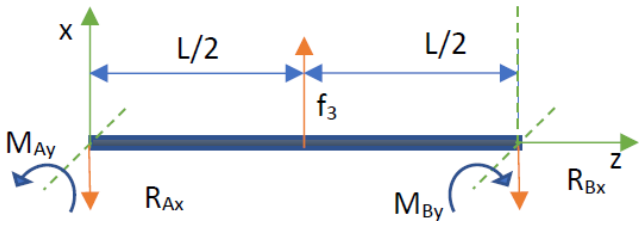

Figure 4-32 FBD of Pin in the x-axis

The bending moment equation on the range of $[0, L/2]$ can be derived from **Figure** 4-33.

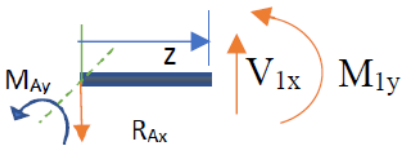

Figure 4-33 FBD of $[0, L/2]$

$$\sum M_z = 0$$

$$M_{Ay} + zR_{Ax} + M_{1y} = 0 \rightarrow M_{1y} = -M_{Ay} - zR_{Ax} = -4.219z - M_{Ay}$$

$$\frac{d^2x}{dy^2} = \frac{M_y}{EI} = \frac{-4.219z - M_{Ay}}{EI}$$

The 1st and 2nd integrals becomes as follows.

$$\frac{dx}{dy} = \theta_1 = \frac{-2.1095z^2 - M_{Ay}\mathrm{z} + C_1}{EI}$$

$$x_1 = \frac{-0.703z^3 - 0.5M_{Ay}z^2 + C_1z + C_2}{EI}$$

The slope and transverse deflection at point A are zero. Hence at z=0 $x = \theta = 0$. This implies that $C_1 = 0$ and $C_2 = 0$

The deflection equations simplified as follows.

$$\theta_1 = \frac{-2.1095z^2 - M_{Ay}\mathrm{z}}{EI}$$

$$x_1 = \frac{-0.703z^3 - 0.5M_{Ay}z^2}{EI}$$

The bending moment equation on the range of $[L/2, \mathrm{L}]$ can be derived from **Figure** 4-34.

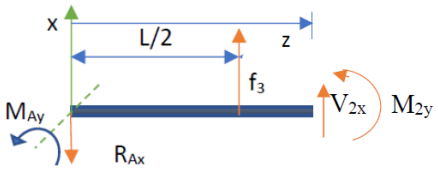

Figure 4-34 FBD of $[L/2, L]$

$$\sum M_z = 0$$

$$M_{Ay} + zR_{Ax} - \left(z - \frac{L}{2}\right)f_3 + M_{2y} = 0 \rightarrow M_{2y} = -M_{Ay} - zR_{Ax} + \left(z - \frac{L}{2}\right)f_3$$

$$= 4.219z - 109.694 - M_{Ay}$$

$$\frac{d^2x}{dy^2} = \frac{M_y}{EI} = \frac{4.219z - 109.694 - M_{Ay}}{EI}$$

The 1st and 2nd integrals becomes as follows.

$$\frac{dx}{dy} = \theta_2 = \frac{2.1095z^2 - 109.694z - M_{Ay}\mathrm{z} + C_3}{EI}$$

$$x_2 = \frac{0.703z^3 - 54.847z^2 - 0.5M_{Ay}z^2 + C_3z + C_4}{EI}$$

The slope and transverse deflection at point A are zero. Hence at z=L, $x = \theta = 0$. This implies that $C_3 = 1426.022 + 26M_{Ay}$ and $C_4 = -12355.928 - 338M_{Ay}$

The deflection equations can be simplified by substituting C_3 and C_4 values.

$$\theta_2 = \frac{2.1095z^2 - 109.694z - M_{Ay}z + 26M_{Ay} + 1426.022}{EI}$$

$$x_2 = \frac{0.703z^3 - 54.847z^2 - 0.5M_{Ay}z^2 + 26M_{Ay}z - 338M_{Ay} - 10929.906}{EI}$$

The reaction bending moment M_{Ay} can be determined by equating θ_1 and θ_2 at the midpoint (L/2).

$$\frac{-2.1095\left(\frac{L}{2}\right)^2 - M_{Ay}\frac{L}{2}}{EI} = \frac{2.1095(L/2)^2 - \frac{109.694L}{2} - \frac{M_{Ay}L}{2} + 26M_{Ay} + 1426.022}{EI}$$

$$-2.1095 \times 13^2 - 13M_{Ay} = 2.1095 \times 13^2 - 109.694 \times 13 - 13M_{Ay} + 26M_{Ay} + 1426.022$$

$$-26M_{Ay} = 4.219 \times 13^2 = 713.011 \rightarrow M_{Ay} = -27.424\ Nmm = M_{By}$$

The bending moment equations can be simplified as follows.

$$M_{1y} = -4.219z - M_{Ay} = -0.16z + 27.424$$

$$M_{2x} = 0.16z - 4.16 - M_{Ax} = 0.16z + 23.264$$

The bending moment equations are linear both in the range of [0, L/2] and [L/2, L] which are [27.424, 25.344] and [25.344, 27.424] respectively.

The deflection equation in y-axis can derived from the free body diagram shown in **Figure** 4-35.

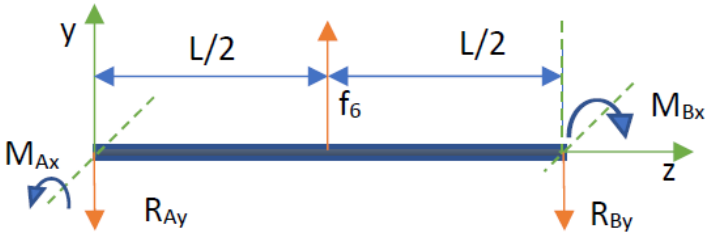

Figure 4-35 FBD of Pin in the y-axis

The bending moment equation on the range of [0, $L/2$] can be derived from Figure 4-36

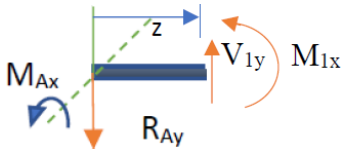

Figure 4-36 FBD of [0, L/2]

$$\sum M_z = 0$$

$$-M_{Ax} - zR_{Ay} - M_{1x} = 0 \rightarrow M_{1x} = -M_{Ax} - zR_{Ay} = -0.16z - M_{Ax}$$

$$\frac{d^2x}{dy^2} = \frac{M_y}{EI} = \frac{-0.16z - M_{Ax}}{EI}$$

The 1st and 2nd integrals becomes as follows.

$$\frac{dx}{dy} = \theta_1 = \frac{-0.08z^2 - M_{Ax}\mathrm{z} + C_1}{EI}$$

$$x_1 = \frac{-0.027z^3 - 0.5M_{Ax}z^2 + C_1z + C_2}{EI}$$

The slope and transverse deflection at point A are zero. Hence at z=0 $x = \theta = 0$. This implies that $C_1 = 0$ and $C_2 = 0$

The deflection equations simplified as follows.

$$\theta_1 = \frac{-0.08z^2 - M_{Ax}\mathrm{z}}{EI}$$

$$x_1 = \frac{-0.027z^3 - 0.5M_{Ax}z^2}{EI}$$

The bending moment equation on the range of $[L/2, \mathrm{L}]$ can be derived from **Figure** 4-37.

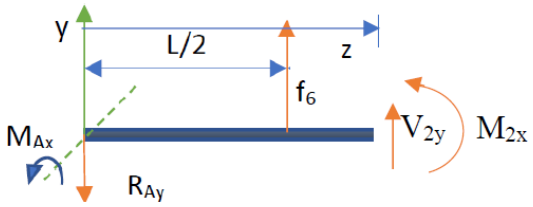

Figure 4-37 FBD of $[L/2, \mathrm{L}]$

$$\sum M_z = 0$$

$$-M_{Ax} - zR_{Ay} + \left(z - \frac{L}{2}\right)f_6 - M_{2x} = 0 \rightarrow M_{2x} = -M_{Ax} - zR_{Ay} + \left(z - \frac{L}{2}\right)f_6$$

$$= 0.16z - 4.16 - M_{Ax}$$

$$\frac{d^2x}{dy^2} = \frac{M_y}{EI} = \frac{0.16z - 4.16 - M_{Ax}}{EI}$$

The 1st and 2nd integrals becomes as follows.

$$\frac{dx}{dy} = \theta_2 = \frac{0.08z^2 - 4.16z - M_{Ax}\mathrm{z} + C_3}{EI}$$

$$x_2 = \frac{0.027z^3 - 2.080z^2 - 0.5M_{Ax}z^2 + C_3z + C_4}{EI}$$

The slope and transverse deflection at point A are zero. Hence at z=L, $x = \theta = 0$. This implies that $C_3 = 54.08 + 26M_{Ax}$ and $C_4 = -474.552 - 338M_{Ax}$

The deflection equations can be simplified by substituting C_3 and C_4 values.

$$\theta_2 = \frac{0.08z^2 - 4.16z - M_{Ax}\mathrm{z} + 26M_{Ax} + 54.08}{EI}$$

$$x_2 = \frac{0.027z^3 - 2.080z^2 - 0.5M_{Ax}z^2 + 26M_{Ax}z + 54.08z - 338M_{Ax} - 474.552}{EI}$$

The reaction of bending moment M_{Ax} can be determined by equating θ_1 and θ_2 at the midpoint (L/2).

$$\frac{-0.08z^2 - M_{Ax}\mathrm{z}}{EI} = \frac{0.08z^2 - 4.16z - M_{Ax}\mathrm{z} + 26M_{Ax} + 54.08}{EI}$$

$$0.16z^2 - 4.16z + 26M_{Ax} + 54.08 = 0 \rightarrow 26M_{Ax} = -54.08 \rightarrow M_{Ax} = -2.08\ Nmm = M_{Bx}$$

The bending moment equations can be simplified as follows.

$$M_{1x} = -0.16z - M_{Ax} = -0.16z + 2.08$$

$$M_{2x} = 0.16z - 4.16 - M_{Ax} = 0.16z - 2.08$$

The bending moment equations are linear both in the range of [0, L/2] and [L/2, L] which are [2.08, 0] and [0, 2.08] respectively.

Materials for Pin: It is made of high carbon steel of Fe870 Indian standard designation and 870 N/mm^2 tensile strength, 210 GPa and 520 N/mm^2 yield stress (σ_y). Since the system is used in the outdoor, its safety factor (n) is four. Hence, the allowable stress becomes:

$$\sigma_{all} = \sigma_w = \frac{\sigma_y}{n} = \frac{520}{4}\frac{N}{mm^2} = 130\ MPa$$

The bending stress can be analyzed by using equation 4.55 of (Beer and et al, 2012).

$$\sigma_z = -\frac{M_y x}{I_y} + \frac{M_x y}{I_x} = -\frac{-27.424x}{I_y} + \frac{M_x y}{I_x}$$

The distances x and y, second moment of area I_y and I_x are equal to $d/2$ and $\pi d^4/64$ respectively.

$$\sigma_z = -\frac{M_y x}{I_y} + \frac{M_x y}{I_x} = -\frac{-27.424 \times 32}{\pi 4^3} + \frac{2.08 \times 32}{\pi 4^3} = 4.696\ MPa$$

Since the induced stress ($4.696\ MPa$) is less than the yield stress ($130\ MPa$), it is safe design.

Rectangular Box for Follower Support: It is square box which is used to hold the pins for follower support see **Figure** 4-30. It has 30X30 mm cross section, 100 mm length and 2 mm wall

thickness. It is subjected to a bearing load of 8.438 N. It is made of high carbon steel of Fe870 Indian standard designation and 870 N/mm^2 tensile strength, 210 GPa and 520 N/mm^2 yield stress (σ_y). Since the system is used in the outdoor, its safety factor (n) is four. Hence, the allowable stress becomes:

$$\sigma_{all} = \sigma_w = \frac{\sigma_y}{n} = \frac{520}{4}\frac{N}{mm^2} = 130\ MPa$$

The bearing stress can be determined by

$$\sigma_b = \sigma_w = \frac{R}{A_b} = \frac{8.438}{dt} = 130\ MPa \rightarrow t = 0.016\ mm$$

The square box is safe because its real thickness (2 mm) is greater than the designed value (0.016 mm).

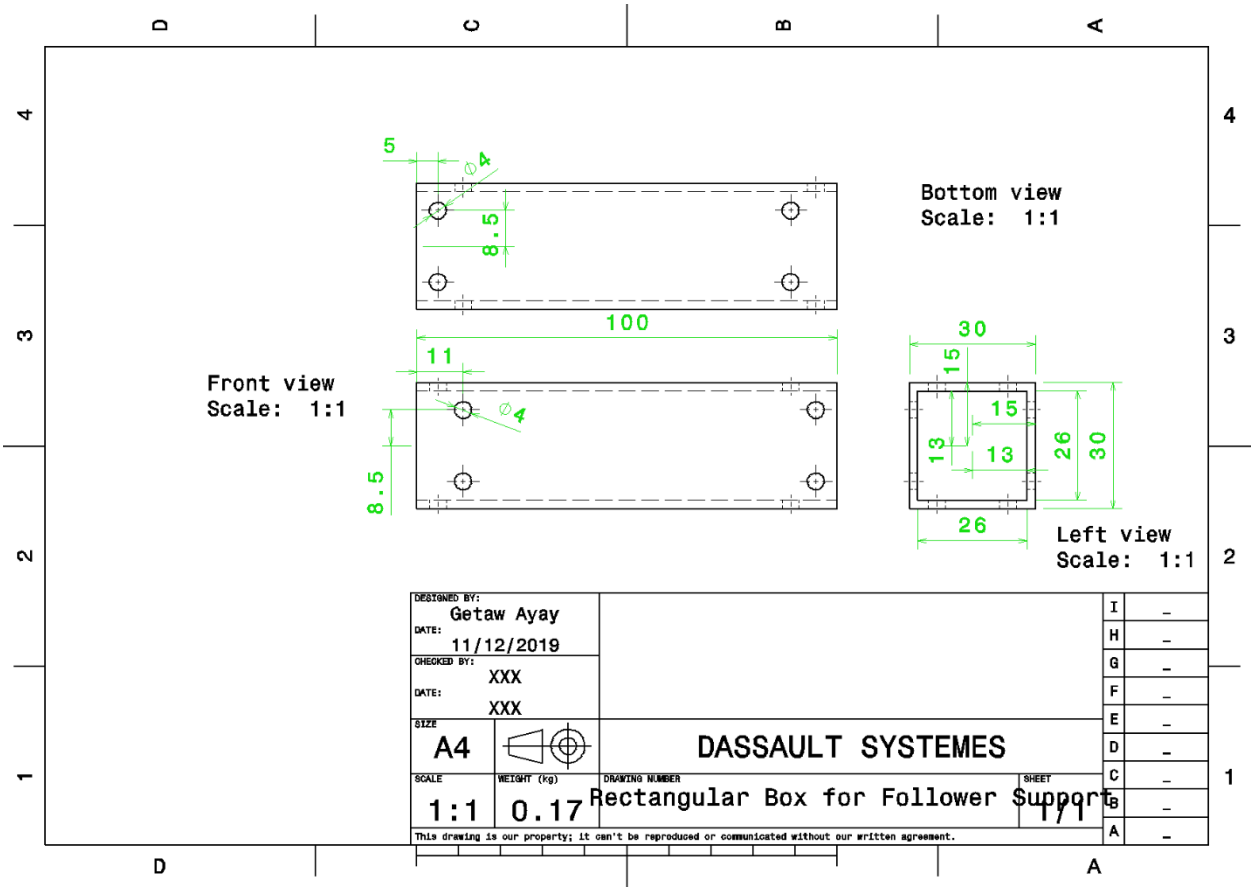

Part Drawing 4-12 Rectangular Box for Follower Support

Follower Head: It is used to transfer power from eccentric cam into follower bar. Its one side is welded on the follower bar and the other on the cutter bar. Its length (38.1+88.7+5.2= 132 mm) depends on the distance (88.7 mm) from center of rotation up to nose of eccentric cam plus

clearance (5.2 mm) between nose of eccentric cam and cutter bar and length of follower head on the opposite of cutter bar (38.1 mm). A maximum of 209.97 N force is applied on it. It is subjected to bending stress. The maximum bending occurs at the joint between follower head and cutter bar i.e., cantilever beam.

$$M_{max} = Fca \times L = 290.97N \times 132\ mm = 38408.04\ Nmm = 38.408\ Nm$$

The shape of the follower head is rectangular cross section. It is made of high carbon steel of Fe870 Indian standard designation and 870 N/mm^2 tensile strength and 520 N/mm^2 yield stress (σ_y). Since the system is used in the outdoor, its safety factor (n) is four. Hence, the allowable stress becomes:

$$\sigma_{all} = \sigma_w = \frac{\sigma_y}{n} = \frac{520}{4}\frac{N}{mm^2} = 130\ MPa$$

Bending stress is induced on it. Hence, it can be related with allowable stress;

$$\sigma_{all} = \sigma_b = \frac{My}{I} = \frac{M_{max}}{Z} \longrightarrow Z = \frac{bh^2}{6} = \frac{M_{max}}{\sigma_{all}} = \frac{38408.04}{130} = 295.446\ mm^3$$

$$bh^2 = 1772.679\ mm^3$$

Where F is transverse force, Z is section modulus of rectangular follower head, b is base (vertical side) and h is height (horizontal side) of the rectangular cross section. The vertical side is greater than the thickness of cam (5 mm). An iteration shows that the value of h is less or equal to 19 mm. It becomes strong when its height h is longer and base b shorter. It is good to use 16 mm and 8 mm height and base respectively for optimum weight to strength ratio.

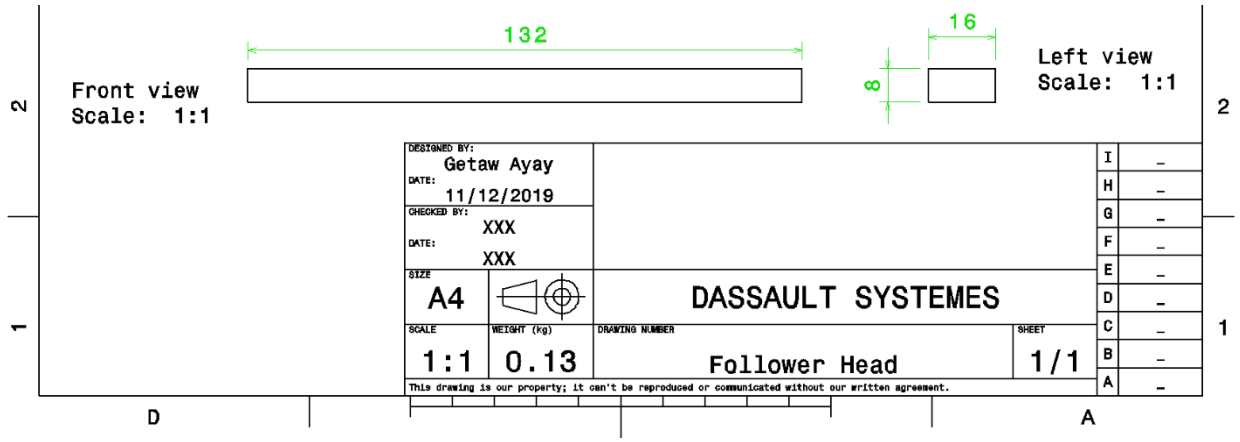

Part Drawing 4-13 Follower Head

Idler Shaft: It is the shaft that holds the driven pulley. The Idler Shaft withstands a torque T_C of 2.095 Nm. The cross section is solid circular. The width of the conveyor pulley is 38 mm.

The force analysis of the Idler Shaft can be done by considering all the machine elements attached on it. The internal diameters of the machine elements are conveyor pulley (d_2), ball bearing (d_3), clearance (d_4) and thrust bearing (d_1) from left to right as shown in

Figure 4-38. The actual position of the shaft is vertical; ball bearing top and thrust bearing bottom end.

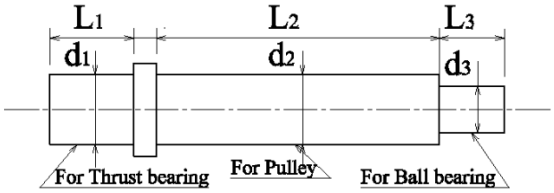

Figure 4-38 2D Sketch of Idler Shaft

Figure 4-39 FBD of Idler Shaft

The conveying force F_C and torque T_C are 28.895 N and 2.095 Nm respectively. The remaining parameters can be analyzed by applying equation of motion.

$$\sum F_z = 0$$

$$R_{Tz} = W_P = m_P g = 4.643 \times 9.81 = 45.548\ N$$

$$\sum F_y = 0$$

$$R_{Ty} + R_{by} - F_C = 0 \longrightarrow R_{Ty} + R_{by} = F_C = 28.895\ N$$

$$\sum M_x = 0$$

$$\left(L_1 + \frac{L_2}{2}\right) F_C - \left(L_1 + L_2 + \frac{L_3}{2}\right) R_{by} = 0$$

Note: In the force analysis of Idler Shaft, there are four unknows (L_1, L_3, R_{Ty} and R_{by}) and two equations which is statically indeterminate. Since the lengths and diameters are unknown, it can't be solved by using the technique of displacement method for statically indeterminate problem. For the time being, the shaft can be designed by considering the applied torque 2.095 Nm.

Materials for Idler Shaft: It is made of high carbon steel of Fe870 Indian standard designation and 870 N/mm^2 tensile strength and 520 N/mm^2 yield stress (σ_y). Since the system is used in the outdoor, its safety factor (n) is four. Hence, the allowable stress becomes:

$$\sigma_{all} = \sigma_w = \frac{\sigma_y}{n} = \frac{520}{4}\frac{N}{mm^2} = 130MPa$$

The allowable shear stress can be determined by using maximum shear stress theory:

$$\tau_{all} = \tau_w = \frac{\sigma_{all}}{2} = \frac{130}{2}\frac{N}{mm^2} = 65\ MPa$$

The shearing stress due to torque T is;

$$\tau = \frac{TC}{J}$$

$$C = \frac{d}{2}\ and\ J = \frac{\pi d^4}{32}$$

$$\tau = \frac{16T}{\pi d^3} = \frac{16 \times 2.095 \times 10^3}{\pi d^3} = 65\ MPa \rightarrow d = 5.475\ mm$$

The diameter of the shaft becomes 6 mm because there is no 5.475 mm bore bearing

Selection of Bearings for Idler Shaft: The bearing on the top end of Idler Shaft is sealed single row deep groove ball bearing. The bore of bearing is 6 mm.

According to bearing catalogue [51], the specification of the sealed single row deep groove 6 mm bore balling bearing is 13 mm outside diameter, 5 mm thickness, 0.88 KN dynamic basic load ratings, 0.35 KN static basic load ratings, 0.015 KN fatigue load limit, 110 000 rpm reference speed ratings, 53 000 rpm limiting speed ratings, 0.0026 Kg mass and 628/6-2Z designation.

The bearing on bottom end of the Idler Shaft is single direction thrust ball bearing. The bore of the bearing is 6 mm. According to bearing [51], the specification of the single direction thrust ball bearing for 6 mm bore thrust balling bearing is 14 mm outside diameter, 5 mm thickness, 2 KN dynamic basic load ratings, 2 KN static basic load ratings, 0.085 KN fatigue load limit, 17 000 rpm reference speed ratings, 24 000 rpm limiting speed ratings, 0.004 Kg mass and BA6 designation.

The lengths L_1, L_4, L_2 and L_3 becomes 5 mm, 5 mm, 38 mm and 5 mm. The length L_4 is a clearance between pulley and thrust bearing which is 5 mm. The reaction forces on both bearings can be determined as follows.

$$29 \times 28.895 - 50.5R_{by} = 0 \rightarrow R_{by} = 16.593N$$

$$R_{Ty} = 28.895 - R_{by} = 28.895 - 16.593 = 12.302\ N$$

Note: The Idler Shaft is subjected to a combined load both shearing and bending. Hence, it should be designed by considering shearing and normal stresses.

The shearing stress due to torque T is;

$$\tau = \frac{TC}{J}$$

$$C = \frac{d}{2}\ and\ J = \frac{\pi d^4}{32}$$

$$\tau = \frac{16T}{\pi d^3} = \frac{16 \times 2.095 \times 10^3}{\pi d^3} = \frac{10669.747}{d^3} =$$

The normal stress in the camshaft can be determined by Beer and et al (2012) equation 4.58 by considering $\sigma_x = \sigma_y = 0$

$$\sigma_z = \frac{W_P}{A} - \frac{M_x y}{I_x} + \frac{M_y x}{I_y} = \frac{W_P}{A} - \frac{M_x y}{I_x} + \frac{0 \times x}{I_y} = \frac{W_P}{A} - \frac{M_x y}{I_x}$$

The above normal stress (σ_z) becomes maximum at y=d/2. The unit of the diameter is millimeter.

$$A = \frac{\pi d^2}{4}, I_x = \frac{\pi d^4}{64} = I_y$$

$$\sigma_z = \frac{4W_p}{\pi d^2} - \frac{32M_x}{\pi d^3}$$

The bending moment M_x can be determined by considering the distributed load w_1, w_2 and w_3 see **Figure** 4-40. The distributed loads are $w_1 = {R_{Ty}}/{L_1} = \frac{16.593}{5} = 3.319\ N/mm$, $w_2 = {F_C}/{L_2} = \frac{28.895}{38} = 0.760\ N/mm$, and $w_3 = {R_{by}}/{L_3} = \frac{12.302}{5} = 2.460\ N/mm$.

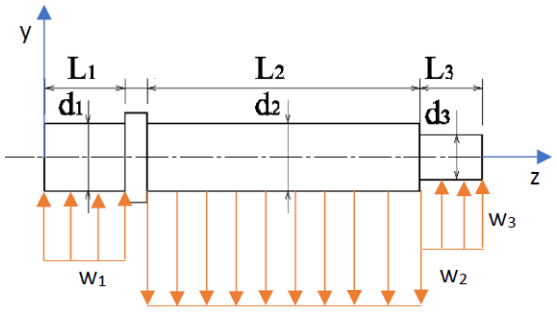

Figure 4-40 FBD of Idler Shaft in the y-axis

The bending moment equation (M_{1x}) on a range of length [0, L_1] can be derived by taking an arbitrary section between this range by using equilibrium equation see **Figure** 4-41.

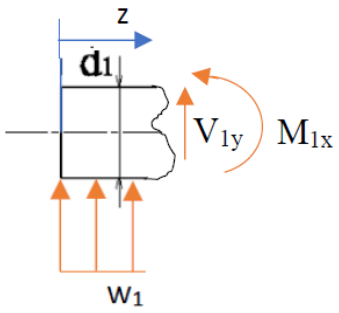

Figure 4-41 FBD between [0, L_1]

$$\sum M_x = 0 = w_1 \frac{z^2}{2} - M_{1x} \longrightarrow M_{1x} = w_1 \frac{z^2}{2} = 1.66z^2$$

The bending moment equation is quadrtic and it becomes maximum at y=L_1=5 mm i.e., M_{1x} [0, 41.500] Nmm.

The bending moment equation (M_{2x}) on a range of length [L_1, $L_1 + L_2$] can be derived by taking an arbitrary section between this range by using equilibrium equation see **Figure** 4-42.

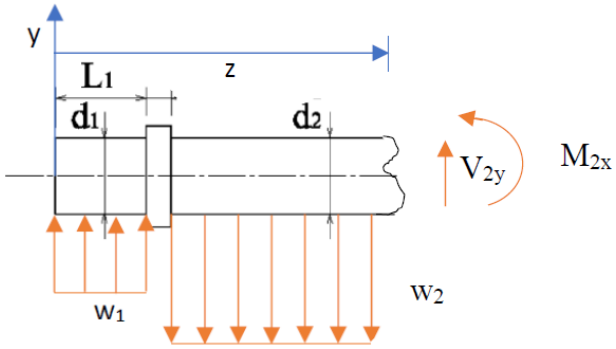

Figure 4-42 FBD between [L_1, $L_1 + L_2$]

$$\sum M_x = 0 = w_1 L_1 (z - \frac{L_1}{2}) - w_2 \frac{(z - L_1)^2}{2} - M_{2x} \longrightarrow M_{2x} = w_1 L_1 (z - \frac{L_1}{2}) - w_2 \frac{(z - L_1)^2}{2}$$

$$= -w_2 \frac{z^2}{2} + (w_2 + w_1) L_1 z - (w_2 + w_1) \frac{{L_1}^2}{2} = -0.38z^2 + 20.395z - 50.988$$

The bending moment equation is quadratic and it becomes maximum at y=L_1+5=10 mm i.e., M_{2x} [114.962, 52.452] Nmm.

The bending moment equation (M_{3x}) on a range of length [$L_1 + L_2$, $L_1 + L_2 + L_3$] can be derived by taking an arbitrary section between this range by using equilibrium equation **Figure** 4-43.

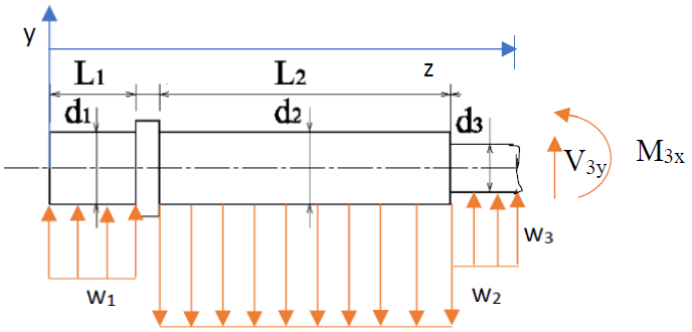

Figure 4-43 FBD between $[L_1 + L_2, L_1 + L_2 + L_3]$

$$\sum \mathrm{M_x} = 0 = \mathrm{w_1 L_1}\left(\mathrm{z} - \frac{\mathrm{L_1}}{2}\right) - \mathrm{w_2 L_2}\left(\mathrm{z} - L_1 - \frac{\mathrm{L_2}}{2}\right) + \mathrm{w_3}\frac{(\mathrm{z} - L_1 - \mathrm{L_2})^2}{2} - \mathrm{M_{3x}}$$

$$\rightarrow \mathrm{M_{3x}} = \mathrm{w_1 L_1}\left(\mathrm{z} - \frac{\mathrm{L_1}}{2}\right) - \mathrm{w_2 L_2}\left(\mathrm{z} - L_1 - \frac{\mathrm{L_2}}{2}\right) + \mathrm{w_3}\frac{(\mathrm{z} - L_1 - \mathrm{L_2})^2}{2} =$$

$$= \mathrm{w_3}\frac{z^2}{2} + \left(\mathrm{w_1 L_1} - \mathrm{w_2 L_2} - \mathrm{w_3}(L_1 + \mathrm{L_2})\right)z - \mathrm{w_1}\frac{{\mathrm{L_1}}^2}{2} + \mathrm{w_2 L_2}\left(L_1 + \frac{\mathrm{L_2}}{2}\right)$$

$$+ \mathrm{w_3}\frac{(L_1 + \mathrm{L_2})^2}{2} = 1.230z^2 - 130.382z + 3713.358$$

The bending moment equation is quadratic and it becomes maximum at y=$\mathrm{L_1}$+$\mathrm{L_2}$+L_3 = 48 mm i.e., $\mathrm{M_{3x}}$ [288.942, 258.182] Nmm.

The maximum shearing stress (τ_{max}) can be analyze by using Beer and et al (2012) equation 7.16.

$$\tau_{max} = \tau_{all} = \sqrt{\left(\frac{\sigma_z}{2}\right)^2 + {\tau_{xz}}^2}$$

The principal stress ($\sigma_{1,2}$) can be determined using Beer and et al (2012) equation 7.13.

$$\sigma_{1,2} = \sigma_{all} = \frac{\sigma_z}{2} \pm \sqrt{\left(\frac{\sigma_z}{2}\right)^2 + {\tau_{xz}}^2}$$

The diameter of the Idler Shaft can be analyzed by using τ_{xz} and σ_z in each section. The torque in the range of [0, $\mathrm{L_{11}}$] is zero i.e., $\tau_{xy} = 0$ and the normal stress σ_y is;

$$R_{Tz} = W_P = m_P g = 4.643 \times 9.81 = 45.548\ N$$

$$\sigma_z = \frac{4W_p}{\pi d^2} - \frac{32M_x}{\pi d^3} = \frac{4 \times 45.548}{\pi d^2} - \frac{32 \times 41.5}{\pi d^3} = -\frac{57.994}{d^2} - \frac{422.716}{d^3}$$

The diameter of the Idler Shaft in the range of [0, $\mathrm{L_1}$] can be analyzed by using maximum shear theory i.e., $\sigma_{1x} = \sigma_{1y} = 0$.

$$\tau_{max} = \tau_{all} = \sqrt{\left(\frac{\sigma_{1z}}{2}\right)^2 + {\tau_{1xz}}^2} = 65\ MPa = \sqrt{\left(-\frac{57.994}{2d^2} - \frac{422.716}{2d^3}\right)^2 + \left(\frac{10669.747}{d^3}\right)^2}$$

$$d^3 = \sqrt{(-0.446d - 3.252)^2 + (164.150)^2} \rightarrow d = 5.476\ mm$$

The diameter of the Idler Shaft in the range of [0, L_1] can also be analyzed by using principal stress i.e., $\sigma_{1x} = \sigma_{1y} = 0$.

$$\sigma_{1,2} = \sigma_{all} = \frac{\sigma_{1z}}{2} + \sqrt{\left(\frac{\sigma_{1z}}{2}\right)^2 + {\tau_{xz}}^2} = 130\ MPa$$

$$= -\frac{57.994}{2d^2} - \frac{422.716}{2d^3} + \sqrt{\left(-\frac{57.994}{2d^2} - \frac{422.716}{2d^3}\right)^2 + \left(\frac{10669.747}{d^3}\right)^2} =$$

$$d^3 = -0.223d - 1.626 + \sqrt{(-0.223d - 1.626)^2 + (82.075)^2} \rightarrow d = 4.300\ mm$$

The diameter of the Idler Shaft in the range of [0, L_1] should be 5.476 mm.

The shearing stress τ_{2xz} and the normal stress σ_{2z} in the range of [L_1, L_1+L_2] are;

$$\tau_{2xy} = \frac{16T_c}{\pi d^3} = \frac{16 \times 2.095 \times 10^3}{\pi d^3} = \frac{10669.747}{d^3}$$

$$\sigma_{2z} = -\frac{4 \times 41.5}{\pi d^2} - \frac{32 \times 114.962}{\pi d^3} = -\frac{57.994}{d^2} - \frac{1170.993}{d^3}$$

The diameter of the Idler Shaft in the range of [L_1, L_1+L_2] can be analyzed by using maximum shear theory i.e., $\sigma_{2x} = \sigma_{2y} = 0$.

$$\tau_{max} = \sqrt{\left(\frac{\sigma_{2z}}{2}\right)^2 + {\tau_{2xz}}^2} = 65\ MPa = \sqrt{\left(-\frac{57.994}{2d^2} - \frac{1170.993}{2d^3}\right)^2 + \left(\frac{10669.747}{d^3}\right)^2}$$

$$d^3 = \sqrt{(-0.446d - 9.002)^2 + (179.535)^2} \rightarrow d = 5.645\ mm$$

The diameter of the Idler Shaft in the range of [L_1, L_1+L_2] can also be analyzed by using principal stress i.e., $\sigma_{2x} = \sigma_{2y} = 0$.

$$\sigma_{1,2} = \sigma_{all} = \frac{\sigma_{2z}}{2} \pm \sqrt{\left(\frac{\sigma_{2z}}{2}\right)^2 + {\tau_{2xz}}^2} = 130\ MPa$$

$$= -\frac{57.994}{2d^2} - \frac{1170.993}{2d^3} + \sqrt{\left(-\frac{57.994}{2d^2} - \frac{1170.993}{2d^3}\right)^2 + \left(\frac{10669.747}{d^3}\right)^2}$$

$$d^3 = -0.223d - 4.504 + \sqrt{(-0.223d - 4.504)^2 + (82.075)^2} \rightarrow d = 4.251\ mm$$

The diameter of the Idler Shaft in the range of [L_1, L_1+L_2]should be 5.645 mm.

The shearing stress τ_{3xz} and the normal stress σ_{3z} in the range of [L_1+L_2, L_1+L_2+L_3] are;

$$\tau_{3xy} = \frac{16T_C}{\pi d^3} = \frac{16 \times 2.095 \times 10^3}{\pi d^3} = \frac{10669.747}{d^3}$$

$$\sigma_{3y} = -\frac{4 \times 0}{\pi d^2} - \frac{32 \times 288.942}{\pi d^3} = -\frac{2943.139}{d^3}$$

The diameter of the Idler Shaft in the range of [L_1+L_2, L_1+L_2+L_3] can be analyzed by using maximum shear theory i.e., $\sigma_{3x} = \sigma_{3y} = 0$.

$$\tau_{max} = \sqrt{\left(\frac{\sigma_{3z}}{2}\right)^2 + {\tau_{3xz}}^2} = 65\ MPa = \sqrt{\left(-\frac{2943.139}{d^3}\right)^2 + \left(\frac{10669.747}{d^3}\right)^2}$$

$$d^3 = \sqrt{(-22.640)^2 + (164.150)^2} \rightarrow d = 5.493\ mm$$

The diameter of the Idler Shaft in the range of [L_1+L_2, L_1+L_2+L_3] can also be analyzed by using principal stress i.e., $\sigma_{3x} = \sigma_{3y} = 0$.

$$\sigma_{1,2} = \sigma_{all} = \frac{\sigma_{3z}}{2} \pm \sqrt{\left(\frac{\sigma_{3z}}{2}\right)^2 + {\tau_{3xz}}^2} = 130\ MPa$$

$$= -\frac{2943.139}{d^3} + \sqrt{\left(-\frac{2943.139}{d^3}\right)^2 + \left(\frac{10669.747}{d^3}\right)^2}$$

$$d^3 = -11.320 + \sqrt{(-11.320)^2 + (82.075)^2} \rightarrow d = 4.151\ mm$$

The diameter of the conveor shaft in the range of [L_1+L_2, L_1+L_2+L_3] should be 5.493 mm.

Discussion on Idler Shaft Diameters: The diameters of the Idler Shaft are 5.476 mm, 5.645 mm and 5.493 mm for the range of [0, L_1], [L_1, L_1+L_2] and [L_1+L_2, $_1$+L_{12}+L_3] lengths respectively. The diameter of Idler Shaft for the ball bearing should be 6 mm. The diameters of the Idler Shaft on the conveyor pulley should be 7 mm because it will support the ball bearing. The diameters of the Idler Shaft on the clearance is 8 mm to support the pulley. Finally, the diameters of the Idler Shaft on the thrust bearing should be 6 mm.

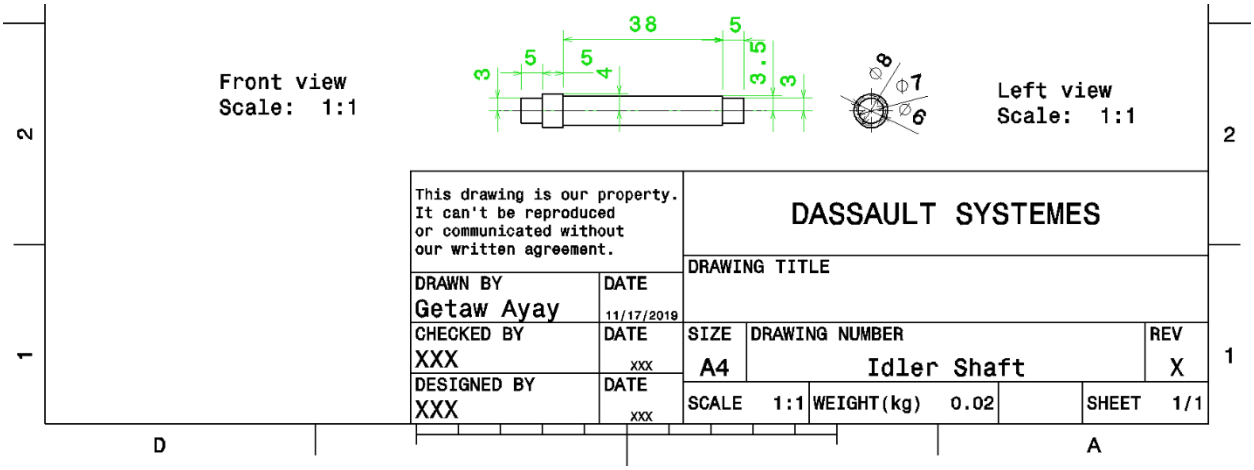

Part Drawing 4-14 Idler Shaft

Camshaft: The force analysis of the camshaft can be done by considering all the machine elements attached on it. The internal diameters of the machine elements are bevel gear (d_{5G}), ball bearing (d_{5b}), conveyor pulley (d_{5p}), cam (d_{5C}) and thrust bearing (d_{5T}) from right to left. The actual position of the shaft is vertical; bevel gear on top end and thrust bearing on bottom end see **Figure** 4-44.

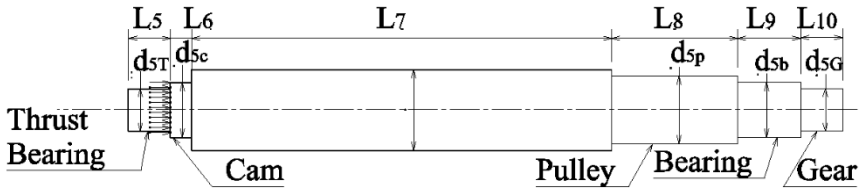

Figure 4-44 Descriptive Diagram of Camshaft

The free body diagram of the camshaft is drawn in **Figure** 4-45.

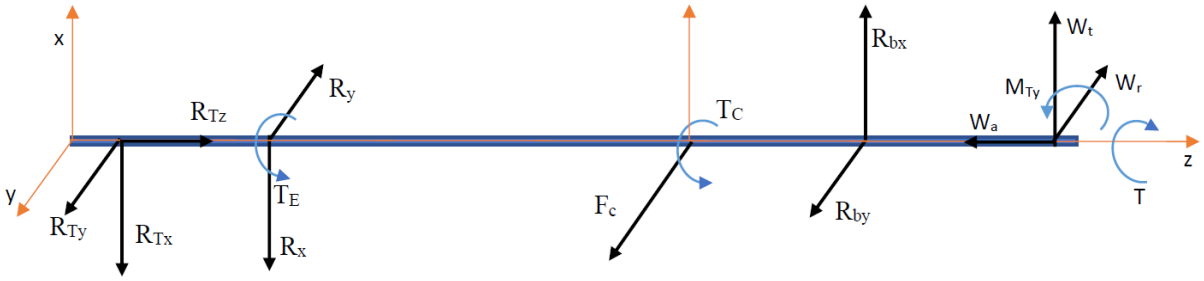

Figure 4-45 FBD of Camshaft

The parameters like torque on eccentric cam (T_E), force of eccentric cam on follower (F), frictional force between cam and follower (f_3), conveying force (F_c=28.895 N), torque on pulley (T_c) and tangential force of bevel gear (W_t) are determined in kinematics and kinetics analysis. The remaining parameters can be analyzed by applying equation of motion.

$$\sum F_x = 0$$

$$-R_{Tx} - R_x + R_{bx} + W_t = 0 \text{ ----------} \textit{4-79}$$

$$\sum F_y = 0$$

$$R_{Ty} - R_y + F_C + R_{by} - W_r = 0 \text{ ----------} \textit{4-80}$$

$$\sum F_z = 0$$

$$R_{Tz} - W_a - W = 0 - - \rightarrow R_{Tz} = W_a = 138.188\ N + W \text{ ----------} \textit{4-81}$$

Where W is the sum of weights of bevel gear, ball bearing, half of belt, half of total lugs, cam and camshaft.

$$\sum M_x = 0$$

$$-\tfrac{L_5}{2} R_{Ty} + \left(L_5 + {}^{L_6}/_2\right) R_y - \left(L_5 + L_6 + L_7 + {}^{L_8}/_2\right) F_c - \left(L_5 + L_6 + L_7 + L_8 + {}^{L_9}/_2\right) R_{by} + \left(L_5 + L_6 + L_7 + L_8 + L_9 + {}^{L_{10}}/_2\right) W_r = 0 \text{ ----------} \textit{4-82}$$

$$\sum M_y = 0$$

$$-\tfrac{L_5}{2} R_{Tx} - \left(L_5 + {}^{L_6}/_2\right) R_x + \left(L_5 + L_6 + L_7 + L_8 + {}^{L_9}/_2\right) R_{bx} + \left(L_5 + L_6 + L_7 + L_8 + L_9 + {}^{L_{10}}/_2\right) W_t + M_{Ty} = 0 \text{ ----------} \textit{4-83}$$

$$\sum M_z = 0$$

$$T_E + T_c + T = 0 \text{ ----------} \textit{4-84}$$

Note: In the force analysis of camshaft, there are seven unknows (L_5, L_6, L_9, R_{Tx}, R_{Ty}, R_{bx} and R_{by}) and five equations which is statically indeterminate. Since the lengths and diameters are unknown, it can't be solved by using the technique of displacement method for statically indeterminate problem. For the time being, the shaft can be designed by considering the part from bevel gear up to ball bearing which is positioned above conveyor pulley. Because it is subjected to a higher load. After analyzing all the above unknowns, it is good to redesign the shaft by considering the whole part.

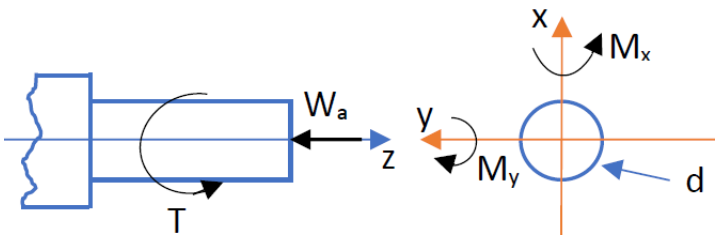

Figure 4-46 FBD of Camshaft on Gear Portion

The loads above the conveyor pulley are axial compressive (W_a=138.188 N), bending loads (W_r and W_t; 442.610 N and 1273.952 N respectively) and torsional moment (T=61.207 Nm) see **Figure** 4-46. This shows that the shaft is subjected to a combined load. The bending moment in the x-axis is the product of radial gear force (W_r) and half of thickness of bevel gear (L_{10}=28 mm).

$$M_x = W_r \frac{L_{10}}{2} = 442.610 \times \frac{28}{2} = 6196.54\ Nmm = 6.197\ Nm$$

The bending moment in the y-axis is the product of tangential gear force (W_t) and half of thickness of bevel gear (L_{10}=28 mm) plus bending moment ($M_{Ty}=W_aR_{mc}$) by axial gear force (W_a=138.188 N).

$$M_y = W_aR_{mc} + W_t \frac{L_{10}}{2} = \left(138.188 \times 48.045 + 1273.952 \times \frac{28}{2}\right) Nmm = 24.475\ Nm$$

Materials for Camshaft: It is made of quenched and tempered steel at 540°c AISI 4340 ASM designation, 1170 MPa tensile stress, 1080 MPa yield stress (σ_y) and 360 BHN. Since the system is used in the outdoor, its safety factor (n) is four. Hence, the allowable stress becomes:

$$\sigma_{all} = \sigma_w = \frac{\sigma_y}{n} = \frac{1080}{4} \frac{N}{mm^2} = 270\ MPa$$

The allowable shear stress can be determined by using maximum shear stress theory:

$$\tau_{all} = \tau_w = \frac{\sigma_{all}}{2} = \frac{270}{2} \frac{N}{mm^2} = 135\ MPa$$

The axial stress in the camshaft can be determined by Beer and et al (2012) equation 4.58 by considering $\sigma_x = \sigma_y = 0$.

$$\sigma_z = \frac{W_a}{A} - \frac{M_y x}{I_y} + \frac{M_x y}{I_x}$$

The above normal stress (σ_z) becomes maximum at 45° between negative x- and y-axes when x=y=$-d/\sqrt{8}$. The unit of the diameter is millimeter.

$$A = \frac{\pi d^2}{4}, I_y = \frac{\pi d^4}{64} = I_x$$

$$\sigma_z = \frac{4W_a}{\pi d^2} + \frac{16\sqrt{2}M_y}{\pi d^3} - \frac{16\sqrt{2}M_x}{\pi d^3} = -\frac{4 \times 138.188}{\pi d^2} - \frac{16\sqrt{2} \times (24.475 + 6.197) \times 10^3}{\pi d^3}$$

$$= -\frac{175.946}{d^2} - \frac{220.926 \times 10^3}{d^3}$$

The shearing stress due to torque T is;

$$\tau_{xz} = \frac{TC}{J}$$

$$C = \frac{d}{2} \; and \; J = \frac{\pi d^4}{32}$$

$$\tau_{xz} = \frac{16T}{\pi d^3} = \frac{16 \times 61.207 \times 10^3}{\pi d^3} = \frac{311.725 \times 10^3}{d^3}$$

The maximum shearing stress (τ_{max}) can be analyze by using Beer and et al (2012) equation 7.16.

$$\tau_{max} = \tau_{all} = \sqrt{\left(\frac{\sigma_z}{2}\right)^2 + {\tau_{xz}}^2}$$

135 MPa=$\sqrt{\left(-\frac{175.946}{2d^2} - \frac{220.926 \times 10^3}{2d^3}\right)^2 + \left(\frac{311.725 \times 10^3}{d^3}\right)^2}$

$$d^3 = \sqrt{(-0.652d - 818.244)^2 + (2309.074)^2}$$

The solution of the above equation is $d = 13.486\, mm$.

The principal stress ($\sigma_{1,2}$) can be determined using Beer and et al (2012) equation 7.13.

$$\sigma_{1,2} = \sigma_{all} = \frac{\sigma_z}{2} \pm \sqrt{\left(\frac{\sigma_z}{2}\right)^2 + {\tau_{xz}}^2} = 270 \; \frac{N}{mm^2} =$$

$$-\frac{175.946}{2d^2} - \frac{220.926 \times 10^3}{2d^3} \pm \sqrt{\left(-\frac{175.946}{2d^2} - \frac{220.926 \times 10^3}{2d^3}\right)^2 + \left(\frac{311.725 \times 10^3}{d^3}\right)^2}$$

$$d^3 = (-0.326d - 409.122) + \sqrt{(-0.326d - 409.122)^2 + (1154.537)^2}$$

The solution of the above equation is $d = 8.336\, mm$. Therefore, the diameter of camshaft is 15 mm because there is no bearing with bore between 15 mm and 13 mm.

Note: Still the numbers of unknowns are greater than number of equations. Hence, it is advisable to know the dimension of bearings and cam in order to get L_6 and L_9.

Selection of Bearings for Camshaft: The bearing on the upper part of camshaft is sealed single row deep groove ball bearing. The bore of bearing is 15 mm.

According to bearing catalogue, the specification of the sealed single row deep groove 15 mm bore

balling bearing is 24 mm outside diameter, 5 mm thickness, 1.56 KN dynamic basic load ratings, 0.8 KN static basic load ratings, 0.034 KN fatigue load limit, 60 000 rpm reference speed ratings, 38 000 rpm limiting speed ratings, 0.0074 Kg mass and 61802 designation.

The bearing on lower part of the camshaft is single direction thrust ball bearing. The bore of the bearing is 15 mm. According to bearing catalogue [53], the specification of the single direction thrust ball bearing for 15 mm bore thrust balling bearing is 28 mm outside diameter, 9 mm thickness, 9 KN dynamic basic load ratings, 15 KN static basic load ratings, 0.56 KN fatigue load limit, 8500 rpm reference speed ratings, 12 000 rpm limiting speed ratings, 0.023 Kg mass and 51102 designation.

Eccentric Cam: It is used to reciprocate the cutter bar through follower bar. Its schematic diagram and FBD is shown in **Figure** 4-5 and **Figure** 4-8 respectively. The cam is subjected to bearing load due to resultant reaction force and shearing due to frictional load (f_3) stresses.

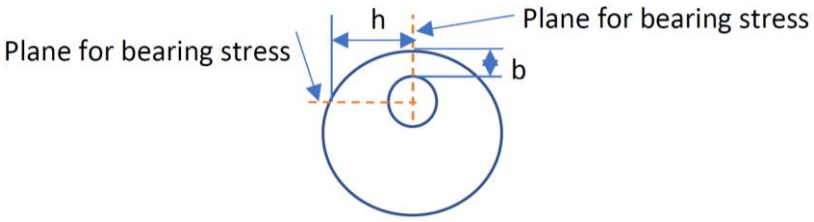

Figure 4-47 Plane of stresses in the Eccentric Cam

The bearing force is determined using **equation** 4-19.

$$\mathbf{R} = \sqrt{F^2(1+\mu^2) + 2Fm_c e\omega^2\,(\mu\sin\theta + \cos\theta) + {m_c}^2 e^2 \omega^4}$$

The bearing load (R) becomes maximum when $(\mu\sin\theta + \cos\theta)$ is maximum because all the other parameters are positive. The maximum value of the equation inside bracket can be determined by setting its derivation with respect to θ zero i.e.,

$$\frac{d\,(\mu\sin\theta + \cos\theta)}{d\theta} = 0 \rightarrow \tan\theta = \mu = 0.0011 \rightarrow \theta = 0.063^o \cong 0^0$$

$$\rightarrow \mathbf{R} = \sqrt{F^2(1+\mu^2) + 2Fm_c e\omega^2 + {m_c}^2 e^2 \omega^4}$$

Note: The bearing load can be determined by neglecting the effect of cam, cutter bar and follower bar masses. That is the follower bar force (F) and cutter bar force becomes same. Hence, the bearing load becomes;

$$\rightarrow \mathbf{R} = F\sqrt{(1+\mu^2)} = 290.97 \times \sqrt{(1+0.029^2)} \cong 295.159\ N$$

Correspondingly, the frictional force (f_3) becomes;

$$f_3 = \mu F = 0.029 \times 290.97 = 8.438\ N$$

Materials for Cam: It is made of high carbon steel of Fe870 Indian standard designation and 870 N/mm^2 tensile strength and 520 N/mm^2 yield stress (σ_y). Since the system is used in the outdoor, its safety factor (n) is four. Hence, the allowable stress becomes:

$$\sigma_{all} = \sigma_w = \frac{\sigma_y}{n} = \frac{520}{4}\frac{N}{mm^2} = 130\ MPa$$

The allowable shear stress can be determined by using maximum shear stress theory:

$$\tau_{all} = \tau_w = \frac{\sigma_{all}}{2} = \frac{130}{2}\frac{N}{mm^2} = 65\ MPa$$

The bearing stress (σ_b) is the ratio of reaction force R and bearing area A_b. The bearing area (A_b) is the product of thickness of cam (t) and diameter of camshaft (d=15 mm).

$$\sigma_b = \sigma_w = \frac{R}{A_b} = \frac{295.159}{dt} = 130\ MPa \rightarrow t = 0.151\ mm$$

The shearing stress is the ratio of shear force (f_3) and shearing area (A=ht).

$$\tau_{all} = \tau_w = \frac{f_3}{ht} = \frac{8.438}{0.151h}\frac{N}{mm^2} = 65\ MPa \rightarrow h = 0.860\ mm$$

The actual thickness of cam should be increased because it is designed by neglecting the effect of masses. Hence, it is recommended to have 5 mm thickness. In addition, its size on the plane of bearing stress (b) is recommended to 5 mm. The size (h) becomes 26.299 mm using the geometry in **Figure** 4-47.

The diameter of the cam becomes 2(t+e+d/2) =2(5+38.1+15/2) =101.2 mm. The length of cam in nose and tail side is 88.7 mm and 12.5 mm respectively.

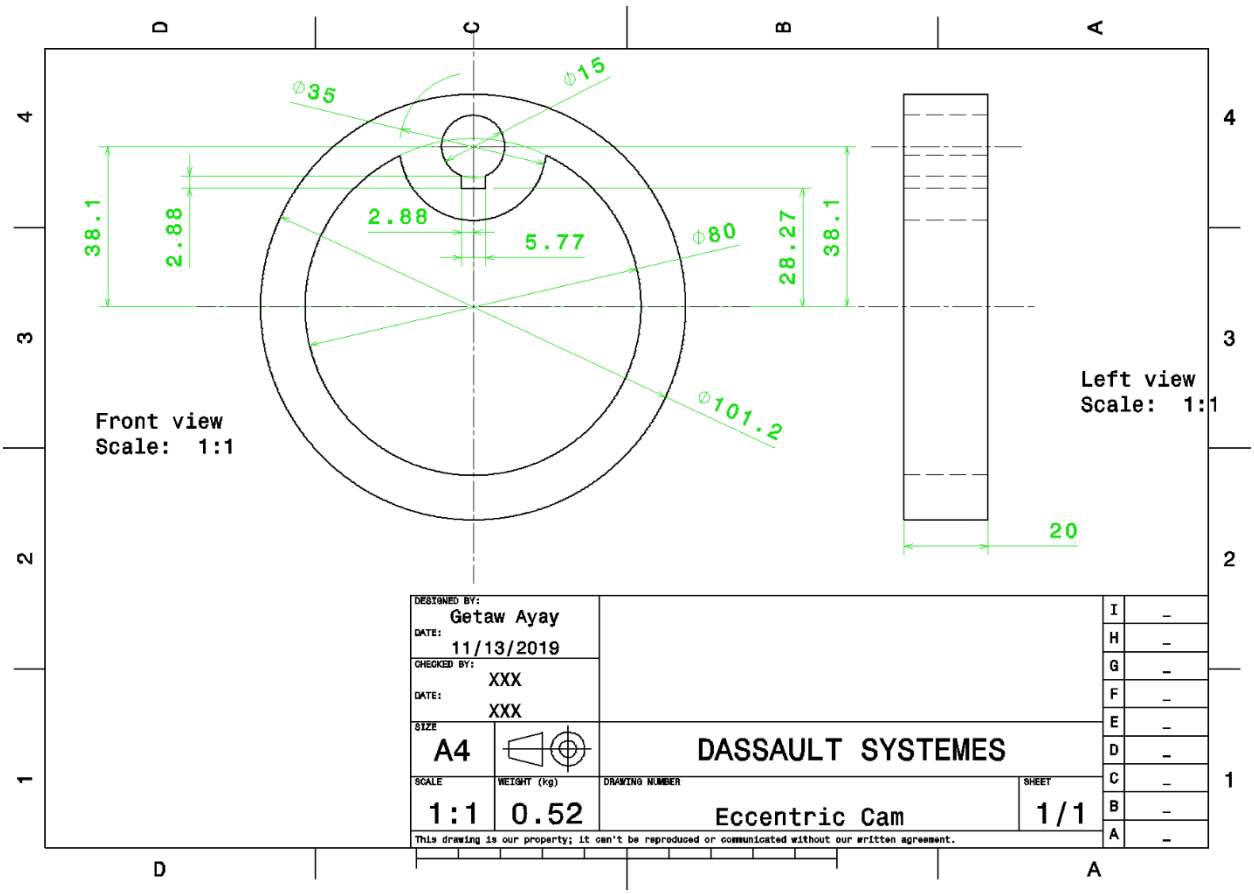

Part Drawing 4-15 Eccentric Cam

Note: The dimension of bearings and cams are already determined in addition to bevel gear and conveyor pulley. Now it is the time to solve from **equation** 4-80 to 4-84 using L_5=9 mm, L_6=5 mm, L_7=377.762 mm, L_8=38 mm, L_9=5 mm, L_{10}=28 mm, F_c=28.895 N, $R_x=f_3$=8.438 N, R_y=F=290.97 N, W_t=1273.952 N, W_a=138.188 N and W_r=442.610 N. The remaiming reaction forces can be determined after substituting these values into **equation** 4-80 to 4-84.

$$-R_{Tx} - R_x + R_{bx} + W_t = -R_{Tx} - 8.438 + R_{bx} + 1273.952 = -R_{Tx} + R_{bx} + 1265.514 = 0$$

$$R_{Ty} - R_y + F_C + R_{by} - W_r = R_{Ty} - 290.97 + 28.895 + R_{by} - 442.610$$
$$= R_{Ty} + R_{by} - 704.685 = 0$$

$$-4.5R_{Ty} + (11.5) \times 290.97 - (410.762) \times 28.895 - (432.262)R_{by} + (448.762) \times 442.610$$
$$= -4.5R_{Ty} - 432.262R_{by} + 190103.736 = 0$$

$$-4.5R_{Tx} - 11.5 \times 8.438 + 432.762R_{bx} + 448.762 \times 1273.952 + 48.045 \times 138.188$$
$$= -4.5R_{Tx} + 432.262R_{bx} + 578243.453 = 0$$

The above equations have four variables and four equations i.e, can be solved by using simultaneous equation.

$$-4.5R_{Tx} + 432.262(R_{Tx} - 1265.514) + 578243.543 = 0 \rightarrow 427.762R_{Tx} = -31209.930$$

$$R_{Tx} = -72.961\ N$$

$$R_{bx} = R_{Tx} - 1265.514 = -72.961 - 1265.514 = 1338.475\ N$$

$$-4.5(-R_{by} + 704.685) - 432.262R_{by} + 190103.736 = 0 \rightarrow -427.762R_{by} = -186932.654$$

$$R_{by} = 437.002\ N$$

$$R_{Ty} = -R_{by} + 704.685 = -437.002 + 704.685 = 267.683\ N$$

The shear force and bending moment diagrams can be constructed after deriving the equations of them in each ranges shown in **Figure** 4-48.

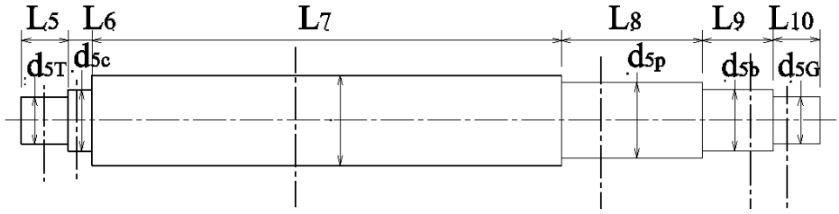

Figure 4-48 Sections for Shear Force and Bending Moment

The transverse forces are applied about x- and y-axes. So that the bending moment is about x-and y-axes. The shaft should be designed for the cumulative or resultant effect of these bending moments. The resultant moment can be determined after determining bending moment about x- and y-axes in each section.

The free body diagram of the camshaft about x-axis is shown in **Figure** 4-49. The loads w_1, w_2, w_3 and w_4 are distributed loads over length L_5, L_6, L_9 and L_{10} respectively i.e., $w_1 = {R_{Tx}}/{L_5} = \frac{72.961}{9} = 8.107\ N/mm$, $w_2 = {R_x}/{L_6} = \frac{8.438}{5} = 1.688\ N/mm$, $w_3 = {R_{bx}}/{L_9} = \frac{1338.475}{5} = 267.697\ N/mm$ and $w_4 = {w_t}/{L_{10}} = \frac{1273.952}{28} = 45.498\ N/mm$.

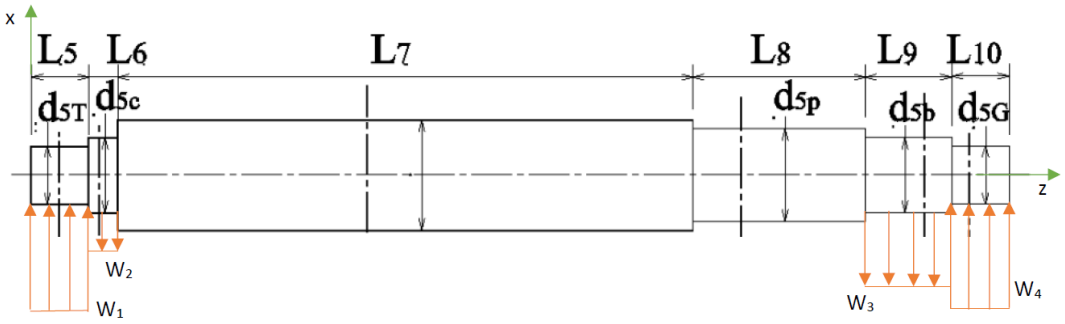

Figure 4-49 FBD Diagram of Camshaft about x-axis

The bending moment equation (M_{1y}) on a range of length [0, L_5] can be derived by taking an arbitrary section between this range by using equilibrium equation see **Figure** 4-50.

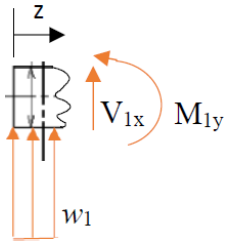

Figure 4-50 FBD between [0, L_5]

$$\sum M_y = 0 = -w_1 \frac{z^2}{2} + M_{1y} \longrightarrow M_{1y} = w_1 \frac{z^2}{2} = 4.054z^2$$

The bending moment equation is quadrtic and it becomes maximum at z=L_5=9 mm i.e., M_{1y} [0, 328.374] Nmm.

The bending moment equation (M_{2y}) on a range of length [L_5, $L_5 + L_6$] can be derived by taking an arbitrary section between this range by using equilibrium equation see **Figure** 4-51.

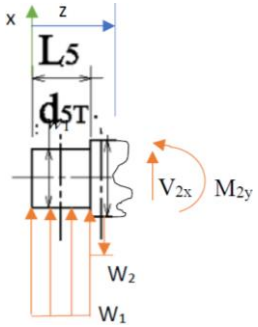

Figure 4-51 FBD between [L_5, $L_5 + L_6$]

$$\sum M_y = 0 = -w_1 L_5(z - \frac{L_5}{2}) + w_2 \frac{(z - L_5)^2}{2} + M_{2y} \longrightarrow M_{2y} = w_1 L_5(z - \frac{L_5}{2}) - w_2 \frac{(z - L_5)^2}{2}$$

$$= -w_2 \frac{z^2}{2} + (w_2 + w_1) L_5 z - (w_2 + w_1) \frac{{L_5}^2}{2} = -0.844z^2 + 88.155z - 396.698$$

The bending moment equation is quadratic and it becomes maximum at z=L_5+L_6=14 mm i.e., M_{2y} [328.333, 672.048] Nmm.

The bending moment equation (M_{3y}) on a range of length $[L_5 + L_6, L_5 + L_6 + L_7]$ can be derived by taking an arbitrary section between this range by using equilibrium equation see **Figure** 4-52.

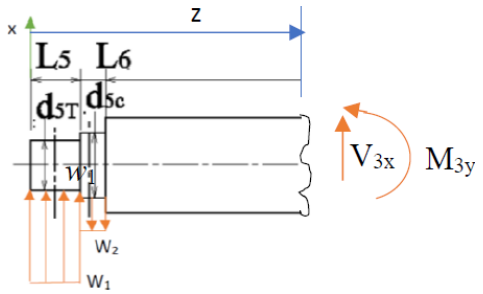

Figure 4-52 FBD between $[L_5 + L_6, L_5 + L_6 + L_7]$

$$\sum M_y = 0 = -w_1 L_5 \left(z - \frac{L_5}{2}\right) + w_2 L_6 \left(z - L_5 - \frac{L_6}{2}\right) + M_{3y}$$

$$\rightarrow M_{3y} = w_1 L_5 \left(z - \frac{L_5}{2}\right) - w_2 L_6 \left(z - L_5 - \frac{L_6}{2}\right)$$

$$= (w_1 L_5 - w_2 L_6)z - w_1 \frac{{L_5}^2}{2} + w_2 L_6 \left(L_5 + \frac{L_6}{2}\right)$$

$$= 64.523z - 231.288$$

The bending moment equation is linear and it becomes maximum at z=L_5+L_6+L_7 =391.762 mm i.e., M_{3y} [672.034, 25046.372] Nmm.

The bending moment equation (M_{4y}) on a range of length $[L_5 + L_6 + L_7, L_5 + L_6 + L_7 + L_8]$ can be derived by taking an arbitrary section between this range by using equilibrium equation see **Figure** 4-53.

$$\sum M_y = 0 = -w_1 L_5 \left(z - \frac{L_5}{2}\right) + w_2 L_6 \left(z - L_5 - \frac{L_6}{2}\right) + M_{4y}$$

$$\rightarrow M_{4y} = w_1 L_5 \left(z - \frac{L_5}{2}\right) - w_2 L_6 \left(z - L_5 - \frac{L_6}{2}\right)$$

$$= (-w_2 L_6 + w_1 L_5)z - w_1 \frac{{L_5}^2}{2} + w_2 L_6 \left(L_5 + \frac{L_6}{2}\right)$$

$$= 64.523z - 231.288$$

The bending moment equation is linear and it becomes maximum at z=L_5+L_6+ L_7+L_8=429.762 mm i.e., M_{4y} [25046.372, 27498.246] Nmm.

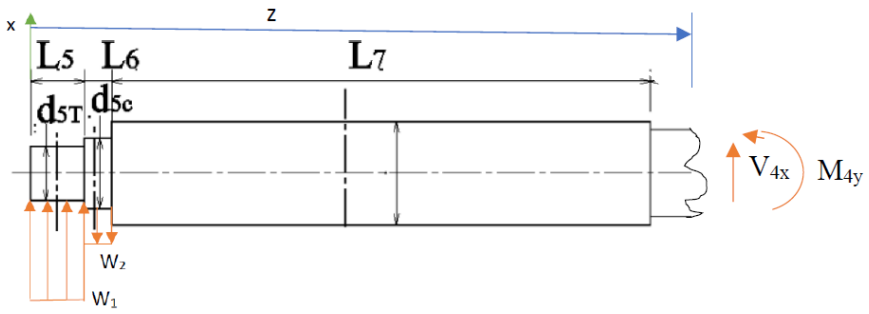

Figure 4-53 FBD between $[L_5 + L_6 + L_7, L_5 + L_6 + L_7 + L_8]$

The bending moment equation (M_{5y}) on a range of length $[L_5 + L_6 + L_7 + L_8, L_5 + L_6 + L_7 + L_8 + L_9]$ can be derived by taking an arbitrary section between this range by using equilibrium equation see **Figure** 4-54.

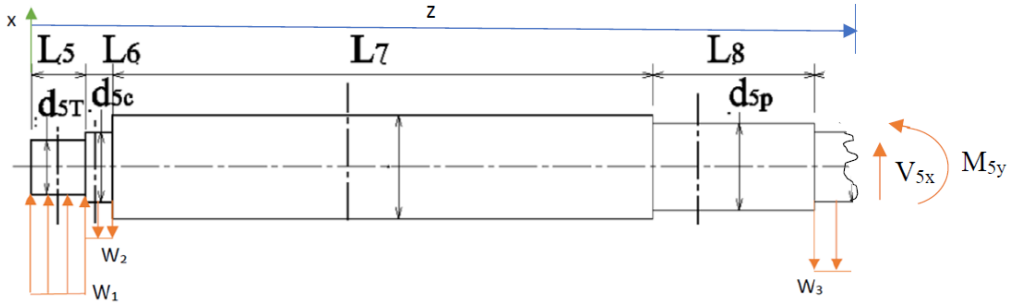

Figure 4-54 FBD between $[L_5 + L_6 + L_7 + L_8, L_5 + L_6 + L_7 + L_8 + L_9]$

$$\sum M_y = 0 = -w_1 L_5 \left(z - \frac{L_5}{2}\right) + w_2 L_6 \left(z - L_5 - \frac{L_6}{2}\right) + w_3 \frac{(Z - L_5 - L_6 - L_7 - L_8)^2}{2} + M_{5y}$$

$$\rightarrow M_{5y} = w_1 L_5 \left(z - \frac{L_5}{2}\right) - w_2 L_6 \left(z - L_5 - \frac{L_6}{2}\right) - w_3 \frac{(z - L_5 - L_6 - L_7 - L_8)^2}{2}$$

$$= -w_3 \frac{z^2}{2} + \left(w_1 L_5 - w_2 L_6 + w_3 (L_5 + L_6 + L_7 + L_8)\right) z - w_1 \frac{{L_5}^2}{2}$$

$$+ w_2 L_6 \left(L_5 + \frac{L_6}{2}\right) - w_3 \frac{(L_5 + L_6 + L_7 + L_8)^2}{2}$$

$$= -133.849 z^2 + 115110.521 z - 24721430.408$$

The bending moment equation is quadratic and it becomes maximum at z=429.762 mm i.e., M_{5y} [27394.049, 24558.356] Nmm.

The bending moment equation (M_{6y}) on a range of length $[L_5 + L_6 + L_7 + L_8 + L_9, L_5 + L_6 + L_7 + L_8 + L_9 + L_{10}]$ can be derived by taking an arbitrary section between this range by using equilibrium equation see **Figure** 4-55.

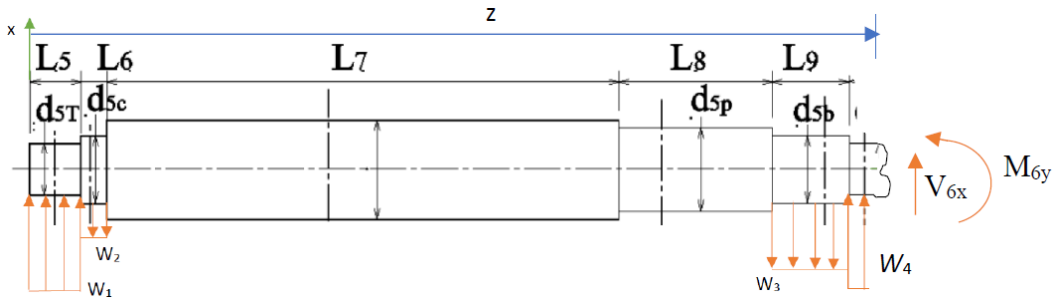

Figure 4-55 FBD between $[L_5 + L_6 + L_7 + L_8 + L_9, L_5 + L_6 + L_7 + L_8 + L_9 + L_{10}]$

$$\sum M_y = 0 = -w_1 L_5 \left(z - \frac{L_5}{2}\right) + w_2 L_6 \left(z - L_5 - \frac{L_6}{2}\right) + w_3 L_9 \left(Z - L_5 - L_6 - L_7 - L_8 - \frac{L_9}{2}\right) - w_4 \frac{(Z - L_5 - L_6 - L_7 - L_8 - L_9)^2}{2} + M_{6y}$$

$$\rightarrow M_{6y} = w_1 L_5 \left(z - \frac{L_5}{2}\right) - w_2 L_6 \left(z - L_5 - \frac{L_6}{2}\right) - w_3 L_9 \left(Z - L_5 - L_6 - L_7 - L_8 - \frac{L_9}{2}\right) + w_4 \frac{(z - L_5 - L_6 - L_7 - L_8 - L_9)^2}{2}$$

$$= w_4 \frac{z^2}{2} + \left(w_1 L_5 - w_2 L_6 - w_3 L_9 - w_4 (L_5 + L_6 + L_7 + L_8 + L_9)\right) z - w_1 \frac{{L_5}^2}{2} + w_2 L_6 \left(L_5 + \frac{L_6}{2}\right) + w_3 L_9 \left(L_5 + L_6 + L_7 + L_8 + \frac{L_9}{2}\right) + w_4 \frac{(L_5 + L_6 + L_7 + L_8 + L_9)^2}{2}$$

$$= 22.749z^2 - 21054.753z + 4874964.811$$

The bending moment equation is quadratic and it becomes maximum at z=$L_5 + L_6 + L_7 + L_8 + L_9 = 462.762$ mm i.e., M_{6y} [21128.693, 3293.266] Nmm.

The free body diagram of the camshaft about y-axis is shown in **Figure** 4-56. The loads w5, w6, w7, w8 and w9 are distributed loads over length L_5, L_6, L_8, L_9 and L_{10} respectively i.e., $w_5 = {R_{Ty}}/{L_5} = \frac{267.683}{9} = 29.743\ N/mm$, $w_6 = {R_y}/{L_6} = \frac{290.97}{5} = 58.194\ N/mm$, $w_7 = {F_c}/{L_8} = \frac{28.895}{38} = 0.760\ N/mm$, $w_8 = {R_{by}}/{L_9} = \frac{437.002}{5} = 87.400\ N/mm$ and $w_9 = {w_r}/{L_{10}} = \frac{442.610}{28} = 15.808\ N/mm$.

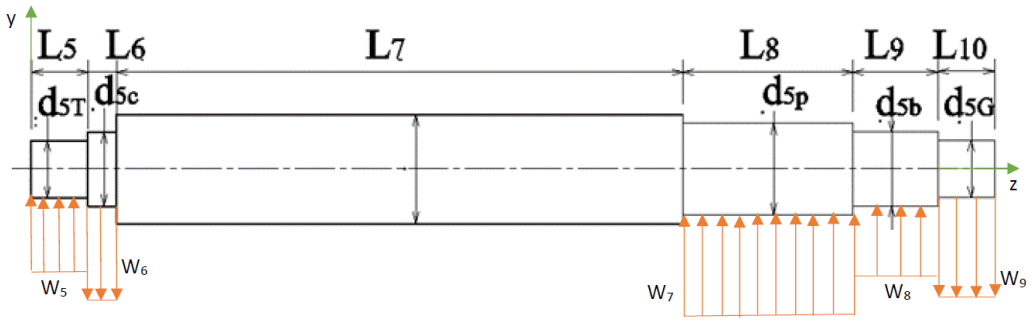

Figure 4-56 FBD Diagram of Camshaft about y-axis

The bending moment equation (M_{1x}) on a range of length [0, L_5] can be derived by using equilibrium equation by taking an arbitrary section between this range see **Figure** 4-57.

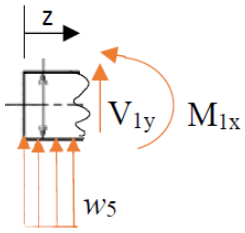

Figure 4-57 FBD between [0, L_5]

$$\sum M_x = 0 = -w_5 \frac{z^2}{2} + M_{1x} \longrightarrow M_{1x} = w_5 \frac{z^2}{2} = 14.872z^2$$

The bending moment equation is quadrtic and it becomes maximum at z=L_5=9 mm i.e., M_{1x} [0, 1204.632] Nmm.

The bending moment equation (M_{2x}) on a range of length [L_5, $L_5 + L_6$] can be derived by taking an arbitrary section between this range by using equilibrium equation see **Figure** 4-58.

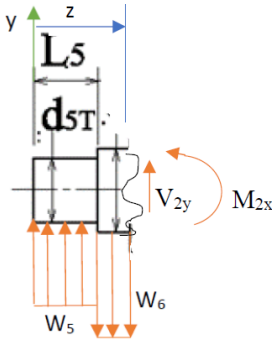

Figure 4-58 FBD between [L_5, $L_5 + L_6$]

$$\sum M_x = 0 = -w_5 L_5 (z - \frac{L_5}{2}) + w_6 \frac{(z - L_5)^2}{2} + M_{2x} \longrightarrow M_{2x} = w_5 L_5 (z - \frac{L_5}{2}) - w_6 \frac{(z - L_5)^2}{2}$$

$$= -w_6\frac{z^2}{2} + (w_6 + w_5)L_5 z - (w_6 + w_5)\frac{{L_5}^2}{2} = -29.097z^2 + 791.433z - 3561.449$$

The bending moment equation is quadratic and it becomes maximum at z=L_5+L_6=14 mm i.e., M_{2x} [1203.664, 1814.159] Nmm.

The bending moment equation (M_{3x}) on a range of length $[L_5 + L_6, L_5 + L_6 + L_7]$ can be derived by taking an arbitrary section between this range by using equilibrium equation see **Figure** 4-59.

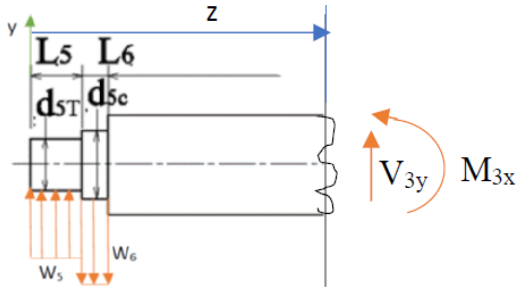

Figure 4-59 FBD between $[L_5 + L_6, L_5 + L_6 + L_7]$

$$\sum M_x = 0 = -w_5 L_5\left(z - \frac{L_5}{2}\right) + w_6 L_6\left(z - L_5 - \frac{L_6}{2}\right) + M_{3x}$$

$$\rightarrow M_{3x} = w_5 L_5\left(z - \frac{L_5}{2}\right) - w_6 L_6\left(z - L_5 - \frac{L_6}{2}\right)$$

$$= (w_5 L_5 - w_6 L_6)z - w_5\frac{{L_5}^2}{2} + w_6 L_6\left(L_5 + \frac{L_6}{2}\right)$$

$$= -23.287z + 2141.582$$

The bending moment equation is linear and it becomes maximum at z=L_5+L_6+L_7 =391.762 mm i.e., M_{3X} [1815.564, -6981.380] Nmm.

The bending moment equation (M_{4X}) on a range of length $[L_5 + L_6 + L_7, L_5 + L_6 + L_7 + L_8]$ can be derived by taking an arbitrary section between this range by using equilibrium equation see **Figure** 4-60.

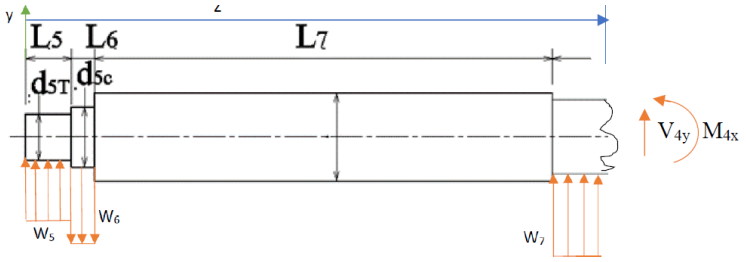

Figure 4-60 FBD between $[L_5 + L_6 + L_7, L_5 + L_6 + L_7 + L_8]$

$$\sum M_x = 0 = -w_5 L_5 \left(z - \frac{L_5}{2}\right) + w_6 L_6 \left(z - L_5 - \frac{L_6}{2}\right) - w_7 \frac{(z - L_5 - L_6 - L_7)^2}{2} + M_{4X}$$

$$\rightarrow M_{4x} = w_5 L_5 \left(z - \frac{L_5}{2}\right) - w_6 L_6 \left(z - L_5 - \frac{L_6}{2}\right) + w_7 \frac{(z - L_5 - L_6 - L_7)^2}{2}$$

$$= w_7 \frac{z^2}{2} + \left(w_5 L_5 - w_6 L_6 - w_7 (L_5 + L_6 + L_7)\right) z - w_5 \frac{{L_5}^2}{2} + w_6 L_6 \left(L_5 + \frac{L_6}{2}\right)$$

$$+ w_7 \frac{(L_5 + L_6 + L_7)^2}{2} = 0.38z^2 - 321.026z + 60463.018$$

The bending moment equation is linear and it becomes maximum at z=L_5+L_6+ L_7 L_8=429.762 mm i.e., M_{4x} [-6981.333, -7317.515] Nmm.

The bending moment equation (M_{5x}) on a range of length $[L_5 + L_6 + L_7 + L_8, L_5 + L_6 + L_7 + L_8 + L_9]$ can be derived by taking an arbitrary section between this range by using equilibrium equation see **Figure** 4-61.

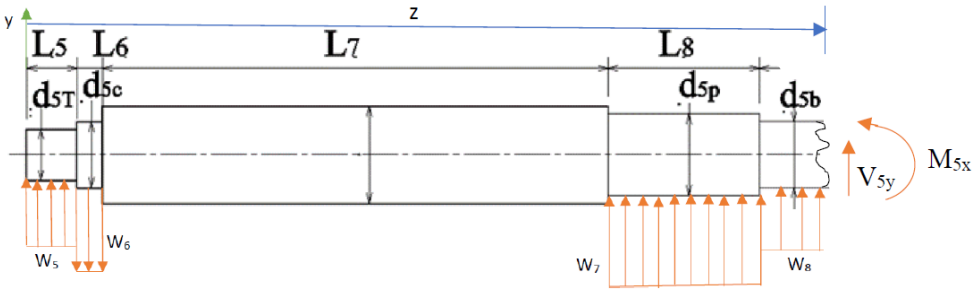

Figure 4-61 FBD between $[L_5 + L_6 + L_7 + L_8, L_5 + L_6 + L_7 + L_8 + L_9]$

$$\sum M_x = 0 = -w_5 L_5 \left(z - \frac{L_5}{2}\right) + w_6 L_6 \left(z - L_5 - \frac{L_6}{2}\right) - w_7 L_8 \left(z - L_5 - L_6 - L_7 - \frac{L_8}{2}\right)$$

$$- w_8 \frac{(Z - L_5 - L_6 - L_7 - L_8)^2}{2} + M_{5x}$$

$$\rightarrow M_{5x} = w_5 L_5 \left(z - \frac{L_5}{2}\right) - w_6 L_6 \left(z - L_5 - \frac{L_6}{2}\right) + w_7 L_8 \left(z - L_5 - L_6 - L_7 - \frac{L_8}{2}\right)$$

$$+ w_8 \frac{(Z - L_5 - L_6 - L_7 - L_8)^2}{2}$$

$$= w_8 \frac{z^2}{2} + \left(w_5 L_5 - w_6 L_6 + w_7 L_8 - w_8 (L_5 + L_6 + L_7 + L_8)\right) z - w_5 \frac{{L_5}^2}{2}$$

$$+ w_6 L_6 \left(L_5 + \frac{L_6}{2}\right) - w_7 L_8 \left(L_5 + L_6 + L_7 + \frac{L_8}{2}\right) + w_8 \frac{(L_5 + L_6 + L_7 + L_8)^2}{2}$$

$$= 43.7z^2 - 37555.591z + 8061460.573$$

The bending moment equation is linear and it becomes maximum at z=$L_5 + L_6 + L_7 +$

L_8=429.762 mm i.e., M_{5x} [-7317.41, -6196.871] Nmm.

The bending moment equation (M_{6x}) on a range of length [$L_5 + L_6 + L_7 + L_8 + L_9$, $L_5 + L_6 + L_7 + L_8 + L_9 + L_{10}$] can be derived by taking an arbitrary section between this range by using equilibrium equation see **Figure** 4-62.

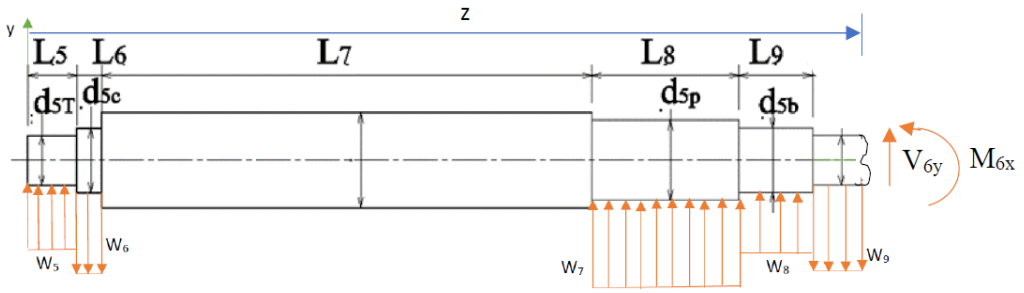

Figure 4-62 FBD between $[L_5 + L_6 + L_7 + L_8 + L_9, L_5 + L_6 + L_7 + L_8 + L_9 + L_{10}]$

$$\sum M_x = 0 = -w_5 L_5\left(z - \frac{L_5}{2}\right) + w_6 L_6\left(z - L_5 - \frac{L_6}{2}\right) - w_7 L_8\left(z - L_5 - L_6 - L_7 - \frac{L_8}{2}\right) - w_8 L_8\left(Z - L_5 - L_6 - L_7 - L_8 - \frac{L_9}{2}\right) + w_9 \frac{(Z - L_5 - L_6 - L_7 - L_8 - L_9)^2}{2} + M_{6x}$$

$$\rightarrow M_{6x} = w_5 L_5\left(z - \frac{L_5}{2}\right) - w_6 L_6\left(z - L_5 - \frac{L_6}{2}\right) + w_7 L_8\left(z - L_5 - L_6 - L_7 - \frac{L_8}{2}\right) + w_8 L_9\left(Z - L_5 - L_6 - L_7 - L_8 - \frac{L_9}{2}\right) - w_9 \frac{(Z - L_5 - L_6 - L_7 - L_8 - L_9)^2}{2}$$

$$= -w_9 \frac{z^2}{2} + \left(w_5 L_5 - w_6 L_6 + w_7 L_8 + w_8 L_9 + w_9(L_5 + L_6 + L_7 + L_8 + L_9)\right)z - w_5 \frac{{L_5}^2}{2} + w_6 L_6\left(L_5 + \frac{L_6}{2}\right) - w_7 L_8\left(L_5 + L_6 + L_7 + \frac{L_8}{2}\right) - w_8 L_9\left(L_5 + L_6 + L_7 + L_8 + \frac{L_9}{2}\right) - w_9 \frac{(L_5 + L_6 + L_7 + L_8 + L_9)^2}{2}$$

$$= -7.904z^2 + 7315.328z - 1692624.990$$

The bending moment equation is quadratic and it becomes maximum at z=$L_5 + L_6 + L_7 + L_8 + L_9 = 434.762$ mm i.e., M_{6x} [-6196.604, 0] Nmm.

The diameter of the camshaft can be analyzed by using τ_{xz} and σ_z in each section. The torque in the range of [0, L_5] is zero i.e., $\tau_{xz} = 0$ and the normal stress σ_z is;

$$\sigma_{1z} = -\frac{4 \times 138.188}{\pi d^2} - \frac{16\sqrt{2} \times (328.374 + 1204.632)}{\pi d^3} = -\frac{175.946}{d^2} - \frac{11041.523}{d^3}$$

The diameter of the camshaft in the range of [0, L_5] can be analyzed by using maximum shear theory i.e., $\sigma_{1x} = \sigma_{1y} = \tau_{1xz} = 0$.

$$\tau_{max} = \tau_{all} = \sqrt{\left(\frac{\sigma_{1z}}{2}\right)^2 + {\tau_{xz}}^2} = 135\ MPa = \frac{\sigma_{1z}}{2} = \frac{175.946}{2d^2} + \frac{11041.523}{2d^3}$$

$$d^3 = 0.652d + 40.895 \rightarrow d = 3.508\ mm$$

The diameter of the camshaft in the range of [0, L_5] can also be analyzed by using principal stress i.e., $\sigma_{1x} = \sigma_{1y} = \tau_{1xz} = 0$.

$$\sigma_{1,2} = \sigma_{all} = \frac{\sigma_{1z}}{2} \pm \sqrt{\left(\frac{\sigma_{1z}}{2}\right)^2 + {\tau_{xz}}^2} = 270\ MPa = \sigma_{1z} = \frac{175.946}{d^2} + \frac{11041.523}{d^3}$$

$$d^3 = 0.652d + 40.895 \rightarrow d = 3.508\ mm$$

The diameter of the camshaft in the range of [0, L_5] should be 3.508 mm.

The shearing stress τ_{2xz} and the normal stress σ_{2z} in the range of [L_5, L_5+L_6] are;

$$\tau_{2xz} = \frac{16T_E}{\pi d^3} = \frac{16 \times 58.270 \times 10^3}{\pi d^3} = \frac{296.767 \times 10^3}{d^3}$$

$$\sigma_{2z} = -\frac{4 \times 138.188}{\pi d^2} - \frac{16\sqrt{2} \times (672.048 + 1814.159\ )}{\pi d^3} = -\frac{175.946}{d^2} - \frac{17906.982}{d^3}$$

The diameter of the camshaft in the range of [L_5, L_5+L_6] can be analyzed by using maximum shear theory i.e., $\sigma_{2x} = \sigma_{2y} = \tau_{2xz} = 0$.

$$\tau_{max} = \sqrt{\left(\frac{\sigma_{1z}}{2}\right)^2 + {\tau_{xz}}^2} = 135\ MPa = \sqrt{\left(-\frac{175.946}{2d^2} - \frac{17906.982}{2d^3}\right)^2 + \left(\frac{296.767 \times 10^3}{d^3}\right)^2}$$

$$d^3 = \sqrt{(-0.652d - 66.322)^2 + (2198.274)^2} \rightarrow d = 13.005\ mm$$

The diameter of the camshaft in the range of [L_5, L_5+L_6] can also be analyzed by using principal stress i.e., $\sigma_{2x} = \sigma_{2y} = 0$.

$$\sigma_{1,2} = \sigma_{all} = \frac{\sigma_{2z}}{2} \pm \sqrt{\left(\frac{\sigma_{2z}}{2}\right)^2 + {\tau_{2xz}}^2} = 270\ MPa$$

$$= -\frac{175.946}{2d^2} - \frac{17906.982}{2d^3}$$

$$+ \sqrt{\left(-\frac{175.946}{2d^2} - \frac{17906.982}{2d^3}\right)^2 + \left(\frac{296.767 \times 10^3}{d^3}\right)^2}$$

$$d^3 = -0.326d - 33.161 + \sqrt{(-0.326d - 33.161)^2 + (1099.137)^2} \rightarrow d = 10.207\ mm$$

The diameter of the camshaft in the range of [L_5, L_5+L_6]should be 13.005 mm.

The shearing stress τ_{3xz} and the normal stress σ_{3z} in the range of [L_5+L_6, L_5+L_6+ L_7] are;

$$\tau_{3xz} = \frac{16T_E}{\pi d^3} = \frac{16 \times 58.270 \times 10^3}{\pi d^3} = \frac{296.767 \times 10^3}{d^3}$$

$$\sigma_{3z} = -\frac{4 \times 138.188}{\pi d^2} - \frac{16\sqrt{2} \times (25046.372 + 6981.380\ )}{\pi d^3} = -\frac{175.946}{d^2} - \frac{230680.862}{d^3}$$

The diameter of the camshaft in the range of [L_5+L_6, L_5+L_6+ L_7] can be analyzed by using maximum shear theory i.e., $\sigma_{3x} = \sigma_{3y} = 0$.

$$\tau_{max} = \sqrt{\left(\frac{\sigma_{3z}}{2}\right)^2 + {\tau_{3xz}}^2} = 135\ MPa = \sqrt{\left(-\frac{175.946}{2d^2} - \frac{230680.862}{2d^3}\right)^2 + \left(\frac{296.767 \times 10^3}{d^3}\right)^2}$$

$$d^3 = \sqrt{(-0.652d - 854.374)^2 + (2198.274)^2} \rightarrow d = 13.317\ mm$$

The diameter of the camshaft in the range of [L_5+L_6, L_5+L_6+ L_7] can also be analyzed by using principal stress i.e., $\sigma_{3x} = \sigma_{3y} = 0$.

$$\sigma_{1,2} = \sigma_{all} = \frac{\sigma_{2z}}{2} \pm \sqrt{\left(\frac{\sigma_{2z}}{2}\right)^2 + {\tau_{2xz}}^2} = 270\ MPa$$

$$= -\frac{175.946}{2d^2} - \frac{230680.862}{2d^3}$$

$$+ \sqrt{\left(= -\frac{175.946}{2d^2} - \frac{230680.862}{2d^3}\right)^2 + \left(\frac{296.767 \times 10^3}{d^3}\right)^2}$$

$$d^3 = -0.326d - 427.187 + \sqrt{(-0.326d - 427.187)^2 + (1099.137)^2} \rightarrow d = 9.086\ mm$$

The diameter of the camshaft in the range of [L_5+L_6, L_5+L_6+ L_7] should be 13.317 mm.

The shearing stress τ_{4xz} and the normal stress σ_{4z} in the range of [L_5+L_6+ L_7, L_5+L_6+ L_7 +L_8] are;

$$\tau_{4xz} = \frac{16T}{\pi d^3} = \frac{16 \times 61.207 \times 10^3}{\pi d^3} = \frac{311.725 \times 10^3}{d^3}$$

$$\sigma_{4z} = -\frac{4 \times 138.188}{\pi d^2} - \frac{16\sqrt{2} \times (27498.246 + 7317.515)}{\pi d^3} = -\frac{175.946}{d^2} - \frac{250761.582}{d^3}$$

The diameter of the camshaft in the range of [L_5+L_6+ L_7, L_5+L_6+ L_7 +L_8] can be analyzed by using maximum shear theory i.e., $\sigma_{4x} = \sigma_{4y} = 0$.

$$\tau_{max} = \sqrt{\left(\frac{\sigma_{4z}}{2}\right)^2 + {\tau_{4xz}}^2} = 135\ MPa = \sqrt{\left(-\frac{175.946}{2d^2} - \frac{250761.582}{2d^3}\right)^2 + \left(\frac{311.725 \times 10^3}{d^3}\right)^2}$$

$$d^3 = \sqrt{(-0.652d - 928.747)^2 + (2309.074)^2} \rightarrow d = 13.558\ mm$$

The diameter of the camshaft in the range of [L_5+L_6+ L_7, L_5+L_6+ L_7 +L_8] can also be analyzed by using principal stress i.e., $\sigma_{4x} = \sigma_{4y} = 0$.

$$\sigma_{1,2} = \sigma_{all} = \frac{\sigma_{4z}}{2} \pm \sqrt{\left(\frac{\sigma_{4z}}{2}\right)^2 + {\tau_{4xz}}^2} = 270\ MPa$$

$$= -\frac{175.946}{2d^2} - \frac{250761.582}{2d^3} + \sqrt{\left(-\frac{175.946}{2d^2} - \frac{250761.582}{2d^3}\right)^2 + \left(\frac{311.725 \times 10^3}{d^3}\right)^2}$$

$$d^3 = -0.326d - 464.373 + \sqrt{(-0.326d - 464.373)^2 + (1154.537)^2} \rightarrow d = 9.198\ mm$$

The diameter of the camshaft in the range of [L_5+L_6+ L_7, L_5+L_6+ L_7 +L_8] should be 13.558 mm.

The shearing stress τ_{5xz} and the normal stress σ_{5z} in the range of [L_5+L_6+ L_7 +L_8, L_5+L_6+ L_7 +L_8+L_9] are;

$$\tau_{5xz} = \frac{16T}{\pi d^3} = \frac{16 \times 61.207 \times 10^3}{\pi d^3} = \frac{311.725 \times 10^3}{d^3}$$

$$\sigma_{5z} = -\frac{4 \times 138.188}{\pi d^2} - \frac{16\sqrt{2} \times (24558.356 + 6196.871)}{\pi d^3} = -\frac{175.946}{d^2} - \frac{221515.461}{d^3}$$

The diameter of the camshaft in the range of [L_5+L_6+ L_7 +L_8, L_5+L_6+ L_7 +L_8+L_9] can be analyzed by using maximum shear theory i.e., $\sigma_{5x} = \sigma_{5y} = 0$.

$$\tau_{max} = \sqrt{\left(\frac{\sigma_{5z}}{2}\right)^2 + {\tau_{5xz}}^2} = 135\ MPa = \sqrt{\left(-\frac{175.946}{2d^2} - \frac{221515.461}{2d^3}\right)^2 + \left(\frac{311.725 \times 10^3}{d^3}\right)^2}$$

$$d^3 = \sqrt{(-0.652d - 820.428)^2 + (2309.074)^2} \rightarrow d = 13.487\ mm$$

The diameter of the camshaft in the range of [L_5+L_6+ L_7 +L_8, L_5+L_6+ L_7 +L_8+L_9] can also be analyzed by using principal stress i.e., $\sigma_{5x} = \sigma_{5y} = 0$.

$$\sigma_{1,2} = \sigma_{all} = \frac{\sigma_{5z}}{2} \pm \sqrt{\left(\frac{\sigma_{5z}}{2}\right)^2 + {\tau_{5xz}}^2} = 270\ MPa$$

$$= -\frac{175.946}{2d^2} - \frac{221515.461}{2d^3} + \sqrt{\left(-\frac{175.946}{2d^2} - \frac{221515.461}{2d^3}\right)^2 + \left(\frac{311.725 \times 10^3}{d^3}\right)^2}$$

$$d^3 = -0.326d - 410.214 + \sqrt{(-0.326d - 410.214)^2 + (1154.537)^2} \rightarrow d = 9.333\ mm$$

The diameter of the camshaft in the range of [L_5+L_6+ L_7 +L_8, L_5+L_6+ L_7 +L_8+L_9] should be 13.487 mm.

The shearing stress τ_{6xz} and the normal stress σ_{6z} in the range of [L_5+L_6+ L_7 +L_8+L_9, L_5+L_6+ L_7 +L_8+L_9+ L_{10}] are;

$$\tau_{6xz} = \frac{16T}{\pi d^3} = \frac{32 \times 61.207 \times 10^3}{\pi d^3} = \frac{311.725 \times 10^3}{d^3}$$

$$\sigma_{6z} = -\frac{4 \times 138.188}{\pi d^2} - \frac{16\sqrt{2} \times (3293.266 + 0)}{\pi d^3} = -\frac{175.946}{d^2} - \frac{23719.849}{d^3}$$

The diameter of the camshaft in the range of [L_5+L_6+ L_7 +L_8+L_9, L_5+L_6+ L_7 +L_8+L_9+ L_{10}] can be analyzed by using maximum shear theory i.e., $\sigma_{6x} = \sigma_{6y} = 0$.

$$\tau_{max} = \sqrt{\left(\frac{\sigma_{6z}}{2}\right)^2 + {\tau_{6xz}}^2} = 135\ MPa = \sqrt{\left(-\frac{175.946}{2d^2} - \frac{23719.849}{2d^3}\right)^2 + \left(\frac{311.725 \times 10^3}{d^3}\right)^2}$$

$$d^3 = \sqrt{(-0.652d - 87.851)^2 + (2309.074)^2} \rightarrow d = 13.221\ mm$$

The diameter of the camshaft in the range of [L_5+L_6+ L_7 +L_8+L_9, L_5+L_6+ L_7 +L_8+L_9+ L_{10}] can also be analyzed by using principal stress i.e., $\sigma_{6x} = \sigma_{6y} = 0$.

$$\sigma_{1,2} = \sigma_{all} = \frac{\sigma_{6z}}{2} \pm \sqrt{\left(\frac{\sigma_{6z}}{2}\right)^2 + {\tau_{6xz}}^2} = 270\ MPa$$

$$= -\frac{175.946}{2d^2} - \frac{23719.849}{2d^3}$$

$$+ \sqrt{\left(= -\frac{175.946}{2d^2} - \frac{23719.849}{2d^3}\right)^2 + \left(\frac{311.725 \times 10^3}{d^3}\right)^2}$$

$$d^3 = -0.326d - 43.926 + \sqrt{(-0.326d - 43.926)^2 + (1154.537)^2} \rightarrow d = 10.348\ mm$$

The diameter of the camshaft in the range of [L_5+L_6+ L_7 +L_8+L_9, L_5+L_6+ L_7 +L_8+L_9+ L_{10}] should be 13.221 mm.

Discussion on Camshaft Diameters: The diameters of the camshaft are 3.508 mm, 13.005 mm, 13.317 mm, 13.558 mm, 13.487 mm and 13.221 mm for the range of [0, L_5], [L_5, L_5+L_6], [L_5+L_6, L_5+L_6+ L_7], [L_5+L_6+ L_7, L_5+L_6+ L_7 +L_8] , [L_5+L_6+ L_7 +L_8, L_5+L_6+ L_7 +L_8+L_9] and [L_5+L_6+ L_7

+L_8+L_9, L_5+L_6+ L_7 +L_8+L_9+ L_{10}] lengths respectively. The diameter of camshaft for the bevel gear is 13.221 mm as it is. However, its diameter for the single row deep groove ball bearing should be 15 mm because there is 13.487 mm bore bearing. The diameters of the camshaft on the conveyor pulley should be 15.5 mm because the pulley is inserted from top and the camshaft should have a shoulder to support the pulley. Therefore the maximum diameter of the camshaft becomes 16 mm. It is between cam and conveyor pulley. The diameters of the camshaft on the cam becomes 15 mm. Finaly, its diameter on the single direction thrust bearing should be 12 mm which was 3.508 mm. The reason to increase this diameter is that the manufacturing cost becomes high during removing on lathe from 16 mm to 3.508 mm.

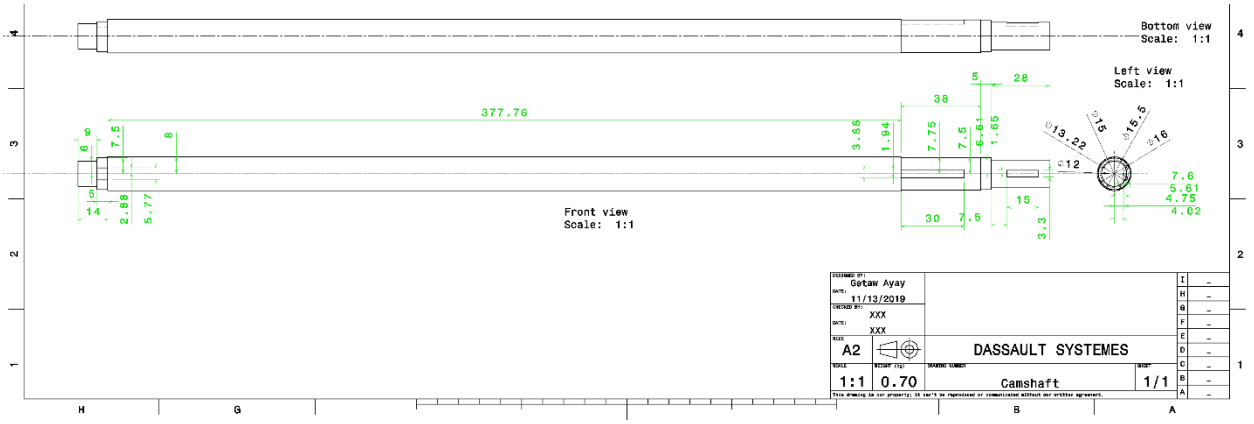

Part Drawing 4-16 Camshaft

Reselection of Thrust Bearings for Camshaft: The bearing on the lower part of camshaft is single direction thrust ball bearing. The bore of bearing was 15 mm. However, after reconsidering all the loads it becomes 12 mm bore single direction thrust ball bearing.

According to bearing catalogue [53], the specification of the single direction thrust ball bearing for 12 mm bore thrust balling bearing is 26 mm outside diameter, 9 mm thickness, 10 KN dynamic basic load ratings, 17 KN static basic load ratings, 0.62 KN fatigue load limit, 9 000 rpm reference speed ratings, 13 000 rpm limiting speed ratings, 0.022 Kg mass and 51101 designation.

Key on Camshaft for Bevel Gear: It is used to transfer power from bevel gear to camshaft and located at top end of camshaft. It is subjected to a torque of 61.207 Nm and the diameter of camshaft on the bevel gear is 13.221 mm. Its cross section is square. The key has taper 1 in 100 on the top side only (R.S. KHURMI and J.K. GUPTA, 2005).

It is made of quenched and tempered (Q&T) steels are from a single heat of 205°c. It has 1640MPa yield strength, 510 BHN and AISI 4140 ASM designation (Budynas Nisbett, 2008). Since, the system is used in the outdoor, its safety factor (n) is three. Hence, the allowable stress becomes:

$$\sigma_{all} = \sigma_w = \frac{\sigma_y}{n} = \frac{1640}{3}\frac{N}{mm^2} = 546.667\ MPa$$

The allowable shear stress can be determined by using maximum shear stress theory:

$$\tau_{all} = \tau_w = \frac{\sigma_{all}}{2} = \frac{546.667}{2}\frac{N}{mm^2} = 273.334\ MPa$$

The shearing stress developed on the key is the ratio of shearing force (F=2T/d) and shearing area (lxt). Where d, T, l and t are diameter of camshaft on the bevel gear, T torque on the camshaft, l length of key and t thickness of the square key. The thickness t is one fourth (t=d/4=13.221/4=3.305 mm) of the diameter of camshaft.

$$\tau = \frac{2T}{dlt} = \frac{8T}{d^2 l} \rightarrow l = \frac{8T}{d^2\tau} = \frac{8 \times 61207}{13.221^2 \times 273.334} = 10.249\ mm$$

The crushing stress developed on the key is the ratio of crushing force (F=2T/d) and resisting area (0.5lt).

$$\sigma_c = \frac{4T}{dlt} = \frac{16T}{d^2 l} \rightarrow l = \frac{16T}{d^2\sigma_c} = \frac{16 \times 61207}{13.221^2 \times 546.667} = 10.249\ mm$$

Discussion of Key on Camshaft for the Bevel Gear: Its length is almost one third of the length of camshaft (28 mm) on the bevel gear part. That means, the length of key way should be at the middle of the length of camshaft on bevel gear part with a length of 15 mm. The depth of key way both on the camshaft and bevel gear becomes 1.653 mm.

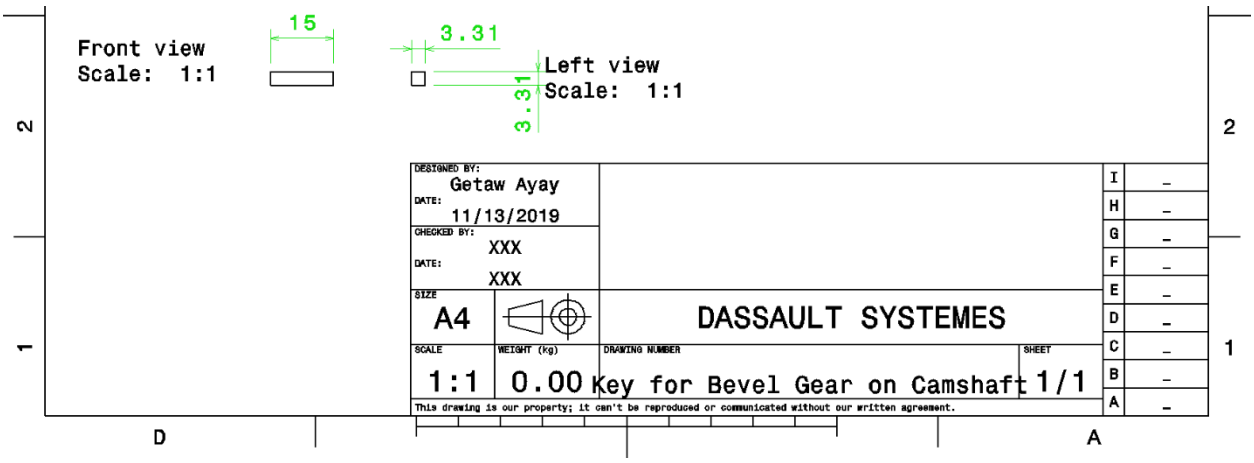

Part Drawing 4-17 Key for Bevel Gear on Camshaft

Key on Camshaft for Conveyor Pulley: It is used to transfer power from camshaft to conveyor pulley and located below the ball bearing. It is subjected to a torque of 2.099 Nm and the diameter of camshaft on the conveyor pulley is 15.5 mm. Its cross section is square. The key has taper 1 in 100 on the top side only (R.S. KHURMI and J.K. GUPTA, 2005).

It is made of high carbon steel of Fe870 Indian standard designation and 870 N/mm^2 tensile strength and 520 N/mm^2 yield stress (σ_y). Since, the system is used in the outdoor, its safety factor (n) is four. Hence, the allowable stress becomes:

$$\sigma_{all} = \sigma_w = \frac{\sigma_y}{n} = \frac{520}{4}\frac{N}{mm^2} = 130MPa$$

The allowable shear stress can be determined by using maximum shear stress theory:

$$\tau_{all} = \tau_w = \frac{\sigma_{all}}{2} = \frac{130}{2}\frac{N}{mm^2} = 65\ MPa$$

The shearing stress developed on the key is the ratio of shearing force (F=2T/d) and shearing area (lxt). Where d, T, l and t are diameter of camshaft on the conveyor pulley, T torque on the camshaft, l length of key and t thickness of the square key. The thickness t is one fourth (t=d/4=15.5/4=3.875 mm) of the diameter of camshaft.

$$\tau = \frac{2T}{dlt} = \frac{8T}{d^2 l} \rightarrow l = \frac{8T}{d^2\tau} = \frac{8 \times 2099}{15.5^2 \times 65} = 1.075\ mm$$

The crushing stress developed on the key is the ratio of crushing force (F=2T/d) and resisting area (0.5lt).

$$\sigma_c = \frac{4T}{dlt} = \frac{16T}{d^2 l} \rightarrow l = \frac{16T}{d^2\sigma_c} = \frac{16 \times 2099}{15.5^2 \times 130} = 1.075\ mm$$

Discussion of Key on Camshaft for the Conveyor Pulley: Its length is smaller than the length of camshaft (38 mm) on the conveyor pulley part. Hence, it is recommended to use 30 mm length of key otherwise it will be difficult to manufacture 1.075 mm length of key and key way in our shop. The depth of key way both on the camshaft and conveyor pulley becomes 1.938 mm.

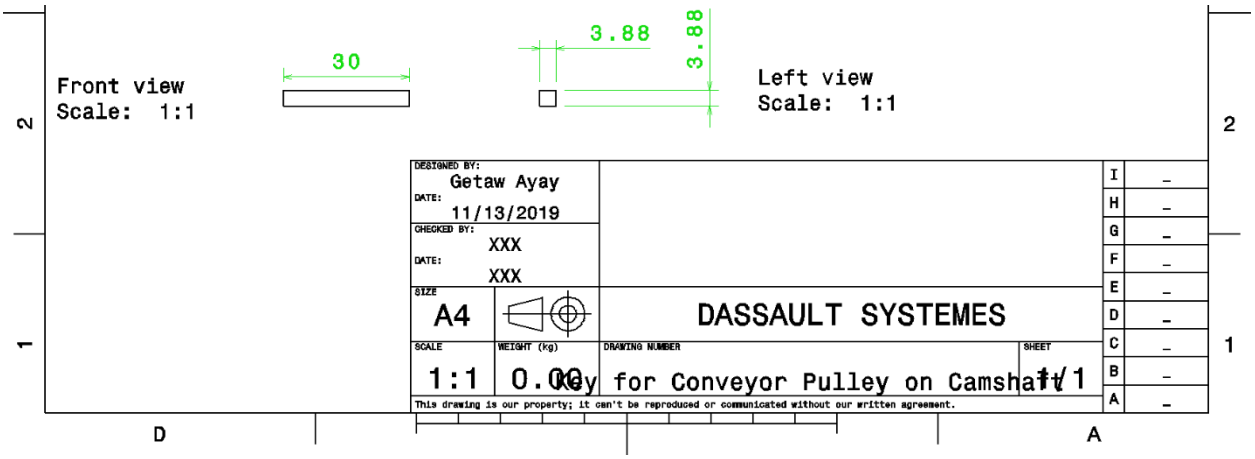

Part Drawing 4-18 Key for Conveyor Pulley on Camshaft

Key on Camshaft for Cam: It is used to transfer power from camshaft to eccentric cam and located above the thrust bearing. It is subjected to a torque of 59.108 Nm and the diameter of camshaft on the cam is 15 mm. Its cross section is square. The maximum length of this key should not greater than 5 mm which is the thickness of eccentric cam. The key has taper 1 in 100 on the top side only (R.S. KHURMI and J.K. GUPTA, 2005).

It is made of quenched and tempered (Q&T) steels are from a single heat of 205^{o}c. It has 1640MPa yield strength, 510 BHN and AISI 4140 ASM designation (Budynas Nisbett, 2008). Since, the system is used in the outdoor, its safety factor (n) is three. Hence, the allowable stress becomes:

$$\sigma_{all} = \sigma_w = \frac{\sigma_y}{n} = \frac{1640}{3}\frac{N}{mm^2} = 546.667\ MPa$$

The allowable shear stress can be determined by using maximum shear stress theory:

$$\tau_{all} = \tau_w = \frac{\sigma_{all}}{2} = \frac{546.667}{2}\frac{N}{mm^2} = 273.334\ MPa$$

The shearing stress developed on the key is the ratio of shearing force (F=2T/d) and shearing area ($l$xt). Where d, T, l and t are diameter of camshaft on the conveyor pulley, T torque on the camshaft, l length of key and t thickness of the square key.

$$\tau = \frac{2T}{dlt} \rightarrow t = \frac{2T}{dl\tau} = \frac{2 \times 59108}{15 \times 5 \times 273.334} = 5.767\ mm$$

The crushing stress developed on the key is the ratio of crushing force (F=2T/d) and resisting area (0.5lt).

$$\sigma_c = \frac{4T}{dlt} \rightarrow t = \frac{4T}{dl\sigma_c} = \frac{4 \times 59108}{15 \times 5 \times 546.667} = 5.767\ mm$$

Discussion of Key on Camshaft for the Bevel Gear: Its length is same as length of cam (5 mm). The depth of key way both on the camshaft and cam becomes 2.883 mm.

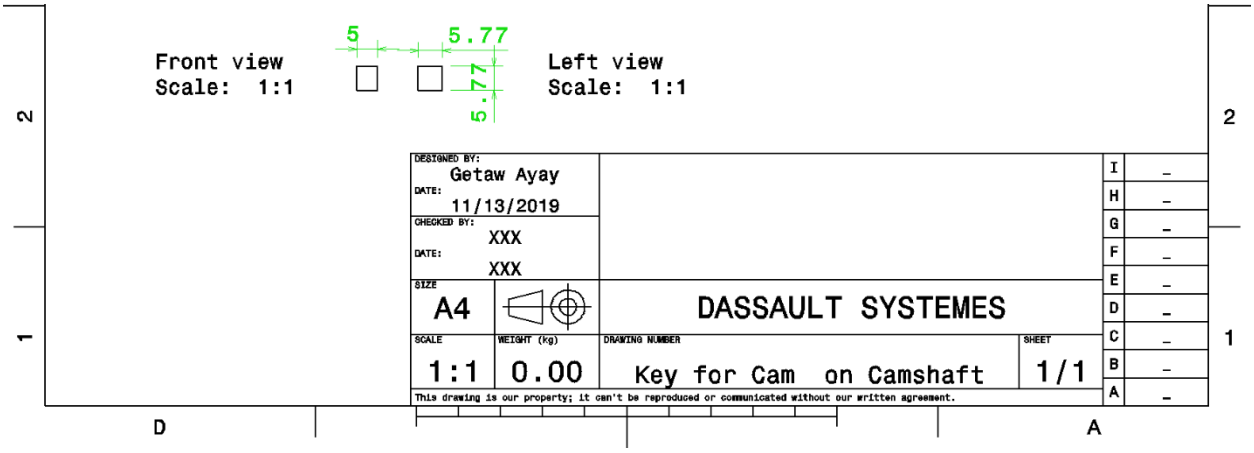

Part Drawing 4-19 Key for Cam on Camshaft

V-Grooved Pulley on Motor Shaft: This pulley is used to transfer power from the DC motor shaft into intermediate shaft. A 5.934 N mm torque is applied on it with 1800 rpm (188.496 rad/s). The pulley is v-grooved with 40 mm groove diameter. The diameter of motor shaft is 16 mm which is taken from the specification of the selected motor. The motor shaft has a 4.768 mm width and 48 mm length square section key.

It is made of grey cast iron (FG 400) with density 7200kg/m^3, 400 MPa tensile strength, proportional limit in tension approximately 40 MPa, E 100 GPa, G 40 GPa and 270 BHN. The properties of cast iron, which make it a valuable material for pulleys, are its low cost, good casting characteristics, high compressive strength, wear resistance and excellent machinability. The compressive strength of cast iron is much greater than the tensile strength (R.S. KHURMI and J.K. GUPTA, 2005). Since the system is used in the outdoor, its safety factor (n) is four. Hence, the allowable stress becomes:

$$\sigma_{all} = \sigma_w = \frac{\sigma_y}{n} = \frac{40}{4}\frac{N}{mm^2} = 10\ MPa$$

The poisons ratio can be calculated using:

$$G = \frac{E}{2(1+v)} \dashrightarrow v = \frac{E}{2G} - 1 = \frac{100}{2 \times 40} - 1 = 0.25$$

The maximum radial and hoop stress set up in the pulley due to rotational speed is given by:

$$\sigma_{r-max} = (3+v)\frac{\rho\omega^2}{8}(R_2 - R_1)^2 = (3+0.25)\frac{7200 \times 188.496^2}{8}(0.02-0.008)^2$$

$$= 14.966 \text{ KPa} \leq \sigma_{all} = 10\ MPa$$

$$\sigma_{H-max} = \frac{\rho\omega^2}{4}\left[(3+v){R_2}^2 + (1-v){R_1}^2\right]$$

$$= \frac{7200 \times 188.496^2}{4}[(3+.25)0.02^2 + (1-.25)0.008^2] = 86.212 \text{ KPa} \leq \sigma_{all} = 10\ MPa$$

Where R_1 and R_2 are internal and external radius of pulley, ϑ is poisson ratio, ρ is density, and ω is rpm of pulley. The internal diameter of pulley is equal to diameter of shaft (18 mm). The above results show that the pulley is safe due to rotational effect.

Based on the international standard (ISO R 155), the distance between shaft centers recommended for lower and upper limit of V-belt drive: $c \geq 0.7(d2 + d1)\ and\ c \leq 2(d2 + d1)\ mm$ respectively and average of 300 mm is selected.

Based on (R.S. KHURMI and J.K. GUPTA, 2005) width of flat or V-belt pulley B= 1.25b; where b= Width of belt and for belt width up to 125 mm, the width of pulley to be greater than belt in mm is by 13. Hence for V-belt of 13 mm width and thickness t=8 mm, the width of the pulley becomes 26 mm. The depth of the groove (d) and groove angle (2β) are 12 mm and 32^o respectively see **Figure** 4-63.

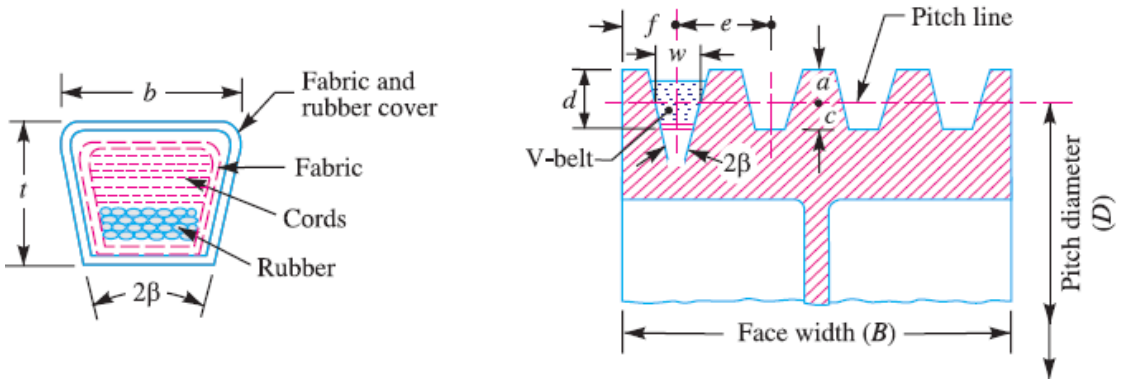

(a) Cross-section of a V-belt (b) Cross-section of V-grooved pulley

Figure 4-63 V-Belt and V-Grooved Pulley [R.S. KHURMI and J.K. GUPTA, 2005]

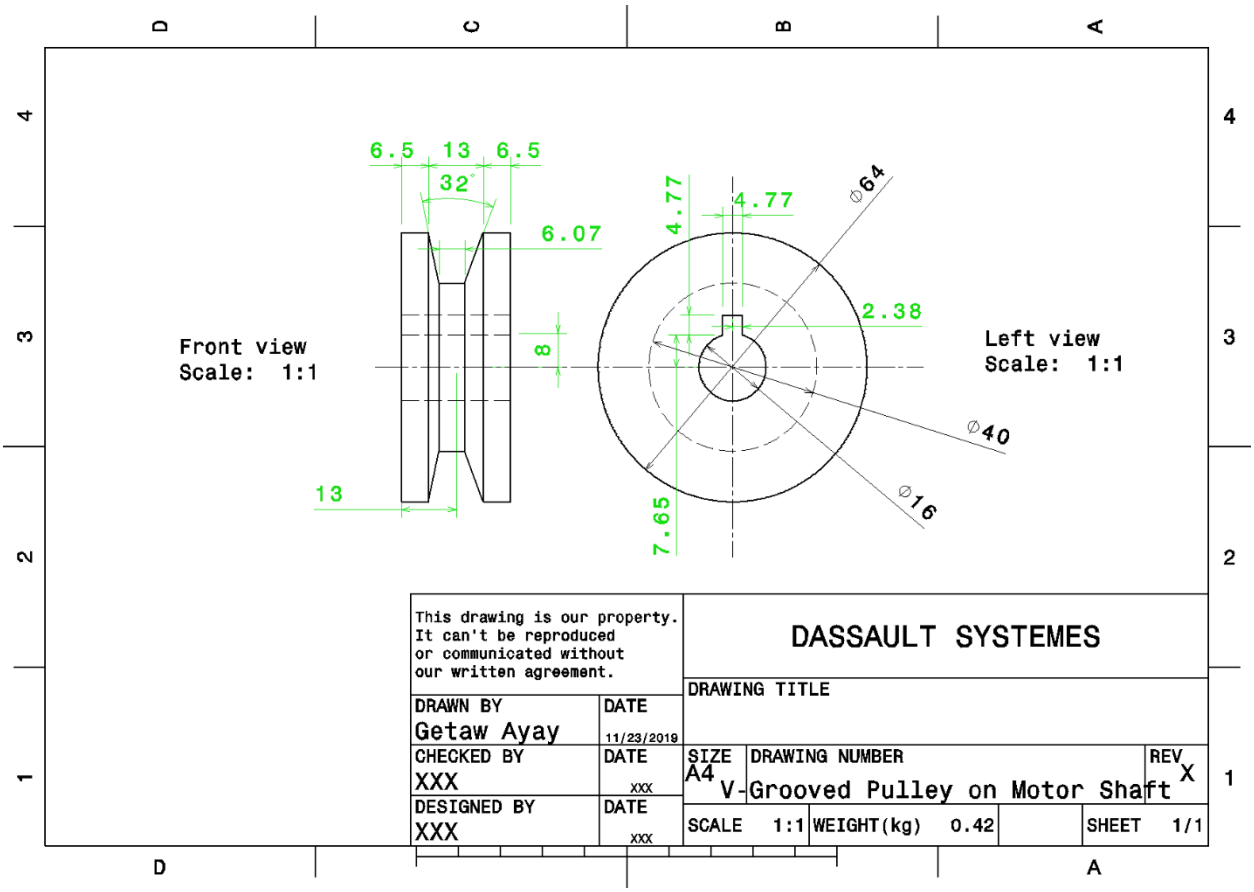

Part Drawing 4-20 V-Grooved Pulley on Motor Shaft

V-Grooved Pulley on Intermediate Shaft: This pulley is used to transfer power from motor shaft pulley into intermediate shaft. A 19.109 Nm torque is applied on it with 561.967 rpm (58.849 rad/s). The pulley is v-grooved 128.12 mm groove diameter. Its width w, depth of groove d and groove angle (2β) are same as the v-grooved pulley on motor shaft which are 26 mm, 12 mm and 32^o respectively see **Figure** 4-63.

It is made of grey cast iron (FG 400) with density 7200 kg/m^3, 400 MPa tensile strength, proportional limit in tension approximately 40 MPa, E 100 GPa, G 40 GPa and 270 BHN. The properties of cast iron, which make it a valuable material for pulleys, are its low cost, good casting characteristics, high compressive strength, wear resistance and excellent machinability. The compressive strength of cast iron is much greater than the tensile strength (R.S. KHURMI and J.K. GUPTA, 2005). Since the system is used in the outdoor, its safety factor (n) is four. Hence, the allowable stress becomes:

$$\sigma_{all} = \sigma_w = \frac{\sigma_y}{n} = \frac{40}{4}\frac{N}{mm^2} = 10\ MPa$$

The poisons ratio can be calculated using:

$$G = \frac{E}{2(1+v)} - - \rightarrow v = \frac{E}{2G} - 1 = \frac{100}{2 \times 40} - 1 = 0.25$$

The maximum radial and hoop stress set up in the pulley due to rotational speed is given by:

$$\sigma_{r-max} = (3+v)\frac{\rho\omega^2}{8}(R_2 - R_1)^2 = (3+0.25)\frac{7200 \times 58.849^2}{8}(0.06406 - 0.0075)^2$$

$$= 32.406\ \text{KPa} = 0.032\ \text{MPa} \leq \sigma_{all} = 10\ MPa$$

$$\sigma_{H-max} = \frac{\rho\omega^2}{4}\left[(3+v){R_2}^2 + (1-v){R_1}^2\right]$$

$$= \frac{7200 \times 58.849^2}{4}[(3+0.25)0.06406^2 + (1-0.25)0.0075^2] = 0.083\ \text{MPa} \leq \sigma_{all}$$

Where R_1 and R_2 are internal and external radius of pulley, ϑ is poison ratio, ρ is density, and ω is rpm of pulley. The internal radius of pulley is equal to diameter of shaft (15 mm). The above results show that the pulley is safe due to rotational effect. The width of the pulley (B), the depth of the groove (d) and groove angle (2β) are 26 mm, 12 mm and 32^o respectively which are determined in the design of v-grooved pulley for the motor shaft.

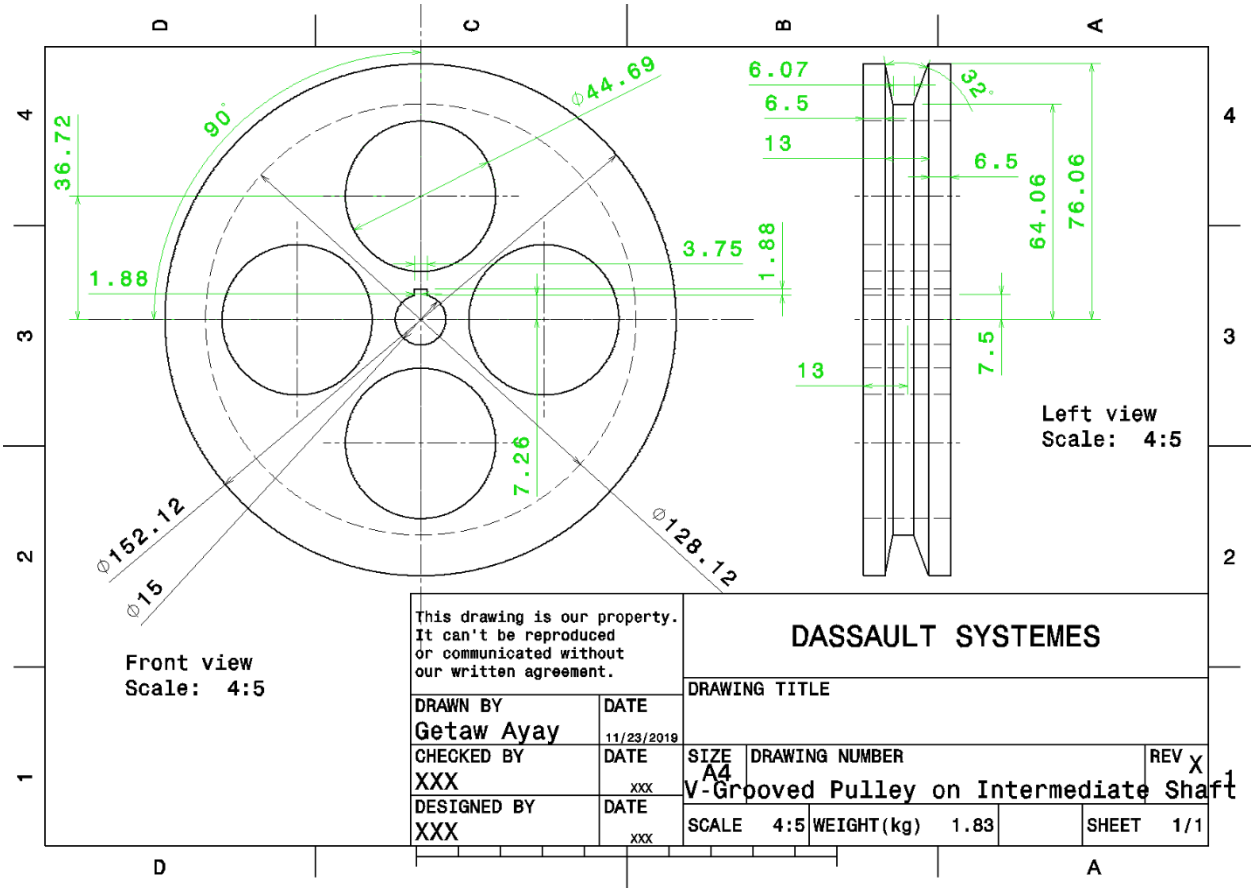

Part Drawing 4-21 V-Grooved Pulley on Intermediate Shaft

Intermediate Shaft: The force analysis of the intermediate shaft can be done by considering all the machine elements attached on it. The internal diameters of the machine elements are bevel gear (d_{4G}), ball bearing (d_{4b}), empty part (d_{4E}), drive pulley (d_{4p}) and thrust bearing (d_{4T}) from right to left as shown in **Figure** 4-64. The actual position of the shaft is horizontal; bevel gear right and thrust bearing left end.

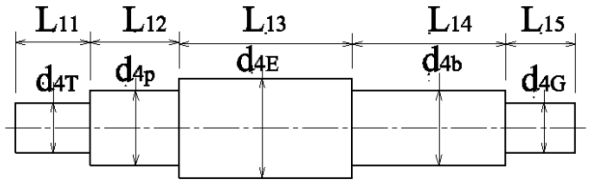

Figure 4-64 2D Sketch of Intermediate Shaft

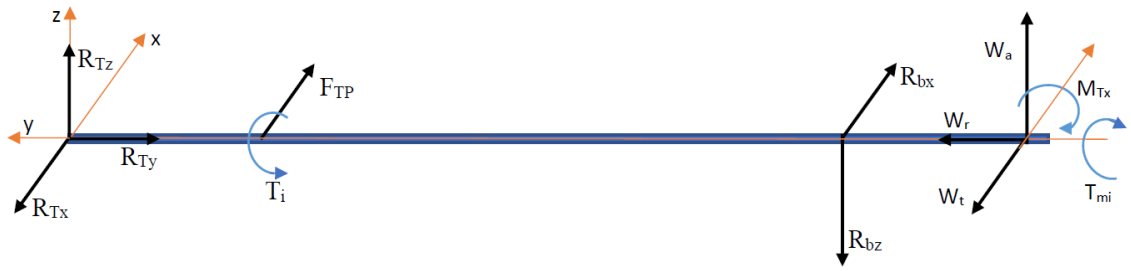

Figure 4-65 FBD of Intermediate Shaft

The parameters like torque on pinion gear (T_{mi}); tangential (W_t=1273.952 N), radial (W_r=442.610 N) and axial (W_a=138.188 N) forces of pinion; tangential force on drive pulley (F_{TP}=298.298 N) and torque on pulley (T_{Pi}=19.109 Nm) are determined in kinematics, kinetics and force analysis of bevel gear. The remaining parameters can be analyzed by applying equation of motion.

$$\sum F_x = 0$$

$$R_{bx} - R_{Tx} - W_t = 0 \longrightarrow R_{bx} - R_{Tx} = W_t = 1273.952\ N \text{ ----------4-85}$$

$$\sum F_y = 0$$

$$R_{Ty} = W_r = 442.6100$$

$$\sum F_z = 0$$

$$R_{Tz} - R_{bz} - W_a = 0 \longrightarrow R_{Tz} - R_{bz} = W_a = 138.188\ N \text{ ----------4-86}$$

$$\sum M_x = 0$$

$$\left(L_{11} + L_{12} + L_{13} + \frac{L_{14}}{2}\right) R_{bz} - \left(L_{11} + L_{12} + L_{13} + L_{14} + \frac{L_{15}}{2}\right) W_a + M_{Tx} = 0 \text{ ----------4-87}$$

$$\sum M_z = 0$$

$$\left(L_{11} + \frac{L_{12}}{2}\right) F_{Tp} + \left(L_{11} + L_{12} + L_{13} + \frac{L_{14}}{2}\right) R_{bx} - \left(L_{11} + L_{12} + L_{13} + L_{14} + \frac{L_{15}}{2}\right) W_t = 0 \text{ -- 4-88}$$

$$\sum T_y = 0$$

$$-T_i + T_{mi} = 0 \text{ ----------4-89}$$

Note: In the force analysis of intermediate shaft, there are six unknows (L_{11}, L_{14}, R_{Tx}, R_{Tz}, R_{bx} and R_{bz}) and four equations which is statically indeterminate. Since the lengths and diameters are unknown, it can't be solved by using the technique of displacement method for statically indeterminate problem. For the time being, the shaft can be designed by considering the part from bevel gear up to ball bearing which is positioned on the right end of the shaft see **Figure** 4-66.

Because it is subjected to a higher load. After analyzing all the above unknowns, it is good to redesign the shaft by considering the whole part.

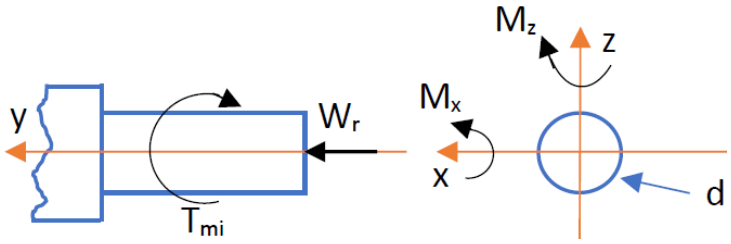

Figure 4-66 FBD of Intermediate Shaft on Gear Portion

The loads on the pinion gear are axial compressive (W_r=442.610 N), bending loads (W_a and W_t; 138.188 N and 1273.952 N respectively) and torsional moment (T_i=19.109 Nm). This shows that the shaft is subjected to a combined load. The bending moment in the z-axis is the product of tangential gear force (W_t) and half of thickness of bevel gear (L_{15}=28 mm).

$$M_z = W_t \frac{L_{15}}{2} = 1273.952 \times \frac{28}{2} = 17835.328\ Nmm = 17.835\ Nm$$

The bending moment in the x-axis is the product of axial gear force (W_a) and half of thickness of bevel gear (L_{15}=28 mm) plus bending moment ($M_{Tx}=W_rR_{mi}$) by axial gear force (W_r=442.610 N).

$$M_x = W_r R_{mi} - W_a \frac{L_{15}}{2} = \left(442.610 \times 15 - 138.188 \times \frac{28}{2}\right) Nmm = 4.705\ Nm$$

Materials for Intermediate Shaft: It is made of high carbon steel of Fe870 Indian standard designation and 870 N/mm^2 tensile strength and 520 N/mm^2 yield stress (σ_y). Since the system is used in the outdoor, its safety factor (n) is four. Hence, the allowable stress becomes:

$$\sigma_{all} = \sigma_w = \frac{\sigma_y}{n} = \frac{520}{4} \frac{N}{mm^2} = 130MPa$$

The allowable shear stress can be determined by using maximum shear stress theory:

$$\tau_{all} = \tau_w = \frac{\sigma_{all}}{2} = \frac{130}{2} \frac{N}{mm^2} = 65\ MPa$$

The axial stress in the camshaft can be determined by Beer and et al (2012) equation 4.58 by considering $\sigma_x = \sigma_z = 0$

$$\sigma_y = \frac{W_a}{A} - \frac{M_x x}{I_x} + \frac{M_z y}{z}$$

The above normal stress (σ_y) becomes maximum at 45^o between negative x- and y-axes when x=y=$d/\sqrt{8}$. The unit of the diameter is millimeter.

$$A = \frac{\pi d^2}{4}, I_x = \frac{\pi d^4}{64} = I_y$$

$$\sigma_z = \frac{4W_a}{\pi d^2} - \frac{16\sqrt{2}M_z}{\pi d^3} - \frac{16\sqrt{2}M_x}{\pi d^3} = -\frac{4 \times 138.188}{\pi d^2} - \frac{16\sqrt{2} \times (17.835 + 4.705) \times 10^3}{\pi d^3}$$

$$= -\frac{175.946}{d^2} - \frac{162.345 \times 10^3}{d^3}$$

The shearing stress due to torque T is;

$$\tau_{xz} = \frac{TC}{J}$$

$$C = \frac{d}{2} \; and \; J = \frac{\pi d^4}{32}$$

$$\tau_{xz} = \frac{16T}{\pi d^3} = \frac{16 \times 19.109 \times 10^3}{\pi d^3} = \frac{97.321 \times 10^3}{d^3}$$

The maximum shearing stress (τ_{max}) can be analyze by using Beer and et al (2012) equation 7.16.

$$\tau_{max} = \tau_{all} = \sqrt{\left(\frac{\sigma_z}{2}\right)^2 + {\tau_{xz}}^2}$$

$$65 \; \frac{N}{mm^2} = \sqrt{\left(-\frac{175.946}{2d^2} - \frac{162.345 \times 10^3}{2d^3}\right)^2 + \left(\frac{97.321 \times 10^3}{d^3}\right)^2}$$

$$d^3 = \sqrt{(-1.353d - 1248.808)^2 + (1497.246)^2}$$

The solution of the above equation is $d = 12.516 \; mm$.

The principal stress ($\sigma_{1,2}$) can be determined using Beer and et al (2012) equation 7.13.

$$\sigma_{1,2} = \sigma_{all} = \frac{\sigma_z}{2} \pm \sqrt{\left(\frac{\sigma_z}{2}\right)^2 + {\tau_{xz}}^2}$$

$$130 \; \frac{N}{mm^2} =$$

$$-\frac{175.946}{2d^2} - \frac{162.345 \times 10^3}{2d^3} \pm \sqrt{\left(-\frac{175.946}{2d^2} - \frac{162.345 \times 10^3}{2d^3}\right)^2 + \left(\frac{97.321 \times 10^3}{d^3}\right)^2}$$

$$d^3 = -0.677d - 624.404 + \sqrt{(-0.677d - 624.404)^2 + (748.623)^2}$$

The solution of the above equation is $d = 4.063 \; mm$.

Therefore, the diameter of intermediate shaft is 15 mm because there is no bore of bearings between 12.948 mm and 15 mm.

Note: Still the numbers of unknowns are greater than number of equations. Hence, it is advisable to know the dimension of bearings thickness.

Selection of Bearings for Intermediate Shaft: The bearing on the right end of intermediate shaft is sealed single row deep groove ball bearing. The bore of bearing is 15 mm.

According to bearing catalogue [51], the specification of the sealed single row deep groove 15 mm bore balling bearing is 24 mm outside diameter, 5 mm thickness, 1.56 KN dynamic basic load ratings, 0.8 KN static basic load ratings, 0.034 KN fatigue load limit, 60 000 rpm reference speed ratings, 38 000 rpm limiting speed ratings, 0.0074 Kg mass and 61802 designation.

The bearing on left end of the intermediate shaft is single direction thrust ball bearing. The bore of the bearing is 15 mm. According to bearing catalogue [53], the specification of the single direction thrust ball bearing for 15 mm bore thrust balling bearing is 28 mm outside diameter, 9 mm thickness, 9 KN dynamic basic load ratings, 15 KN static basic load ratings, 0.56 KN fatigue load limit, 8500 rpm reference speed ratings, 12 000 rpm limiting speed ratings, 0.023 Kg mass and 51102 designation.

The lengths L_{11}, L_{12}, L_{14} and L_{15} becomes 9 mm, 26 mm, 5 mm and 28 mm. The length L13 is a clearance between v-grooved pulley and bevel gear box which is 5 mm. The reaction forces on both bearings can be determined as follows.

$$R_{bx} - R_{Tx} = W_t = 1273.952\ N$$

$$R_{Ty} = W_r = 442.6100$$

$$R_{Tz} - R_{bz} = W_a = 138.188\ N$$

$$37.5R_{bz} - 59 \times 138.188 + 15 \times 442.610 = 0 \rightarrow 37.5R_{bz} = 1513.942 \rightarrow R_{bz} = 40.372\ N$$

$$\rightarrow R_{Tz} = 40.372 + 138.188 = 178.56\ N$$

$$22 \times 298.298\ + 37.5R_{bx} - 59 \times 1273.952 = 0 \rightarrow 37.5R_{bx} = 68600.612$$

$$\rightarrow R_{bx} = 1829.350\ N$$

$$\rightarrow R_{Tx} = 1829.350 - 1273.952 = 555.398\ N$$

The shear force and bending moment diagrams can be constructed after deriving the equations of them in each ranges.

The transverse forces are applied about x- and z-axes. So that the bending moment is about x-and z-axes. The shaft should be designed for the cumulative or resultant effect of these bending moments as well as the torsional moment. The resultant moment can be determined after determining bending moment about x- and z-axes in each section.

The free body diagram of the intermediate shaft about x-axis is shown in **Figure** 4-67. The loads w_1, w_2, w_3 and w_4 are distributed loads over length L_{11}, L_{12}, L_{14} and L_{15} respectively i.e., $w_1 = {R_{Tx}}/{L_{11}} = \frac{555.398}{9} = 61.711\ N/mm,$ $w_2 = {F_{Tp}}/{L_{12}} = \frac{298.298}{26} = 11.473\ N/mm,$ $w_3 = {R_{bx}}/{L_{14}} = \frac{1829.350}{5} = 365.87\ N/mm$ and $w_4 = {w_t}/{L_{15}} = \frac{1273.952}{28} = 45.498\ N/mm.$

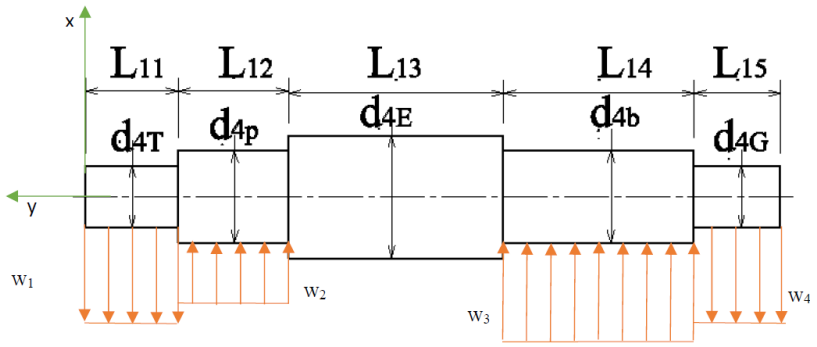

Figure 4-67 FBD Diagram of Intermediate Shaft about x-axis

The bending moment equation (M_{1z}) on a range of length [0, L_{11}] can be derived by taking an arbitrary section between this range by using equilibrium equation see **Figure** 4-68.

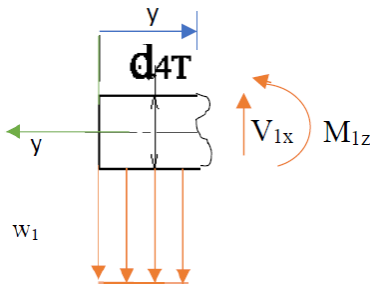

Figure 4-68 FBD between [0, L_{11}]

$$\sum \mathrm{M_z} = 0 = \mathrm{w_1}\frac{y^2}{2} + \mathrm{M_{1y}} \longrightarrow \mathrm{M_{1z}} = -\mathrm{w_1}\frac{\mathrm{y}^2}{2} = 30.856\mathrm{z}^2$$

The bending moment equation is quadrtic and it becomes maximum at y=L_{11}=9 mm i.e., M_{1z} [0, 2499.336] Nmm.

The bending moment equation (M_{2z}) on a range of length [L_{11}, $L_{11} + L_{12}$] can be derived by taking an arbitrary section between this range by using equilibrium equation see **Figure** 4-69.

$$\sum \mathrm{M_z} = 0 = \mathrm{w_1 L_{11}}(\mathrm{y} - \frac{\mathrm{L_{11}}}{2}) - \mathrm{w_2}\frac{(\mathrm{y} - L_{11})^2}{2} + \mathrm{M_{2z}} \longrightarrow \mathrm{M_{2z}} = -\mathrm{w_1 L_{11}}\left(\mathrm{y} - \frac{\mathrm{L_{11}}}{2}\right)$$
$$+ \mathrm{w_2}\frac{(\mathrm{y} - L_{11})^2}{2} = \mathrm{w_2}\frac{y^2}{2} - (\mathrm{w_2} + \mathrm{w_1})\mathrm{L_{11}}y + (\mathrm{w_2} + \mathrm{w_1})\frac{{\mathrm{L_{11}}}^2}{2}$$

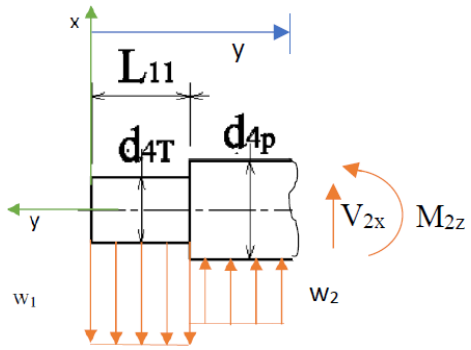

Figure 4-69 FBD between $[L_{11}, L_{11} + L_{12}]$

$$= 5.737y^2 - 658.656y + 2963.952$$

The bending moment equation is quadratic and it becomes maximum at y=L_{11}+L_{12}=35 mm i.e., M_{2z} [2499.255, -13061.183] Nmm.

The bending moment equation (M_{3z}) on a range of length $[L_{11} + L_{12}, L_{11} + L_{12} + L_{13}]$ can be derived by taking an arbitrary section between this range by using equilibrium equation see **Figure** 4-70.

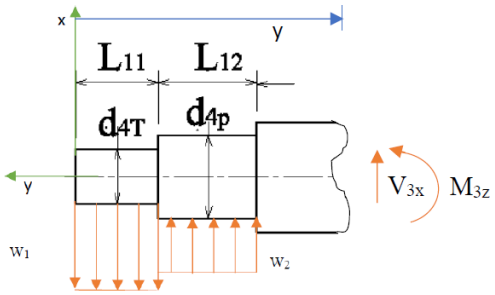

Figure 4-70 FBD between $[L_{11} + L_{12}, L_{11} + L_{12} + L_{13}]$

$$\sum \mathrm{M_z} = 0 = \mathrm{w_1 L_{11}}\left(\mathrm{y} - \frac{\mathrm{L_{11}}}{2}\right) - \mathrm{w_2 L_{12}}\left(\mathrm{z} - L_{11} - \frac{\mathrm{L_{12}}}{2}\right) + \mathrm{M_{3z}}$$

$$\rightarrow \mathrm{M_{3z}} = -\mathrm{w_1 L_{11}}\left(\mathrm{y} - \frac{\mathrm{L_{11}}}{2}\right) + \mathrm{w_2 L_{12}}\left(\mathrm{z} - L_{11} - \frac{\mathrm{L_{12}}}{2}\right)$$

$$= (-\mathrm{w_1 L_{11}} + \mathrm{w_2 L_{12}})z + \mathrm{w_1}\frac{{\mathrm{L_{11}}}^2}{2} - \mathrm{w_2 L_{12}}\left(L_{11} + \frac{\mathrm{L_{12}}}{2}\right)$$

$$= -257.1z - 4063.265$$

The bending moment equation is linear and it becomes maximum at y=L_{11}+L_{12}+L_{13} = 40 mm i.e., M_{3z} [-13061.765, -14347.265] Nmm.

The bending moment equation (M_{4z}) on a range of length $[L_{11} + L_{12} + L_{13}, L_{11} + L_{12} + L_{13} + L_{14}]$ can be derived by taking an arbitrary section between this range by using equilibrium equation see **Figure** 4-71.

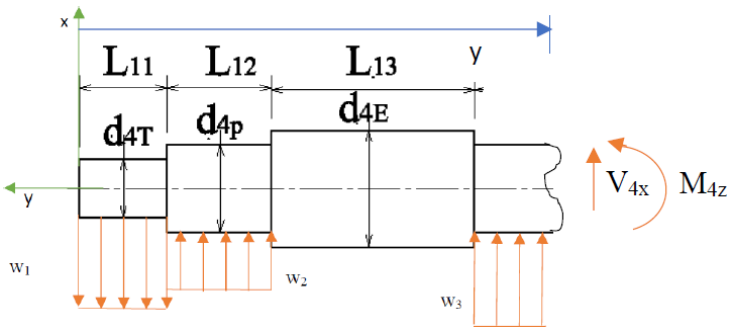

Figure 4-71 FBD between $[L_{11} + L_{12} + L_{13}, L_{11} + L_{12} + L_{13} + L_{14}]$

$$\sum M_z = 0 = w_1 L_{11}\left(y - \frac{L_{11}}{2}\right) - w_2 L_{12}\left(z - L_{11} - \frac{L_{12}}{2}\right) - w_3 \frac{(z - L_{11} - L_{12} - L_{13})^2}{2} + M_{4z}$$

$$\rightarrow M_{4z} = -w_1 L_{11}\left(y - \frac{L_{11}}{2}\right) + w_2 L_{12}\left(z - L_{11} - \frac{L_{12}}{2}\right) + w_3 \frac{(z - L_{11} - L_{12} - L_{13})^2}{2}$$

$$= w_3 \frac{y^2}{2} + \left(-w_1 L_{11} + w_2 L_{12} - w_3(L_{11} + L_{12} + L_{13})\right)y + w_1 \frac{{L_{11}}^2}{2}$$

$$- w_2 L_6 \left(L_{11} + \frac{L_{12}}{2}\right) + w_3 \frac{(L_{11} + L_{12} + L_{13})^2}{2}$$

$$= 182.935y^2 - 14891.900y + 288632.735$$

The bending moment equation is linear and it becomes maximum at y=$L_{11} + L_{12} + L_{13}$=40 mm i.e., M_{4z} [-14347.265, -11059.390] Nmm.

The bending moment equation (M_{5z}) on a range of length $[L_{11} + L_{12} + L_{13} + L_{14}, L_{11} + L_{12} + L_{13} + L_{14} + L_{15}]$ can be derived by taking an arbitrary section between this range by using equilibrium equation see **Figure** 4-72.

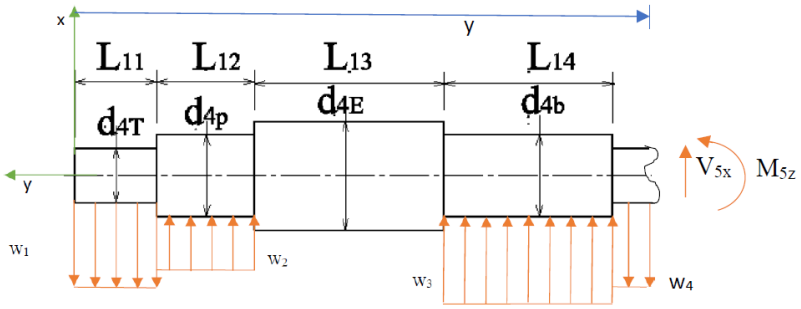

Figure 4-72 FBD between $[L_{11} + L_{12} + L_{13} + L_{14}, L_{11} + L_{12} + L_{13} + L_{14} + L_{15}]$

$$\sum M_z = 0 = w_1 L_{11}\left(y - \frac{L_{11}}{2}\right) - w_2 L_{12}\left(z - L_{11} - \frac{L_{12}}{2}\right) - w_3 L_{14}\left(z - L_{11} - L_{12} - L_{13} - \frac{L_{14}}{2}\right)$$

$$+ w_4 \frac{(z - L_{11} - L_{12} - L_{13} - L_{14})^2}{2} + M_{5z}$$

$$\rightarrow M_{5z} = -w_1 L_{11}\left(y - \frac{L_{11}}{2}\right) + w_2 L_{12}\left(z - L_{11} - \frac{L_{12}}{2}\right) + w_3 L_{14}\left(z - L_{11} - L_{12} - L_{13} - \frac{L_{14}}{2}\right) - w_4 \frac{(z - L_{11} - L_{12} - L_{13} - L_{14})^2}{2}$$

$$= -w_4 \frac{y^2}{2} + \left(-w_1 L_{11} + w_2 L_{12} + w_3 L_{11} + w_4 (L_{11} + L_{12} + L_{13} + L_{14})\right) y + w_1 \frac{L_{11}^2}{2} - w_2 L_{12}\left(L_{11} + \frac{L_{12}}{2}\right) - w_3 L_{14}\left(L_{11} + L_{12} + L_{13} + \frac{L_{14}}{2}\right) - w_4 \frac{(L_{11} + L_{12} + L_{13} + L_{14})^2}{2} = -22.749y^2 + 3619.660y - 128181.115$$

The bending moment equation is linear and it becomes maximum at z=45 mm i.e., M_{5z} [-11363.14, 9566.684] Nmm.

The free body diagram of the intermediate shaft about z-axis is shown in **Figure** 4-73. The loads w_5, w_6, and w_7 are distributed loads over length L_{11}, L_{14} and L_{15} respectively i.e., $w_5 = {}^{R_{Tz}}/_{L_{11}} = \frac{178.56}{9} = 19.84\ N/mm$, $w_6 = {}^{R_{bz}}/_{L_{14}} = \frac{40.372}{5} = 8.074\ N/mm$, and $w_7 = {}^{W_a}/_{L_{15}} = \frac{138.188}{28} = 4.935\ N/mm$.

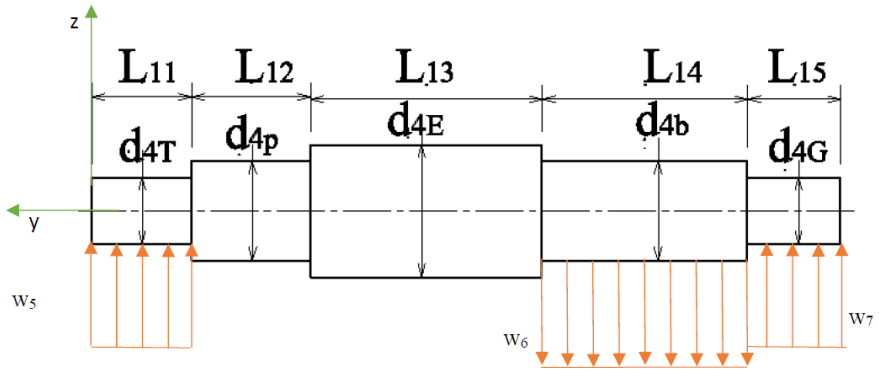

Figure 4-73 FBD Diagram of Intermediate Shaft about z-axis

The bending moment equation (M_{1x}) on a range of length [0, L_{11}] can be derived by using equilibrium equation by taking an arbitrary section between this range see **Figure** 4-74.

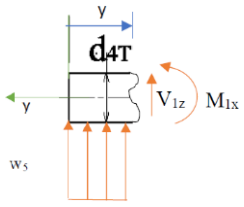

Figure 4-74 FBD between [0, L_{11}]

$$\sum M_x = 0 = -w_5 \frac{y^2}{2} + M_{1x} \longrightarrow M_{1x} = w_5 \frac{y^2}{2} = 9.92y^2$$

The bending moment equation is quadrtic and it becomes maximum at y=L_{11}=9 mm i.e., M_{1x} [0, 803.52] Nmm.

The bending moment equation (M_{2x}) on a range of length $[L_{11}, L_{11} + L_{12}]$ can be derived by taking an arbitrary section between this range by using equilibrium equation see **Figure** 4-75.

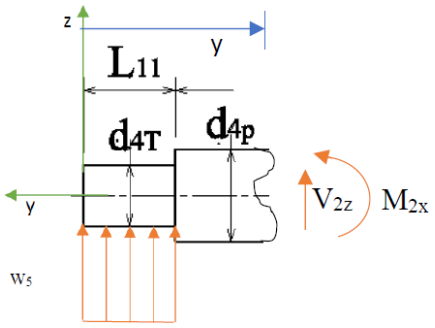

Figure 4-75 FBD between $[L_{11}, L_{11} + L_{12}]$

$$\sum M_x = 0 = -w_5 L_{11}\left(y - \frac{L_{11}}{2}\right) + M_{2x} \longrightarrow M_{2x} = w_5 L_{11}\left(y - \frac{L_{11}}{2}\right) = w_5 L_{11} y - w_5 \frac{{L_{11}}^2}{2}$$
$$= 178.56y - 803.52$$

The bending moment equation is linear and it becomes maximum at y=L_{11}+L_{12}=35 mm i.e., M_{2x} [803.52, 5446.08] Nmm.

The bending moment equation (M_{3x}) on a range of length $[L_{11} + L_{12}, L_{11} + L_{12} + L_{13}]$ can be derived by taking an arbitrary section between this range by using equilibrium equation see **Figure** 4-76.

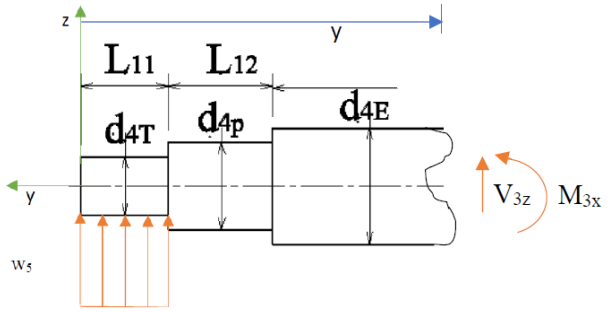

Figure 4-76 FBD between $[L_{11} + L_{12}, L_{11} + L_{12} + L_{13}]$

$$\sum M_x = 0 = -w_5 L_{11}\left(y - \frac{L_{11}}{2}\right) + M_{3x} \longrightarrow M_{3x} = w_5 L_{11}\left(y - \frac{L_{11}}{2}\right) = w_5 L_{11} y - w_5 \frac{{L_{11}}^2}{2}$$
$$= 178.56y - 803.52$$

The bending moment equation is linear and it becomes maximum at y=L_{11}+L_{13}+L_{13} =40 mm i.e.,

M_{3X} [5446.08, 6338.88] Nmm.

The bending moment equation (M_{4X}) on a range of length $[L_{11} + L_{12} + L_{13}, L_{11} + L_{12} + L_{13} + L_{14}]$ can be derived by taking an arbitrary section between this range by using equilibrium equation see **Figure** 4-77.

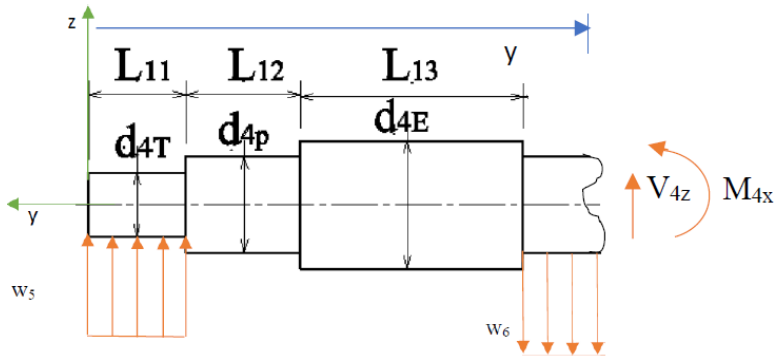

Figure 4-77 FBD between $[L_{11} + L_{12} + L_{13}, L_{11} + L_{12} + L_{13} + L_{14}]$

$$\sum M_x = 0 = -w_5 L_{11}\left(y - \frac{L_{11}}{2}\right) + w_6 \frac{(y - L_{11} - L_{12} - L_{13})^2}{2} + M_{4x} \rightarrow M_{4x}$$

$$= w_5 L_{11}\left(y - \frac{L_{11}}{2}\right) - w_6 \frac{(y - L_{11} - L_{12} - L_{13})^2}{2}$$

$$= -w_6 \frac{y^2}{2} + \left(w_5 L_{11} + w_6(L_{11} + L_{12} + L_{13})\right)y - w_5 \frac{{L_{11}}^2}{2}$$

$$- w_6 \frac{(L_{11} + L_{12} + L_{13})^2}{2}$$

$$= -4.037y^2 + 501.52y - 7262.72$$

The bending moment equation is quadratic and it becomes maximum at y=L_{11}+L_{12}+ L_{13} +L_{14}=40 mm i.e., M_{4x} [6338.88, 7130.755] Nmm.

The bending moment equation (M_{5x}) on a range of length $[L_{11} + L_{12} + L_{13} + L_{14}, L_{11} + L_{12} + L_{13} + L_{14} + L_{15}]$ can be derived by taking an arbitrary section between this range by using equilibrium equation see **Figure** 4-78.

$$\sum M_x = 0 = -w_5 L_{11}\left(y - \frac{L_{11}}{2}\right) + w_6 L_{14}\left(y - L_{11} - L_{12} - L_{13} - \frac{L_{14}}{2}\right)$$

$$- w_7 \frac{(y - L_{11} - L_{12} - L_{13} - L_{14})^2}{2} + M_{5x}$$

$$\rightarrow \mathrm{M_{5x}} = \mathrm{w_5 L_{11}}\left(\mathrm{y} - \frac{\mathrm{L_{11}}}{2}\right) - \mathrm{w_6 L_{14}}\left(\mathrm{y} - L_{11} - L_{12} - L_{13} - \frac{\mathrm{L_{14}}}{2}\right) + \mathrm{w_7}\frac{(\mathrm{y} - L_{11} - L_{12} - L_{13} - \mathrm{L_{14}})^2}{2}$$

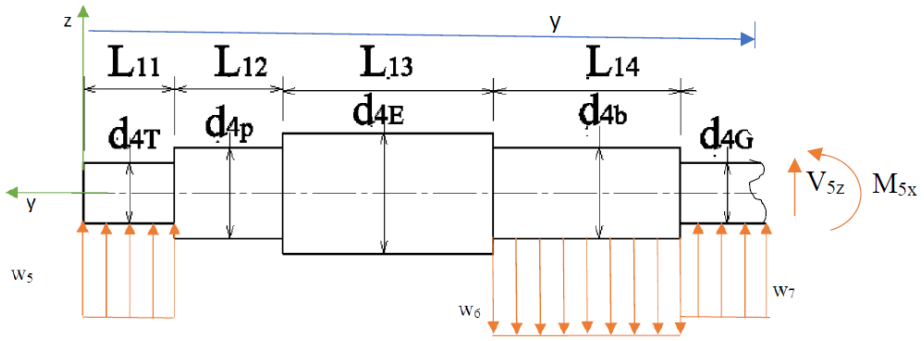

Figure 4-78 FBD between $[L_{11} + L_{12} + L_{13} + L_{14}, L_{11} + L_{12} + L_{13} + L_{14} + L_{15}]$

$$= \mathrm{w_7}\frac{\mathrm{y}^2}{2} + \left(\mathrm{w_5 L_{11}} - \mathrm{w_6 L_{14}} - \mathrm{w_7}(L_{11} + L_{12} + L_{13} + \mathrm{L_{14}})\right)y - \mathrm{w_5}\frac{{\mathrm{L_{11}}}^2}{2} + \mathrm{w_6 L_{14}}\left(L_{11} + L_{12} + L_{13} + \frac{\mathrm{L_{14}}}{2}\right) + \mathrm{w_7}\frac{(L_{11} + L_{12} + L_{13} + \mathrm{L_{14}})^2}{2}$$

$$= 2.468\mathrm{y}^2 - 82.887y + 5908.978$$

The bending moment quadratic is linear and it becomes maximum at y= $L_{11} + L_{12} + L_{13} + L_{14} + L_{15}$=63 mm i.e., $\mathrm{M_{5x}}$ [7176.763, 10482.589] Nmm.

The diameter of the intermediate shaft can be analyzed by using τ_{xz} and σ_z in each section. The torque in the range of [0, $\mathrm{L_{11}}$] is zero i.e., $\tau_{xy} = 0$ and the normal stress σ_y is;

$$\sigma_{1y} = -\frac{4 \times 442.610}{\pi d^2} - \frac{8\sqrt{2} \times (2499.336 + 803.52)}{\pi d^3} = -\frac{563.549}{d^2} - \frac{23788.92}{d^3}$$

The diameter of the intermediate shaft in the range of [0, $\mathrm{L_{11}}$] can be analyzed by using maximum shear theory i.e., $\sigma_{1x} = \sigma_{1z} = \tau_{1xy} = 0$.

$$\tau_{max} = \tau_{all} = \sqrt{\left(\frac{\sigma_{1y}}{2}\right)^2 + {\tau_{xy}}^2} = 65\ MPa = \frac{\sigma_{1y}}{2} = \frac{563.549}{2d^2} + \frac{23788.92}{2d^3}$$

$$d^3 = 4.335d + 182.992 \rightarrow d = 5.932\ mm$$

The diameter of the intermediate shaft in the range of [0, $\mathrm{L_{11}}$] can also be analyzed by using principal stress i.e., $\sigma_{1x} = \sigma_{1z} = \tau_{1xy} = 0$.

$$\sigma_{1,2} = \sigma_{all} = \frac{\sigma_{1y}}{2} \pm \sqrt{\left(\frac{\sigma_{1y}}{2}\right)^2 + {\tau_{xy}}^2} = 130\ MPa = \sigma_{1y} = \frac{563.549}{d^2} + \frac{23788.92}{d^3}$$

$$d^3 = 4.335d + 182.992 \rightarrow d = 5.932\,mm$$

The diameter of the intermediate shaft in the range of [0, L_{11}] should be 5.932 mm.

The shearing stress τ_{2xy} and the normal stress σ_{2y} in the range of [L_{11}, L_{11}+L_{12}] are;

$$\tau_{2xy} = \frac{16T_{mi}}{\pi d^3} = \frac{16 \times 19.109 \times 10^3}{\pi d^3} = \frac{97.321 \times 10^3}{d^3}$$

$$\sigma_{2z} = -\frac{4 \times 442.610}{\pi d^2} - \frac{16\sqrt{2} \times (13061.183 + 5446.08\,)}{\pi d^3} = -\frac{563.549}{d^2} - \frac{133299.127}{d^3}$$

The diameter of the intermediate shaft in the range of [L_{11}, L_{11}+L_{12}] can be analyzed by using maximum shear theory i.e., $\sigma_{2x} = \sigma_{2z} = 0$.

$$\tau_{max} = \sqrt{\left(\frac{\sigma_{2z}}{2}\right)^2 + {\tau_{2xz}}^2} = 65\,MPa = \sqrt{\left(-\frac{563.549}{2d^2} - \frac{133299.127}{2d^3}\right)^2 + \left(\frac{97.321 \times 10^3}{d^3}\right)^2}$$

$$d^3 = \sqrt{(-4.335d - 1025.378)^2 + (1497.251)^2} \rightarrow d = 12.266\,mm$$

The diameter of the intermediate shaft in the range of [L_{11}, L_{11}+L_{12}] can also be analyzed by using principal stress i.e., $\sigma_{2x} = \sigma_{2z} = 0$.

$$\sigma_{1,2} = \sigma_{all} = \frac{\sigma_{2y}}{2} \pm \sqrt{\left(\frac{\sigma_{2y}}{2}\right)^2 + {\tau_{2xy}}^2} = 130\,MPa$$

$$= -\frac{563.549}{2d^2} - \frac{66649.563}{2d^3} + \sqrt{\left(-\frac{563.549}{2d^2} - \frac{133299.127}{2d^3}\right)^2 + \left(\frac{97.321 \times 10^3}{d^3}\right)^2}$$

$$d^3 = -2.167d - 512.689 + \sqrt{(-2.167d - 512.689)^2 + (748.627)^2} \rightarrow d = 7.293\,mm$$

The diameter of the intermediate shaft in the range of [L_{11}, L_{11}+L_{12}]should be 12.266 mm.

The shearing stress τ_{3xy} and the normal stress σ_{3y} in the range of [L_{11}+L_{12}, L_{11}+L_{12}+L_{13}] are;

$$\tau_{3xy} = \frac{16T_{mi}}{\pi d^3} = \frac{16 \times 19.109 \times 10^3}{\pi d^3} = \frac{97.321 \times 10^3}{d^3}$$

$$\sigma_{3y} = -\frac{4 \times 442.610}{\pi d^2} - \frac{16\sqrt{2} \times (14347.265 + 6338.88\,)}{\pi d^3} = -\frac{563.549}{d^2} - \frac{148992.591}{d^3}$$

The diameter of the intermediate shaft in the range of [L_{11}+L_{12}, L_{11}+L_{12}+L_{13}] can be analyzed by using maximum shear theory i.e., $\sigma_{3x} = \sigma_{3z} = 0$.

$$\tau_{max} = \sqrt{\left(\frac{\sigma_{3y}}{2}\right)^2 + {\tau_{3xz}}^2} = 65\,MPa = \sqrt{\left(-\frac{563.549}{2d^2} - \frac{148992.591}{2d^3}\right)^2 + \left(\frac{97.321 \times 10^3}{d^3}\right)^2}$$

$$d^3 = \sqrt{(-4.335d - 1146.097)^2 + (1497.251)^2} \rightarrow d = 12.426\,mm$$

The diameter of the intermediate shaft in the range of [L_{11}+L_{12}, L_{11}+L_{12}+L_{13}] can also be analyzed by using principal stress i.e., $\sigma_{3x} = \sigma_{3z} = 0$.

$$\sigma_{1,2} = \sigma_{all} = \frac{\sigma_{3y}}{2} \pm \sqrt{\left(\frac{\sigma_{3y}}{2}\right)^2 + {\tau_{3xy}}^2} = 130\ MPa =$$

$$= -\frac{563.549}{2d^2} - \frac{74496.295}{2d^3}$$

$$+ \sqrt{\left(-\frac{563.549}{2d^2} - \frac{148992.591}{2d^3}\right)^2 + \left(\frac{97.321 \times 10^3}{d^3}\right)^2}$$

$$d^3 = -2.167d - 573.048 + \sqrt{(-2.167d - 573.048)^2 + (748.626)^2} \rightarrow d = 7.138\ mm$$

The diameter of the intermediate shaft in the range of [L_{11}+L_{12}, L_{11}+L_{12}+L_{13}] should be 12.426 mm.

The shearing stress τ_{4xy} and the normal stress σ_{4y} in the range of [L_{11}+L_{12}+ L_{13}, L_{11}+L_{12}+L_{13}+ L_{14}] are;

$$\tau_{4xy} = \frac{16T_{mi}}{\pi d^3} = \frac{16 \times 19.109 \times 10^3}{\pi d^3} = \frac{97.321 \times 10^3}{d^3}$$

$$\sigma_{4y} = -\frac{4 \times 442.610}{\pi d^2} - \frac{16\sqrt{2} \times (11059.390 + 7130.755)}{\pi d^3} = -\frac{563.549}{d^2} - \frac{131015.075}{d^3}$$

The diameter of the intermediate shaft in the range of [L_{11}+L_{12}+ L_{13}, L_{11}+L_{12}+L_{13}+ L_{14}] can be analyzed by using maximum shear theory i.e., $\sigma_{4x} = \sigma_{4z} = 0$.

$$\tau_{max} = \sqrt{\left(\frac{\sigma_{4y}}{2}\right)^2 + {\tau_{4xy}}^2} = 65\ MPa = \sqrt{\left(-\frac{563.549}{2d^2} - \frac{131015.075}{2d^3}\right)^2 + \left(\frac{97.321 \times 10^3}{d^3}\right)^2}$$

$$d^3 = \sqrt{(-4.335d - 1007.808)^2 + (1497.251)^2} \rightarrow d = 12.242\ mm$$

The diameter of the intermediate shaft in the range of [L_{11}+L_{12}+ L_{13}, L_{11}+L_{12}+L_{13}+ L_{14}] can also be analyzed by using principal stress i.e., $\sigma_{4x} = \sigma_{4z} = 0$.

$$\sigma_{1,2} = \sigma_{all} = \frac{\sigma_{4y}}{2} \pm \sqrt{\left(\frac{\sigma_{4y}}{2}\right)^2 + {\tau_{4xy}}^2} = 130\ MPa$$

$$= -\frac{563.549}{2d^2} - \frac{131015.075}{2d^3}$$

$$+ \sqrt{\left(-\frac{563.549}{2d^2} - \frac{131015.075}{2d^3}\right)^2 + \left(\frac{97.321 \times 10^3}{d^3}\right)^2}$$

$$d^3 = -2.167d - 503.904 + \sqrt{(-2.167d - 503.904)^2 + (748.626)^2} \rightarrow d = 7.316\ mm$$

The diameter of the intermediate shaft in the range of [L_{11}+L_{12}+ L_{13}, L_{11}+L_{12}+L_{13}+ L_{14}] should be 12.242 mm.

The shearing stress τ_{5xy} and the normal stress σ_{5y} in the range of [L_{11}+L_{12}+ L_{13}+L_{14}, L_{11}+L_{12}+L_{13}+ L_{14}+L_{15}] are;

$$\tau_{5xy} = \frac{16T_{mi}}{\pi d^3} = \frac{16 \times 19.109 \times 10^3}{\pi d^3} = \frac{97.321.643 \times 10^3}{d^3}$$

$$\sigma_{5z} = -\frac{4 \times 442.610}{\pi d^2} - \frac{16\sqrt{2} \times (9566.684 + 10482.589)}{\pi d^3} = -\frac{563.549}{d^2} - \frac{144405.501}{d^3}$$

The diameter of the intermediate shaft in the range of [L_{11}+L_{12}+ L_{13}+L_{14}, L_{11}+L_{12}+L_{13}+ L_{14}+L_{15}] can be analyzed by using maximum shear theory i.e., $\sigma_{5x} = \sigma_{5z} = 0$.

$$\tau_{max} = \sqrt{\left(\frac{\sigma_{5y}}{2}\right)^2 + {\tau_{5xy}}^2} = 65\ MPa = \sqrt{\left(-\frac{563.549}{2d^2} - \frac{144405.501}{2d^3}\right)^2 + \left(\frac{97.321 \times 10^3}{d^3}\right)^2}$$

$$d^3 = \sqrt{(-4.335d - 1110.812)^2 + (1497.251)^2} \rightarrow d = 12.379\ mm$$

The diameter of the intermediate shaft in the range of [L_{11}+L_{12}+ L_{13}+L_{14}, L_{11}+L_{12}+L_{13}+ L_{14}+L_{15}] can also be analyzed by using principal stress i.e., $\sigma_{5x} = \sigma_{5z} = 0$.

$$\sigma_{1,2} = \sigma_{all} = \frac{\sigma_{5z}}{2} \pm \sqrt{\left(\frac{\sigma_{5z}}{2}\right)^2 + {\tau_{5xz}}^2} = 130\ MPa$$

$$= -\frac{563.549}{2d^2} - \frac{144405.501}{2d^3}$$

$$+ \sqrt{\left(-\frac{563.549}{2d^2} - \frac{144405.501}{2d^3}\right)^2 + \left(\frac{97.321 \times 10^3}{d^3}\right)^2}$$

$$d^3 = -2.167d - 555.406 + \sqrt{(-2.167d - 555.406)^2 + (748.626)^2} \rightarrow d = 7.183\ mm$$

The diameter of the intermediate shaft in the range of [L_{11}+L_{12}+ L_{13}+L_{14}, L_{11}+L_{12}+L_{13}+ L_{14}+L_{15}] should be 12.379 mm.

Discussion on Intermediate Shaft Diameters: The diameters of the intermediate shaft are 5.932 mm, 12.266 mm, 12.426, 12.242 mm and 12.379 mm for the range of [0, L_{11}], [L_{11}, L_{11}+L_{12}], [L_{11}+L_{12}, L_{11}+L_{12}+L_{13}], [L_{11}+L_{12}+ L_{13}, L_{11}+L_{12}+L_{13}+ L_{14}], and [L_{11}+L_{12}+ L_{13}+L_{14}, L_{11}+L_{12}+L_{13}+ L_{14}+L_{15}] lengths respectively. The diameter of intermediate shaft for the bevel gear is 12.379 mm as it is. However, its diameter for the single row deep groove ball bearing should be 15 mm because

there is bore bearing12.379 mm and 15 mm. The diameters of the intermediate shaft on the clearance between ball bearing and v-grooved pulley should be 16 mm because it will support the ball bearing. Therefore, the maximum diameter of the intermediate shaft becomes 16 mm. It is on the clearance between ball bearing and v-grooved pulley. The diameters of the intermediate shaft on the v-grooved pulley becomes 15 mm. Finaly, its diameter on the single direction thrust bearing should be 12 mm which was 5.932 mm. The reason to increase this diameter is that the manufacturing cost becomes high during removing on lathe from 16 mm to 5.932 mm.

Reselection of Bearing on Left end of the Intermediate Shaft: The bearing on left end of the intermediate shaft is single direction thrust ball bearing. The bore of the bearing is 12 mm. According to bearing catalogue [53], the specification of the single direction thrust ball bearing for 12 mm bore thrust balling bearing is 26 mm outside diameter, 9 mm thickness, 10 KN dynamic basic load ratings, 17 KN static basic load ratings, 0.62 KN fatigue load limit, 9000 rpm reference speed ratings, 13 000 rpm limiting speed ratings, 0.022 Kg mass and 51101 designation.

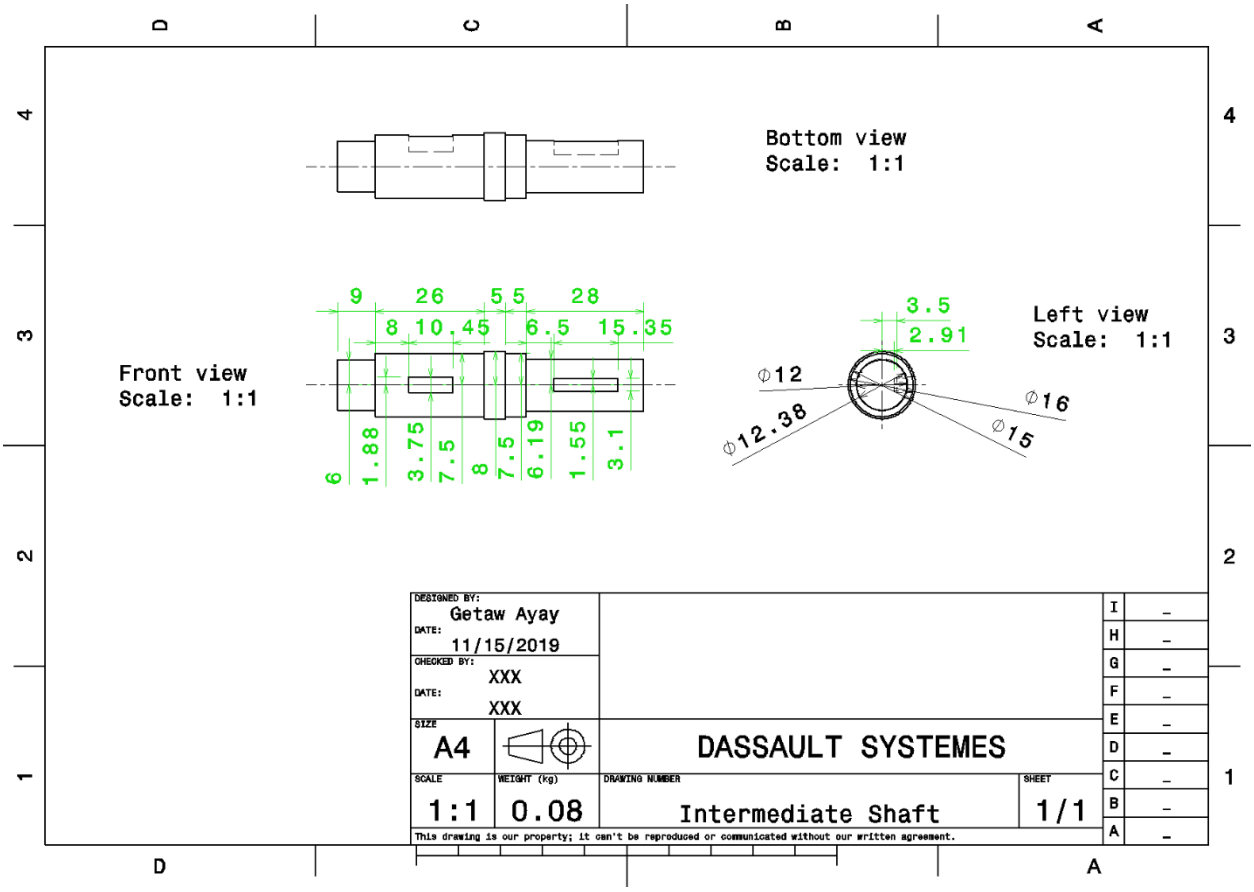

Part Drawing 4-22 Intermediate Shaft

Key on Intermediate Shaft for Bevel Gear: It is used to transfer power from intermediate shaft to bevel gear and located at right end of intermediate shaft. It is subjected to a torque of 19.109 Nm and the diameter of intermediate shaft on the bevel gear is 12.379 mm. Its cross section is square. The key has taper 1 in 100 on the top side only (R.S. KHURMI and J.K. GUPTA, 2005). It is made of high carbon steel of Fe870 Indian standard designation and 870 N/mm^2 tensile strength and 520 N/mm^2 yield stress (σ_y). Since, the system is used in the outdoor, its safety factor (n) is four. Hence, the allowable stress becomes:

$$\sigma_{all} = \sigma_w = \frac{\sigma_y}{n} = \frac{520}{4}\frac{N}{mm^2} = 130MPa$$

The allowable shear stress can be determined by using maximum shear stress theory:

$$\tau_{all} = \tau_w = \frac{\sigma_{all}}{2} = \frac{130}{2}\frac{N}{mm^2} = 65\ MPa$$

The shearing stress developed on the key is the ratio of shearing force (F=2T/d) and shearing area (lxt). Where d, T, l and t are diameter of intermediate shaft on the bevel gear, T torque on the intermediate shaft, l length of key and t thickness of the square key. The thickness t is one fourth (t=d/4=12.379/4=3.095 mm) of the diameter of intermediate shaft.

$$\tau = \frac{2T}{dlt} = \frac{8T}{d^2 l} \rightarrow l = \frac{8T}{d^2\tau} = \frac{8 \times 19109}{12.379^2 \times 65} = 15.348\ mm$$

The crushing stress developed on the key is the ratio of crushing force (F=2T/d) and resisting area (0.5lt).

$$\sigma_c = \frac{4T}{dlt} = \frac{16T}{d^2 l} \rightarrow l = \frac{16T}{d^2\sigma_c} = \frac{16 \times 19109}{12.379^2 \times 130} = 15.348\ mm$$

Discussion of Key on intermediate Shaft for the Bevel Gear: Its length (15.348 mm) is smaller than length bevel gear (28 mm) on intermediate shaft. That means, the length of key way should be on the mid span of the length of intermediate shaft on bevel gear part. The depth of key way both on the camshaft and bevel gear becomes 1.547 mm.

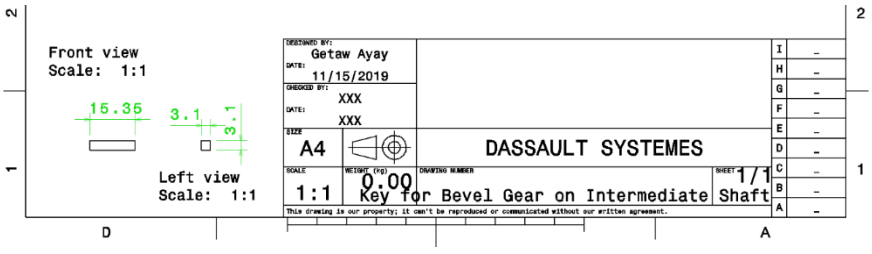

Part Drawing 4-23 Key for Bevel Gear on Intermediate Shaft

Key on Intermediate Shaft for V-Grooved Pulley: It is used to transfer power from v-grooved pulley to intermediate shaft and located between the thrust and ball bearings. It is subjected to a torque of 19.109 Nm and the diameter of intermediate shaft on the v-grooved pulley is 15 mm. Its cross section is square. The key has taper 1 in 100 on the top side only (R.S. KHURMI and J.K. GUPTA, 2005).

It is made of high carbon steel of Fe870 Indian standard designation and 870 N/mm^2 tensile strength and 520 N/mm^2 yield stress (σ_y). Since, the system is used in the outdoor, its safety factor (n) is four. Hence, the allowable stress becomes:

$$\sigma_{all} = \sigma_w = \frac{\sigma_y}{n} = \frac{520}{4}\frac{N}{mm^2} = 130MPa$$

The allowable shear stress can be determined by using maximum shear stress theory:

$$\tau_{all} = \tau_w = \frac{\sigma_{all}}{2} = \frac{130}{2}\frac{N}{mm^2} = 65\ MPa$$

The shearing stress developed on the key is the ratio of shearing force (F=2T/d) and shearing area (lxt). Where d, T, l and t are diameter of intermediate shaft on the conveyor pulley, T torque on the intermediate shaft, l length of key and t thickness of the square key. The thickness t is one fourth (t=d/4=15/4=3.75 mm) of the diameter of intermediate shaft.

$$\tau = \frac{2T}{dlt} = \frac{8T}{d^2 l} \rightarrow l = \frac{8T}{d^2\tau} = \frac{8 \times 19109}{15^2 \times 65} = 10.453\ mm$$

The crushing stress developed on the key is the ratio of crushing force (F=2T/d) and resisting area (0.5lt).

$$\sigma_c = \frac{4T}{dlt} = \frac{16T}{d^2 l} \rightarrow l = \frac{16T}{d^2\sigma_c} = \frac{16 \times 19109}{15^2 \times 130} = 10.453\ mm$$

Discussion of Key on Intermediate Shaft for the V-Grooved Pulley: Its length (10.453 mm) is smaller than the length of intermediate shaft (26 mm) on the v-grooved pulley part. Hence, it is recommended to make it at the mid span of intermediate shaft on v-grooved part. The depth of key way both on the camshaft and conveyor pulley becomes 1.875 mm.

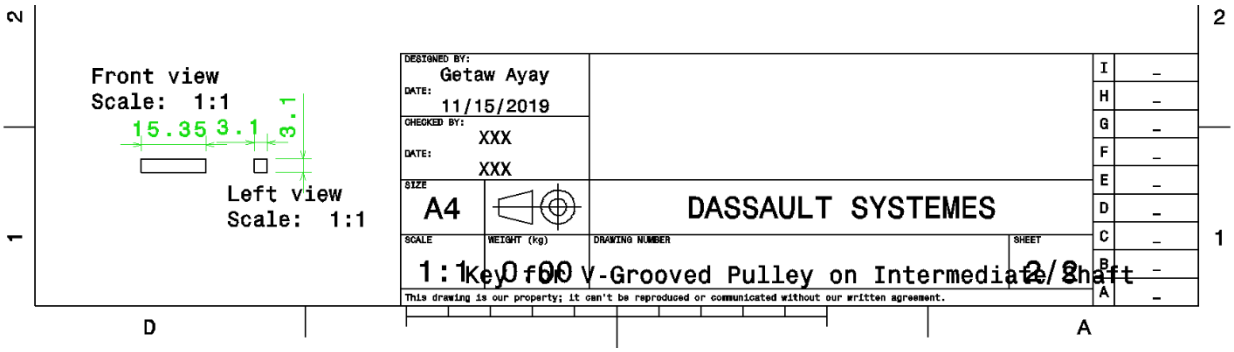

Part Drawing 4-24 Key for V-Grooved Pulley on Intermediate Shaft

Star Wheel Assembly: It is used to collect, control and feed the grain into the cutter and then convey the cut straw together with the lug. It has star wheel vertical rod, star wheel arm and roller between them as shown in **Figure** 4-79.

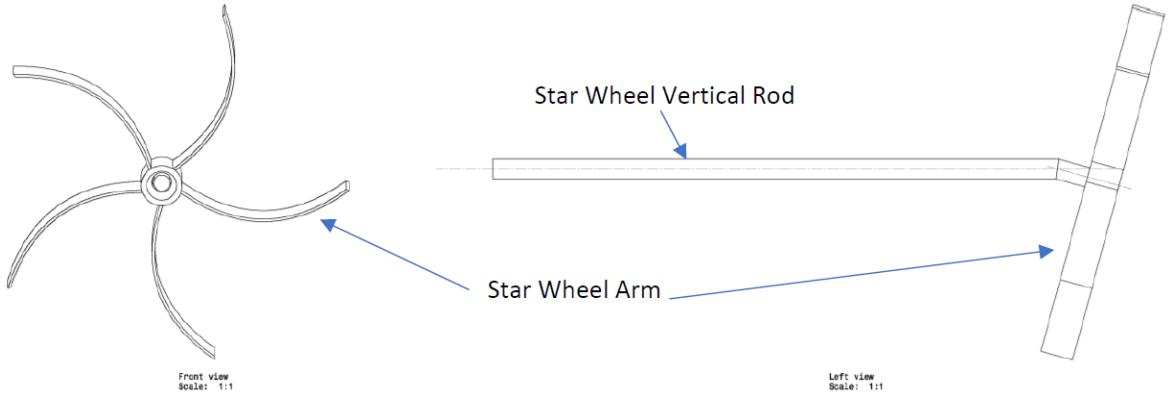

Figure 4-79 Star Wheel Assembly

Star Wheel vertical Rod: It is used to maintain the star wheel in its position. A conveying force of 28.895 N is applied on at a distance of the radius of star wheel 76.125 mm i.e., it creates a torque of 2199.632 Nmm. The height of this rod must be equal to or greater than the vertical height (y_c=399.262 mm) between lug center and cutter bar position. The rod is fixed on its bottom end and free at the top end. Hence, it is a cantilever beam which is in vertical position. The maximum stress occurs at the bottom fixed end with a combination of torsional and bending stress. The bending moment becomes the product of height y_c and conveying force F_c.

$$M_x = F_c y_c = 28.895 \times 399.262 = 11536.675\ Nmm$$

Materials for Star Wheel Rod: It is made of high carbon steel of Fe870 Indian standard designation and 870 N/mm^2 tensile strength and 520 N/mm^2 yield stress (σ_y). Since, the system is used in the outdoor, its safety factor (n) is four. Hence, the allowable stress becomes:

$$\sigma_{all} = \sigma_w = \frac{\sigma_y}{n} = \frac{520}{4}\frac{N}{mm^2} = 130MPa$$

The allowable shear stress can be determined by using maximum shear stress theory:

$$\tau_{all} = \tau_w = \frac{\sigma_{all}}{2} = \frac{130}{2}\frac{N}{mm^2} = 65\ MPa$$

The bending stress and shearing stress can be determined as follows

$$\sigma_z = \frac{M_x y}{I_x} = \frac{11536.675 \times d/2}{\pi d^4/64} = \frac{32 \times 11536.675}{\pi d^3} = \frac{117511.612}{d^3}$$

The shearing stress due to torque T is;

$$\tau_{yz} = \frac{TC}{J}$$

$$C = \frac{d}{2}\ and\ J = \frac{\pi d^4}{32}$$

$$\tau_{yz} = \frac{32T}{\pi d^3} = \frac{16 \times 2199.632}{\pi d^3} = \frac{11202.634}{d^3}$$

The diameter of the star wheel rod can be analyzed by using maximum shear theory i.e., $\sigma_x = \sigma_y = 0$

$$\tau_{max} = \tau_{all} = \sqrt{\left(\frac{\sigma_z}{2}\right)^2 + {\tau_{yz}}^2} = 65\ MPa = \sqrt{\left(\frac{117511.612}{2d^3}\right)^2 + \left(\frac{11202.634}{d^3}\right)^2}$$

$$d^3 = \sqrt{903.935^2 + 172.348^2} \rightarrow d = 9.727\ mm$$

The diameter of the star wheel rod can also be analyzed by using principal stress i.e., $\sigma_x = \sigma_y = 0$.

$$\sigma_{1,2} = \sigma_{all} = \frac{\sigma_y}{2} \pm \sqrt{\left(\frac{\sigma_y}{2}\right)^2 + {\tau_{yz}}^2} = 130\ MPa$$

$$= \frac{117511.612}{2d^3} \pm \sqrt{\left(\frac{117511.612}{2d^3}\right)^2 + \left(\frac{11202.634}{d^3}\right)^2}$$

$$d^3 = 451.968 \pm \sqrt{451.968^2 + 86.174^2} \rightarrow d = 9.698\ mm$$

The diameter of the star wheel rod should be 10 mm.

Discussion on the Length of Star Wheel Rod: the length of star wheel should be the sum of the vertical height (y_c=399.262 mm), the height of the star wheel arm (20 mm), thickness of divider (1 mm) and clearance between divider and star wheel arm (9 mm).

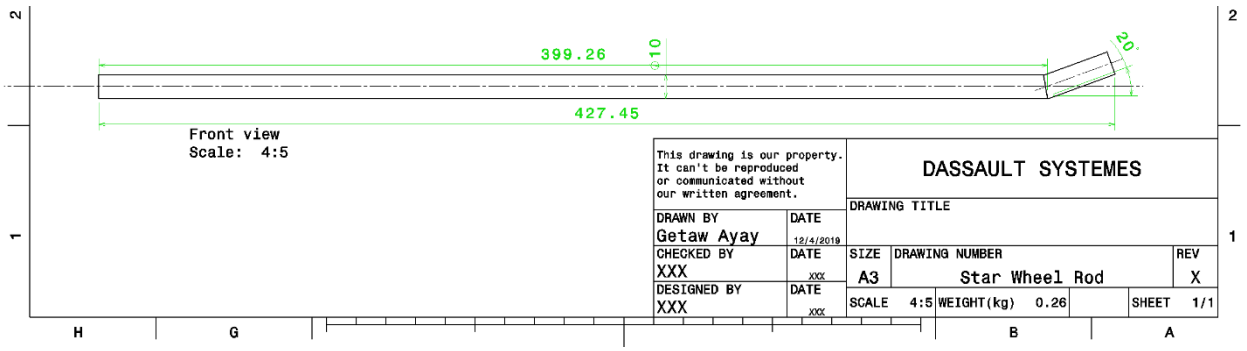

The mass of the star wheel rod can be reduced by using hollow round bar. The proportional dimension can be determined by considering same second moment of area both for solid and hollow bar. The solid rod has a diameter of 10 mm and it has the following mathematical relation with the internal (d_i) and external (d_o) diameter of the hollow rod.

$$d^4 = {d_o}^4 - {d_i}^4 = 100$$

The values of the internal (d_i) and external (d_o) diameter of the hollow rod becomes 8 mm and 11 mm respectively [54].

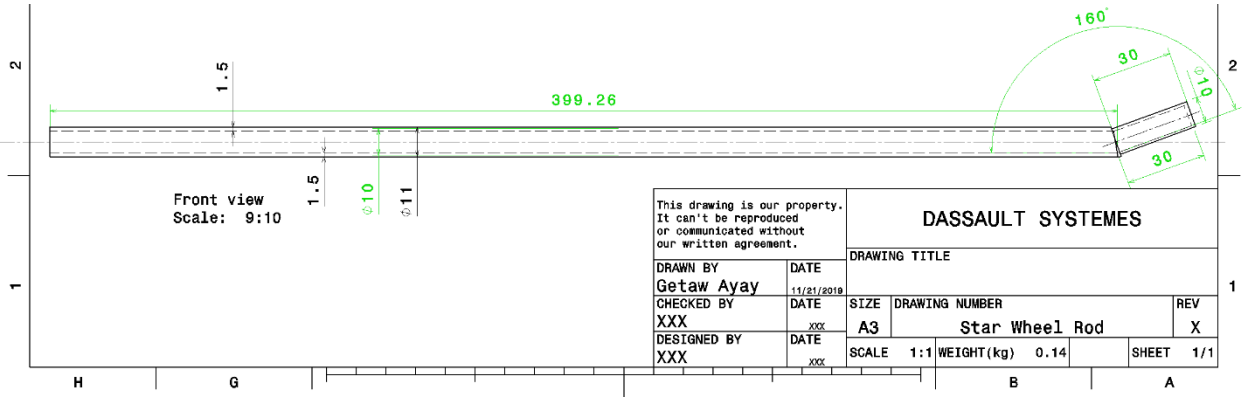

Part Drawing 4-25 Star Wheel Rod

Selection of Bearing Between Star Wheel Arm and Rod: This bearing is used to reduce the frictional losses between the star wheel arm and rod. Since the orientation of the bearing is vertical, it should be single direction thrust ball 8 mm bore bearing. According to bearing catatlogue [53], 8 mm bore single direction thrust balling bearing has 19 mm outside diameter, 7 mm thickness, 3 KN dynamic basic load rating, 4 KN static basic load rating, 0.15 KN fatigue load limit, 12 000 rpm reference speed ratings, 17 000 rpm limiting speed ratings, 0.007 Kg mass and BA 8 designation.

Selection of Round Tube for Bearing Seat: The outer diameter and thickness of the bearing between star wheel arm and rod is 19 mm and 7 mm respectively. The seat for the bearing should

have 19 mm internal diameter. It is selected 21.3 mm outer diameter and 2.5 mm thickness steel which has 1.16 Kg/m weight from RFL steel ltd [52].

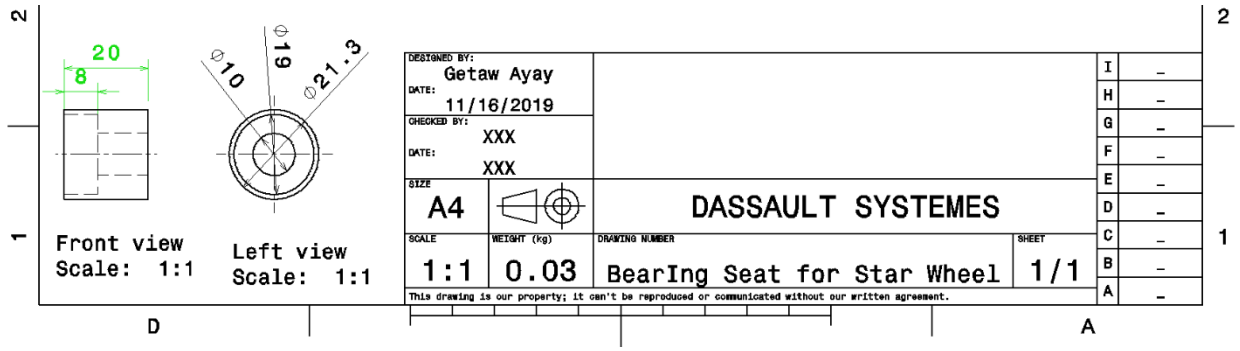

Part Drawing 4-26 Bearing Seat for Star Wheel

Star Wheel Arm: It is used to collect and convey the straw. It is installed at the top end of the star wheel rod. It has a radius of 76.125 mm. It is subjected to a transverse load of 28.895 N. Its cross section is rectangular.

The maximum bending moment becomes;

$$M_z = F_c L = 28.895 \times 76.625 = 2199.632\ Nmm$$

Materials for Star Wheel Arm: It is made of high carbon steel of Fe E 650 Indian standard designation and 870 N/mm^2 tensile strength and 650 N/mm^2 yield stress (σ_y). Since, the system is used in the outdoor, its safety factor (n) is four. Hence, the allowable stress becomes:

$$\sigma_{all} = \sigma_w = \frac{\sigma_y}{n} = \frac{650}{4}\frac{N}{mm^2} = 162.5MPa$$

The bending stress and shearing stress can be determined as follows

$$\sigma_x = \frac{M_z y}{I_z} = \frac{2199.632 \times 6}{hb^2} = \frac{13197.762}{hb^2} = 162.5$$

The height h and base b of the cross section of the star wheel arm becomes 20 mm and 2 mm respectively.

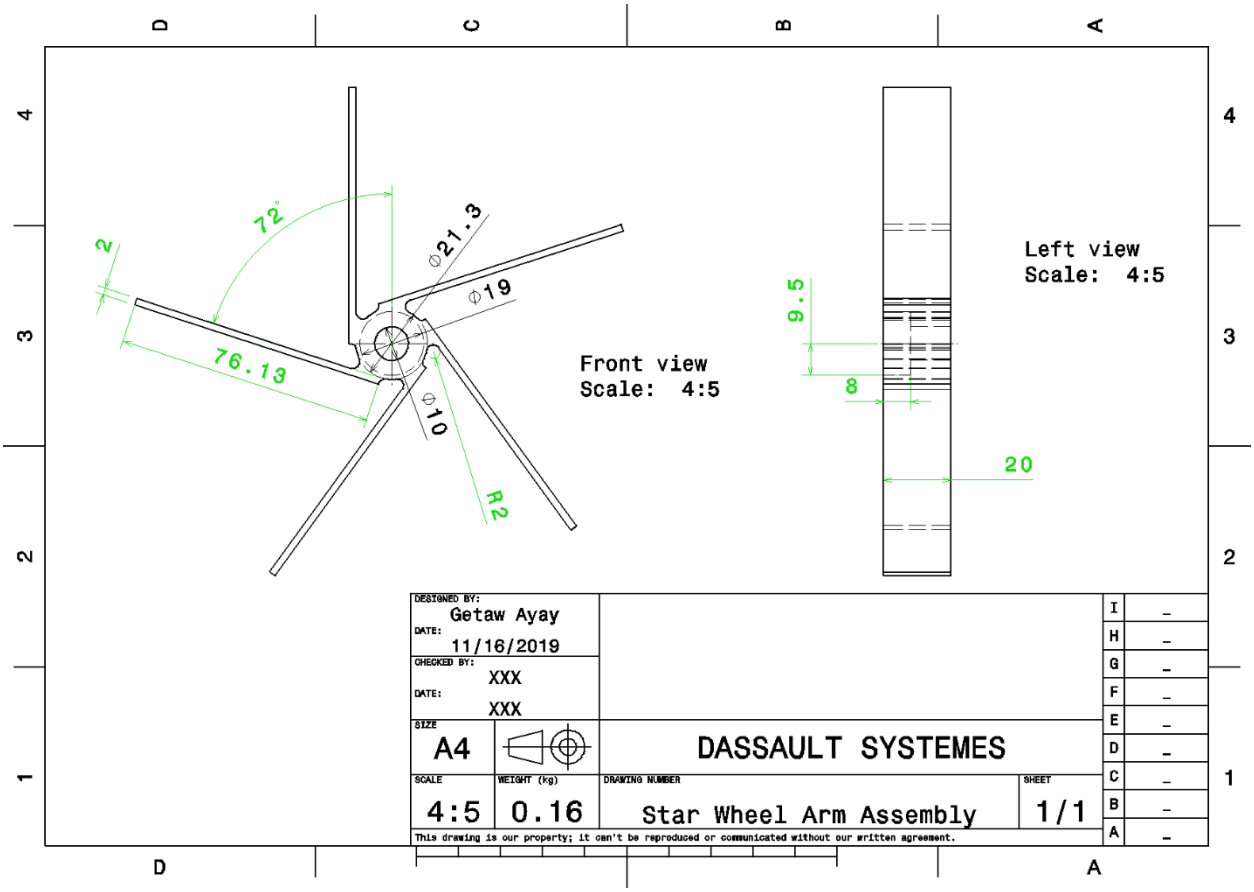

Part Drawing 4-27 Star Wheel Arm Assembly

Divider: It divides the crop uniformly. The divider is load free. Hence, it should be designed only its geometry. The divider has two ends. These are tail in the star wheel arm side and nose in the uncut side of the crop. The tail depends on the diameter of the star wheel arm and the nose has arrow. So that the divider has a kind of triangular shape with arc at the tail side. The star wheel arm is completely covered in cut side but one third in the uncut side of the crop by the divider. The part of divider becomes 76.125 mm and 25.375 mm in the cut and uncut side of the crop respectively. According to Bailling (1985), the recommended values for the nose angle and inclination angle of the divider is 28^o and 20^o respectively.

It is made of high carbon steel of Fe E 650 Indian standard designation and 870 N/mm^2 tensile strength and 650 N/mm^2 yield stress (σ_y).

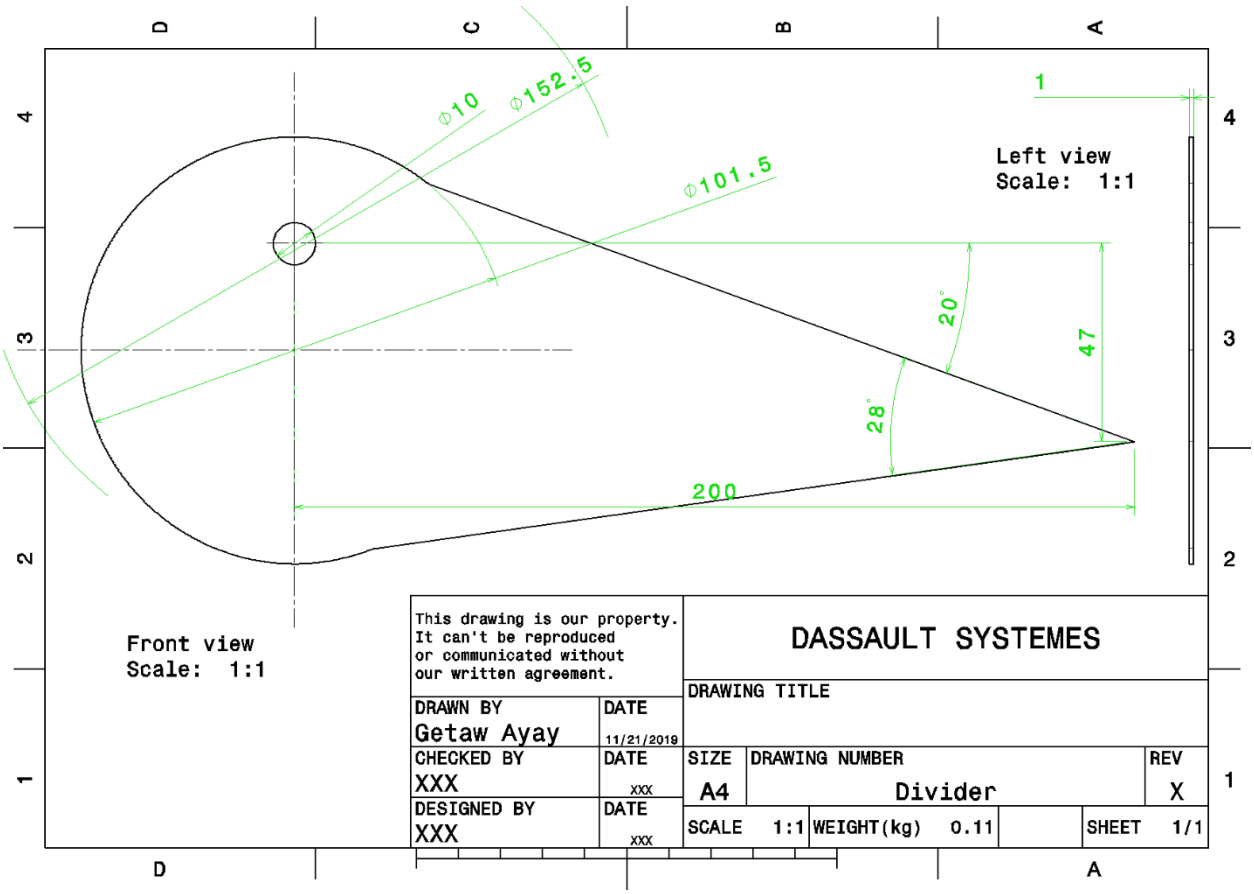

Part Drawing 4-28 Divider

Star Wheel and Divider Assembly Support: It is installed below the guard lip bar which supports the star wheel and divider assembly. It is subjected to a cobination of weight and conveying loads. The downward weight is the sum of star wheel arm assembly (0.16 Kg),star wheel roller (0.007 Kg), star wheel rod (0.14 Kg) and divider (0.11 Kg) which is 0.417 Kg or 4.091 N. The horintal conveying force is 28.895 N. These loads are applied at a maximum distance 346.564 mm cantilever beam. The normal stesses created by the two loads are in the x-axis. The cross section of the support is hollow square section in order to get good contanct for weld joint.

The loads creates two bending and torsional moments. The bending moments are about y-axis (M_y) and z-axis (M_z) whereas the torsional moment is about x-axis (T).

$$M_y = W \times L = 4.022 \times 346.564 = 1394.186\ Nmm$$

$$M_z = F_c \times L = 28.895 \times 346.564 = 10016.163\ Nmm$$

$$T = F_c \times L = 28.895 \times 399.262\ mm = 11536.675\ Nmm$$

It is made of high carbon steel of Fe E 650 Indian standard designation and 870 N/mm^2 tensile strength and 650 N/mm^2 yield stress (σ_y). Since, the system is used in the outdoor, its safety factor

(n) is four. Hence, the allowable stress becomes:

$$\sigma_{all} = \sigma_w = \frac{\sigma_y}{n} = \frac{650}{4}\frac{N}{mm^2} = 162.5\ MPa$$

The allowable shear stress can be determined by using maximum shear stress theory:

$$\tau_{all} = \tau_w = \frac{\sigma_{all}}{2} = \frac{162.5}{2}\frac{N}{mm^2} = 81.25\ MPa$$

The bending and shearing stresses can be determined as follows for the square section.

$$\sigma_x = \frac{M_y z}{I_y} + \frac{M_z y}{I_z}$$

$$\tau = \frac{Tt}{J_\alpha}$$

The second moment of area about y- and z-axes are same because it is square section.

$I_y = I_z = \frac{S^4}{12}$, $t = S$, z=y=$\frac{S}{2}$ and $J_\alpha = \alpha b t^3 = \alpha S^4 = 0.208S^4$

$$\sigma_x = \frac{M_y z}{I_y} + \frac{M_z y}{I_z} = \frac{1394.186 \times 6}{S^3} + \frac{10016.163 \times 6}{S^3} = \frac{68462.094}{S^3}$$

$$\tau = \frac{T}{0.208S^3} = \frac{11536.675}{0.208S^3} = \frac{55464.784}{S^3}$$

The side of the square cross section beam can be analyzed by using maximum shear theory i.e., $\sigma_z = \sigma_y = 0$.

$$\tau_{max} = \tau_{all} = \sqrt{\left(\frac{\sigma_x}{2}\right)^2 + {\tau_{xy}}^2} = 81.25\ MPa = \sqrt{\left(\frac{68462.094}{2S^3}\right)^2 + \left(\frac{55464.784}{S^3}\right)^2}$$

$$S^3 = \sqrt{421.305^2 + 682.643^2} \rightarrow S = 9.292\ mm$$

The side of the square cross section beam can also be analyzed by using principal stress i.e., $\sigma_z = \sigma_y = 0$.

$$\sigma_{1,2} = \sigma_{all} = \frac{\sigma_x}{2} \pm \sqrt{\left(\frac{\sigma_x}{2}\right)^2 + {\tau_{xy}}^2} = 162.5\ MPa$$

$$= \frac{68462.094}{2S^3} \pm \sqrt{\left(\frac{68462.094}{2S^3}\right)^2 + \left(\frac{55464.784}{S^3}\right)^2}$$

$$d^3 = 210.653 \pm \sqrt{210.653^2 + 341.322^2} \rightarrow d = 8.489\ mm$$

The side of the square cross section becomes 9.292 mm. However, the beam has hollow section in

order to maximum the strength to weight ratio i.e., the second moment of area should be same both for solid (S) and hollow section (S_o and S_i).

$$S^4 = {S_o}^4 - {S_i}^4 = 7454.814$$

The internal (S_i) and external (S_o) sides of the square section can be optimized by iteration to 10 mm and 12 mm respectively [54].

The shearing stress should be checked for closed thin wall section.

$$t = \frac{S_o - S_i}{2} = \frac{12 - 10}{2} = 1\ mm\ and\ A = 11 \times 11 = 121\ mm^2$$

$$\tau = \frac{T}{2tA} = \frac{11536.675}{2 \times 1 \times 121} = 47.672\ MPa$$

The bending stress in the x-axis becomes as follows.

$$\sigma_x = \frac{68462.094 S_o}{{S_o}^4 - {S_i}^4} = \frac{68462.094 \times 12}{12^4 - 10^4} = 76.522\ MPa$$

The maximum shear stress becomes;

$$\tau_{max} = \sqrt{\left(\frac{\sigma_x}{2}\right)^2 + {\tau_{xy}}^2} = \sqrt{\left(\frac{76.522}{2}\right)^2 + (47.672)^2} = 61.127\ MPa < \tau_{all}$$

The maximum principal stress also becomes;

$$\sigma_{1,2} = \frac{\sigma_x}{2} \pm \sqrt{\left(\frac{\sigma_x}{2}\right)^2 + {\tau_{xy}}^2} = \frac{76.522}{2} \pm \sqrt{\left(\frac{76.522}{2}\right)^2 + 47.672^2} = 99.388\ MPa < \sigma_{all}$$

The applied normal and shearing stresses are less than the allowable corresponding stresses which indicates that the beam design is safe.

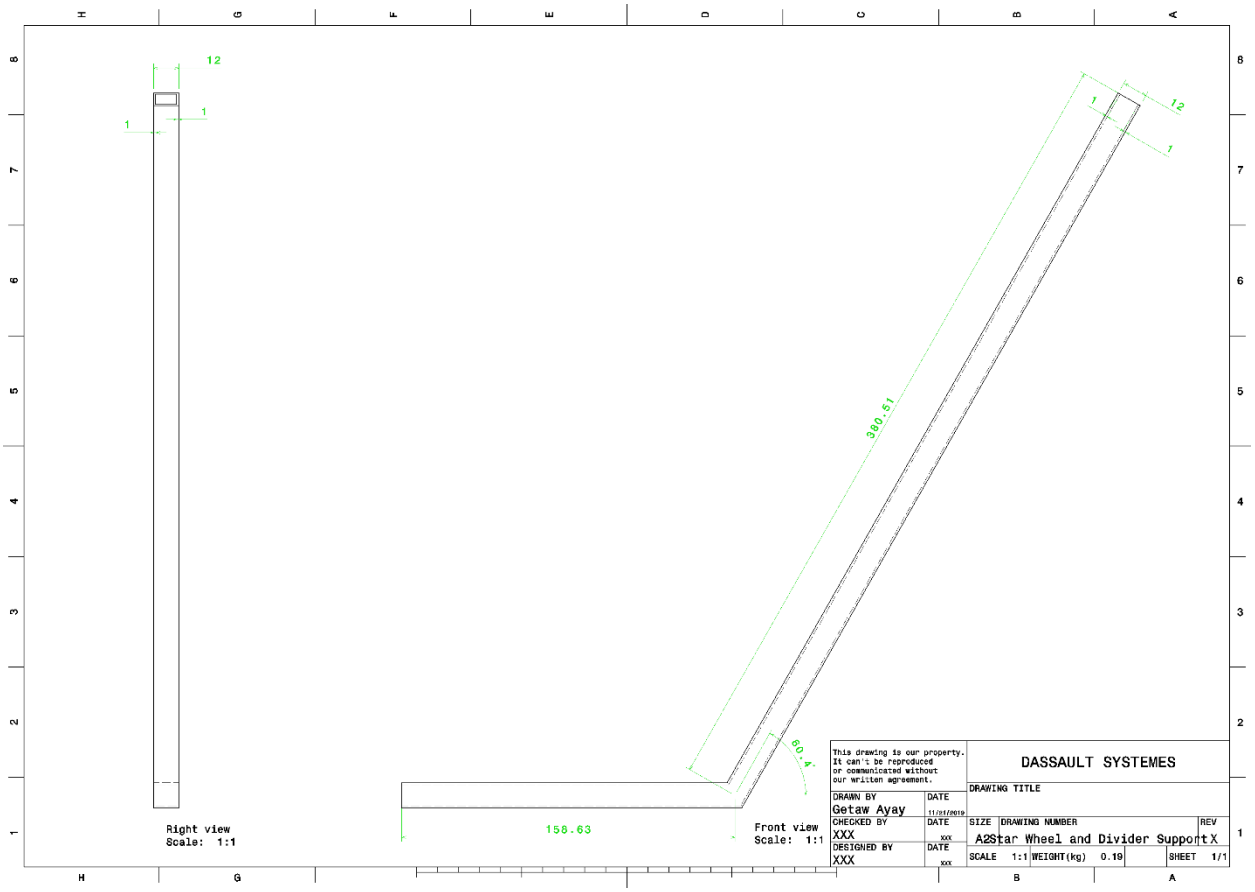

Part Drawing 4-29 Star Wheel and Divider Support

Frame for Solar Panel Support: It is used to spport the solar panel. It has four legs, five long beams, two short beams and two stiffners as shown in **Figure** 4-80. Its cross section is square. It also supports two solar panels i.e., W is 15 Kg each. The solar panel has 1580X808X40 mm dimension. The length L in **Figure** 4-81 is 808 mm.

Figure 4-80 Solar Panel Support Isometric View

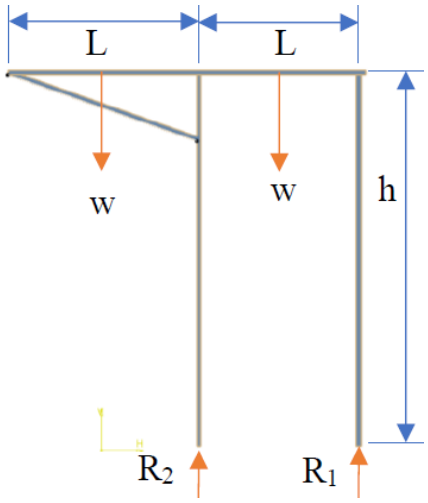

Figure 4-81 Side View of Solar Panel Support

The reaction forces R_1 and R_2 can be determined by applying the equalibrium equations.

$$\sum M_{R1} = 0$$

$$1.5LW + 0.5LW - LR_2 = 0 \rightarrow R_2 = 2W = 2 \times 15 \times 9.81 = 294.3\ N$$

$$\sum F = 0$$

$$R_1 + R_2 - 2W = 0 \rightarrow R_1 = -R_2 + 2W = -294.3 + 294.3 = 0\ N$$

Discussion on the Reaction Force R_2 and Height h: There is no load on the right-side leg (R_1=0 N). The solar panel has only two legs. It can be strengthened by using stiffeners on both sides. There are two vertical supports at R_2 which share the weight equally i.e., 147.15 N each. The vertical support is subjected to a compressive load of 147.15 N. It should be designed by

considering compressive stress and buckling of column fixed end on both sides. The height from the ground up to the solar panel is approximately 2 m by considering the tallest person. The diameter of the wheel is 394.165 mm. Hence, the height h becomes approximately 1.6 m.

Materials for the Solar Panel Support: It is made of high carbon steel of Fe870 Indian standard designation and 870 N/mm^2 tensile strength and 520 N/mm^2 yield stress (σ_y). Since, the system is used in the outdoor, its safety factor (n) is four. Hence, the allowable stress becomes:

$$\sigma_{all} = \sigma_w = \frac{\sigma_y}{n} = \frac{520}{4}\frac{N}{mm^2} = 130MPa$$

The compressive stress is the ratio of compressive force 98.1 N and cross-sectional area S^2.

$$\sigma_{all} = \frac{R_2/2}{S^2} \rightarrow S^2 = \frac{\frac{R_2}{2}}{\sigma_{all}} = \frac{147.15}{130} \rightarrow S = 0.566\ mm$$

The side of the cross section is very small (less than 1 mm). Hence, it should be designed by considering the buckling. The critical load (F$_c$) can be determined as follows.

$$P_c = \frac{4\pi^2 EI}{L^2} = \frac{\pi^2 ES^4}{3L^2} \rightarrow S^4 = \frac{3L^2 P_c}{\pi^2 E} = \frac{3 \times 1600^2 \times 147.15}{\pi^2 \times 210000} \rightarrow S = 4.832\ mm$$

The buckling stress σ_c is the ratio of critical load P_c and area s^2.

$$\sigma_c = \frac{P_c}{S^2} = \frac{147.15}{4.832^2} = 6.302\ MPa$$

Discussion: the dimension of the cross section of the leg of the solar panel support is very small. Hence, it is advisable to make it hollow square section. The smallest available hollow square has 10 mm outside dimension. The possible thickness for 10 mm can be determined using side of solid square section (4.832 mm).

$$S^2 = {S_o}^2 - {S_i}^2 \rightarrow {S_i}^2 = {S_o}^2 - S^2 = 10^2 - 4.832^2 \rightarrow S_i = 8.755\ mm$$

The thickness can be determined by subtracting S_i from S_o.

$$t = \frac{S_o - S_i}{2} = \frac{10 - 8.755}{2} = 0.623\ mm$$

The minimum available thickness is 1 mm. Hence, the leg has 10X10X1 mm hollow square dimensions and 0.281 Kg/m [54].

The beam supports the solar panel at two sides i.e., a single solar panel is supported by two cantilever beams. Half of the weight (73.575 N) of a solar panel is distributed over a length of L (808 mm) cantilever beam i.e., w=W/2*1/L=73.575/808=0.091 N/mm. A maximum bending moment is created at the fixed end of the cantilever beam see **Figure** 4-82.

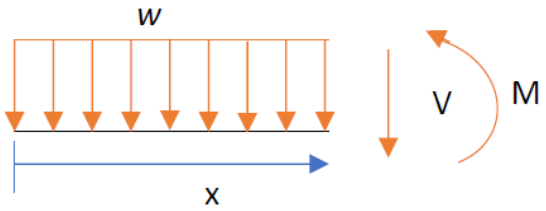

Figure 4-82 FBD of Cantilever Beam of Solar Panel

$$\sum M_x = 0$$

$$-w\frac{x^2}{2} - M = 0 \rightarrow M = w\frac{x^2}{2} = \frac{Wx^2}{4L}$$

The maximum bending moment becomes 29724.3 Nmm. The bending stress can be determined for this maximum bending moment.

$$\sigma_b = \frac{M_y y}{I_y} = \frac{29724.3 \times S/2}{S^4/12} \rightarrow S^3 = \frac{29724.3 \times 6}{130} \rightarrow S = 11.111\ mm$$

As it is obvious hollow section with same cross sectional area is more stronger than solid section. So the 11.111 mm solid square section can be changed to hollow square section as follows.

$$S^4 = {S_o}^4 - {S_i}^4$$

The size of the hollow section can be descided by iteration starting from 11.111 mm for S_o value. It is economical to select 14 mm and 1.5 mm for S_o and t respectively from [54].

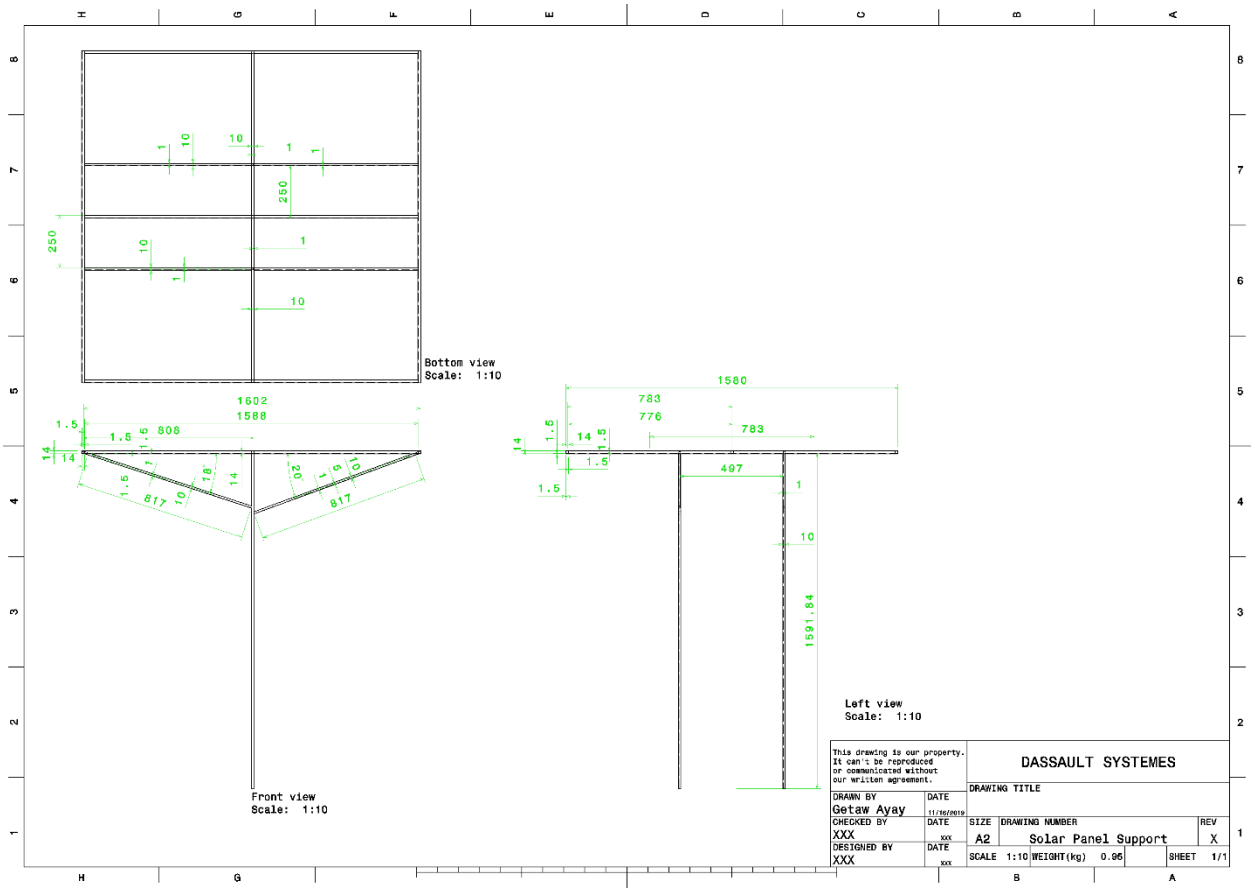

Part Drawing 4-30 Solar Panel Support

Gear Box: It is used to hold the bevel gears. It is also installed on the left top beam of cutter frame. The gear box has hollow square cross section with size greater than the gear diameter (147.37 mm) see **Figure** 4-83. It is subjected to a bearings loads which come from camshaft and intermediate shaft. The bearing loads are 1338.475 N and 437.002 N in the x-and y-axes respectively from camshaft and 1829.350 N and 40.372 N in the x-and z-axes respectively from intermediate shaft. The resultant bearing loads become 1408.008 N and 1829.795 N from camshaft and intermediate shaft respectively. The bearing outside daimeters and thicknesses are 24 mm and 5 mm respectively both for intermediate shaft and camshaft.

The cross section of the square gear box is preferred to 160 mm outside dimension and 6.3 mm thickness [54].

Material for Gear Box: It is made of high carbon steel of Fe E 650 Indian standard designation and 870 N/mm^2 tensile strength and 650 N/mm^2 yield stress (σ_y). Since, the system is used in the outdoor, its safety factor (n) is ten. Hence, the allowable stress becomes:

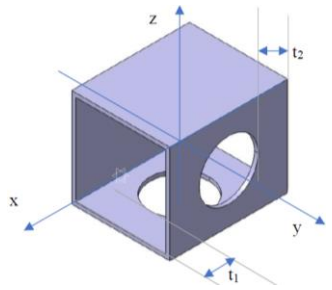

Figure 4-83 Gear Box

$$\sigma_{all} = \sigma_w = \frac{\sigma_y}{n} = \frac{650}{10}\frac{N}{mm^2} = 65\ MPa$$

The allowable shear stress can be determined by using maximum shear stress theory:

$$\tau_{all} = \tau_w = \frac{\sigma_{all}}{2} = \frac{65}{2}\frac{N}{mm^2} = 32.5\ MPa$$

The bearing stress (σ_b) on the gear box from camshaft side is the ratio of 1408.008 N force (R_b) and bearing area (A_b).

$$\sigma_b = \frac{R_b}{A_b} = \frac{1408.008}{24 \times 5} = 11.733\ MPa < \sigma_{all}$$

The shearing stress (τ) on the gear box from camshaft side is the ratio of 1408.008 N force (R_b) and shearing area.

$$\tau = \frac{R_b}{A} = \frac{1408.008}{6.3t_1} = 32.5 \rightarrow t_1 = 6.877\ mm$$

The bearing stress (σ_b) on the gear box from intermediate shaft side is the ratio of 1829.795 N force (R_b) and bearing area (A_b).

$$\sigma_b = \frac{R_b}{A_b} = \frac{1829.795}{24 \times 5} = 15.249\ MPa < \sigma_{all}$$

The shearing stress (τ) on the gear box from intermediate shaft side is the ratio of 1829.795 N force (R_b) and shearing area.

$$\tau = \frac{R_b}{A} = \frac{1829.795}{6.3t_2} = 32.5 \rightarrow t_2 = 8.937\ mm$$

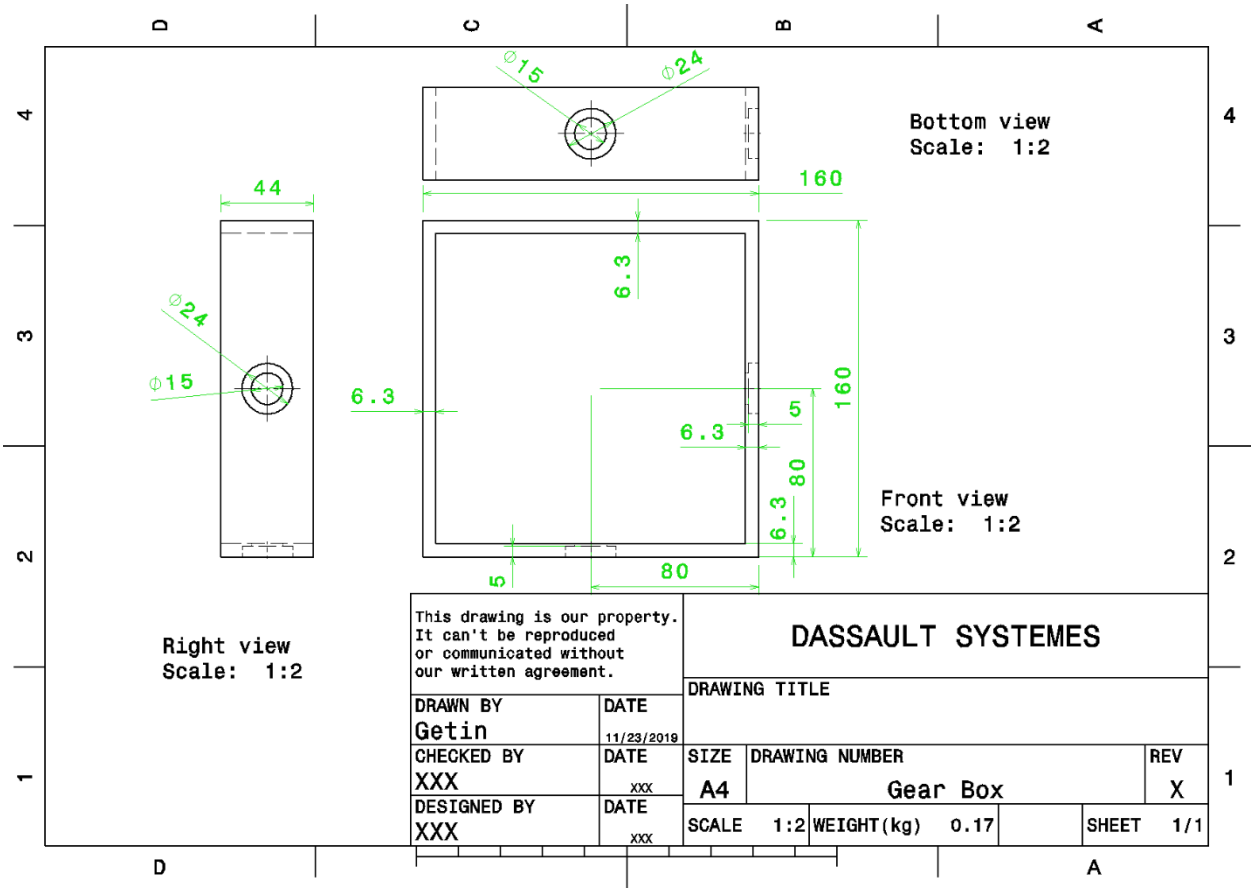

Part Drawing 4-31 Gear Box

Frame for Cutter: It is the main structure which is used to support all the power transmission, cutter, conveyor and divider parts see in **Figure** 4-84. It transmits all the weight to tires. It is subjected to a cummulative weight of 42.972 Kg or 421.555 N at different potition. So that it is mainly under bending load. The beam has square cross section.

Table 4-4 Weight of Components on Cutter Frame

S. No	Part Name	Quantity	Mass in Kg	Total Mass
1.	Bevel Pinion	1	0.230	0.230
2.	Bevel Gear	1	2.310	2.310
3.	Conveyor Pulleys on Conveyor	1	2.740	2.740
4.	Conveyor Pulleys on Cam Shaft	1	2.780	2.780
5.	Flat Belt	1	0.180	0.180
6.	Lug	13	0.030	0.390
7.	Rivet for Lug	30	0.002	0.060
8.	Bolt for Blade	16	0.007	0.106
9.	Nut for Blade	16	0.004	0.056

10.	Blade or Cutter	8	0.030	0.240
11.	Cutter Bar	1	0.230	0.230
12.	Guard Lip	10	0.010	0.100
13.	Bolt for Guard Lip	24	0.009	0.209
14.	Nut for Guard Lip	24	0.003	0.067
15.	Guard Lip Bar	1	0.140	0.140
16.	Bearing for Cutter Bar Support	4	0.005	0.022
17.	Follower Bar	1	0.100	0.100
18.	Rollers for follower bar	8	0.004	0.031
19.	Rectangular Box for Follower Bar	1	0.170	0.170
20.	Vertical Position Pin for Follower Support	4	0.057	0.229
21.	Horizontal Position Pin for Follower Support	4	0.032	0.130
22.	Follower Head	2	0.130	0.260
23.	Idler Shaft	1	0.020	0.020
24.	Ball Bearing for Idler Shaft	1	0.003	0.003
25.	Thrust Bearing for Idler Shaft	1	0.004	0.004
26.	Camshaft	1	0.700	0.700
27.	Ball Bearing for Camshaft	1	0.007	0.007
28.	Thrust Bearing for Camshaft	1	0.022	0.022
29.	Eccentric Cam	1	0.520	0.520
30.	Key on Camshaft for Bevel Gear	1	0.001	0.001
31.	Key on Camshaft for Conveyor Pulley	1	0.004	0.004
32.	Key on Camshaft for Cam:	1	0.001	0.001
33.	V-Grooved Pulley on Motor Shaft	1	0.420	0.420
34.	V-Grooved Pulley on Intermediate Shaft	1	1.830	1.830
35.	Intermediate Shaft	1	0.080	0.080
36.	Ball Bearing on Intermediate Shaft	1	0.007	0.007
37.	Thrust Bearing on Intermediate Shaft	1	0.023	0.023
38.	Key on Intermediate Shaft for Bevel Gear	1	0.001	0.001
39.	Key on Intermediate Shaft for V-Grooved Pulley	1	0.001	0.001
40.	Star Wheel vertical Rod	4	0.140	0.560
41.	Star Wheel Arm	4	0.160	0.640
42.	Bearing Between Star Wheel Arm and Rod	4	0.007	0.028
43.	Frame for Solar Panel Support	1	0.950	0.950
44.	Crop Divider	4	0.110	0.440
45.	Star Wheel and Divider Assembly Support	4	0.190	0.760
46.	DC Motor	1	25.000	25.000
47.	Gear Box	1	0.170	0.170
Total		212	39.574	42.972

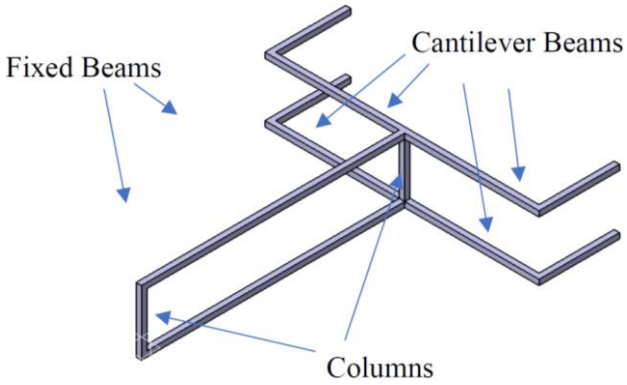

Figure 4-84 Frame for Cutter System

The frame has four cantilever beams, two fixed beams and two columns. The cantilever beams are not loaded equally. The weight in **Table** 4-4 is shared by the four beams which have similar shape. The camshaft assembly is supported by the left bottom cantilever beam on its shoulder as the reader is considered as observer. The weight becomes 8.436 Kg or 82.757 N see **Table** 4-5.

Table 4-5 Weight Supported by left bottom cantilever beam on its shoulder

Part Name	**Quantity**	**Mass in Kg**	**Total Mass**
Bevel Gear	1	2.310	2.310
Conveyor Pulleys on Cam Shaft	1	2.780	2.780
Flat Belt	0.5	0.180	0.090
Lug	6.5	0.030	0.195
Rivet for Lug	15	0.002	0.030
Follower Bar	1	0.100	0.100
Rollers for follower bar	8	0.004	0.031
Rectangular Box for Follower Bar	1	0.170	0.170
Vertical Position Pin for Follower Support	4	0.000	0.000
Horizontal Position Pin for Follower Support	4	0.000	0.000
Follower Head	2	0.130	0.260
Camshaft	1	0.700	0.700
Ball Bearing for Camshaft	1	0.007	0.007
Thrust Bearing for Camshaft	1	0.022	0.022
Eccentric Cam	1	0.520	0.520
Key on Camshaft for Bevel Gear	1	0.001	0.001
Key on Camshaft for Conveyor Pulley	1	0.004	0.004
Key on Camshaft for Cam:	1	0.001	0.001
Star Wheel vertical Rod	2	0.140	0.280
Star Wheel Arm	2	0.160	0.320
Bearing Between Star Wheel Arm and Rod	2	0.007	0.014
Crop Divider	2	0.110	0.220
Star Wheel and Divider Assembly Support	2	0.190	0.380

			8.435

The free end of the left bottom cantilever beam also supports half of the weight (0.585 Kg or 5.739 N) of the cutter and guard lip assembly see **Table** 4-6.

Table 4-6 Free End of the Left Bottom Cantilever Beam

S. No	Part Name	Quantity	Mass in Kg	Total Mass
1	Bolt for Blade	8	0.007	0.053
2	Nut for Blade	8	0.004	0.028
3	Blade or Cutter	4	0.030	0.120
4	Cutter Bar	0.5	0.230	0.115
5	Guard Lip	5	0.010	0.050
6	Bolt for Guard Lip	12	0.009	0.104
7	Nut for Guard Lip	12	0.003	0.034
8	Guard Lip Bar	0.5	0.140	0.070
9	Bearing for Cutter Bar Support	2	0.005	0.011
Total				0.585

The beam is also sbjected to 138.188 N vertical downward force from axial component of bevel gear, 290.97 N compressive force from cutting force and 8.438 N horizontal force from frictional force on its shoulder. The total vertical downward force is 210.089 N which is the sum of 138.188 N vertical downward force and total weight 71.901 N at the shoulder. There is also 290.97 N horizontal bending load at the free end which comes from cutter bar see **Figure** 4-85.

In general, the beam is subjected to three dimensional forces. These forces creates a normal stress in the y-axis because the vertical downward force (210.089 N) creates a bending stress in y-axis, the axial compress force (290.97 N) creates normal stress and the horizontal force (8.438 N) creates bending stress in the y-axis. Finally the weight (5.739 N) on its free end creates normal stress in the y-axis and torsional stress xy plane.

The length of the beam is equal to half of the width of cut (304.8 mm) in the cam side and (88.7+5.2+10+3=96.9 mm) in cutter bar side see **Figure** 4-85.

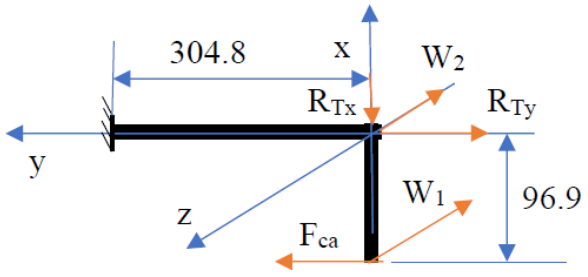

Figure 4-85 FBD of Left Bottom Beam of Cutter Frame

The loads W_1, F_{ca}, R_{Ty}, W_2 and R_{TX} have a values of 5.739 N, 290.97 N, 267.683 N, 210.089 N and 72.961 N respectively.

The bending moments in the x- and z-axes on any arbitrary section between fixed end and origin can be defined by the following equations.

$$M_x = W_1 y + W_2 y = 215.828y$$

$$M_z = -R_{Tx} y - F_{ca} \times 96.9 = -72.961y - 28194.993$$

The net axial force in the y-axis;

$$F_y = F_{ca} - R_{Ty} = 290.67 - 267.683 = 23.287\ N$$

The bending moments (M_x and M_z) becomes maximum at the fixed end which are 65784.374 Nmm and -50433.506 Nmm respectively.

The beam is also subjected to torsional moment (T).

$$T = W_1 \times 96.9 = 5.739 \times 96.9 = 556.109\ Nmm$$

It is made of high carbon steel of Fe E 650 Indian standard designation and 870 N/mm^2 tensile strength and 650 N/mm^2 yield stress (σ_y). Since, the system is used in the outdoor, its safety factor (n) is four. Hence, the allowable stress becomes:

$$\sigma_{all} = \sigma_w = \frac{\sigma_y}{n} = \frac{650}{4}\frac{N}{mm^2} = 162.5\ MPa$$

The allowable shear stress can be determined by using maximum shear stress theory:

$$\tau_{all} = \tau_w = \frac{\sigma_{all}}{2} = \frac{162.5}{2}\frac{N}{mm^2} = 81.25\ MPa$$

The bending and shearing stresses can be determined as follows for the square section.

$$\sigma_y = \frac{F_y}{A} - \frac{M_x z}{I_x} + \frac{M_z x}{I_z}$$

$$\tau = \frac{Tt}{J_\alpha}$$

The second moment of area about y- and z-axes are same because it is square section.

$I_x = I_z = \frac{S^4}{12}$, $t = S$, z=y=$\frac{S}{2}$, $A = S^2$ and $J_\alpha = \alpha b t^3 = \alpha S^4 = 0.208S^4$

$$\sigma_y = -\frac{23.287}{S^2} - \frac{65784.374 \times 6}{S^3} - \frac{30766.895 \times 6}{S^3} = -\frac{23.287}{S^2} - \frac{579307.614}{S^3}$$

$$\tau = \frac{T}{0.208S^3} = \frac{556.109}{0.208S^3} = \frac{2673.601}{S^3}$$

The side of the square cross section of the beam can be analyzed by using maximum shear theory

i.e., $\sigma_x = \sigma_z = 0$.

$$\tau_{max} = \tau_{all} = \sqrt{\left(\frac{\sigma_y}{2}\right)^2 + {\tau_{xy}}^2} = 81.25\ MPa = \sqrt{\left(-\frac{23.287}{2S^2} - \frac{579307.614}{2S^3}\right)^2 + \left(\frac{2673.601}{S^3}\right)^2}$$

$$S^3 = \sqrt{(-0.143S - 3564.97)^2 + 32.906^2} \rightarrow S = 15.280\ mm$$

The side of the square cross section beam can also be analyzed by using principal stress i.e.,$\sigma_x = \sigma_z = 0$.

$$\sigma_{1,2} = \sigma_{all} = \frac{\sigma_x}{2} \pm \sqrt{\left(\frac{\sigma_y}{2}\right)^2 + {\tau_{xy}}^2} = 162.5\ MPa$$

$$= -\frac{23.287}{2S^2} - \frac{579307.614}{2S^3} \pm \sqrt{\left(-\frac{23.287}{2S^2} - \frac{579307.614}{2S^3}\right)^2 + \left(\frac{2673.601}{S^3}\right)^2}$$

$$S^3 = -0.072S - 1782.485 \pm \sqrt{(-0.072 - 1782.485)^2 + 16.453^2} \rightarrow S = 15.274\ mm$$

The side of the square cross section becomes 15.280 mm. However, the beam should be hollow section to maximize the strength to weight ratio i.e., the second moment of area should be same both for solid (S) and hollow section (S_o and S_i).

$$S^4 = {S_o}^4 - {S_i}^4 = 54512.163$$

The internal (S_i) and external (S_o) sides of the square section can be optimized by iteration to 23 mm and 25 mm respectively [54].

The shearing stress should be checked for closed thin wall section.

$$t = \frac{S_o - S_i}{2} = \frac{25 - 23}{2} = 1\ mm\ and\ A = 24 \times 24 = 576\ mm^2$$

$$\tau = \frac{T}{2tA} = \frac{556.109}{2 \times 1 \times 576} = 0.483\ MPa$$

The bending stress in the x-axis becomes as follows.

$$\sigma_y = \frac{F_y}{A} - \frac{M_x z}{I_x} + \frac{M_z x}{I_z} = -\frac{23.287}{{S_o}^2 - {S_i}^2} - \frac{65784.374\ \times 6S_o}{{S_o}^4 - {S_i}^4} - \frac{30766.895 \times 6S_o}{{S_o}^4 - {S_i}^4}$$

$$= -\frac{23.287}{25^2 - 23^2} - \frac{65784.374\ \times 6 \times 25}{25^4 - 23^4} - \frac{30766.895 \times 6 \times 25}{25^4 - 23^4}$$

$$= -130.972\ MPa$$

The maximum shear stress becomes;

$$\tau_{max} = \sqrt{\left(\frac{\sigma_y}{2}\right)^2 + {\tau_{xy}}^2} = \sqrt{\left(\frac{-130.972}{2}\right)^2 + (0.483)^2} = 65.488\ MPa < \tau_{all}$$

The maximum principal stress also becomes;

$$\sigma_{1,2} = \frac{\sigma_y}{2} \pm \sqrt{\left(\frac{\sigma_y}{2}\right)^2 + {\tau_{xy}}^2} = \frac{-130.972}{2} \pm \sqrt{\left(\frac{-130.972}{2}\right)^2 + 0.483^2} = |130.974|\ MPa < \sigma_{all}$$

The applied normal and shearing stresses are less than the allowable corresponding stresses which indicates that the beam design is safe.

Discussion on Lower Cantilever Beams: There are two cantilever beam on lower side; one is left bottom beam on camshaft side and the other is right bottom beam on idler shaft side. They have symmetrical shape and their cros sections depends on the loads applied on it. The magnitude of loads on the left bottom beam are greater than the right bottom beam. The cross section of right bottom should be less than the left bottom beam which is 25mm and 23 mm external and internal side of a square section respectively. It is recommended to make the left and right beams from one uniform square pipe. Therefore, the cross section of the right bottom beam becomes 25mm and 23 mm external and internal side of a square section respectively.

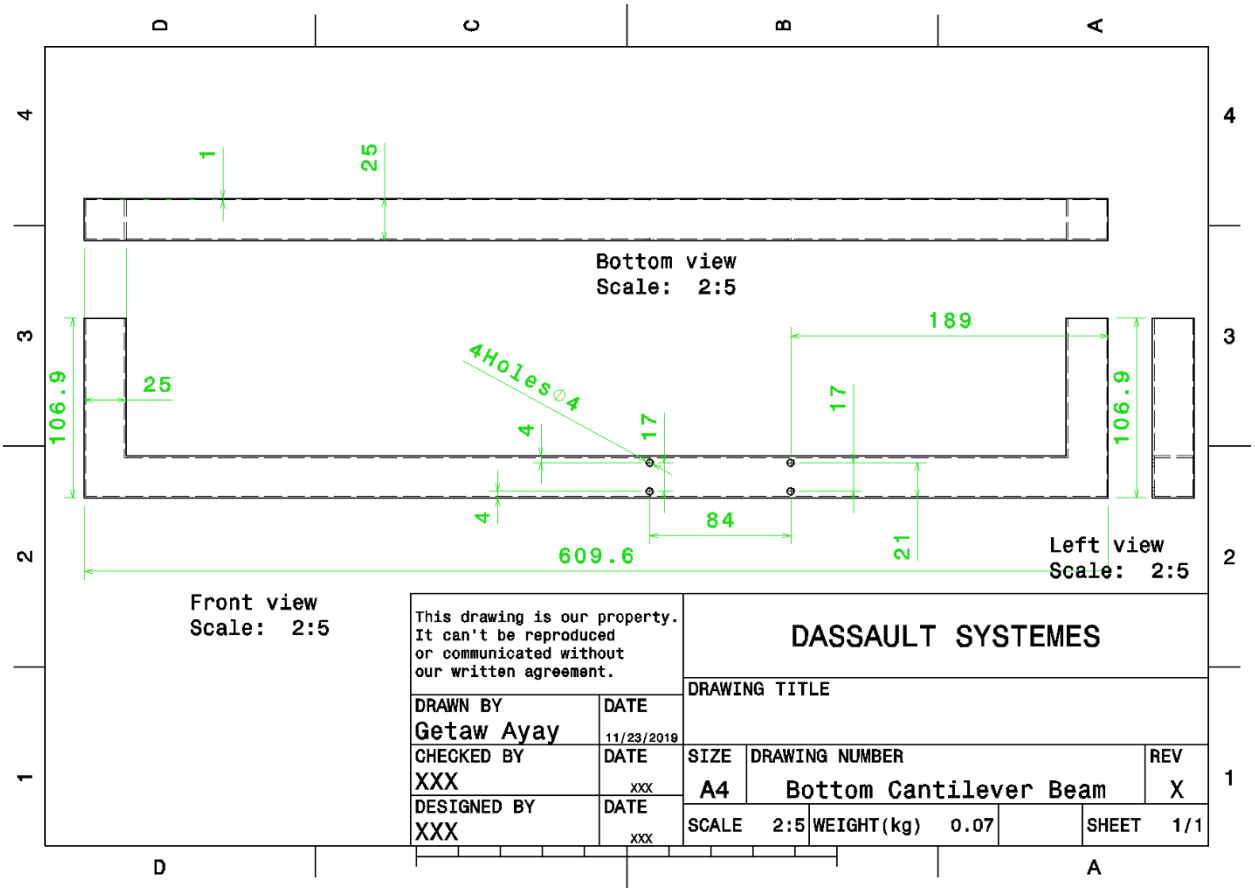

Part Drawing 4-32 Bottom Cantilever Beam

The DC motor and gear box assembly is supported by the left top cantilever beam on its shoulder as the reader is considered as observer. The weight becomes 27.762Kg or W=272.345 N see in **Table** 4-7. This weight is applied aroud the shoulder of the beam.

Table 4-7 Masses of Motor Gear Box Assembly

S. No	Part Name	Quantity	Mass in Kg	Total Mass
1.	Bevel Pinion	1	0.230	0.230
2.	V-Grooved Pulley on Motor Shaft	1	0.420	0.420
3.	V-Grooved Pulley on Intermediate Shaft	1	1.830	1.830
4.	Intermediate Shaft	1	0.080	0.080
5.	Ball Bearing on Intermediate Shaft	1	0.007	0.007
6.	Thrust Bearing on Intermediate Shaft	1	0.023	0.023
7.	Key on Intermediate Shaft for Bevel Gear	1	0.001	0.001
8.	Key on Intermediate Shaft for V-Grooved Pulley	1	0.001	0.001
9.	DC Motor	1	25.000	25.000
10.	Gear Box	1	0.170	0.170

Total	10	27.762	27.762

The beam is also sbjected to R_{bz}=40.372 N vertical downward and R_{bx}=1829.350 N horizntal to positive x-axis forces from intermediate shaft ball bearing and R_{bx}=1338.475 N horizntal to positive x-axis and R_{by}=437.002 N horizontal to left forces from camshaft ball bearing. In general, the beam is subjected to three dimensional forces. These forces create a normal stress in the y-axis. The length of the beam is equal to half of the width of cut (304.8 mm) in the cam side and (88.7+5.2+10+3=96.9 mm) in cutter bar side see **Figure** 4-86.

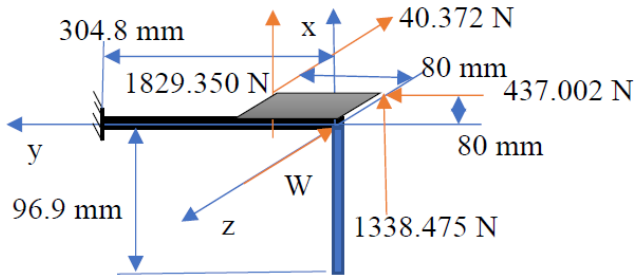

Figure 4-86 FBD of Left Top Beam of Cutter Frame

The loads can be collected to the origin by considering their corresponding moments.

$$F_x = 1829.350 + 1338.475 = 3167.798\ N, F_y = 437.002\ N\ and\ F_z = -40.372 - 272.345 = -312.718\ N$$

$$M_x = 437.002 \times 80 + 40.372 \times 80 = 38189.92\ Nmm$$

$$M_z = -1829.350 \times 80 = -146348\ Nmm$$

$$T = -1338.475 \times 80 - 1829.350 \times 80 = -253426\ Nmm$$

The bending moments in the x- and z-axes on any arbitrary section between fixed end and origin can be defined by the following equations.

$$M_x = 38189.92 + 312.718y$$

$$M_z = -146348 + 3167.798y$$

The net axial force in the y-axis;

$$F_y = 437.002\ N$$

The bending moments (M_x and M_z) becomes maximum at the fixed end which are 133503.928 Nmm and 819196.830 Nmm respectively.

It is made of high carbon steel of Fe E 650 Indian standard designation and 870 N/mm^2 tensile strength and 650 N/mm^2 yield stress (σ_y). Since, the system is used in the outdoor, its safety factor (n) is four. Hence, the allowable stress becomes:

$$\sigma_{all} = \sigma_w = \frac{\sigma_y}{n} = \frac{650}{4}\frac{N}{mm^2} = 162.5\ MPa$$

The allowable shear stress can be determined by using maximum shear stress theory:

$$\tau_{all} = \tau_w = \frac{\sigma_{all}}{2} = \frac{162.5}{2}\frac{N}{mm^2} = 81.25\ MPa$$

The bending and shearing stresses can be determined as follows the square section.

$$\sigma_y = \frac{F_y}{A} - \frac{M_x z}{I_x} + \frac{M_z x}{I_z}\ and\ \tau = \frac{Tt}{J_\alpha}$$

The second moment of area about y- and z-axes are same because it is square section.

$I_x = I_z = \frac{S^4}{12}$, z=y=$\frac{S}{2}$, $t = S$, $A = S^2$ and $J_\alpha = \alpha b t^3 = \alpha S^4 = 0.208S^4$

$$\sigma_y = -\frac{437.002}{S^2} - \frac{133503.928\ \times 6}{S^3} - \frac{819196.830 \times 6}{S^3} = -\frac{437.002}{S^2} - \frac{5716204.548}{S^3}$$

$$\tau = \frac{T}{0.208S^3} = \frac{253426}{0.208S^3} = \frac{905092.857}{S^3}$$

The side of the square cross section of the beam can be analyzed by using maximum shear theory i.e., $\sigma_x = \sigma_z = 0$.

$$\tau_{max} = \tau_{all} = \sqrt{\left(\frac{\sigma_y}{2}\right)^2 + {\tau_{xy}}^2} = 81.25\ MPa$$

$$= \sqrt{\left(-\frac{437.002}{2S^2} - \frac{5716204.548}{2S^3}\right)^2 + \left(\frac{905092.857}{S^3}\right)^2}$$

$$S^3 = \sqrt{(-2.689S - 35176.643)^2 + 11139.604^2} \rightarrow S = 33.317\ mm$$

The side of the square cross section beam can also be analyzed by using principal stress i.e.,$\sigma_x = \sigma_z = 0$.

$$\sigma_{1,2} = \sigma_{all} = \frac{\sigma_x}{2} \pm \sqrt{\left(\frac{\sigma_y}{2}\right)^2 + {\tau_{xy}}^2} = 162.5\ MPa$$

$$= -\frac{437.002}{2S^2} - \frac{5716204.548}{2S^3}$$

$$\pm \sqrt{\left(-\frac{437.002}{2S^2} - \frac{5716204.548}{2S^3}\right)^2 + \left(\frac{905092.857}{S^3}\right)^2}$$

$$S^3 = -1.345S - 17588.322 \pm \sqrt{(-1.345S - 17588.322)^2 + 5569.802^2} \rightarrow S = 9.511\ mm$$

The side of the square cross section becomes 33.317 mm. However, the beam should be hollow

section to maximize the strength to weight ratio i.e., the second moment of area should be same both for solid (S) and hollow section (S_o and S_i).

$$S^4 = {S_o}^4 - {S_i}^4 = 1232149.926$$

The internal (S_i) and external (S_o) sides of the square section can be optimized by iteration to 35 mm and 40 mm respectively [54].

The shearing stress should be checked for closed thin wall section.

$$t = \frac{S_o - S_i}{2} = \frac{40 - 35}{2} = 2.5\ mm\ and\ A = 37.5 \times 37.5 = 1406.25\ mm^2$$

$$\tau = \frac{T}{2tA} = \frac{253426}{2 \times 2.5 \times 1406.25} = 36.043\ MPa$$

The bending stress in the x-axis becomes as follows.

$$\sigma_y = \frac{F_y}{A} - \frac{M_x z}{I_x} + \frac{M_z x}{I_z} = -\frac{437.002}{{S_o}^2 - {S_i}^2} - \frac{133503.928\ \times 6S_o}{{S_o}^4 - {S_i}^4} - \frac{819196.830 \times 6S_o}{{S_o}^4 - {S_i}^4} =$$

$$= -\frac{437.002}{40^2 - 35^2} - \frac{133503.928\ \times 6 \times 40}{40^4 - 35^4} - \frac{819196.830 \times 6 \times 40}{40^4 - 35^4}$$

$$= -62.342\ MPa$$

The maximum shear stress becomes;

$$\tau_{max} = \sqrt{\left(\frac{\sigma_y}{2}\right)^2 + {\tau_{xy}}^2} = \sqrt{\left(\frac{-62.342}{2}\right)^2 + (36.043)^2} = 47.652\ MPa < \tau_{all}$$

The maximum principal stress also becomes;

$$\sigma_{1,2} = \frac{\sigma_y}{2} \pm \sqrt{\left(\frac{\sigma_y}{2}\right)^2 + {\tau_{xy}}^2} = \frac{-62.342}{2} \pm \sqrt{\left(\frac{-62.342}{2}\right)^2 + 36.043^2} = |78.823|\ MPa < \sigma_{all}$$

The applied normal and shearing stresses are less than the allowable corresponding stresses which indicates that the beam design is safe.

Discussion on Upper Cantilever Beams: There are two cantilever beam on upper side; one is left top beam on camshaft side and the other is right top beam on idler shaft side. They have symmetrical shape and their cros sections depends on the loads applied on it. The magnitude of loads on the left top beam are greater than the right top beam. The cross section of right top should be less the left top beam which is 40 mm and 35 mm external and internal side of a square section respectively. It is recommended to make the left and right beams from one uniform square pipe. Therefore, the cross section of the right top beam becomes 40 mm and 35 mm external and internal

side of a square section respectively.

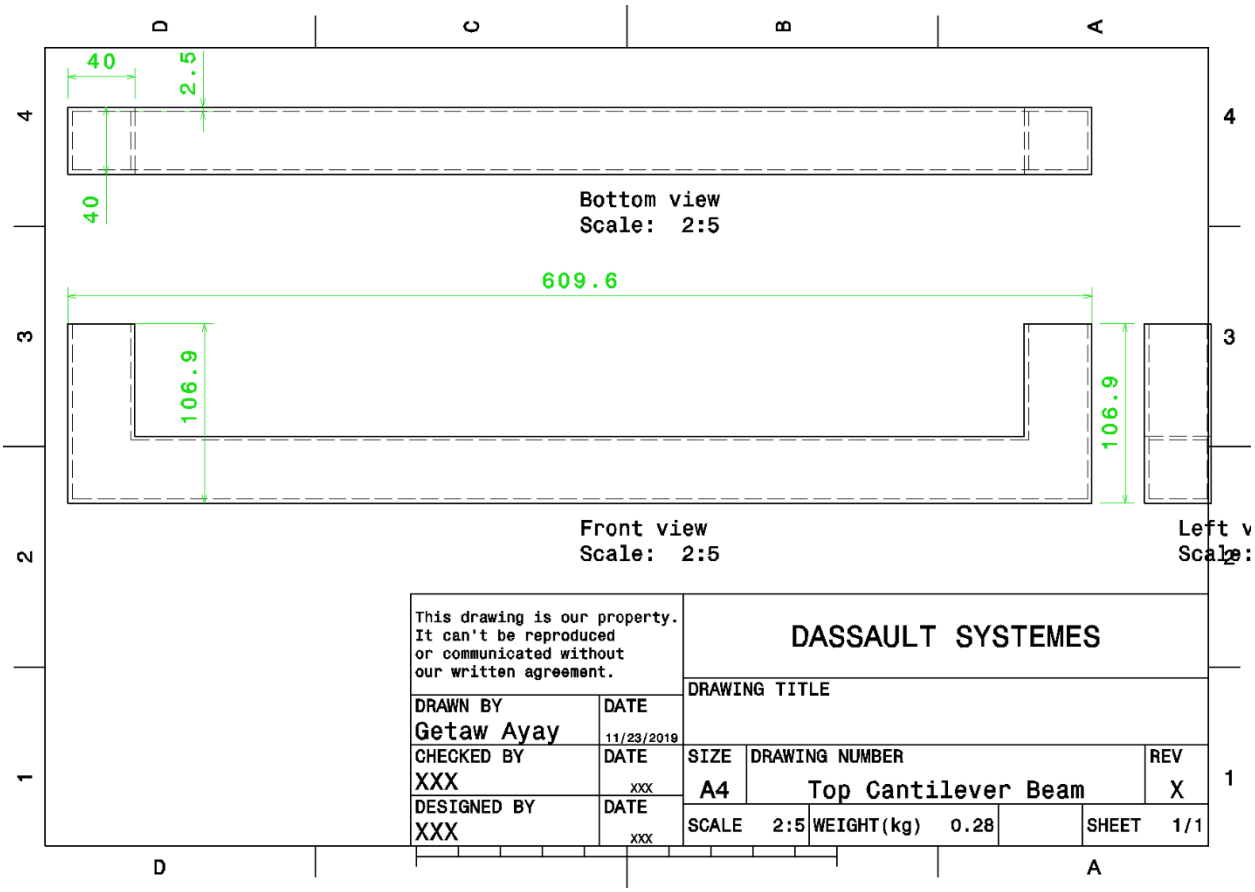

Part Drawing 4-33 Top Cantilever Beam

Fixed Beams: There two fixed beams; one is on the top and the other on bottom sides. These two beams become fixed when we use the vertical stiffener. The stiffener can be neglected to simplify the analysis. When the stiffener is removed the beams become cantilever. The lengths of the beams are same (L_1=303.983 mm) which is the sum of length of the length of cantilever beams (L_4=106.9 mm) and radius of tires (394.165/2=197.083 mm).

The two beams are loaded in different magnitudes of loads see **Figure** 4-87 and **Figure** 4-88.

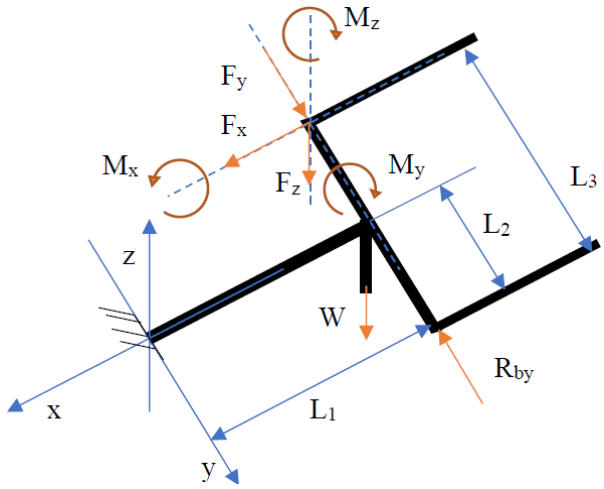

Figure 4-87 FBD for Top Fixed beam

The value of loads in top fixed beam are 16.593 N, 137.154 N, -253426 Nmm, -312.718 N, 38189.92 Nmm, 3167.798 N, 437.002 N and -146348 Nmm for R_{by}, W, M_y, F_z, M_x, F_x, F_y and M_z respectively. The lengths L_1, L_2 and L_3 are 197.083 mm, 304.8 mm and 609.6 mm respectively.

Table 4-8 Weight W of Bottom Beam Assembly on Top Fixed Beam

S. No	Part Name	Quantity	Mass in Kg	Total Mass
1	Bevel Gear	1	2.310	2.310
2	Conveyor Pulleys on Conveyor	1	2.740	2.740
3	Conveyor Pulleys on Cam Shaft	1	2.780	2.780
4	Flat Belt	1	0.180	0.180
5	Lug	13	0.030	0.390
6	Rivet for Lug	30	0.002	0.060
7	Bolt for Blade	16	0.007	0.106
8	Nut for Blade	16	0.004	0.056
9	Blade or Cutter	8	0.030	0.240
10	Cutter Bar	1	0.230	0.230
11	Guard Lip	10	0.010	0.100
12	Bolt for Guard Lip	24	0.009	0.209
13	Nut for Guard Lip	24	0.003	0.067
14	Guard Lip Bar	1	0.140	0.140
15	Bearing for Cutter Bar Support	4	0.005	0.022
16	Follower Bar	1	0.100	0.100
17	Rollers for follower bar	8	0.004	0.031
18	Rectangular Box for Follower Bar	1	0.170	0.170
19	Vertical Position Pin for Follower Support	4	0.000	0.000
20	Horizontal Position Pin for Follower Support	4	0.000	0.000
21	Follower Head	2	0.130	0.260
22	Idler Shaft	1	0.020	0.020

23	Ball Bearing for Idler Shaft	1	0.003	0.003
24	Thrust Bearing for Idler Shaft	1	0.004	0.004
25	Camshaft	1	0.700	0.700
26	Ball Bearing for Camshaft	1	0.007	0.007
27	Thrust Bearing for Camshaft	1	0.022	0.022
28	Eccentric Cam	1	0.520	0.520
29	Key on Camshaft for Bevel Gear	1	0.001	0.001
30	Key on Camshaft for Conveyor Pulley	1	0.004	0.004
31	Key on Camshaft for Cam:	1	0.001	0.001
32	Star Wheel vertical Rod	4	0.140	0.560
33	Star Wheel Arm	4	0.160	0.640
34	Bearing Between Star Wheel Arm and Rod	4	0.007	0.028
35	Crop Divider	4	0.110	0.440
36	Star Wheel and Divider Assembly Support	4	0.190	0.760
37	Bottom Cantilever Beam	1	0.080	0.080
	Total	202	10.853	13.981

The axial stress is induced due to load F_x. The torsional moment T can be analyzed as follows.

$$T = F_z \times L_1 + \mathrm{M}_x = 312.718 \times 197.083 + 38189.92 = 100067.187\ Nmm$$

The bending moment on the fixed between the origin and T connection can be defined as follows both about y- and z-axes.

$$\mathrm{M}_y = -\mathrm{M}_y - (F_z + W)x = -253426 - (312.718 + 137.154)x = -449.872x - 253426$$

$$\mathrm{M}_z = -\mathrm{M}_z - \left(F_y - R_{by}\right)x = -146348 - (437.002 - 16.593)x = -420.409x - 146348$$

The bending moments M_y and M_z becomes maximum at x=L_1 which are -342088.123 Nmm and -229203.467 Nmm.

These loads create normal and shearing plane stresses.

Materials: The beam has square section. It is made of high carbon steel of Fe E 650 Indian standard designation and 870 N/mm^2 tensile strength and 650 N/mm^2 yield stress (σ_y). Since, the system is used in the outdoor, its safety factor (n) is four. Hence, the allowable stress becomes:

$$\sigma_{all} = \sigma_w = \frac{\sigma_y}{n} = \frac{650}{4}\frac{N}{mm^2} = 162.5\ MPa$$

The allowable shear stress can be determined by using maximum shear stress theory:

$$\tau_{all} = \tau_w = \frac{\sigma_{all}}{2} = \frac{162.5}{2}\frac{N}{mm^2} = 81.25\ MPa$$

The bending and shearing stresses can be determined as follows the square section.

$$\sigma_x = \frac{F_x}{A} - \frac{M_y z}{I_y} + \frac{M_z y}{I_z}$$

$$\tau = \frac{Tt}{J_\alpha}$$

The second moment of area about y- and z-axes are same because it is square section.

$I_y = I_z = \frac{S^4}{12}$, z=y=$\frac{S}{2}$, $t = S$, $A = S^2$ and $J_\alpha = \alpha b t^3 = \alpha S^4 = 0.208 S^4$

$$\sigma_x = -\frac{3167.798}{S^2} - \frac{342088.123 \times 6}{S^3} - \frac{229203.467 \times 6}{S^3} = -\frac{3167.798}{S^2} - \frac{3427749.540}{S^3}$$

$$\tau = \frac{T}{0.208 S^3} = \frac{100067.187}{0.208 S^3} = \frac{481092.245}{S^3}$$

The side of the square cross section of the beam can be analyzed by using maximum shear theory i.e., $\sigma_y = \sigma_z = 0$.

$$\tau_{max} = \tau_{all} = \sqrt{\left(\frac{\sigma_x}{2}\right)^2 + {\tau_{xy}}^2} = 81.25\ MPa$$

$$= \sqrt{\left(-\frac{3167.798}{2S^2} - \frac{3427749.540}{2S^3}\right)^2 + \left(\frac{481092.245}{S^3}\right)^2}$$

$$S^3 = \sqrt{(-19.494S - 2109.228)^2 + 5921.135^2} \rightarrow S = 18.582\ mm$$

The side of the square cross section beam can also be analyzed by using principal stress i.e.,$\sigma_y = \sigma_z = 0$.

$$\sigma_{1,2} = \sigma_{all} = \frac{\sigma_x}{2} \pm \sqrt{\left(\frac{\sigma_x}{2}\right)^2 + {\tau_{xy}}^2} = 162.5\ MPa$$

$$= -\frac{3167.798}{2S^2} - \frac{3427749.540}{2S^3}$$

$$\pm \sqrt{\left(-\frac{3167.798}{2S^2} - \frac{3427749.540}{2S^3}\right)^2 + \left(\frac{481092.245}{S^3}\right)^2}$$

$$d^3 = -9.747S - 10546.922 \pm \sqrt{(-9.747S - 10546.922)^2 + 2960.568^2} \rightarrow d = 7.399\ mm$$

The side of the square cross section becomes 18.582 mm. However, the beam should be hollow section to maximize the strength to weight ratio i.e., the second moment of area should be same both for solid (S) and hollow section (S_o and S_i).

$$S^4 = {S_o}^4 - {S_i}^4 = 119223.684$$

The internal (S_i) and external (S_o) sides of the square section can be optimized by iteration to 35 mm and 40 mm respectively [54].

The shearing stress should be checked for closed thin wall section.

$$t = \frac{S_o - S_i}{2} = \frac{40 - 35}{2} = 2.5\ mm\ and\ A = 37.5 \times 37.5 = 1406.25\ mm^2$$

$$\tau = \frac{T}{2tA} = \frac{100067.187}{2 \times 2.5 \times 1406.25} = 14.232\ MPa$$

The bending stress in the x-axis becomes as follows.

$$\sigma_x = \frac{F_x}{A} - \frac{M_x z}{I_x} + \frac{M_z x}{I_z} = -\frac{3167.798}{{S_o}^2 - {S_i}^2} - \frac{342088.123 \times 6S_o}{{S_o}^4 - {S_i}^4} - \frac{229203.467 \times 6S_o}{{S_o}^4 - {S_i}^4}$$

$$= -\frac{3167.798}{40^2 - 35^2} - \frac{342088.123 \times 6 \times 40}{40^4 - 35^4} - \frac{229203.467 \times 6 \times 40}{40^4 - 35^4}$$

$$= -137.873\ MPa$$

The maximum shear stress becomes;

$$\tau_{max} = \sqrt{\left(\frac{\sigma_x}{2}\right)^2 + {\tau_{xy}}^2} = \sqrt{\left(\frac{-137.873}{2}\right)^2 + (14.232)^2} = 70.390\ MPa < \tau_{all}$$

The maximum principal stress also becomes;

$$\sigma_{1,2} = \frac{\sigma_y}{2} \pm \sqrt{\left(\frac{\sigma_y}{2}\right)^2 + {\tau_{xy}}^2} = \frac{-137.873}{2} \pm \sqrt{\left(\frac{-137.873}{2}\right)^2 + 14.232^2} = |139.327|\ MPa$$

$$< \sigma_{all}$$

The applied normal and shearing stresses are less than the allowable corresponding stresses which indicates that the beam design is safe.

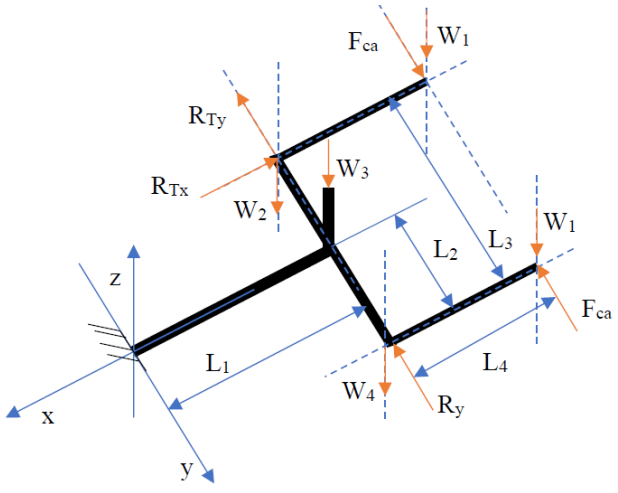

Figure 4-88 FBD for Bottom Fixed beam

The value of loads in bottom fixed beam are 12.302 N, 30.230 N, 284.419 N, 210.089 N, 72.961

N, 267.683 N, 290.97 N and 5.739 N for R_y, W_4, W_3, W_2, R_{Tx}, R_{Ty}, F_{ca}, and W_1 respectively. The lengths L_1, L_2, L_3 and L_4 are 197.083 mm, 304.8 mm, 609.6 mm and 106.9 mm respectively.

Table 4-9 Weight W_3 of Top Beam Assembly on Bottom Fixed Beam

S. No	Part Name	Quantity	Mass in Kg	Total Mass in Kg
1	Bevel Pinion	1	0.23	0.23
2	V-Grooved Pulley on Motor Shaft	1	0.42	0.42
3	V-Grooved Pulley on Intermediate Shaft	1	1.83	1.83
4	Intermediate Shaft	1	0.08	0.08
5	Ball Bearing on Intermediate Shaft	1	0.0074	0.0074
6	Thrust Bearing on Intermediate Shaft	1	0.023	0.023
7	Key on Intermediate Shaft for Bevel Gear	1	0.0012	0.0012
8	Key on Intermediate Shaft for V-Grooved Pulley	1	0.0012	0.0012
9	Frame for Solar Panel Support	1	0.95	0.95
10	DC Motor	1	25	25
11	Gear Box	1	0.17	0.17
12	Top Cantilever Beam	1	0.28	0.28
	Total	12	28.9928	28.9928

Table 4-10 Weight W_4 of Idler Shaft Assembly on Bottom Fixed Beam

S. No	Part Name	Quantity	Mass in Kg	Total Mass in Kg
3	Conveyor Pulleys on Conveyor	1	2.74	2.74
5	Flat Belt	0.5	0.18	0.09
6	Lug	6.5	0.03	0.195
7	Rivet for Lug	15	0.002	0.03
23	Idler Shaft	1	0.02	0.02
24	Ball Bearing for Idler Shaft	1	0.0026	0.0026
25	Thrust Bearing for Idler Shaft	1	0.004	0.004
Total		26	2.9786	3.0816

All the above loads create normal and shearing plane stresses. The normal stress is due to axial and bending loads and shearing stress due to twisting moment. The axial stress is induced due to load R_{Tx}=72.961 N. The torsional moment T can be analyzed as follows.

$$T = (W_2 - W_4)L_2 = (210.089 - 30.230)304.8 = 54821.023\ Nmm$$

The bending moment on the fixed beam between the origin and T connection can be defined as follows both about y- and z-axes.

$$\mathrm{M}_y = -(W_2 + W_3 + W_4)x - 2W_1x = -(210.089 + 284.419 + 30.230)x - 2 \times 5.739x$$

$$= -536.216x$$

$$\mathrm{M}_z = \left(R_y + R_{Ty}\right)x - R_{Tx}L_2 = (12.302 + 267.683)x - 72.961 \times 304.8$$

$$= 279.985x - 22238.513$$

The bending moments M_y and M_z becomes maximum at origin (x=L_1=197.083 mm) which are -105679.058 Nmm and 32941.771 Nmm.

These loads create normal and shearing plane stresses.

Materials: The beam has square section. It is made of high carbon steel of Fe E 650 Indian standard designation and 870 N/mm^2 tensile strength and 650 N/mm^2 yield stress (σ_y). Since, the system is used in the outdoor, its safety factor (n) is four. Hence, the allowable stress becomes:

$$\sigma_{all} = \sigma_w = \frac{\sigma_y}{n} = \frac{650}{4}\frac{N}{mm^2} = 162.5\ MPa$$

The allowable shear stress can be determined by using maximum shear stress theory:

$$\tau_{all} = \tau_w = \frac{\sigma_{all}}{2} = \frac{162.5}{2}\frac{N}{mm^2} = 81.25\ MPa$$

The bending and shearing stresses can be determined as follows the square section.

$$\sigma_x = \frac{F_x}{A} - \frac{M_y z}{I_y} + \frac{M_z y}{I_z}$$

$$\tau = \frac{Tt}{J_\alpha}$$

The second moment of area about y- and z-axes are same because it is square section.

$I_y = I_z = \frac{S^4}{12}$, z=y=$\frac{S}{2}$, $t = S$, $A = S^2$ and $J_\alpha = \alpha b t^3 = \alpha S^4 = 0.208S^4$

$$\sigma_x = \frac{72.961}{S^2} + \frac{105679.058 \times 6}{S^3} + \frac{32941.771 \times 6}{S^3} = \frac{72.961}{S^2} + \frac{831724.974}{S^3}$$

$$\tau = \frac{T}{0.208S^3} = \frac{54821.023}{0.208S^3} = \frac{264043.380}{S^3}$$

The side of the square cross section of the beam can be analyzed by using maximum shear theory i.e., $\sigma_y = \sigma_z = 0$.

$$\tau_{max} = \tau_{all} = \sqrt{\left(\frac{\sigma_x}{2}\right)^2 + {\tau_{xy}}^2} = 81.25\ MPa$$

$$= \sqrt{\left(\frac{72.961}{2S^2} + \frac{831724.974}{2S^3}\right)^2 + \left(\frac{264043.380}{S^3}\right)^2}$$

$$S^3 = \sqrt{(0.449S + 5118.308)^2 + 3249.765^2} \rightarrow S = 18.241\ mm$$

The side of the square cross section beam can also be analyzed by using principal stress i.e.,$\sigma_y =$

$\sigma_z = 0.$

$$\sigma_{1,2} = \sigma_{all} = \frac{\sigma_x}{2} \pm \sqrt{\left(\frac{\sigma_x}{2}\right)^2 + {\tau_{xy}}^2} = 162.5\ MPa$$

$$= \frac{72.961}{2S^2} + \frac{831724.974}{2S^3} \pm \sqrt{\left(\frac{72.961}{2S^2} + \frac{831724.974}{2S^3}\right)^2 + \left(\frac{264043.380}{S^3}\right)^2}$$

$$d^3 = 0.224S + 2559.154 \pm \sqrt{(0.224S + 2559.154)^2 + 1624.882^2} \rightarrow d = 17.756\ mm$$

The side of the square cross section becomes 18.241 mm. However, the beam should be hollow section to maximize the strength to weight ratio i.e., the second moment of area should be same both for solid (S) and hollow section (S_o and S_i).

$$S^4 = {S_o}^4 - {S_i}^4 = 110711.969$$

The internal (S_i) and external (S_o) sides of the square section can be optimized by iteration to 22 mm and 25 mm respectively.

The shearing stress should be checked for closed thin wall section.

$$t = \frac{S_o - S_i}{2} = \frac{25 - 22}{2} = 1.5\ mm\ and\ A = 23.5 \times 23.5 = 552.25\ mm^2$$

$$\tau = \frac{T}{2tA} = \frac{54821.023}{2 \times 1.5 \times 552.25} = 33.089\ MPa$$

The bending stress in the x-axis becomes as follows.

$$\sigma_x = \frac{F_x}{A} - \frac{M_x z}{I_x} + \frac{M_z x}{I_z} = \frac{72.961}{{S_o}^2 - {S_i}^2} + \frac{105679.058\ \times 6S_o}{{S_o}^4 - {S_i}^4} + \frac{32941.771 \times 6S_o}{{S_o}^4 - {S_i}^4}$$

$$= \frac{72.961}{25^2 - 22^2} + \frac{105679.058 \times 6 \times}{3025^4 - 22^4} + \frac{32941.771 \times 6 \times 25}{25^4 - 22^4} = 133.492\ MPa$$

The maximum shear stress becomes;

$$\tau_{max} = \sqrt{\left(\frac{\sigma_x}{2}\right)^2 + {\tau_{xy}}^2} = \sqrt{\left(\frac{133.492}{2}\right)^2 + (33.089\ )^2} = 74.498\ MPa < \tau_{all}$$

The maximum principal stress also becomes;

$$\sigma_{1,2} = \frac{\sigma_y}{2} \pm \sqrt{\left(\frac{\sigma_y}{2}\right)^2 + {\tau_{xy}}^2} = \frac{133.492}{2} \pm \sqrt{\left(\frac{133.492}{2}\right)^2 + (33.089\ )^2} = 141.244\ MPa < \sigma_{all}$$

The applied normal and shearing stresses are less than the allowable corresponding stresses which indicates that the beam design is safe.

The **column** has square cross section. It supports vertical load which creates compressive load. The load is the sum of W_1, W_2, W_3 and W_4.

$$W = 2W_1 + W_2 + W_3 + W_4 = 2 \times 5.739 + 210.089 + 284.419 + 30.230 = 536.216 \text{ N}$$

Materials: The column is made of high carbon steel of Fe E 650 Indian standard designation and 870 N/mm^2 tensile strength and 650 N/mm^2 yield stress (σ_y). Since, the system is used in the outdoor, its safety factor (n) is four. Hence, the allowable stress becomes:

$$\sigma_{all} = \sigma_w = \frac{\sigma_y}{n} = \frac{650}{4}\frac{N}{mm^2} = 162.5\ MPa$$

The compressive stress can be determined as follows the square section.

$$\sigma_x = \frac{F_x}{A} = 162.5\ MPa = \frac{536.216\ N}{S^2} \rightarrow S = 1.817\ mm$$

The column can be designed by considering buckling for fixed ends. The column has a length from bottom to top beam (542.762 mm) which is the sum of height of camshaft (462.762) and half of the gear box (160/2=80 mm). The critical load can be determined as follows.

$$P_c = \frac{\pi^2 EI}{4L^2} \rightarrow I = \frac{S^4}{12} = \frac{4WL^2}{\pi^2 E} = \frac{4 \times 536.216 \times 542.762^2}{\pi^2 \times 210000} \rightarrow S = 7.777\ mm$$

The side of the square cross section of the column becomes 7.777 mm. However, the column should be hollow section to maximize the strength to weight ratio i.e., the second moment of area should be same both for solid (S) and hollow section (S_o and S_i).

$$S^4 = {S_o}^4 - {S_i}^4 = 3658.040$$

The internal (S_i) and external (S_o) sides of the square section can be optimized by iteration to 8 mm and 10 mm respectively [54].

The critical load can be determined as follows.

$$P_c = \frac{\pi^2 EI}{4L^2} = \frac{\pi^2 E}{4L^2}\left(\frac{{S_o}^4 - {S_i}^4}{12}\right) = \frac{\pi^2 \times 210000}{4 \times 542.762^2}\left(\frac{10^4 - 8^4}{12}\right) = 865.377 \text{ N}$$

The designed critical load is greater than the applied load which indicates that the column design is safe.

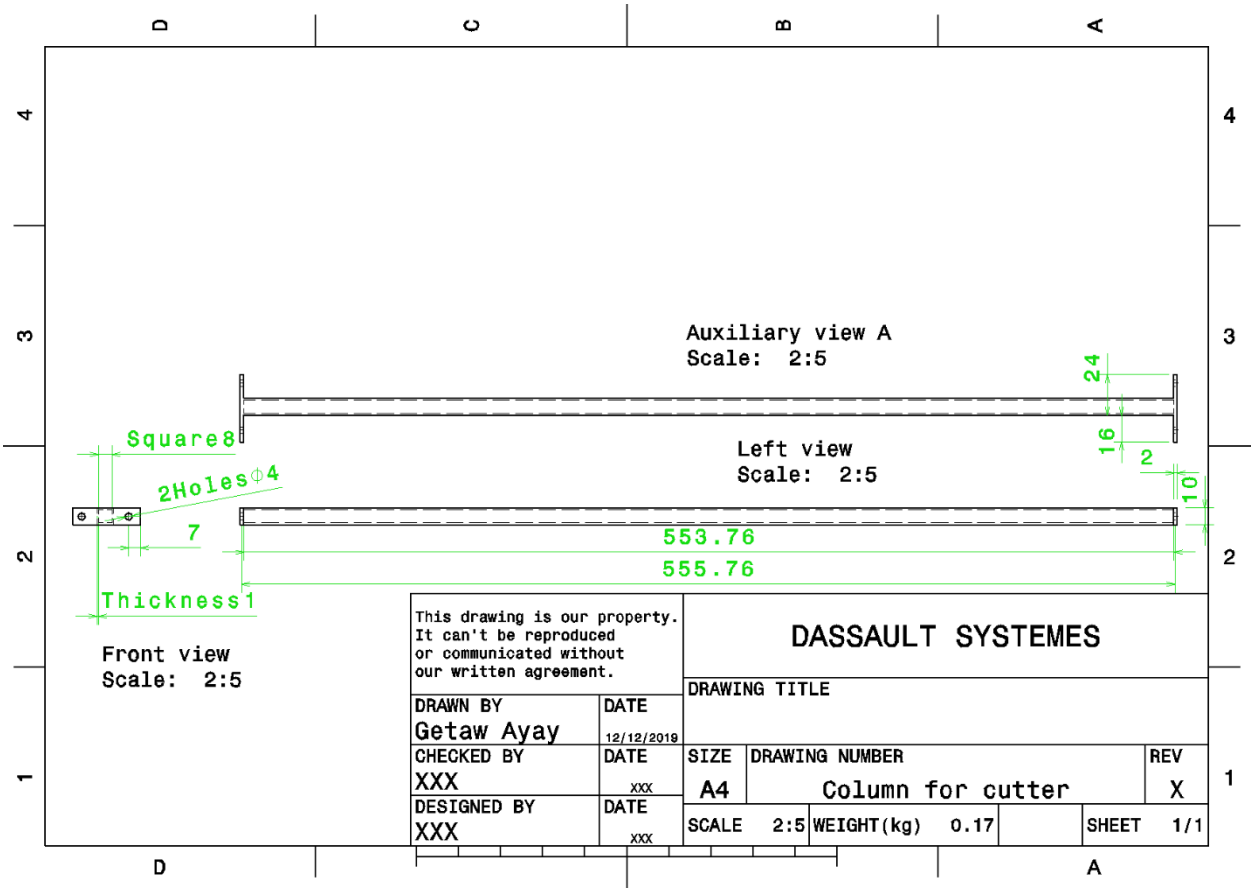

Part Drawing 4-34 Column for Cutter Frame

Axel: It connects the two tires and supports all the weight attached on the cutter frame. The weight is **74.438** Kg or 730.237 N see **Table** 4-11.

Table 4-11 Weight on Axel

S. No	Part Name	Quantity	Mass in Kg	Total Mass in Kg
1	Bevel Pinion	1	0.230	0.230
2	Bevel Gear	1	2.310	2.310
3	Conveyor Pulleys on Conveyor	1	2.740	2.740
4	Conveyor Pulleys on Cam Shaft	1	2.780	2.780
5	Flat Belt	1	0.180	0.180
6	Lug	13	0.030	0.390
7	Rivet for Lug	30	0.002	0.060
8	Bolt for Blade	16	0.007	0.106
9	Nut for Blade	16	0.004	0.056
10	Blade or Cutter	8	0.030	0.240
11	Cutter Bar	1	0.230	0.230

12	Guard Lip	10	0.010	0.100
13	Bolt for Guard Lip	24	0.009	0.209
14	Nut for Guard Lip	24	0.003	0.067
15	Guard Lip Bar	1	0.140	0.140
16	Bearing for Cutter Bar Support	4	0.005	0.022
17	Follower Bar	1	0.100	0.100
18	Rollers for follower bar	8	0.004	0.031
19	Rectangular Box for Follower Bar	1	0.170	0.170
20	Vertical Position Pin for Follower Support	4	0.057	0.229
21	Horizontal Position Pin for Follower Support	4	0.032	0.130
22	Follower Head	2	0.130	0.260
23	Idler Shaft	1	0.020	0.020
24	Ball Bearing for Idler Shaft	1	0.003	0.003
25	Thrust Bearing for Idler Shaft	1	0.004	0.004
26	Camshaft	1	0.700	0.700
27	Ball Bearing for Camshaft	1	0.007	0.007
28	Thrust Bearing for Camshaft	1	0.022	0.022
29	Eccentric Cam	1	0.520	0.520
30	Key on Camshaft for Bevel Gear	1	0.001	0.001
31	Key on Camshaft for Conveyor Pulley	1	0.004	0.004
32	Key on Camshaft for Cam:	1	0.001	0.001
33	V-Grooved Pulley on Motor Shaft	1	0.420	0.420
34	V-Grooved Pulley on Intermediate Shaft	1	1.830	1.830
35	Intermediate Shaft	1	0.080	0.080
36	Ball Bearing on Intermediate Shaft	1	0.007	0.007
37	Thrust Bearing on Intermediate Shaft	1	0.023	0.023
38	Key on Intermediate Shaft for Bevel Gear	1	0.001	0.001
39	Key on Intermediate Shaft for V-Grooved Pulley	1	0.001	0.001
40	Star Wheel vertical Rod	4	0.140	0.560
41	Star Wheel Arm	4	0.160	0.640
42	Bearing Between Star Wheel Arm and Rod	4	0.007	0.028
43	Frame for Solar Panel Support	1	0.950	0.950
44	DC Motor	1	25.000	25.000
45	Crop Divider	4	0.110	0.440
46	Star Wheel and Divider Assembly Support	4	0.190	0.760
47	Gear Box	1	0.170	0.170
48	Top Fixed Beam	1	0.581	0.581

49	Bottom Fixed Beam	1	0.218	0.218
48	Bottom Cantilever Beam	1	0.080	0.080
49	Top Cantilever Beam	1	0.280	0.280
49.4	Column	2	0.154	0.307
50	Solar Panels	2	15.000	30.000
Total		**220**	**55.887**	**74.438**

The axel has fixed ends on the tires. Hence, it is fixed beam. Its length is 609.6 mm.

The forces and bending moments on the axel can be determined from the free body diagram shown in **Figure** 4-89. Since the weight (W) is applied at the mid span of the axel and the support of axel is same at its ends, the reaction forces and moments should be equal. This implies that $R_1 = R_2$, and $M_1 = M_2$.

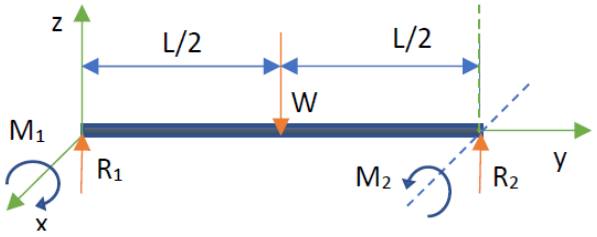

Figure 4-89 FBD of Axel

$$\sum F_z = 0 \rightarrow 2R_1 - \mathrm{W} = 0 \rightarrow R_1 = \frac{\mathrm{W}}{2} = \frac{730.237}{2} = 365.119\ N = R_2$$

$$\sum M_x = 0 \rightarrow -M_1 - \frac{L}{2}\mathrm{W} + M_2 + LR_2 = 0 \rightarrow -M_1 + M_2 = 0 \rightarrow M_1 = M_2$$

Note: The axel is statically indeterminate because there are two unknowns and one equation. Therefore, the unknowns can be determined by considering deflection (both transverse and slope) either at point 1 or 2 using elastic curve equations.

$$\frac{d^2z}{dy^2} = \frac{M_y}{EI}$$

The bending moment equation on the range of $[0, L/2]$ can be derived from **Figure** 4-90.

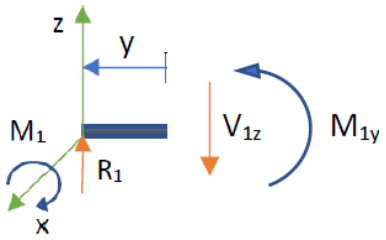

Figure 4-90 FBD of Axel Between [0, L/2]

$$\sum M_x = 0 \rightarrow -M_1 - yR_1 + M_{1y} = 0 \rightarrow M_{1y} = M_1 + yR_1 = 365.119\text{y} + M_1$$

$$\frac{d^2z}{dy^2} = \frac{M_y}{EI} = \frac{365.119\text{y} + M_1}{EI}$$

The 1st and 2nd integrals become as follows.

$$\frac{dz}{dy} = \theta_1 = \frac{182.560y^2 + M_1\text{y} + C_1}{EI}$$

$$z_1 = \frac{60.853y^3 + 0.5M_1y^2 + C_1y + C_2}{EI}$$

The slope and transverse deflection at point 1 are zero. Hence at y=0, $z = \theta = 0$. This implies that $C_1 = 0$ and $C_2 = 0$

The deflection equations simplified as follows.

$$\theta_1 = \frac{182.560y^2 + M_1\text{y}}{EI}$$

$$z_1 = \frac{60.853y^3 + 0.5M_1y^2}{EI}$$

The bending moment equation on the range of $[L/2, \text{L}]$ can be derived from **Figure** 4-91.

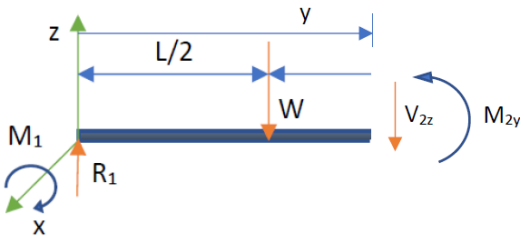

Figure 4-91 FBD of [L/2, L]

$$\sum M_x = 0 \rightarrow -M_1 - yR_1 + \text{W}\left(y - \frac{L}{2}\right) + M_{2y} = 0 \rightarrow M_{2y} = M_1 + yR_1 - \text{W}\left(y - \frac{L}{2}\right)$$

$$= -365.119\text{y} + 222576.238 + M_1$$

$$\frac{d^2z}{dy^2} = \frac{M_y}{EI} = \frac{-365.119\text{y} + 222576.238 + M_1}{EI}$$

The 1st and 2nd integrals becomes as follows.

$$\frac{dz}{dy} = \theta_2 = \frac{-182.560y^2 + 222576.238\text{y} + M_1\text{y} + C_3}{EI}$$

$$z_2 = \frac{-60.853y^3 + 111288.119y^2 + 0.5M_1y^2 + C_3y + C_4}{EI}$$

The slope and transverse deflection at point 2 are zero. Hence at y=L, $z = \theta = 0$. This implies that $C_3 = -67.841 \times 10^6 - 609.6M_1$ and $C_4 = 13.785 \times 10^9 + 304.8M_1$

The deflection equations can be simplified by substituting C_3 and C_4 values.

$$\theta_2 = \frac{-182.560y^2 + 222576.238\text{y} + M_1\text{y} - 67.841 \times 10^6 - 609.6M_1}{EI}$$

$$z_2 = \frac{-60.853y^3 + 111288.119y^2 + 0.5M_1y^2 - (67.841 \times 10^6 + 609.6M_1)y + 13.785 \times 10^9 + 304.8M_1}{EI}$$

The reaction bending moment M_1 can be determined by equating θ_1 and θ_2 at the midpoint (L/2).

$$\frac{182.560\left(\frac{L}{2}\right)^2 + M_1\left(\frac{L}{2}\right)}{EI} = \frac{-182.560\left(\frac{L}{2}\right)^2 + 222576.238\left(\frac{L}{2}\right) + M_1\left(\frac{L}{2}\right) - 67.841 \times 10^6 - 609.6M_1}{EI}$$

$$-91.28L^2 - 111288.119\text{L} - 67.841 \times 10^6 - 609.6M_1 = 0$$

$$609.6M_1 = -91.28L^2 - 111288.119\text{L} - 67.841 \times 10^6 \rightarrow M_1 = -278220.137\ Nmm = M_2$$

The bending moment equations can be simplified as follows.

$$M_{1y} = 365.119y + M_1 = 365.119y - 278220.137$$

$$M_{2y} == -365.119y + 222576.238 + M_1 = -365.119y - 55643.899$$

The bending moment equations are linear both in the range of [0, L/2] and [L/2, L] which are [-278220.137, -166931.866] and [-166932.170, -278220.441] Nmm respectively. The Maximum bending moment is 278220.137 Nmm which occurs at the fixed end. So that the axel should be designed for this bending moment.

Note: The axel is inserted in the bearing of the tire which has d=19.073 mm bore bearing. This implies that the diameter of the axel should be greater than or equal to the bore of bearing. So that it is advisable to analyze the materials property to decide its type because the diameter of the axel is already known.

$$\sigma_{all} = \frac{M_x z}{I_x} = \frac{32M_x}{\pi d^3} = \frac{32 \times 278220.137}{\pi 19.073^3} = 408.443\ MPa = \sigma_{all}$$

$I_x = \frac{\pi d^4}{64}$ and $z = \frac{d}{2}$

The yield strength of the material can be determined by using your factor of safety (n).

$$\sigma_y = n\sigma_{all} = 4 \times 408.443 = 1633.773\ MPa$$

The next strong available material is quenched and tempered (Q&T) steel at 205 ^{o}C with 1640 MPa yield strength, 510 BHN and 4140 AISI number.

Discussion on the Diameter of Axel: The axel has 19.073 mm diameter. However, the diameter should be increased to 20 mm because first there is no 19.073 mm diameter standard rod and second there should be shoulder to fix the tire in a position.

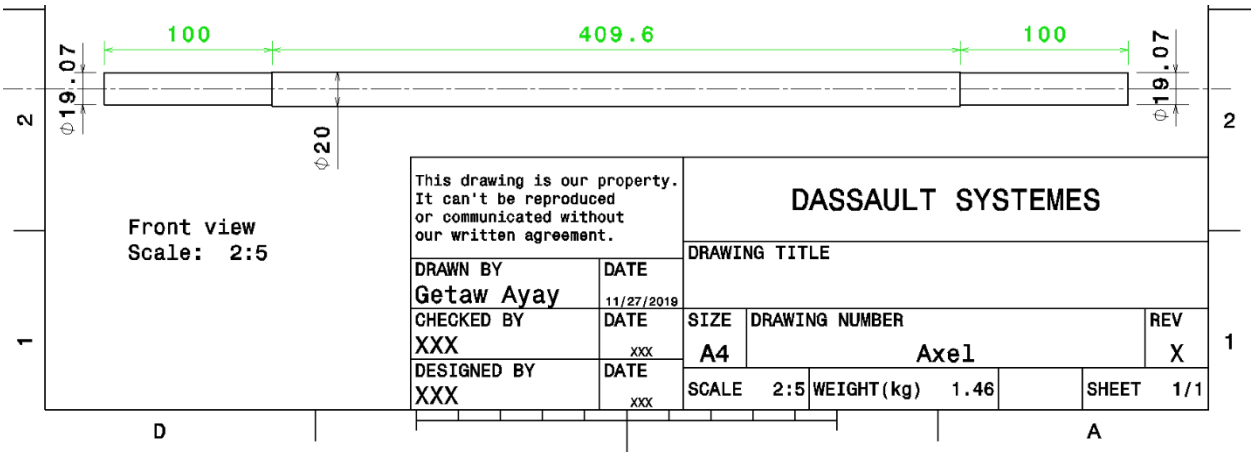

Part Drawing 4-35 Axel

Selection of Tires: It is used to transport the whole harvester. The tire is solid because it will be used in fields where there is no maintenance of tires. Hence, Carlisle branded with solid micro-cellular polyurethane material is selected. It has 4.80/4.00-8 size, 483781 product code, ribbed tread, 3" centered hub, 3/4" (19.073 mm) precision bearings, 15.5'' (394.165 mm) overall diameter, 3.4'' (86.462 mm) width 8.0-pound (3.629 Kg) tire + wheel weight and 500-pound (226.796 Kg) weight capacity [55].

Mathematical Modeling for Pushing the Harvester

The harvester should be stable during movement in a leveled field about the centroid of the axel. The harvester is pushed by human hand force (F_h).

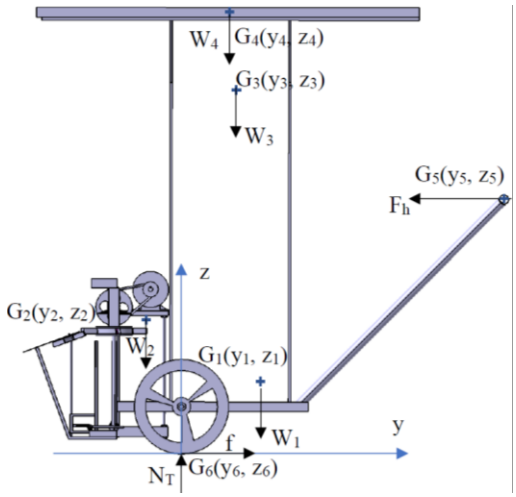

Figure 4-92 2D Side View of Solar Harvester about yz-Plane

The pushing human hand force (F_h) can be determined by applying equilibrium equations for **Figure** 4-92. The assembly has four sub-assemblies which has a centroid coordinates about the local axis a local axis; tire sub assembly G_1 (x_1,y_1,z_1), whole cutter system sub assembly G_2 (x_2,y_2,z_2), solar panel support G_3 (x_3,y_3,z_3) and solar panel G4 (x_4,y_4,z_4). The position of human hand force is located at (x_5,y_5,z_5) and the contact between ground and land has a coordinate of (x_6,y_6,z_6).

The summation of forces in the y-axis of the harvester can be defined as follows see **Figure** 4-92.

$$\sum F_y \leq 0 \rightarrow -F_h + f \leq 0 \rightarrow F_h \geq f = \mu_6 N_T$$ ---------- *4-90*

The frictional resistance of the ground with the tires f is equal to $\mu_6 N_T$.

The summation of forces in the z-axis of the harvester can be defined as follows see **Figure** 4-92.

$$\sum F_z = 0 - - \rightarrow N_T = W_1 + W_2 + W_3 + W_4 + W_4$$ ---------- *4-91*

The summation of moments about centroid (G) of the axel axis can be defined as follows by considering diameter (d) of tires see **Figure** 4-92.

$$\sum \mathrm{M}_{Gx} = 0 \rightarrow F_h(z_5 - \mathrm{d}/2) - W_4 y_4 - W_3 y_3 + W_2 y_2 - W_1 y_1 + \mathrm{f}d/2 = 0$$ ---------- 4-92

The pushing human hand force (F_h) can be defined by using the **equations** 4-90**,** 4-91 and 4-9**2**.

$$F_h \geq \mu_6(W_1 + W_2 + W_3 + W_4 + W_4) \; or \; F_h = \frac{W_4 y_4 + W_3 y_3 - W_2 y_2 + W_1 y_1 - \mathrm{f}d/2}{(z_5 - \mathrm{d}/2)}$$ ---------- 4-93

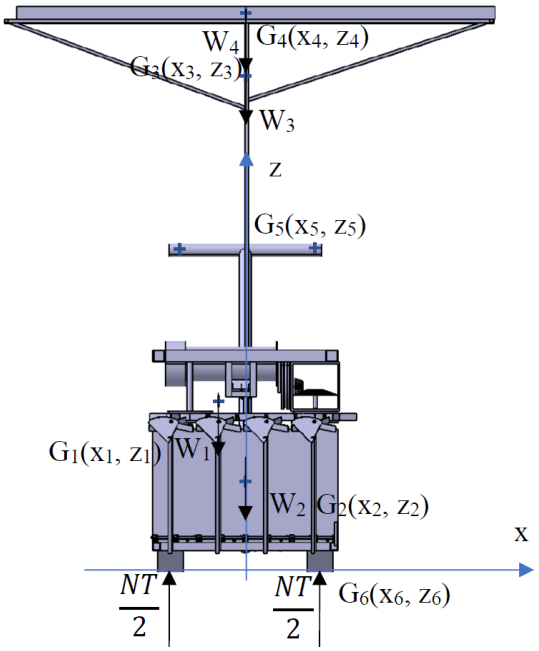

Figure 4-93 2D Front View of Solar Harvester about xz-Plane

The summation of moments about centroid (G) of the axel in the y-axis can be defined as follows by considering diameter (d) of tires see **Figure** 4-93. The weights w_2, w_3 and w_4 passes through the origin or centroid of axel in the y-axis. Hence, they cannot create moment about y-axis of the centroid of axel.

$$\sum M_{Gy} = 0 \rightarrow W_1 x_1 = 0 \quad \text{---------- 4-94}$$

Discussion about Coordinate x_1: **Equation** 4-94 shows that the value of x_1 must as small as possible otherwise it will unbalance the stability of the harvester. The harvester will try to rotate in the positive y-axis. Therefore, the position of solar panel and its support should be shifted to the positive x-axis to counter act this moment. **Equation** 4-94 can be modified as follows**.**

$$\sum M_{Gy} = 0 \rightarrow W_1 x_1 - (W_3 + W_4) x_3 = 0 \rightarrow x_3 = \frac{W_1 x_1}{(W_3 + W_4)} \quad \text{---------- 4-95}$$

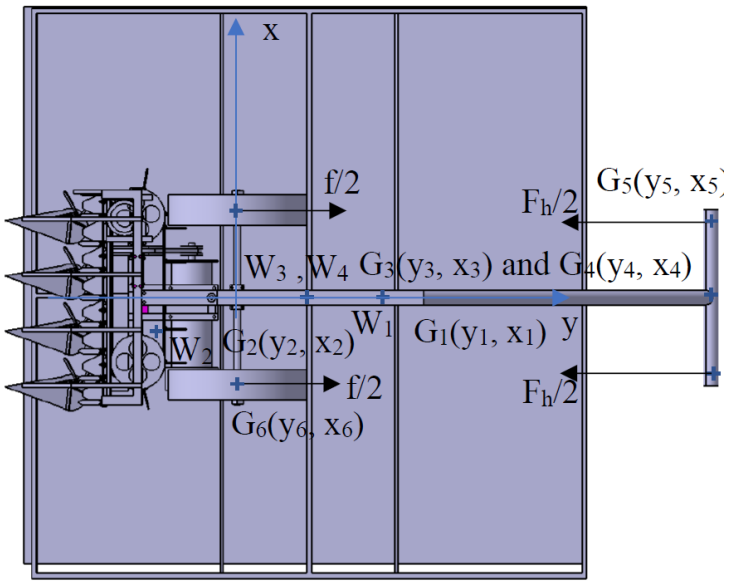

Figure 4-94 2D Bottom View of Solar Harvester about yx-Plane

Gathered Information: the weights (w_1, w_2, w_3 and w_4) and centroidal coordinates (x_1, x_2, x_3, x_4, x_5, x_6, y_1, y_2, y_3, y_4, y_5, y_6, z_1, z_2, z_3, z_4, z_5, z_6) with respect to local axis. The four sub-assemblies have a global coordinate which are taken from CATIA drawing. The global coordinate of sub-assemblies are for tire sub assembly G_1 (235.991, 422.734, -37.789), whole cutter system sub assembly G_2 (216.135, -37.5, 217.78), solar panel support G_3 (247.991, 379.521, 1344.582) and solar panel G4 (247.991, 379.521, 1486.335). In addition, the axel, tire 1 and tire 2 have centroidal coordinates with respect to global axes (235.991, 174.434, -160.926), (-11.809, 174.434, -160.926) and (483.791,174.434, -160.926) respectively. The diameter of the tire is 394.165 mm. The local axis (0,0,0) is located at the mid-point of the tires in the x-axis 235.991, 174.434 in the y-axis and -358.009 below z-axis with respect to the global axis. The centroidal coordinates of G_1, G_2, G_3, G_4, G_5, and G_6 can be redefined in terms of local axis (0,0,0) i.e., tire sub assembly G_1 (0, 248.3, 320.22), whole cutter system sub assembly G_2 (-19.856, -211.934, 575.789), solar panel support G_3 (12, 205.087, 1702.591) and solar panel G4 (12, 205.087, 1844.344). The position of the contact between ground and land has a coordinate of G_6 (±247.8, 0, 0). All dimensions are in mm. The weights w_1, w_2, w_3 and w_4 are 14.655 Kg, 48.074 Kg, 7.432 Kg and 29.868 Kg or 143.766 N, 471.606 N, 72.908 N and 293.005 N respectively.

The coefficient of rolling friction μ_6 between the ground and tire is 0.03 [**56**].

Discussion on Mathematical Modeling for Pushing the Harvester: The pushing human hand force (F_h) can be determined by using the **equations** 4-93.

$$F_h \geq 0.03(143.766 + 471.606 + 72.908 + 293.005) = 29.005\ N$$

Any adult person can apply up to 300 N pushing force for prolonged time which indicate that the harvester can be easily transported by a single person.

$$F_h = \frac{293.005 \times 205.087 + 72.908 \times 205.087 - 471.606 \times 211.934 + 143.766 \times 248.3 - 29.005 \times 197.083}{(z_5 - 197.083)}$$

$$= \frac{5{,}075.359}{z_5 - 197.083} \text{ ---------- } \textit{4-96}$$

The value of the pushing force in **equation** 4-96 is less or equal to 300 N which is a force applied by adult person.

$$\frac{5{,}075.359}{z_5 - 197.083} \leq 300 \rightarrow z_5 \geq 214.000\ mm$$

The value of z_5 is the height of the handle from ground which depends on the height of the user. Its value is estimated between 910 mm and 1120 mm [**45**]. It is preferable to choose average for the time being 1015 mm. The width and diameter of the handle is recommended to 460 mm and [25,38] mm respectively [**45**]. The width should be maximized to 500 mm by considering longest shoulder. Hence, the x_5 value becomes 250 mm.

The moment about y-axis can be determined by using **equation** 4-94 as follows.

$$W_1 x_1 = 14.655 \times 0 = 0$$

This shows that, there is no need to shift the position of solar panel and its support. Hence, **equation** 4-95 becomes useless.

$$x_3 = \frac{W_1 x_1}{(W_3 + W_4)} = \frac{W_1 \times 0}{(W_3 + W_4)} = 0$$

The stability of harvester about centroid (G) of the axel axis can be determined by using **equation** 4-93 as follows.

$$F_h(z_5 - d/2) - W_4 y_4 - W_3 y_3 + W_2 y_2 - W_1 y_1 + \frac{fd}{2} \geq 0$$

$$29.005(z_5 - 197.083) - 293.005 \times 205.087 - 72.908 \times 205.087 + 471.606 \times 211.934$$
$$- 143.766 \times 248.3 + 29.005 \times 197.083 \geq 0$$

$$29.005 z_5 - 10791.751 \geq 0 \rightarrow z_5 \geq 372.065\ mm$$

Therefore, the height z_5 (1015 mm) is more capable to push the harvester.

Handle: the handle is used to transfer power from hand to axel. It is subjected to 300 pushing force and has 1015 mm height from ground. However, it is located on top of the handle and axel holder which is fixed on axel. The axel is located at the center of the tire 197.083 mm above ground and

the height of the handle above the tire becomes 817.917 mm.

The length l of the handle is determined from the height 817.917 mm and base 600 mm [**56**] using Pythagoras theorem see **Figure** 4-95.

$$l = \sqrt{817.917^2 + 600^2} = 1014.391\ mm$$

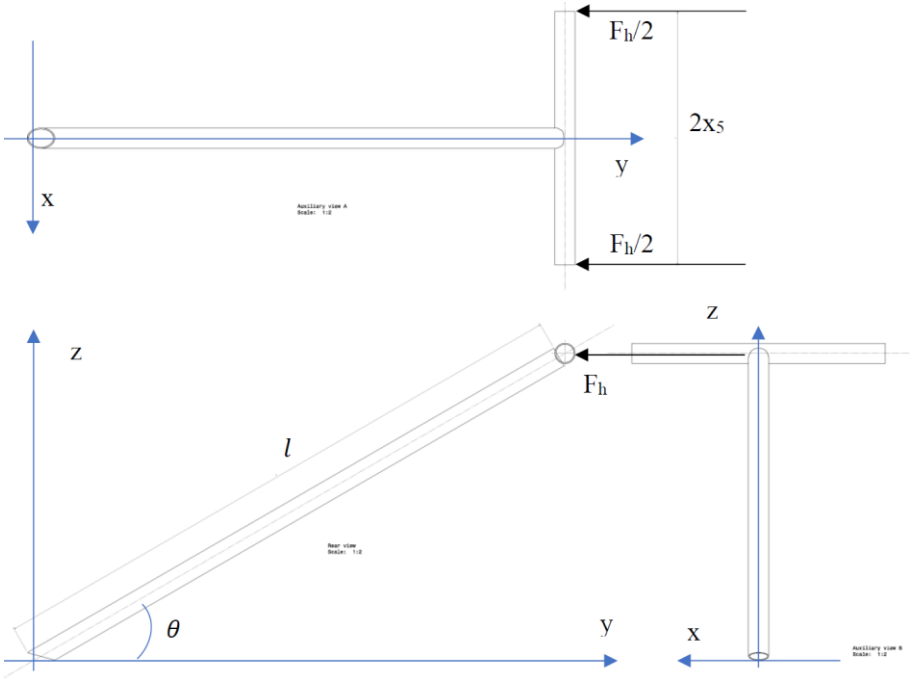

Figure 4-95 Multi View of Handle Sketch

The handle has T-shape i.e., the handle head is under bending stress whereas the leg under compressive and bending stresses.

Handle Head: It is cantilever beam about the joint. The maximum bending moment becomes

$$M_{max} = \frac{F_h}{2} x_5 = 150 \times 250 = 37500\ Nmm$$

Handle Leg: it is also a cantilever beam about the joint between itself and handle holder. The compressive load is equal to;

$$F_c = F_h \cos\theta = 300 \times \frac{600}{1014.391} = 177.446\ N$$

The bending load and maximum bending moment become as follows.

$$F_b = F_h \sin\theta = 300 \times \frac{817.917}{1014.391} = 241.894\ N$$

$$M_{max} = F_b l = 241.894 \times 1014.391 = 245375.097\ Nmm$$

Note: Both the handle head and leg are circular cross section.

Materials for handle: Both the handle head and leg are made of high carbon steel of Fe E 650 Indian standard designation and 870 N/mm^2 tensile strength and 650 N/mm^2 yield stress (σ_y). Since, the system is used in the outdoor, its safety factor (n) is four. Hence, the allowable stress becomes:

$$\sigma_{all} = \sigma_w = \frac{\sigma_y}{n} = \frac{650}{4}\frac{N}{mm^2} = 162.5\ MPa$$

The combined stress on the handle leg can be determined as follows for the circular section.

$$\sigma = -\frac{F_c}{A} \pm \frac{M_x y}{I_x}$$

The above normal stress (σ) becomes maximum at y=d/2. The unit of the diameter is millimeter.

$$A = \frac{\pi d^2}{4}, I_x = \frac{\pi d^4}{64}$$

$$\sigma = -\frac{4F_c}{\pi d^2} \pm \frac{32M_{max}}{\pi d^3} = -\frac{4 \times 177.446}{\pi d^2} \pm \frac{32 \times 245375.097}{\pi d^3} = 162.5MPa$$

$$d = \sqrt[3]{-1.390d \pm 15380.740} \longrightarrow d = 24.850\ mm$$

The handle leg can be designed by considering buckling for fixed ends. The critical load can be determined as follows.

$$P_c = \frac{\pi^2 EI}{4L^2} \longrightarrow I = \frac{\pi d^4}{64} = \frac{4F_c L^2}{\pi^2 E} = \frac{4 \times 177.446 \times 1014.391^2}{\pi^2 \times 210000} \rightarrow d = 12.255\ mm$$

The diameter of the leg of the handle should be 24.850 mm. However, the handle should be hollow section to maximize the strength to weight ratio i.e., the second moment of area should be same both for solid (S) and hollow section (S_o and S_i).

$$d^4 = {d_o}^4 - {d_i}^4 = 381334.038$$

The internal (d_i) and external (d_o) diameters of the square section can be optimized by iteration to 24 mm and 30 mm respectively [54].

The critical load can be determined as follows.

$$P_c = \frac{\pi^2 EI}{4L^2} = \frac{\pi^2 E}{4L^2}\pi\left(\frac{{d_o}^4 - {d_i}^4}{64}\right) = \frac{\pi^3 \times 210000}{4 \times 1014.391^2}\left(\frac{30^4 - 24^4}{64}\right) = 11820.873\ \text{N}$$

The designed critical load is greater than the applied load which indicates that the handle leg design is safe.

The normal stress is also determined for the hollow section as follows.

$$\sigma = -\frac{4 \times 177.446}{\pi(30^2 - 24^2)} \pm \frac{32 \times 245375.097 \times 30}{\pi(30^4 - 24^4)} = 157.489\ MPa$$

The applied normal stress is less than the allowable stress which indicates that the handle leg design is safe.

Handle Head: The bending stress on the handle head can be determined as follows for the circular section.

$$\sigma = \frac{M_x y}{I_x}$$

The above normal stress (σ) becomes maximum at y=d/2. The unit of the diameter is millimeter.

$$I_x = \frac{\pi d^4}{64}$$

$$\sigma = \frac{32M_{max}}{\pi d^3} = \frac{32 \times 37500}{\pi d^3} = 162.5MPa$$

$$d = 13.296\, mm$$

The diameter of the head of the handle is 13.296 mm. However, the handle should be hollow section to maximize the strength to weight ratio i.e., the second moment of area should be same both for solid (S) and hollow section (S_o and S_i).

$$d^4 = {d_o}^4 - {d_i}^4 = 31252.447$$

The internal (d_i) and external (d_o) diameters of the square section can be optimized by iteration to 28 mm and 30 mm respectively [54].

The normal stress is also determined for the hollow section as follows.

$$\sigma = \frac{32 \times 37500 \times 30}{\pi(30^4 - 28^4)} = 58.661\, MPa$$

The applied normal stress is less than the allowable stress which indicates that the handle head design is safe.

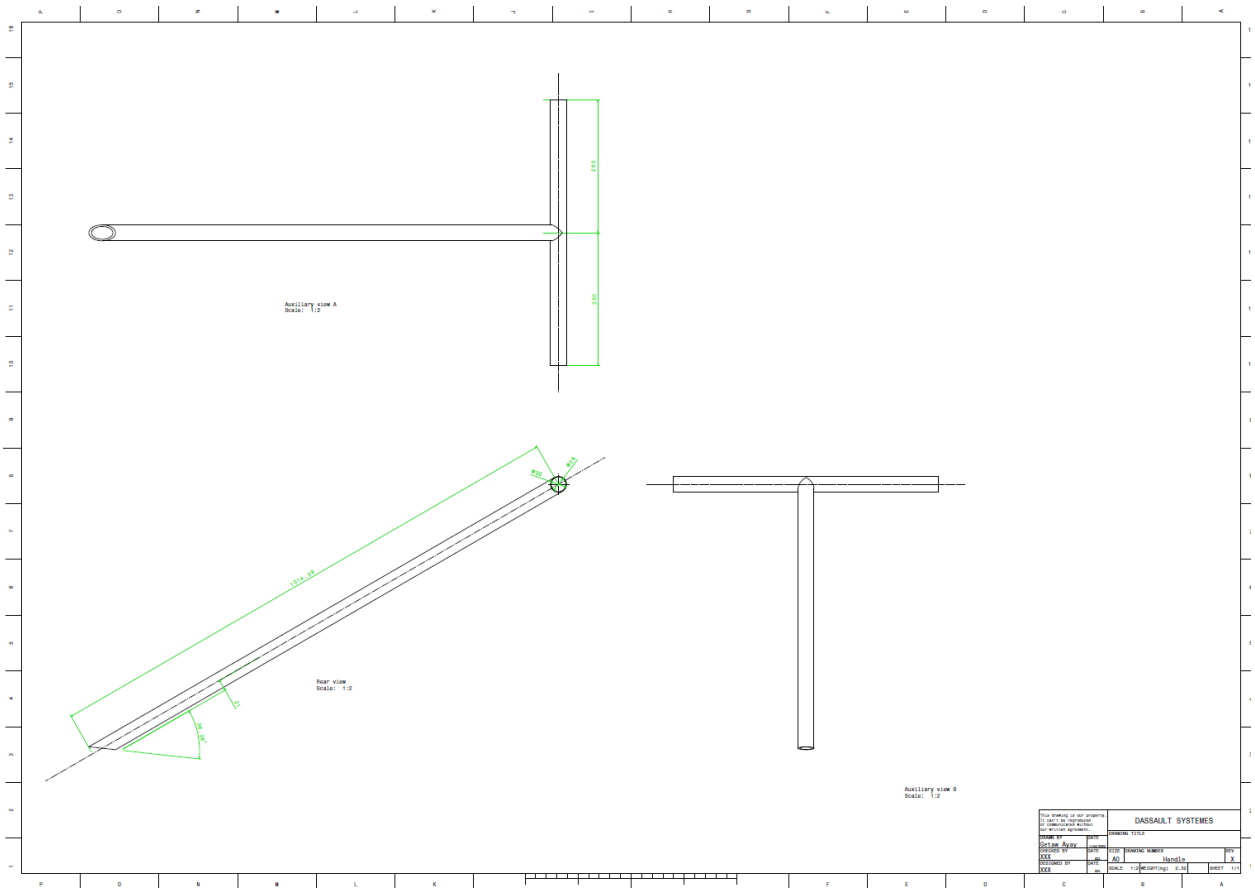

Part Drawing 4-36 Handle

Threaded Rod: It is used to join the main harvester with the vehicle. In addition it is used to adjust the height of cutting. The whole weight W_2 of the main harvester (471.606 N) is applied on it at G_2 (-19.856, -211.934, 575.789) with respect to the local axis. The location of the centroid of the threaded rod is at (235.991, 101.763, -22.711) mm with respect to the global coordinate system. Its centroid becomes (0, -72.723, 335.298) with respect to the local axis. The weight W_2 creates compressive and bending stresses. The bending moments are about x- and y-axes.

$$M_x = -471.606 \times (-211.934 + 72.723) = 65652.743\ Nmm$$

$$M_y = -471.606 \times (-19.856 - 0) = 9364.209\ Nmm$$

Materials for Thread Rod: Both the handle head and leg are made of high carbon steel of Fe E 650 Indian standard designation and 870 N/mm^2 tensile strength and 650 N/mm^2 yield stress (σ_y). Since, the system is used in the outdoor, its safety factor (n) is four. Hence, the allowable stress becomes:

$$\sigma_{all} = \sigma_w = \frac{\sigma_y}{n} = \frac{650}{4}\frac{N}{mm^2} = 162.5\ MPa$$

The normal stress due to the combined stresses becomes;

$$\sigma_z = -\frac{W_2}{A} \pm \frac{M_x y}{I_x} \pm \frac{M_y x}{I_y}$$

The above normal stress (σ_z) becomes maximum at y=d/2. The unit of the diameter is millimeter.

$$A = \frac{\pi d^2}{4}, I_x = \frac{\pi d^4}{64} = I_y$$

$$\sigma_z = -\frac{4 \times 471.606}{\pi d^2} \pm \frac{32(65652.743 + 9364.209)}{\pi d^3} = 162.5$$

$$d = \sqrt[3]{-3.695d \pm 4702.255} = 16.827\ mm$$

This diameter is the core diameter of the threaded rod. The next available standard thread rod is Mfr. Model # M20130.200.1000, Country of Origin Taiwan, Material Steel, Grade Class 10.9, Threaded Rod Finish Black Oxide, Thread Size M20-2.5mm, Length 1m, Thread Direction Right Hand, Min. Tensile Strength 145,000 psi, Temp. Range -58 Degrees to 302 Degrees F and Yield Strength 130,000 psi [**58**].

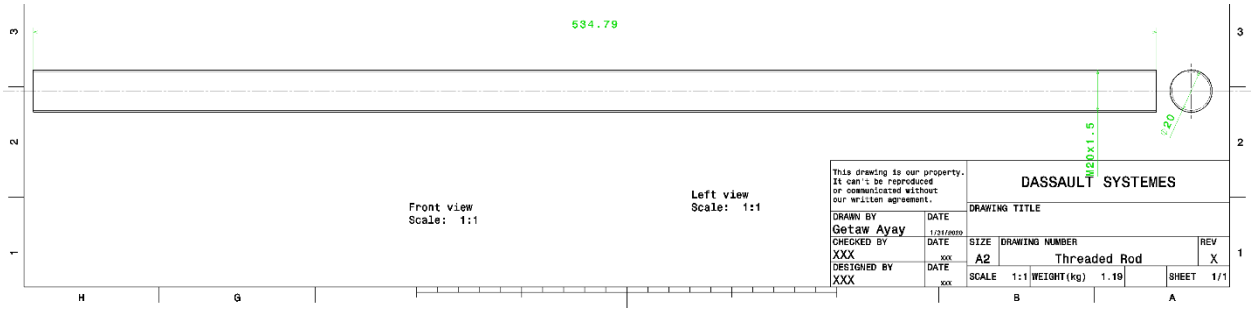

Part Drawing 4-37 Threaded Rod

Fit and Tolerance

Fit and Tolerance of Gear on its Hole: The fits between the hole of gear and both camshaft and intermediate shaft is transition H7/k6. The magnitude of the common tolerance (IT) of the pinion and gear can be determined as follows by using the Renard R5 geometric series of numbers (i) (Joseph E. Shigley and Charles R. Mischke, 1996).

$$i = \frac{(0.45D^{1/3} + 0.001D)}{1000} \quad \text{---------- 4-97}$$

Where D is the geometric mean of the size range under consideration and is obtained from the formula

$$D = \sqrt{D_{max} D_{min}} \quad \text{---------- 4-98}$$

The basic size of hole of bevel gear is 13.221 mmm. It is in the size range between 10 and 18.

$$D = \sqrt{18 \times 10} = 13.416$$

$$\rightarrow i = \frac{\left(0.45 \times 13.416^{1/3} + 0.001 \times 13.416\right)}{1000} = 0.0011\ mm$$

The tolerance of the shaft is IT6 for transition fit k6.

$$IT6 = 10i = 10 \times 0.0011 = 0.011\ mm$$

The formula for fundamental deviation of the shaft is determined as follows using $\alpha = 0$, $\beta = 0.6$ and $\gamma = 0.33$ for k fundamental deviation using (Joseph E. Shigley and Charles R. Mischke, 1996 table 19.4).

$$Fundamental\ Deviation = \alpha + \frac{\beta D^{\gamma}}{1000} = 0 + \frac{0.6 \times 13.416^{0.33}}{1000} = 0.001\ mm$$

The lower deviation of the shaft is equal to the fundamental deviation (0.001 mm). The upper deviation is the sum of IT6 grade and fundamental deviation.

$$Upper\ deviation\ of\ shaft = 0.001 + 0.011 = 0.012\ mm$$

The shaft limits are;

$$Upper\ shaft\ limit = 13.221 + 0.001 = 13.222\ mm$$

$$Lower\ shaft\ limit = 13.221 + 0.012 = 13.233\ mm$$

The tolerance of the hole of bevel gear is IT7 for H7 transition fit. The formula for IT7 is:

$$IT7 = 16i = 0.0011 \times 16 = 0.017\ mm$$

The formula for fundamental deviation of the hole is determined as follows using $\alpha = 0$, $\beta = 0$ and $\gamma = 0$ for h fundamental deviation using (Joseph E. Shigley and Charles R. Mischke, 1996 table 19.4).

$$Fundamental\ Deviation = \alpha + \frac{\beta D^{\gamma}}{1000} = 0 + \frac{0 \times 13416^{0}}{1000} = 0.000\ mm$$

The lower deviation of the hole is the negative of the upper deviation of the shaft i.e., -0.012 mm. The upper deviation of the gear hole is equal to the sum of IT7 grade and lower deviation of hole (Joseph E. Shigley and Charles R. Mischke, 1996).

$$upper\ deviation\ (hole) = \text{lower deviation (shaft)} + \text{IT7 (Hole)} = -0.012 + 0.017$$

$$= 0.005\text{mm}$$

The gear limits are;

$$Upper\ gear\ limit = 13.221 + 0.005 = 13.226\ mm$$

$$Lower\ gear\ limit = 13.221 - 0.012 = 13.209\ mm$$

The hole of the pinion gear is 12.379 mmm. It is in the size range between 10 and 18.

$$D = \sqrt{18 \times 10} = 13.416$$

$$\rightarrow i = \frac{\left(0.45 \times 13.416^{1/3} + 0.001 \times 13.416\right)}{1000} = 0.0011\ mm$$

The tolerance of the shaft is IT6 for transition fit k6.

$$IT6 = 10i = 10 \times 0.0011 = 0.011\ mm$$

The formula for fundamental deviation of the shaft is determined as follows using $\alpha = 0$, $\beta = 0.6$ and $\gamma = 0.33$ for k fundamental deviation using (Joseph E. Shigley and Charles R. Mischke, 1996 table 19.4).

$$Fundamental\ Deviation = \alpha + \frac{\beta D^{\gamma}}{1000} = 0 + \frac{0.6 \times 13416^{0.33}}{1000} = 0.001\ mm$$

The lower deviation of the shaft is equal to the fundamental deviation (0.001 mm). The upper deviation is the sum of IT grade IT6 and fundamental deviation.

$$Upper\ deviation\ of\ shaft = 0.001 + 0.011 = 0.012\ mm$$

The shaft limits are;

$$Upper\ shaft\ limit = 13.221 + 0.001 = 13.222\ mm$$

$$Lower\ shaft\ limit = 13.221 + 0.012 = 13.233\ mm$$

The tolerance of the hole of bevel gear is IT7 for H7 transition fit. The formula for IT7 is:

$$IT7 = 16i = 0.0011 \times 16 = 0.017\ mm$$

The formula for fundamental deviation of the hole is determined as follows using $\alpha = 0$, $\beta = 0$ and $\gamma = 0$ for h fundamental deviation using (Joseph E. Shigley and Charles R. Mischke, 1996 table 19.4).

$$Fundamental\ Deviation = \alpha + \frac{\beta D^{\gamma}}{1000} = 0 + \frac{0 \times 13416^{0}}{1000} = 0.000\ mm$$

The lower deviation of the hole is the negative of the upper deviation of the shaft i.e., -0.012 mm. The upper deviation of the gear hole is equal to the sum of IT7 grade and lower deviation of hole (Joseph E. Shigley and Charles R. Mischke, 1996).

$$upper\ deviation\ (hole) = \text{lower deviation (shaft)} + \text{IT7 (Hole)} = -0.012 + 0.017$$

$$= 0.005\text{mm}$$

The gear limits are;

$$Upper\ gear\ limit = 13.221 + 0.005 = 13.226\ mm$$

$$Lower\ gear\ limit = 13.221 - 0.012 = 13.209\ mm$$

Fit and Tolerance of Conveyor Pulleys on its Hole: The fits between the hole of conveyor pulley and camshaft is transition H7/k6. The magnitude of the common tolerance (IT) of the conveyor pulley and shafts can be determined as follows by using the Renard R5 geometric series of numbers (i) (Joseph E. Shigley and Charles R. Mischke, 1996).

$$i = \frac{\left(0.45D^{1/3} + 0.001D\right)}{1000}$$

Where D is the geometric mean of the size range under consideration and is obtained from the formula

$$D = \sqrt{D_{max}D_{min}}$$

The hole of the conveyor pulley on camshaft is 15.5 mmm. It is in the size range between 10 and 18.

$$D = \sqrt{18 \times 10} = 13.416$$

$$\rightarrow i = \frac{\left(0.45 \times 13.416^{1/3} + 0.001 \times 13.416\right)}{1000} = 0.0011\ mm$$

The tolerance of conveyor pulley on camshaft is IT7 for H7 transition fit. The formula for IT7 is:

$$IT7 = 16i = 0.0011 \times 16 = 0.017\ mm$$

Correspondingly, the tolerance of the shaft is IT6 for transition fit k6.

$$IT6 = 10i = 10 \times 0.0011 = 0.011\ mm$$

The formula for fundamental deviation of the shaft is determined as follows $\alpha = 0$, $\beta = 0.6$ and $\gamma = 0.33$ using (Joseph E. Shigley and Charles R. Mischke, 1996 table 19.4).

$$Fundamental\ Deviation = \alpha + \frac{\beta D^{\gamma}}{1000} = 0 + \frac{0.6 \times 13.416^{0.33}}{1000} = 0.001\ mm$$

The upper deviation is equal the fundamental deviation (0.001 mm). The lower deviation can be determined by subtracting IT6 from fundamental deviation.

$$Lower\ deviation\ of\ shaft = 0.001 - 0.011 = -0.010\ mm$$

The shaft limits are;

$$Upper\ shaft\ limit = 15.5 + 0.001 = 15.501\ mm$$

$$Lower\ shaft\ limit = 15.500 - 0.010 = 15.490\ mm$$

The lower deviation of the hole is the negative of the upper deviation of the shaft i.e., -0.001 mm. The upper deviation of the conveyor hole is equal to the negative of the lower deviation of the shaft plus the change in tolerance of that grade and the next finer grade (Joseph E. Shigley and Charles R. Mischke, 1996).

$$upper\ deviation\ (hole) = -\text{lower deviation (shaft)} + \text{IT6 (shaft)} = 0.010 + 0.011$$

$$= 0.021\text{mm}$$

The conveyor hole limits are;

$$Upper\ conveyor\ pulley\ on\ camshaft\ limit = 15.500 + 0.021 = 15.521\ mm$$

$$Lower\ conveyor\ pulley\ on\ camshaft\ limit = 15.500 - 0.001 = 15.499\ mm$$

Fit and Tolerance of Conveyor Pulleys on its Hole: The fits between the hole of conveyor pulley and Idler Shaft is transition H7/k6. The magnitude of the common tolerance (IT) of the conveyor pulley and shafts can be determined as follows by using the Renard R5 geometric series of numbers (i) (Joseph E. Shigley and Charles R. Mischke, 1996).

$$i = \frac{\left(0.45D^{1/3} + 0.001D\right)}{1000}$$

The hole of the conveyor on Idler Shaft is 7 mmm. It is in the size range between 6 and 10.

$$D = \sqrt{10 \times 6} = 7.746$$

$$\rightarrow i = \frac{\left(0.45 \times 7.746^{1/3} + 0.001 \times 7.746\right)}{1000} = 0.001\ mm$$

The tolerance IT is IT7 for H7 transition fit. The formula for IT7 is:

$$IT7 = 16i = 16 \times 0.001 = 0.016\ mm$$

Correspondingly, the tolerance of the shaft is IT6 for transition fit k6.

$$IT6 = 10i = 10 \times 0.001 = 0.010\ mm$$

The formula for fundamental deviation of the shaft is determined as follows $\alpha = 0$, $\beta = 0.6$ and $\gamma = 0.33$ for k6 using (Joseph E. Shigley and Charles R. Mischke, 1996 table 19.4).

$$Fundamental\ Deviation = \alpha + \frac{\beta D^{\gamma}}{1000} = 0 + \frac{0.6 \times 7.746^{0.33}}{1000} = 0.001\ mm$$

The upper deviation is equal the fundamental deviation (0.001 mm). The lower deviation can be determined by subtracting IT6 from fundamental deviation.

$$Lower\ deviation\ of\ shaft = 0.001 - 0.010 = -0.009\ mm$$

The shaft limits are;

$$Upper\ shaft\ limit = 7 + 0.001 = 7.001\ mm$$

$$Lower\ shaft\ limit = 7 - 0.010 = 6.990\ mm$$

The lower deviation of the hole is the negative of the upper deviation of the shaft i.e., -0.001 mm. The upper deviation of the conveyor pulley hole is equal to the negative of the lower deviation of the shaft plus the change in tolerance of that grade and the next finer grade (Joseph E. Shigley and Charles R. Mischke, 1996).

$$upper\ deviation\ (hole) = -\text{lower deviation (shaft)} + \text{IT6 (shaft)} = 0.009 + 0.010$$

$$= 0.019\ \text{mm}$$

The gear limits are;

$$Upper\ conveyor\ pulley\ on\ conveyor\ shaft\ limit = 7 + 0.019 = 7.019\ mm$$

$$Lower\ conveyor\ pulley\ on\ conveyor\ shaft\ limit = 7 - 0.001 = 6.999\ mm$$

Flat Belt Tolerance: total length of belt=1281.993+50=1331.993 mm, width=25 mm and 5 mm. The center distance between the two pulleys is 413.231 mm. The tolerance should be conducted for the center distance. The magnitude of the common tolerance (IT) of the belt can be determined as follows by using the Renard R5 geometric series of numbers (i) (Joseph E. Shigley and Charles R. Mischke, 1996).

$$i = \frac{\left(0.45D^{1/3} + 0.001D\right)}{1000}$$

Where D is the geometric mean of the size range under consideration and is obtained from the formula

$$D = \sqrt{D_{max}D_{min}}$$

The center distance of the pulleys is 413.231 mm. It is in the size range between 400 and 500.

$$D = \sqrt{500 \times 400} = 447.214$$

$$\rightarrow i = \frac{\left(0.45 \times 447.214^{1/3} + 0.001 \times 447.214\right)}{1000} = 0.004\ mm$$

The tolerance of pulley assembly is IT7 for H7 transition fit. The formula for IT7 is:

$$IT7 = 16i = 0.004 \times 16 = 0.064\ mm$$

Correspondingly, the tolerance of the shaft is IT6 for transition fit k6.

$$IT6 = 10i = 10 \times 0.004 = 0.040\ mm$$

The formula for fundamental deviation of the shaft is determined as follows $\alpha = 0$, $\beta = 0.6$ and $\gamma = 0.33$ for k6 using (Joseph E. Shigley and Charles R. Mischke, 1996 table 19.4).

$$Fundamental\ Deviation = \alpha + \frac{\beta D^{\gamma}}{1000} = 0 + \frac{0.6 \times 447.214^{0.33}}{1000} = 0.005\ mm$$

The upper deviation is equal the fundamental deviation (0.005 mm). The lower deviation can be determined by subtracting IT6 from fundamental deviation.

$$Lower\ deviation\ of\ shaft = 0.005 - 0.040 = -0.035\ mm$$

The center distance limits in terms of shafts are;

$$Upper\ shaft\ limit = 413.231 + 0.005 = 413.226\ mm$$

$$Lower\ shaft\ limit = 413.231 - 0.035 = 413.196\ mm$$

The lower deviation of the center distance is the negative of the upper deviation of the shaft i.e., -0.005 mm. The upper deviation of the center distance is equal to the negative of the lower deviation of the shaft plus the change in tolerance of that grade and the next finer grade (Joseph E. Shigley and Charles R. Mischke, 1996).

$$upper\ deviation\ (hole) = -\text{lower deviation (shaft)} + \text{IT6 (shaft)} = 0.035 + 0.040$$
$$= 0.075 \text{ mm}$$

The center distance limits are;

$$Upper\ center\ distance\ limit = 413.231 + 0.075 = 413.306\ mm$$
$$Lower\ center\ distance\ limit = 413.231 - 0.005 = 413.236\ mm$$

Lug: The center distance between the two holes is 11mm. The tolerance should be conducted for the center distance. The fit between the two holes is H7/k6 locational transition fit. The magnitude of the common tolerance (IT) of the holes of lug center distance can be determined as follows by using the Renard R5 geometric series of numbers (i) (Joseph E. Shigley and Charles R. Mischke, 1996).

$$i = \frac{\left(0.45D^{1/3} + 0.001D\right)}{1000}$$

Where D is the geometric mean of the size range under consideration and is obtained from the formula

$$D = \sqrt{D_{max}D_{min}}$$

The center distance between the holes is 11 mm. It is in the size range between 10 and 18.

$$D = \sqrt{18 \times 10} = 13.416$$
$$\rightarrow i = \frac{\left(0.45 \times 13.416^{1/3} + 0.001 \times 13.416\right)}{1000} = 0.001\ mm$$

The tolerance of center distance is IT7 for H7 locational transition fit. The formula for IT7 is:

$$IT7 = 16i = 0.001 \times 16 = 0.016\ mm$$

Correspondingly, the tolerance of the shaft is IT6 for locational transition fit k6.

$$IT6 = 10i = 10 \times 0.001 = 0.001\ mm$$

The formula for fundamental deviation of the shaft is determined as follows $\alpha = 0$, $\beta = 0.6$ and $\gamma = 0.33$ for p6 using (Joseph E. Shigley and Charles R. Mischke, 1996 table 19.4).

$$Fundamental\ Deviation = \alpha + \frac{\beta D^{\gamma}}{1000} = 0 + \frac{0.6 \times 13.416^{0.33}}{1000} = 0.001\ mm$$

The upper deviation is equal the fundamental deviation (0.001 mm). The lower deviation can be determined by subtracting IT6 from fundamental deviation.

$$Lower\ deviation\ of\ shaft = 0.001 - 0.001 = 0\ mm$$

The center distance limits in terms of shafts are;

$$Upper\ shaft\ limit = 11 + 0.001 = 11.001mm$$

$$Lower\ shaft\ limit = 11 + 0 = 11.0\ mm$$

The lower deviation of the center distance is the negative of the upper deviation of the shaft i.e., -0.001 mm. The upper deviation of the center distance is equal to the negative of the lower deviation of the shaft plus the change in tolerance of that grade and the next finer grade (Joseph E. Shigley and Charles R. Mischke, 1996).

$$upper\ deviation\ (hole) = -\text{lower deviation (shaft)} + \text{IT6 (shaft)} = 0 + 0.001$$

$$= 0.001\ \text{mm}$$

The center distance limits are;

$$Upper\ center\ distance\ limit = 11 + 0.001 = 11.001\ mm$$

$$Lower\ center\ distance\ limit = 11 - 0.001 = 10.999\ mm$$

Rivet Tolerance: The magnitude of the common tolerance (IT) of the diameter 4 mm of the rivet can be determined as follows by using the Renard R5 geometric series of numbers (i) (Joseph E. Shigley and Charles R. Mischke, 1996).

$$i = \frac{\left(0.45D^{1/3} + 0.001D\right)}{1000}$$

Where D is the geometric mean of the size range under consideration and is obtained from the formula

$$D = \sqrt{D_{max}D_{min}}$$

The diameter of the rivet is 4 mm. It is in the size range between 3 and 6.

$$D = \sqrt{6 \times 3} = 4.243$$

$$\rightarrow i = \frac{\left(0.45 \times 4.243^{1/3} + 0.001 \times 4.243\right)}{1000} = 0.001\ mm$$

The tolerance of the hole of the lug is IT7 for H7 clearance fit. The formula for IT7 is:

$$IT7 = 16i = 0.001 \times 16 = 0.016\ mm$$

Correspondingly, the tolerance of the rivet is IT6 for locational transition fit k6.

$$IT6 = 10i = 10 \times 0.001 = 0.001\ mm$$

The formula for fundamental deviation of the shaft is determined as follows $\alpha = 0$, $\beta = 0.6$ and $\gamma = 0.33$ for k6 using (Joseph E. Shigley and Charles R. Mischke, 1996 table 19.4).

$$Fundamental\ Deviation = \alpha + \frac{\beta D^{\gamma}}{1000} = 0 + \frac{0.6 \times 4.243^{0.33}}{1000} = 0.001\ mm$$

The upper deviation is equal the fundamental deviation (0.001 mm). The lower deviation can be determined by subtracting IT6 from fundamental deviation.

$$Lower\ deviation\ of\ shaft = 0.001 - 0.001 = 0\ mm$$

The diameters of the rivet are;

$$Upper\ shaft\ limit = 4 + 0.001 = 4.001mm$$

$$Lower\ shaft\ limit = 4 + 0 = 4.0\ mm$$

The lower deviation of the hole is the negative of the upper deviation of the shaft i.e., -0.001 mm. The upper deviation of the diameter of the hole is equal to the negative of the lower deviation of the shaft plus the change in tolerance of that grade and the next finer grade (Joseph E. Shigley and Charles R. Mischke, 1996).

$$upper\ deviation\ (hole) = -\text{lower deviation (shaft)} + \text{IT6 (shaft)} = 0 + 0.001$$
$$= 0.001\ \text{mm}$$

The hole limits are;

$$Upper\ hole\ limit = 4 + 0.001 = 4.001\ mm$$

$$Lower\ hole\ limit = 4 - 0.001 = 3.999\ mm$$

Note: The remaining fit and tolerances are calculated and put together in **Table** 4-26

Analysis of Solar Panels and Batteries

The DC Motor is driven by using solar power source. The total daily energy (E_d) requirement to drive the motor is the product of total power (P) to drive the motor at a time and working hours per day (t_w).

$E_d = Pt_w$ ----------*4-99*

The average sun peak power (P_p) is the ratio of the total daily energy (E_d) requirement and peak power collecting time from sun (t_s) per day.

$P_p = \frac{E_d}{t_s} = \frac{Pt_w}{t_s}$----------*4-100*

The total numbers of solar panels (N_p) needed to collect the peak power becomes the ratio of peak power (P_p) and capacity of single solar panel (E_p).

$$N_p = \frac{P_p}{E_p} = \frac{Pt_w}{E_p t_s} \text{----------4-101}$$

The power is taken from batteries. In order to drive the motor, enough amount of batteries should be installed. At a time, total power (P) is required to drive the motor. The capacity of the battery (P_b) in KW is defined by multiplying its voltage V (v) and current I (A).

$$P_b = VI \text{----------4-102}$$

The number of batteries (N_b) becomes the ratio of total power (P) to drive the motor at a time and capacity of the battery (P_b) in KW.

$$N_b = \frac{P}{P_b} = \frac{P}{VI} \text{----------4-103}$$

Discussion on Solar Panels and Batteries

The specifications of the DC motor are already decided mathematical modeling of power requirement for the harvester. It has a specification of 1.5 hp power, 24 V, 1800 rpm, 62.5 Amps Armature Full Load. The total power (P) to drive the motor at a time becomes 1.5 hp or 1118.55 watt. The standard working time (t_w) is 8 hours per day. So that the total daily energy (E_d) requirement can be analyzed using **equation** 4-99.

$$E_d = Pt_w = 1118.55 \times 8 = 8945.4\ Wh$$

The average sun peak power (P_p) and collecting time from sun (t_s) per day are depends the exact location if the field. Solar harvester is recommended on places where the solar power is available during harvesting time. Ethiopia is one of those places where there is plenty of solar power throughout the year. Hence, our country Ethiopia can be considered as example. In Ethiopia, the intensity of sun ray is good in between 7:30 Am and 5:30 Pm. Among this, the time between 8:00 Am and 5:00 Pm is preferable for harvesting which was proofed during the observational test in the shop. Hence, there is 9 hours sun peak time (t_s) to collect solar power.

$$P_p = \frac{8945.4}{9} = 994.267\ Watt$$

The total numbers of solar panels (N_p) needed to collect the peak power and capacity of single solar panel (E_p) relation be seen in **Table** 4-12. A maximum of 200-Watt solar power was available in Ethiopian market during proforma collection on 2017. Hence, five 200-watt Solarmax solar panels are selected.

$$N_p = \frac{P_p}{E_p} = \frac{994.267}{E_p}$$

Table 4-12 Relation Between Number of Solar Panels and Capacity of Single Solar Panel

capacity of single solar panel W	994	497	331	249	199	166	142	124	110	99	90	83
Number of Solar Panels	1	2	3	4	5	6	7	8	9	10	11	12

At the same, 12 V and 200 Ah Copex solar battery was bought on 2017. The capacity of a single battery can be determined using **equation** 4-102.

$$P_b = VI = 12 \times 200 = 2400\ KWh$$

The number of batteries (N_b) can be determined using **equation** 4-103.

$$N_b = \frac{1118.55}{2400} = 0.466$$

This implies that a single battery can be enough to drive the system for one hour. An additional of one battery is required to drive for the remaining time. Hence using two batteries it is possible to drive the system for a day by substituting the charged battery.

Therefore, five solar panels (200W each) and two batteries (12v and 200Ah each) are used. Carrying those elements is tiresome. The solar panels and one of the batteries should be place on the ground. When the used battery becomes low in charge, the other battery replaces it. By doing so, the weight to be pushed by the operator becomes reduced.

Discussion on Kinematic Analysis of Eccentric Cam and Flat Face Follower

The values of eccentric distance and radius of cam are 38.1 mm and 50.6 mm respectively. The equation of displacement, velocity and acceleration can be simplified as follows.

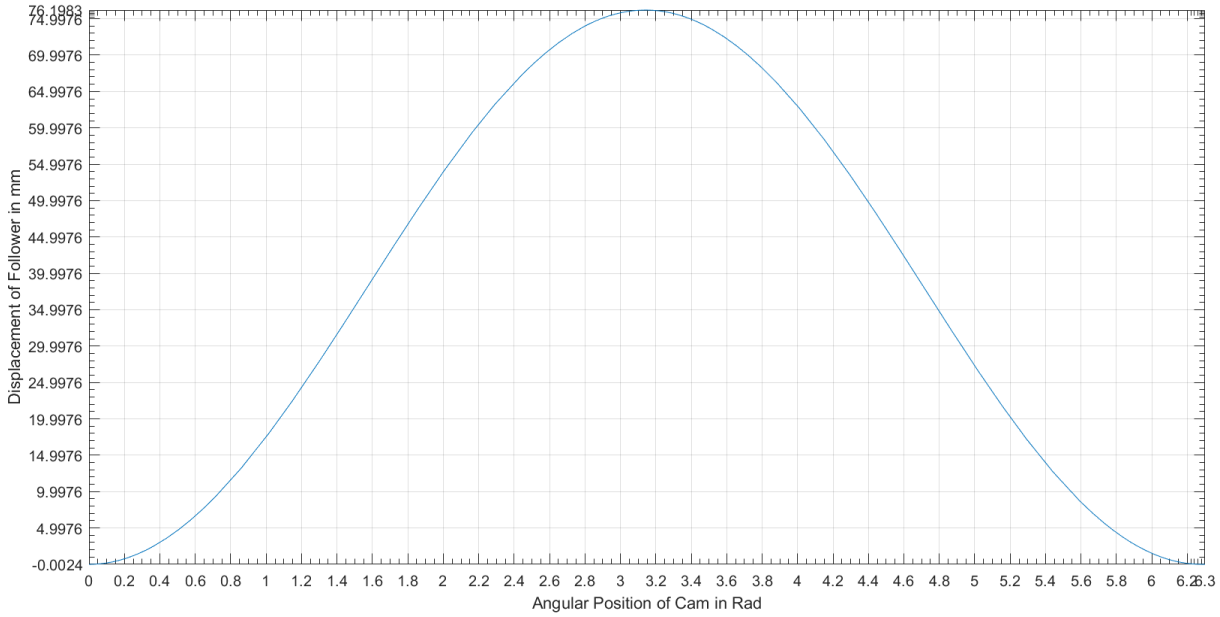

Figure 4-96 Relation between Displacement and Angular Position Graph

$$S = \sqrt{R^2 + e^2 - 2Re\cos\theta - e^2 sin^2\theta} - R + e$$

$$S = \sqrt{4011.91 - 3855.72\cos\theta - 1451.61 sin^2\theta} - 12.5\ mm$$

The graph in **Figure** 4-96 shows that the motion of the follower is sinusoidal simple harmonic motion with 180^o rise and the remaining 180^o dwell. The displacement has maximum (76.2 mm) and minimum positions (0 mm) at 180^o and 0^o respectively.

$$V_f = \frac{dS}{dt} = \frac{2Re\sin\theta - e^2\sin 2\theta}{2\sqrt{R^2 + e^2 - 2Re\cos\theta - e^2 sin^2\theta}}\omega_3$$

$$= \frac{35420.572\sin\theta - 13335.215\sin 2\theta}{\sqrt{4011.91 - 3855.72\cos\theta - 1451.61 sin^2\theta}}\frac{mm}{s}$$

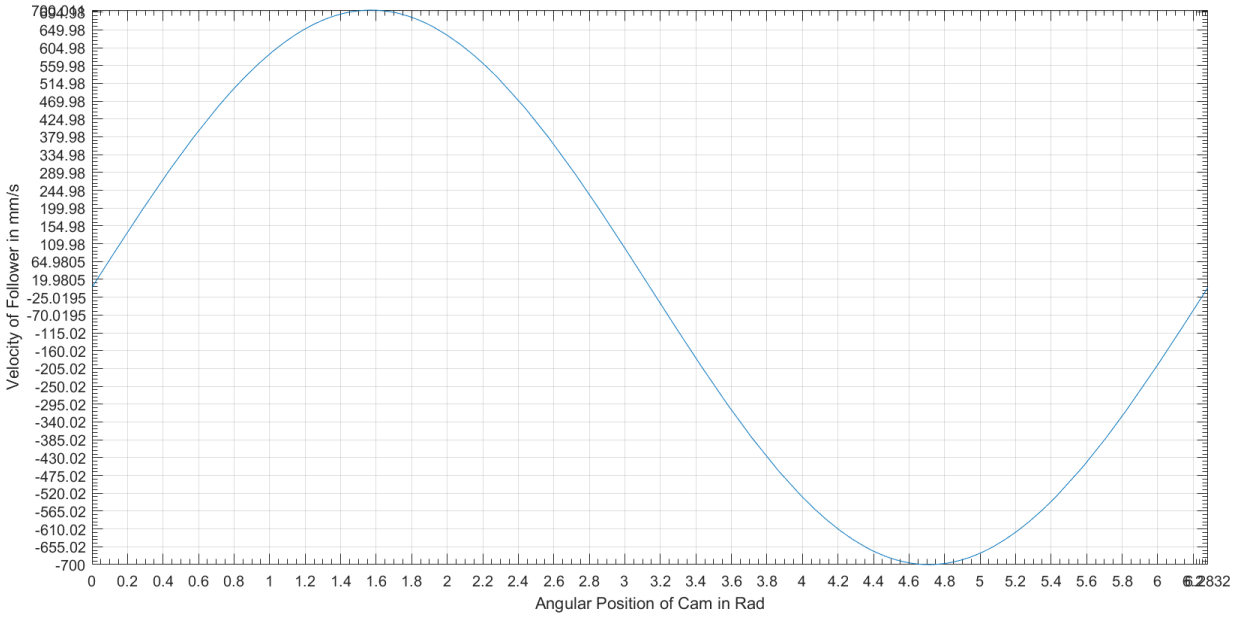

Figure 4-97 Relation between Velocity and Angular Position Graph

The graph in **Figure** 4-97 shows that the velocity of the follower is in a range of [-700, 700] mm/s minimum (0 mm) at 0º and 180º whereas maximum at 90º and 270º (700 mm/s) at the minimum angular speed (18.373 rad/s) of the camshaft. However, whenever there is an increase on the speed of camshaft, the velocity of the follower becomes increased.

$$a_f = \left[\frac{Re\cos\theta - e^2\cos 2\theta}{\sqrt{R^2 + e^2 - 2Re\cos\theta - e^2\sin^2\theta}} - \frac{(2Re\sin\theta - e^2\sin 2\theta)^2}{4(R^2 + e^2 - 2Re\cos\theta - e^2\sin^2\theta)^{1.5}}\right]{\omega_3}^2$$

$$= \left[\frac{650782.165\cos\theta - 490015.820\cos 2\theta}{\sqrt{4011.91 - 3855.72\cos\theta - 1451.61\sin^2\theta}} - \frac{(17710.286\sin\theta - 6667.608\sin 2\theta)^2}{(4011.91 - 3855.72\cos\theta - 1451.61\sin^2\theta)^{1.5}}\right]\frac{mm}{s^2}$$

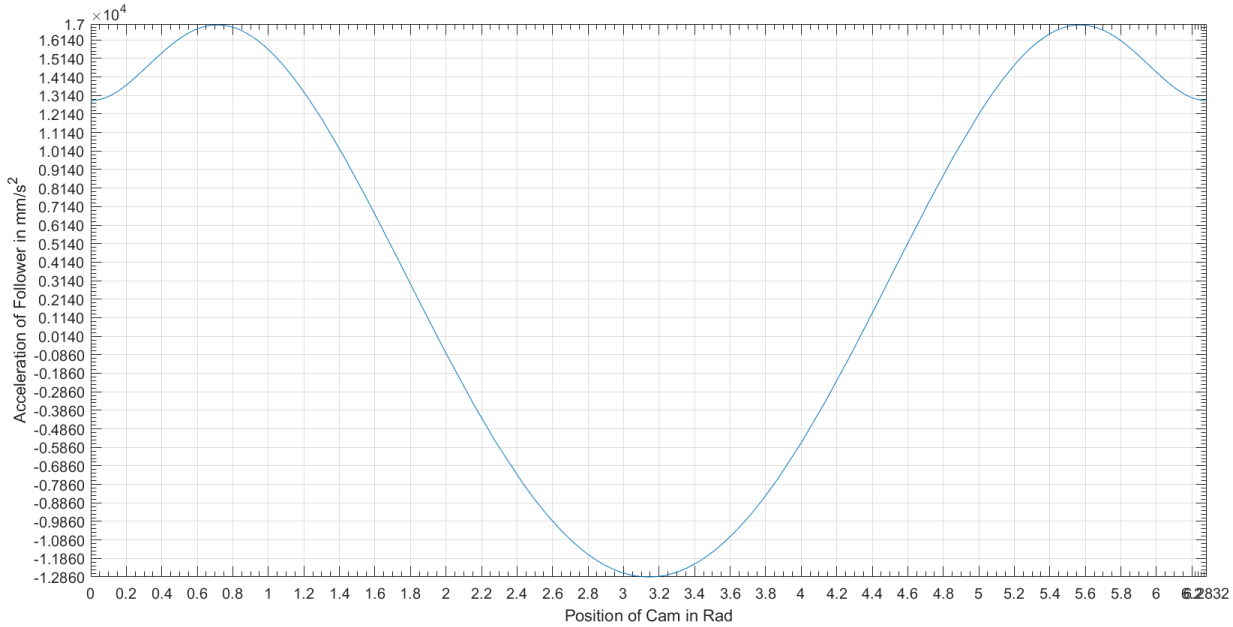

Figure 4-98 Relation between Acceleration and Angular Position Graph

The graph in **Figure** 4-98 shows that the acceleration of the follower is in a range of -12861.357, 17000] mm/s^2 minimum (0 mm) at 112.162º and 247.838º whereas maximum at 41.2253º and 318.747º (1700 mm/ s^2) at the minimum angular speed (18.373 rad/s) of the camshaft. However, whenever there is an increase on the speed of camshaft, the acceleration of the follower becomes increased.

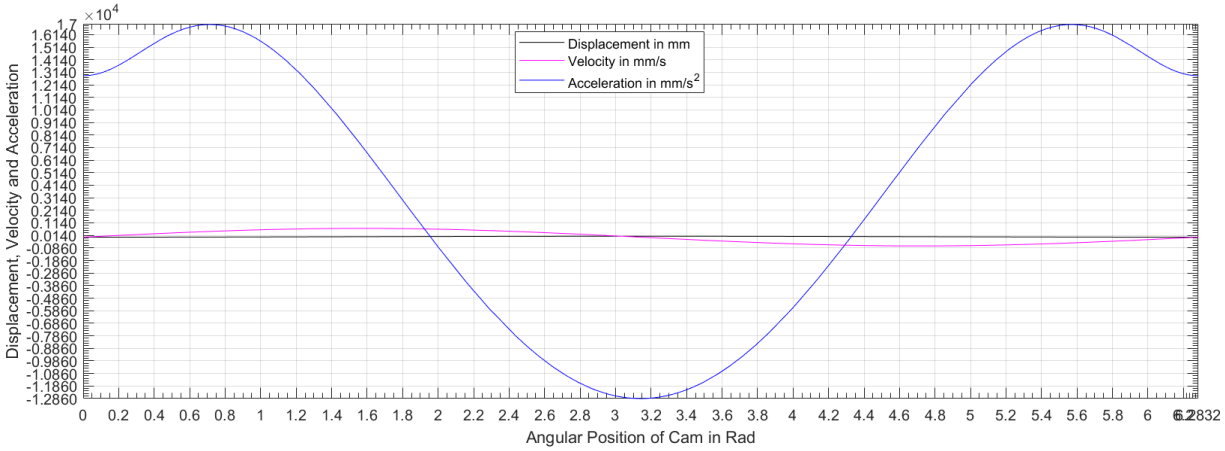

Figure 4-99 Relative of Value of S, V_f and a_f versus Angular Position

Discussion on Kinetic Analysis of Eccentric Cam and Flat Face Follower

The vales of F_{ca}, μ, L_1, L_2, m, a_f, L_3, m_{cb}, g, e, μ_3, R and b are 290.97 N, 0.0011, 78 mm, 98.9 mm, 0.992 Kg, 12.861 m/s^2, 0.632 Kg, 9.81 m/s^2, 38.1 mm, 0.029, 50.6 mm and 609.6 mm respectively.

Table 4-13 Mass m_{cb} of Cutter Assembly

S. No	Part Name	Quantity	Mass in Kg	Total Mass in Kg
8	Bolt for Blade	16	0.007	0.106
9	Nut for Blade	16	0.004	0.056
10	Blade or Cutter	8	0.030	0.240
11	Cutter Bar	1	0.230	0.230
Total		41	0.271	0.632

Table 4-14 Mass m_f of Follower Assembly

S. No	Part Name	Quantity	Mass in Kg	Total Mass in Kg
17	Follower Bar	1	0.100	0.100
22	Follower Head	2	0.130	0.260
Total		3	0.23	0.36

The mass m of cutter bar and follower assemblies becomes 0.992 Kg. The driving force applied on the follower by the cam can be simplified by substituting all the parameters except a_f in mm/s^2.

$$F = \frac{F_{ca}(L_1 + 2\mu L_2) + mL_1(\mu g + a_f) + 2\mu^2 L_3 m_{cb} g}{2\mu e \sin\theta + 2\mu\mu_3\sqrt{R^2 + e^2 - 2Re\cos\theta - e^2\sin^2\theta} + \mu^2\mu_3 b - 2\mu\mu_3 R - 2\mu\mu_3 e + (1 - \mu\mu_3)L_1}$$

$$= \frac{22.760 + 7.738 \times 10^{-5} a_f}{8.382 \times 10^{-5}\sin\theta + 6.38 \times 10^{-5}\sqrt{4.012 \times 10^{-3} - 3.856 \times 10^{-3}\cos\theta - 1.452 \times 10^{-3}\sin^2\theta} + 7.799 \times 10^{-2}} N$$

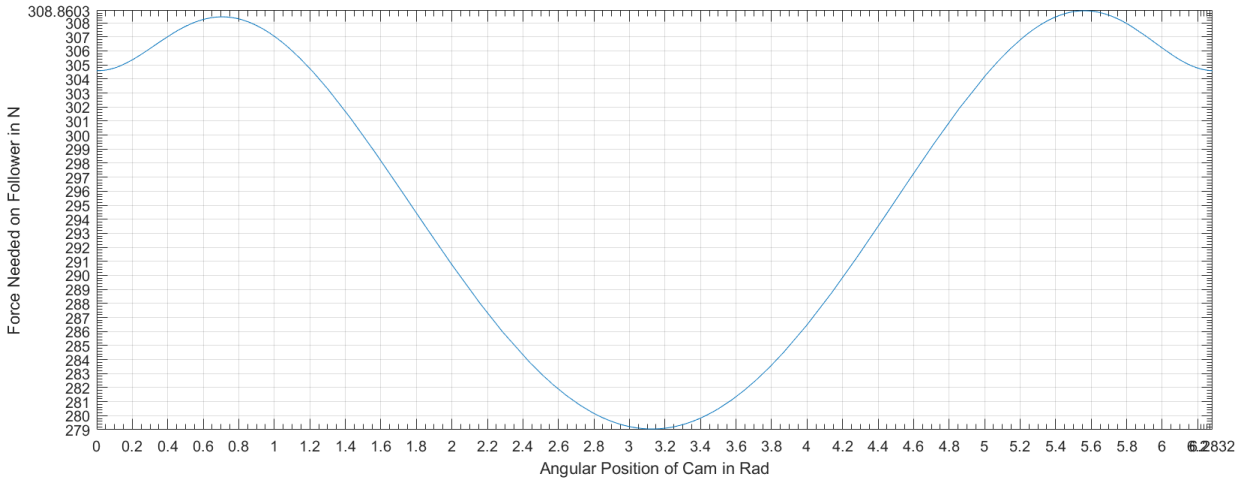

Figure 4-100 Force on Follower Versus Angular Position of Cam

The graph in **Figure** 4-100 shows that the force needed on the follower is between [279, 308.860] N at the minimum angular speed (18.373 rad/s) of the camshaft. The applied force is between [664.397, 4714.56] N which is much greater than the required force. Therefore, the harvester can be operated at any position of cam. The applied force is calculated by dividing the torque on cam to the extreme positions of cam (12.5 mm and 88.7 mm). However, whenever there is an increase

on the speed of camshaft, the applied and required force on the follower becomes increased. The torque T_E needed by the eccentric cam on the camshaft can be analyzed as follows.

$$T_E = F\left(\mu_3\sqrt{R^2 + e^2 - 2Re\cos\theta - e^2\sin^2\theta} + e\sin\theta\right)$$
$$= F\left(0.029\sqrt{4.012\times10^{-3} - 3.856\times10^{-3}\cos\theta - 1.452\times10^{-3}\sin^2\theta} + 0.0381\sin\theta\right)\ Nm$$

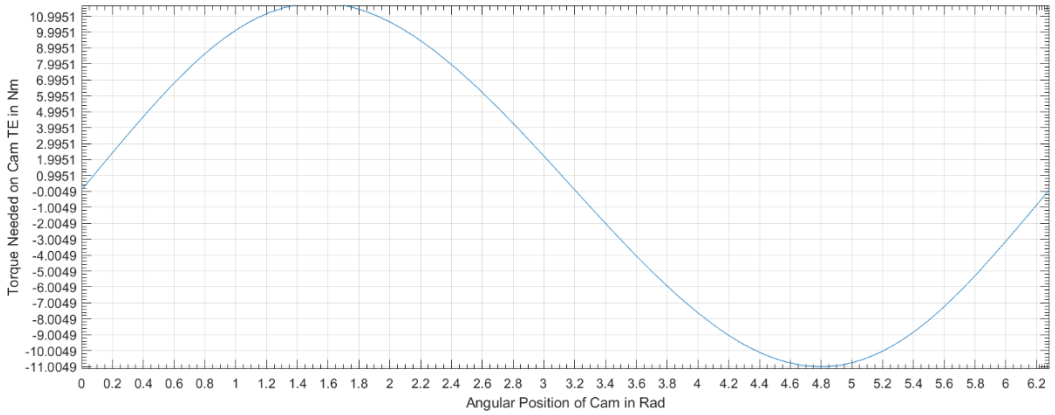

Figure 4-101 Torque on Cam versus Position of Cam

The applied torque T_E on the cam is 58.932 Nm whereas it is needed between -11.163 and 11.670 Nm at the minimum angular speed (18.373 rad/s) of the camshaft. This indicates that the applied torque is much greater than the required torque.

The total torque (T) needed to drive the camshaft becomes the sum of torques in the eccentric cam (T_E) and conveyor pulley (T_c), i.e.;

$$T = T_E + T_c$$

The values of d_3, μ_4, m_s, g, n_k, V_m, P, ω_3 and d_s are 145 mm, 0.13, 34.7 mm, 9.81 m/s^2, 8, 0.5 m/s, 95.819 mm, 18.373 rad/s and 1.983 mm respectively.

$$T_c = \mu_4 m_s g\sum_{i\to1}^{n_k} i\frac{V_m p}{\omega_3 d_s} = 0.13\times34.7\times10^{-3}\times9.81\sum_{i\to1}^{8} i\frac{0.5\times0.095819}{18.373\times1.983\times10^{-3}}$$
$$= 2.095\ Nm$$

$$T = F\left(0.029\sqrt{4.012\times10^{-3} - 3.856\times10^{-3}\cos\theta - 1.452\times10^{-3}\sin^2\theta} + 0.0381\sin\theta\right)$$
$$+ 2.095\ Nm$$

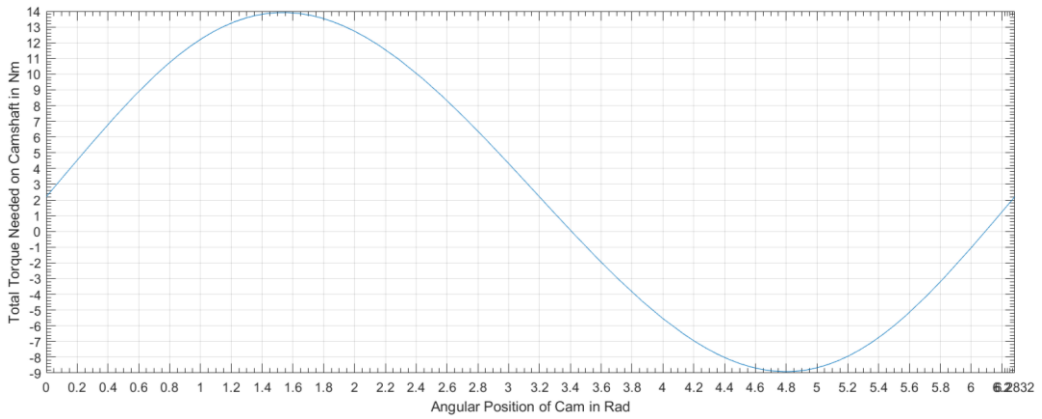

Figure 4-102 Total Torque on Camshaft versus Angular Position of Cam

Th graph in **Figure** 4-102 shows that the total torque needed to operate both the conveyor and cam is between 9 Nm and 14 Nm whereas 61.027 Nm total torque is applied on it at the minimum angular speed (18.373 rad/s) of the camshaft. Hence, the applied torque is greater than the required.

Discussion on Mass of Harvester

The prototype is manufactured from materials which are purchased and collected from locally available materials. Some materials are purchased with exact size whereas others nearest available. The remaining materials collected from old spare shop around post office, ASTU production shop, ASTU production garbage, MDME garbage and MDME store for those materials which were not included in the proposal.

Table 4-15 Design and Prototype of Basic Parts

S. N$_o$	**Part Name**	**Design**		**Prototype**	
		Specification	Qty	Specification	Qty
1.	DC Motor	1.5 hp	1	1 hp	1
2.	Solar Panel	200 Watt	5	200 Watt	2
3.	Solar Battery	12V200Ah	2	12V200Ah	2
4.	Pulley Drive M	Φ64xϕ16x26	1	Φ82xϕ19x19.43	1
5.	Pulley Drive I	Φ82xϕ19x19.43	1	Φ152.12xϕ15x15	1
6.	Cam	Φ101.2x5	1	Φ112x6	1
7.	Camshaft	Φ16x462.76	1	Φ20x450	1
8.	Conveyor Pulley C	Φ145xϕ15.5x38	1	Φ300xϕ19x100	1
9.	Conveyor Pulley I	Φ145xϕ7x38	1	Φ300xϕ19x100	1
10	Cutter Bar	609.6x10x5	1	610x50x5	1

11	Cutter or Blade	76.2x68.63x1	8	76.2x112.2x3	8
12	Gear Box	44x160x160	1	125x80x80	1
13	Guard Lip Bar	609.6x10x3	1	600x80x4	1
14	Guard Lip	96.92x15x4	10	154x20x4	9
15	Idler Shaft	Φ8x55	1	Φ 20x435	1
16	Intermediate Shaft	Φ8x73	1	Φ20x124.5	1
17	Lug	70x25x2	13	132x75x1	14
18	Rectangular Box for Follower Support	100x30x30x2	1	110x80x80x1.5	1
19	Star Wheel Assembly	Φ152.4x20	4	Φ213.9x20	3
20	Axel	Φ20x609.6	1	Φ38x145	1
21	Belt for Conveyor	1281.99x25x5	1	1729x100x5	1
22	Bevel Gear	Φ147x Φ13x44	1	Φ62.4x Φ16x19	1
23	Pinion Gear	Φ55x Φ12x44	1	Φ62.4x Φ16x19	1
24	Frame for Cutter	1.466 Kg	1	24.3 Kg	1
25	Divider	276.25x152.5x1	4	466.956x210x2	3
26	Follower Head	132x16x8	1	120x120x15x2	1
27	Solar Panel Support	0.95 Kg	1	22.77 Kg	1
28	Star Wheel and Divider Support	539x12x12x1	4	818x20x20x2	3

Table 4-15 shows that the weight of the prototype components is greater than the weight of the design component except the DC motor and bevel gear. Hence, the whole weight of the prototype (190 Kg) is greater than the designed harvester (93.03 Kg). Due to the big weight of the prototype, we were forced to use three tires; two at the rear and one at the front.

All the components are manufactured in our shop except drilling works which are more than 28 mm holes. The status of the machines in our work shop are very old. This made the manufacturing of components very tedious and the components were manufactured far from the design value specially for components which need drilling, milling and turning. Because, the machines were not work properly in addition their vices were damaged and worn out. In general, the machines needed maintenance during the prototype manufacturing period especially drilling machines.

Testing

The harvester was tested in the shop in two stages. The first test was a test of the harvester after completing the assembly in order to record the speed at different shafts and to make some modification if it is required. The second test was conducted by feeding the row of straws in to the harvester in order to check the functionality of the machine for real harvesting.

Shop (After Assembly) Test

Test Equipment: Two solar batteries, two solar panels, charge controller, Digital Tachometer, multi meter, stop watch and harvester machine. The capacities of a single battery and solar panel are 200 Ah and 200 Watt respectively

The shop test was carried out by using solar panel and solar battery separately. There are two solar panels and solar batteries as a source of power available in order to drive the harvester. The experiment was carried six times. These are using single battery, two batteries in series, two batteries in parallel, single solar panel, two solar panel in series and two solar panel in parallel.

The testing of the harvest was carried out on October 31, 2018 around 3:15 PM.

Table 4-16 Voltage Recorded during the Test

Power source	1 Battery	2 Series Batteries	2 Batteries Parallel	1 Solar Panel	2 series Solar Panel	2 parallel Solar Panel
Measured Voltage in V	13.01	25.77	13.01	39.7	79.6	39.7

Table 4-17 Measured RPM Values of Shafts

S No	Shafts	Speed in RPM					
		1 Battery	2 Series Batteries	2 Batteries Parallel	1 Solar Panel	2 series Solar Panel	2 parallel Solar Panel
1.	Motor output shaft	0	64	0	138	347.18	267
2.	Intermediate Shaft	0	59	0	136	223.52	171.9
3.	Cam shaft	0	56	0	129	176	135.4
4.	Idler Shaft	0	47	0	49.9	75.12	57.8

The power requirement of the harvester becomes clear. The cutter system was in rotation when the voltage supplied into the DC Motor becomes greater than 24 V, which is attained by using two batteries in series, single solar panel, two solar panels in series and two solar panel in parallel. However, the weight of the two batteries (Lead Acid) is 130 Kg, which is not feasible due to its

high weight. Even if the cutter works by using single solar panel, it is not recommended to use it as sole source of power because the test was conducted without load. Hence, two solar panel either in series or in parallel can be used to drive the harvester.

Note: The DC motor used in the prototype is different from the selected DC motor both in size and type due to unavailability during proforma collection period in Adama and Addis Ababa. The only available DC motor with high power was 1 hp. The specifications of the motor were not clear because it is written in Chinese language. The relation between voltage (V) supplied into DC motor and its angular speed (ω) is defined as follows (**Daniel Collins, 2015)**.

$$\omega = \frac{V}{k} - \frac{TR}{k^2} \text{ ----------} \textit{4-104}$$

Where T is the torque of the DC motor, R is the resistance of the armature of the DC motor and k is the torque and electrical inherent constant of DC motor.

The resistance R of the armature of the DC motor is constant. The speed of the DC motor shaft was measured without a load hence the torque is also constant. The torque and electrical inherent constant k of DC motor can be approximated by substituting the different corresponding values of ω and V from **Table** 4-16 and **Table** 4-17 in comparison with main plate attached on the motor i.e., 200V and 1800 rpm.

$$0 = \frac{13.01}{k} - \frac{TR}{k^2} \text{ ----------} \textit{4-105}$$

$$64\frac{2\pi}{60} = \frac{25.77}{k} - \frac{TR}{k^2} \text{ ----------} \textit{4-106}$$

$$138\frac{2\pi}{60} = \frac{39.7}{k} - \frac{TR}{k^2} \text{ ----------} \textit{4-107}$$

$$347.18\frac{2\pi}{60} = \frac{79.6}{k} - \frac{TR}{k^2} \text{ ----------} \textit{4-108}$$

$$1800\frac{2\pi}{60} = \frac{200}{k} - \frac{TR}{k^2} \text{ ----------} \textit{4-109}$$

Using simultaneous **equation** 4-105 and 4-109, k becomes;

$$(1800 - 0)\frac{2\pi}{60} = \frac{200 - 13.01}{k} \rightarrow k = 0.992$$

Using simultaneous **equation** 4-106 and 4-109, k becomes;

$$(1800 - 64)\frac{2\pi}{60} = \frac{200 - 25.77}{k} \rightarrow k = 0.958$$

Using simultaneous **equation** 4-107 and 4-109, k becomes;

$$(1800 - 138)\frac{2\pi}{60} = \frac{200 - 39.7}{k} \rightarrow k = 0.921$$

Using simultaneous **equation** 4-108 and 4-109, k becomes;

$$(1800 - 347.18)\frac{2\pi}{60} = \frac{200 - 79.6}{k} \rightarrow k = 0.791$$

The value of k can be considered by taking the average of the k values at different voltages.

$$k = \frac{0.992 + 0.958 + 0.921 + 0.791}{4} = 0.916$$

Using **equation** 4-105, TR can be determined as follows

$$TR = Vk - \omega k^2 = 13.01 * 0.916 - 0 = 11.917$$

Using **equation** 4-106, TR can be determined as follows

$$TR = Vk - \omega k^2 = 25.77 * 0.916 - 64\frac{2\pi}{60} * 0.916^2 = 17.982$$

Using **equation** 4-107, TR can be determined as follows

$$TR = Vk - \omega k^2 = 39.7 * 0.916 - 138 * \frac{2\pi}{60} * 0.916^2 = 24.24$$

Using **equation** 4-108, TR can be determined as follows

$$TR = Vk - \omega k^2 = 79.6 * 0.916 - 347.18 * \frac{2\pi}{60} * 0.916^2 = 42.41$$

Using **equation** 4-109, TR can be determined as follows

$$TR = Vk - \omega k^2 = 200 * 0.916 - 1800 * \frac{2\pi}{60} * 0.916^2 = 25.04$$

Since the values of TR is different at different voltage it is advisable to take average.

$$TR = \frac{11.917 + 17.982 + 24.24 + 42.41 + 25.04}{5} = 24.318$$

The general formula can be simplified by substituting k and TR values, i.e.,

$\omega = \frac{V}{0.916} - \frac{24.318}{0.916^2} = 1.092V - 28.983$ ----------*4-110*

The DC motor needs more than 26.54V to begin rotation.

The above equation shows that the relation between ω and V is direct. The smallest angular velocity of cam shaft is 18.373 rad/s 175.499 rpm) which is between 129 rpm and 176 rpm with speed slippage ratio of 129/138=0.935 and 176/347.18=0.507 respectively. The average speed slippage ratio (0.721) can be taken. The motor shaft speed becomes 18.373/0.721=25.483 rad/s or 175.499/0.721=243.411 rpm. Therefore, the minimum voltage supplied to get angular velocity of 25.483 rad/s becomes;

$$\omega = 1.092V - 28.983 \rightarrow V = \frac{\omega + 28.983}{1.092} = \frac{25.483 + 28.983}{1.092} = 49.877\ V$$

This result shows that, two series 12V batteries, single solar panel or two parallel solar panels cannot drive the harvester sufficiently to cut the grain.

In general, the above analysis helps us to characterize the DC motor i.e., the relation of the torque T, the resistance R of the armature and the torque and electrical inherent constant k of DC motor. The voltage supply should be greater than or equal to 49.877 V only for this prototype which is attained by using two solar panel in series. This voltage will vary by using a different DC motor or modifying the prototype for this possessed DC motor.

Shop (Functionality) Test

Test Equipment: Harvester, straw holder, wheat straws and grass (**ነጠፍጮ**) straws.

Test Preparations: The straw holder is made of 10x10 mm square pipe. It has seven rows and two beams see **Photo** 4-1. The purpose of the beams is to hold the rows in a position whereas the rows are used to hold the straws of grains in a vertical position. Each row has more than 20 holes using 4 mm drill bit.

Photo 4-1 Straw Holder

The straight and unbroken straws were separated from bent and broken straws.

Testing Method: The test was conducted by inserting straws into the holes in rows. It was carried in successive five stages. The first test was carried by using one row of straws i.e., straws were inserted into only one row see **Photo** 4-2.

Photo 4-2 Single Row of Straws before Cutting

The harvester cuts nicely the straws. This shows that the energy from two series solar panel is enough to harvest the row of straws see **Photo** 4-3.

Photo 4-3 Single Row of Straws after Cutting

The second test was carried by using double rows of straws i.e., straws were inserted into two rows see **Photo** 4-4.

Photo 4-4 Double Rows of Straws before Cutting

The harvester cuts nicely the straws. This shows that the energy from two series solar panel is enough to harvest two rows of straws see **Photo** 4-5.

Photo 4-5 Double Rows of Straws after Cutting

The third test was carried by using triple rows of straws i.e., straws were inserted into three rows see **Photo** 4-6.

Photo 4-6 Triple Rows of Straws before Cutting

The harvester cuts nicely the straws. This shows that the energy from two series solar panel is enough to harvest three rows of straws see **Photo** 4-7.

Photo 4-7 Triple Rows of Straws after Cutting

The fourth test was carried by using quadruple rows of straws i.e., straws were inserted into three rows see **Photo** 4-8.

Photo 4-8 Quadruple Rows of Straws before Cutting

The harvester cuts nicely the straws. This shows that the energy from two series solar panel is enough to harvest four rows of straws see **Photo** 4-9.

Photo 4-9 Quadruple Rows of Straws after Cutting

The fifth test was carried by using quintuple rows of straws i.e., straws were inserted into five rows see **Photo** 4-10.

Photo 4-10 Quintuple Rows of Straws before Cutting

The harvester cuts nicely the straws. This shows that the energy from two series solar panel is enough to harvest five rows of straws see **Photo** 4-11.

Photo 4-11 Quintuple Rows of Straws after Cutting

The test was also carried by using septuple rows of straws i.e., straws were inserted into seven rows.

The harvester cuts nicely the straws. This shows that the energy from two series solar panel is enough to harvest five rows of straws see **Photo** 4-12.

Photo 4-12 Septuple Rows of Straws after Cutting

In general, the energy was energetic to cut for the designed width of cut (609.6 mm) using two series solar panels 200 watt each.

Photo 4-13 Cross Section of Wheat (Left) and Gomech (ጎመጫ) Right

The harvester was also tested for harvesting grass called Gomech (ጎመጫ local name). The relative strength of Gomech (ጎመጫ) is relatively stronger than wheat. Even if it is not supported by numerical values, it is was proofed by three techniques. The first technique was by observation during cutting the wheat and grass. The second technique was proofed by crushing the wheat and

the grass using our hand. Lastly, it was checked by their difference in cross section. The grass sold cross section whereas wheat hollow as shown in **Photo** 4-13.

Even if the grass is stronger than the wheat, the harvester was tested up to three rows of straws. It cut the grass nicely these rows of straws.

Assembly Procedures

The harvester has 271 components with three main sub-assemblies see **Assembly** Tree 4-1.

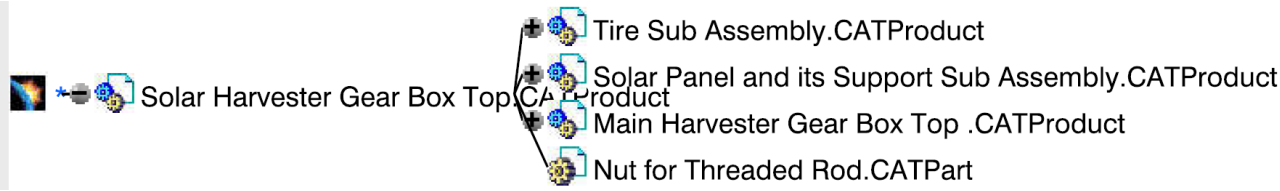

Assembly Tree 4-1 Solar Harvester Main Sub-Assemblies

As shown in the **Assembly** Tree 4-1, there are three main sub-assemblies in the harvester. The main harvesting component sub-assemblies should be first assembled on to the tire sub assembly through the threaded rod. The height of the main harvesting component sub-assemblies is adjusted then after fixed by using the nut for threaded rod.

The components in the tire sub assembly are shown in **Assembly** Tree 4-2. They are assembled as follows.

1. Weld the handle on the handle and axel holder
2. Insert the axel into the tire and tight it by nut for the axel
3. Insert the axel into the handle and axel holder
4. Insert the axel into the second tire and tight it by using nut for the axel
5. Adjust the position of handle and axel holder at mid span between the two tires
6. Finally fix the handle and axel hold by the axel grips and bolt for axel grips

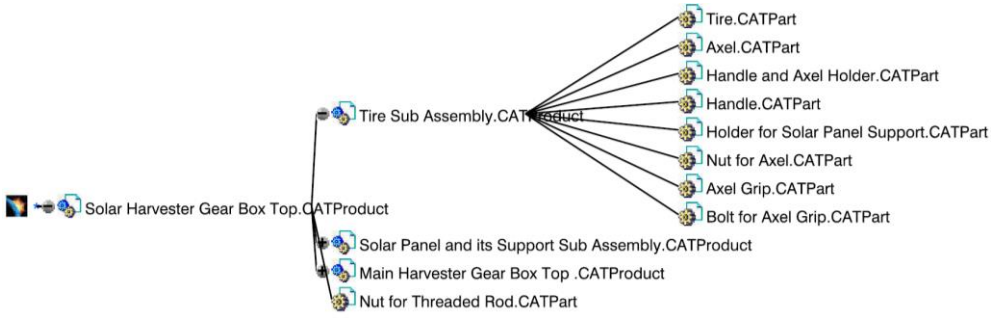

Assembly Tree 4-2 Components in Tire Sub Assembly

The components in the solar panel and its support sub assembly are shown in **Assembly** Tree 4-3.

They are assembled as follows.

1. Weld the beams and columns
2. Weld the stiffeners for solar panels support one on the beam and the other end on the beam
3. Fix the solar panels on top of the support using wire

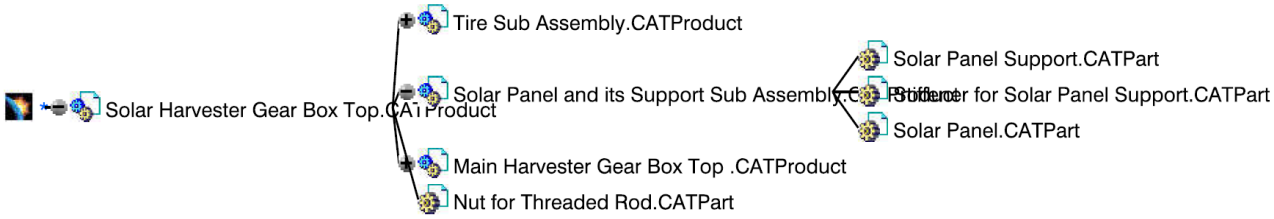

Assembly Tree 4-3 Components in Solar Panel and its Support Sub Assembly

The components in the main harvesting sub assembly are shown in **Assembly** Tree 4-4. It has 10 another sub-assembly. They are assembled as follows.

1. Weld star wheel sub assembly on to frame for cutter sub assembly
2. Weld Guard lip sub assembly on to frame for cutter sub assembly
3. Insert cutter sub assembly into guard lip sub-assembly
4. Insert the follower bar into follower bar support and fix on the bottom frame
5. Insert conveyor belt sub assembly into camshaft sub assembly
6. Insert camshaft sub assembly into frame for cutter sub assembly
7. Insert idler shaft into the conveyor belt sub assembly and fix the idler shaft sub assembly on its position
8. Insert V-belt into the pulley on the intermediate shaft and then
9. Insert this sub assembly in the gear box
10. Fix the DC motor on the top frame by tight the v-belt on the pulley of the motor
11. Strengthen the top and bottom frame by using the thread rod and its nut

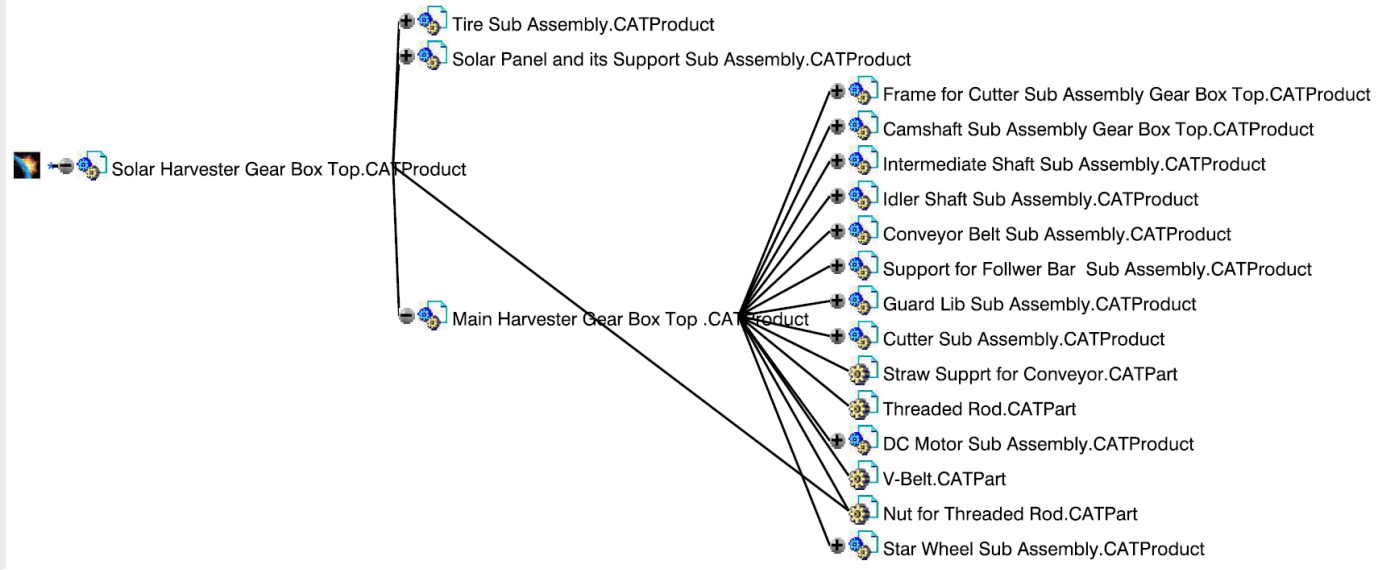

Assembly Tree 4-4 Components in Main Harvesting Sub Assembly

The components in the frame for cutter sub assembly are shown in **Assembly** Tree 4-5. They are assembled as follows.

The top and bottom frame for cutter sub-assemblies are connected by using the column. The column is fixed on them using nut for column

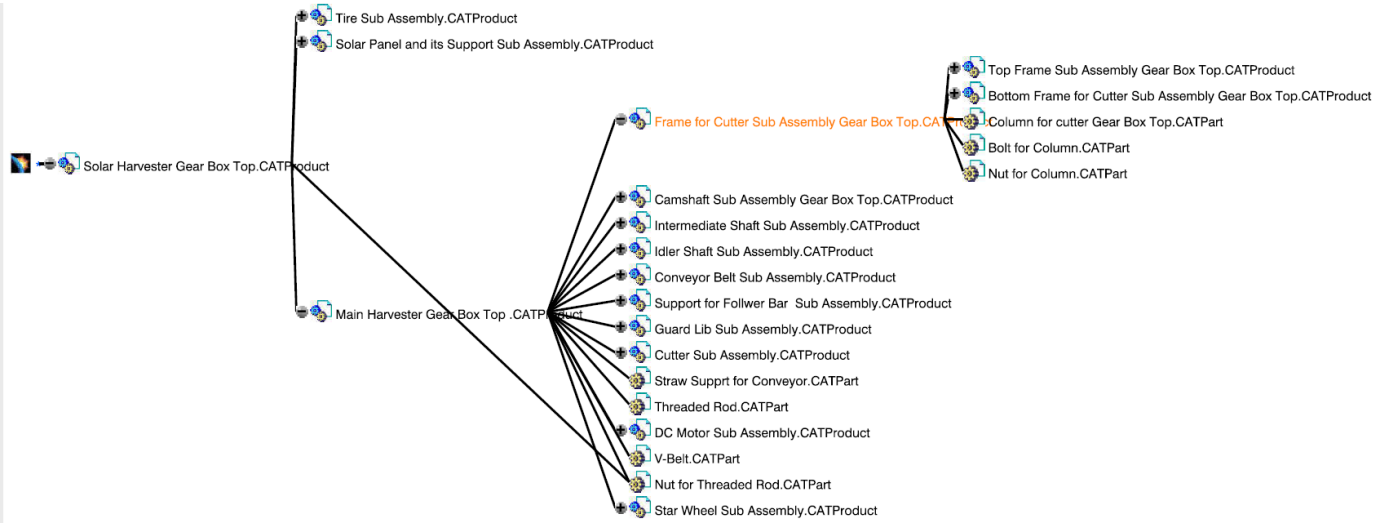

Assembly Tree 4-5 Components in Frame for Cutter Sub Assembly

The components in the camshaft sub assembly are shown in **Assembly** Tree 4-6. They are assembled as follows.

1. Insert key for cam into the camshaft on its lower end
2. Insert cam into the camshaft in the position of it key
3. Insert thrust bearing in camshaft below cam

4. Insert key for conveyor pulley into the middle key way of camshaft
5. Insert conveyor pulley into the camshaft on its top end
6. Insert ball bearing into camshaft
7. Insert key for bevel gear at top end of camshaft
8. Insert bevel gear into camshaft on the position of the key for bevel gear

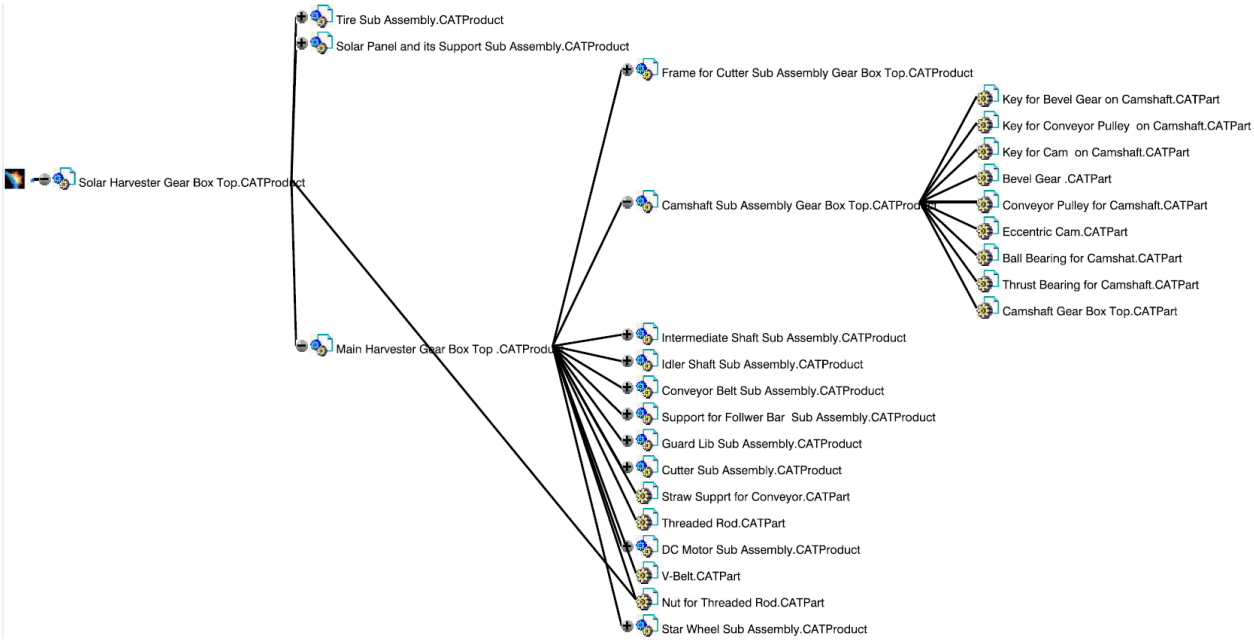

Assembly Tree 4-6 Components in Camshaft Sub Assembly

The components in the intermediate shaft sub assembly are shown in **Assembly** Tree 4-7. They are assembled as follows.

1. Insert ball bearing into intermediate shaft
2. Insert key for bevel gear into intermediate shaft
3. Insert key for v-grooved pulley into intermediate shaft
4. Insert V-grooved pulley into intermediate shaft
5. Insert thrust bearing into intermediate shaft

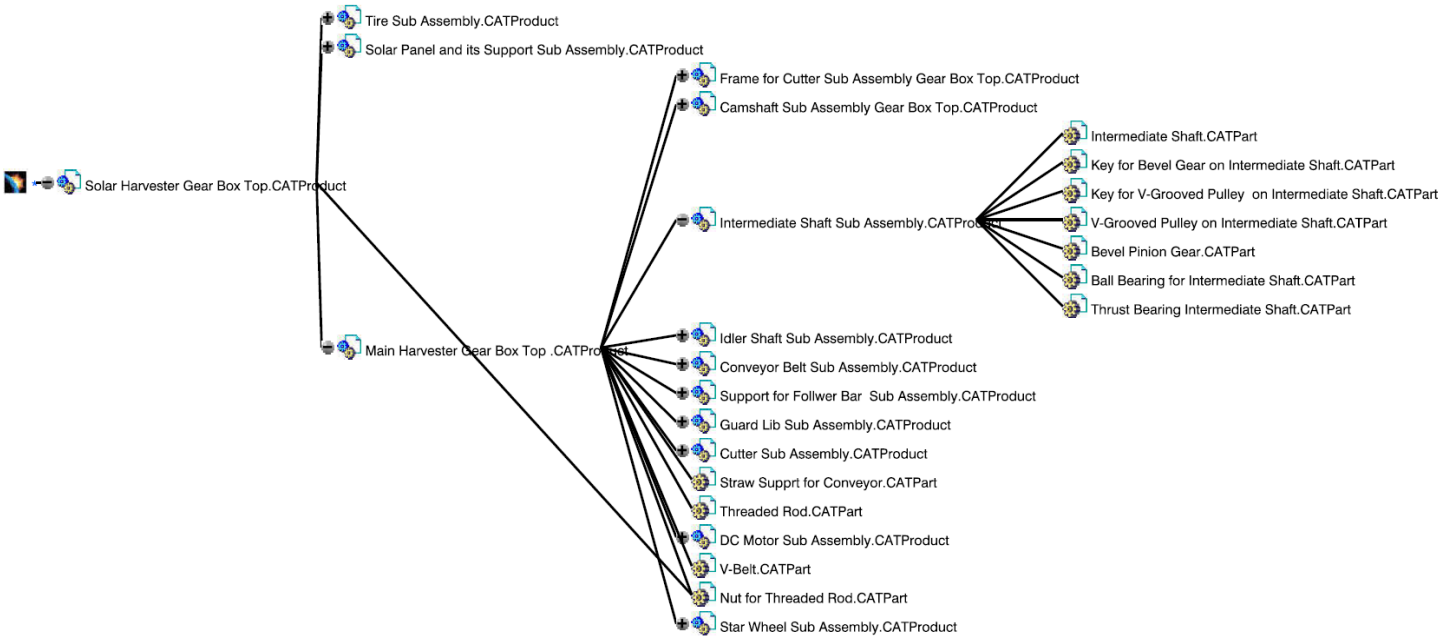

Assembly Tree 4-7 Components in Intermediate Shaft Sub Assembly

The components in the idler shaft sub assembly are shown in **Assembly** Tree 4-8. They are assembled as follows.

1. Insert conveyor pulley into idler shaft
2. Insert ball bearing into idler shaft on top end
3. Insert thrust bearing into idler shaft on its lower end

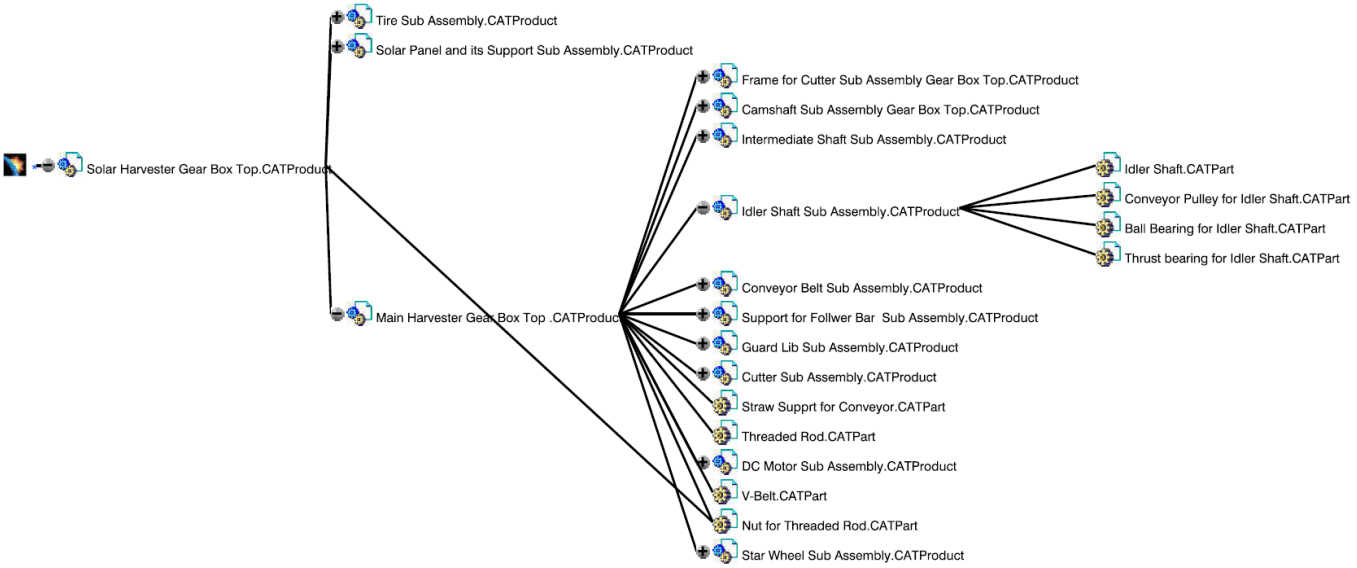

Assembly Tree 4-8 Components in Idler Shaft Sub Assembly

The components in the conveyor belt sub assembly are shown in **Assembly** Tree 4-9. They are

assembled as follows.

1. Align the holes of lug and flat belt
2. Fix them together by using rivet

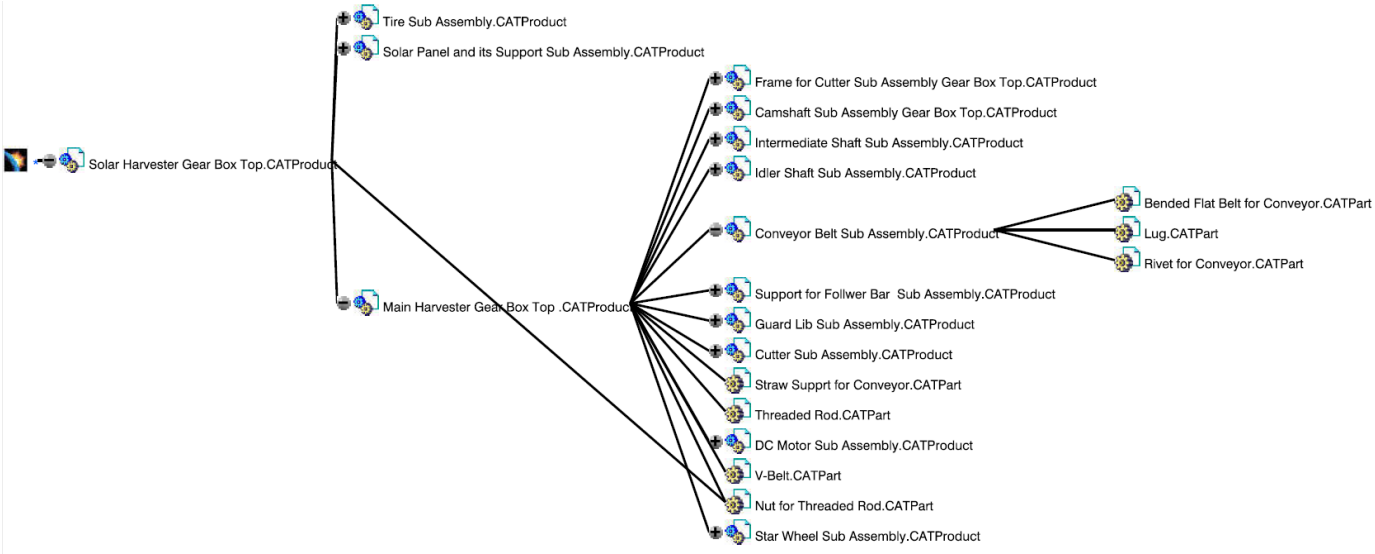

Assembly Tree 4-9 Components in Conveyor Belt Sub Assembly

The components in the support for follower bar sub assembly are shown in **Assembly** Tree 4-10. There are one roller and two spacers in each bolt. The longer bolts are aligned vertically whereas shorter horizontally. They are assembled as follows.

1. Insert half part of the bolt into the follower bar support
2. Insert one of the spacers into the bolt
3. Insert the roller into the bolt next to the spacer
4. Insert the remaining spacer into the bolt next to the roller
5. Finally fix the bolt on the follower bar support by using nut for follower bar support

The components in the Guard lip sub assembly are shown in **Assembly** Tree 4-11. They are assembled as follows.

1. Align the holes of the guard lip bar and guard lip
2. Fix them together buy using bolts and nuts for guard lip bar
3. Insert bolt for bearing on guard lip into guard lip bar
4. Insert bearing for cutter bar support into guard lip bar
5. Fix the bearing on guard lip bar using nut for bearings on guard lip bar

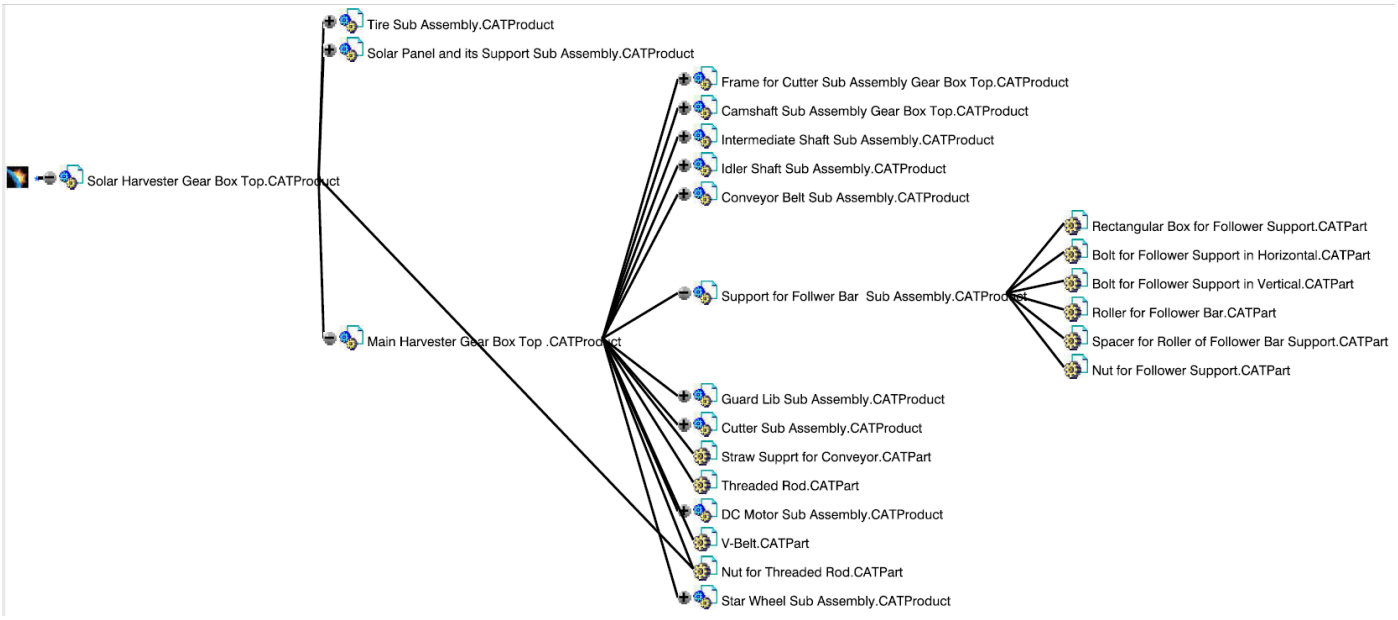

Assembly Tree 4-10 Components in Support for Follower bar Sub Assembly

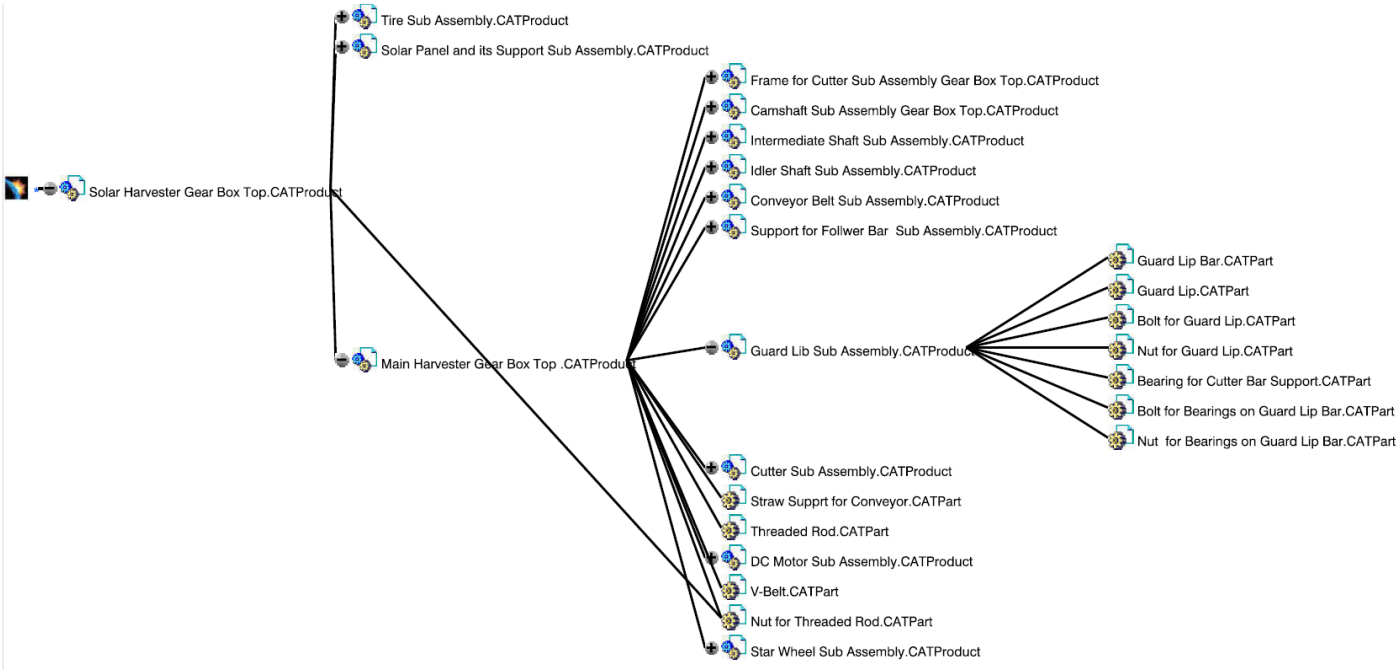

Assembly Tree 4-11 Components in Guard Lip Sub Assembly

The components in the cutter sub assembly are shown **Assembly** Tree 4-12. They are assembled as follows.

1. Weld follower bar on the follower bar head
2. Weld follower bar head on cutter bar
3. Align the holes blade and cutter bar and fix them by using bolt and nut for cutter or blade

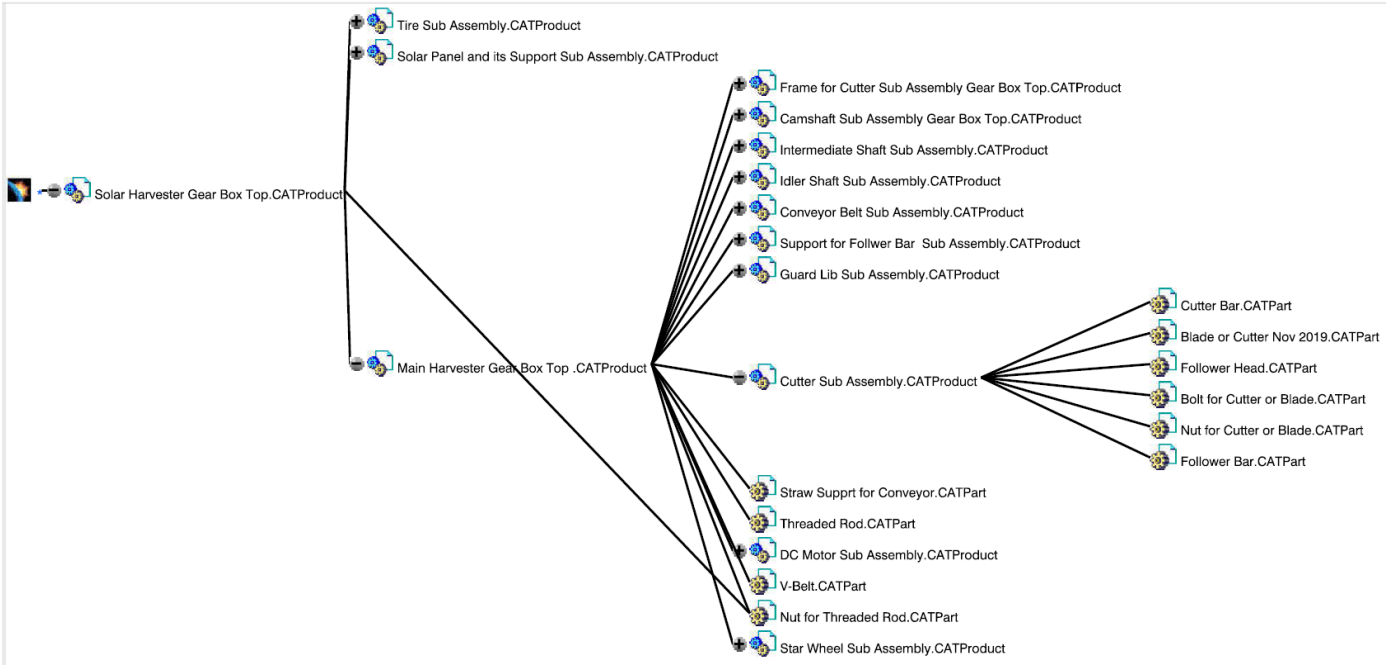

Assembly Tree 4-12 Components in Cutter Sub Assembly

The components in the DC motor sub assembly are shown in **Assembly** Tree 4-13. They are assembled as follows.

1. Insert key for V-grooved pulley into DC Motor shaft
2. Insert V-grooved pulley into DC Motor shaft

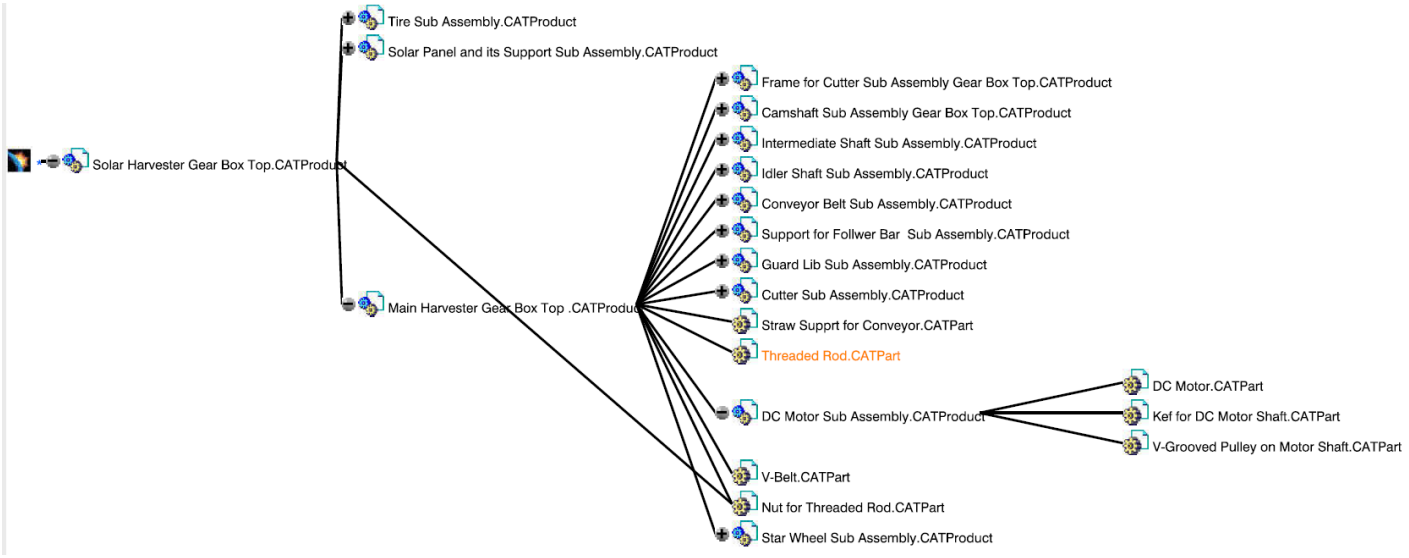

Assembly Tree 4-13 Components in DC Motor Sub Assembly

The components in the star wheel sub assembly are shown in Assembly Tree 4-14. They are assembled as follows.

1. Weld star wheel rod onto the star wheel and divider support
2. Insert bearing for star wheel arm into star wheel rod
3. Insert star wheel arm into star wheel rod on the bearing part
4. Insert divider into star wheel rod on top of star wheel arm

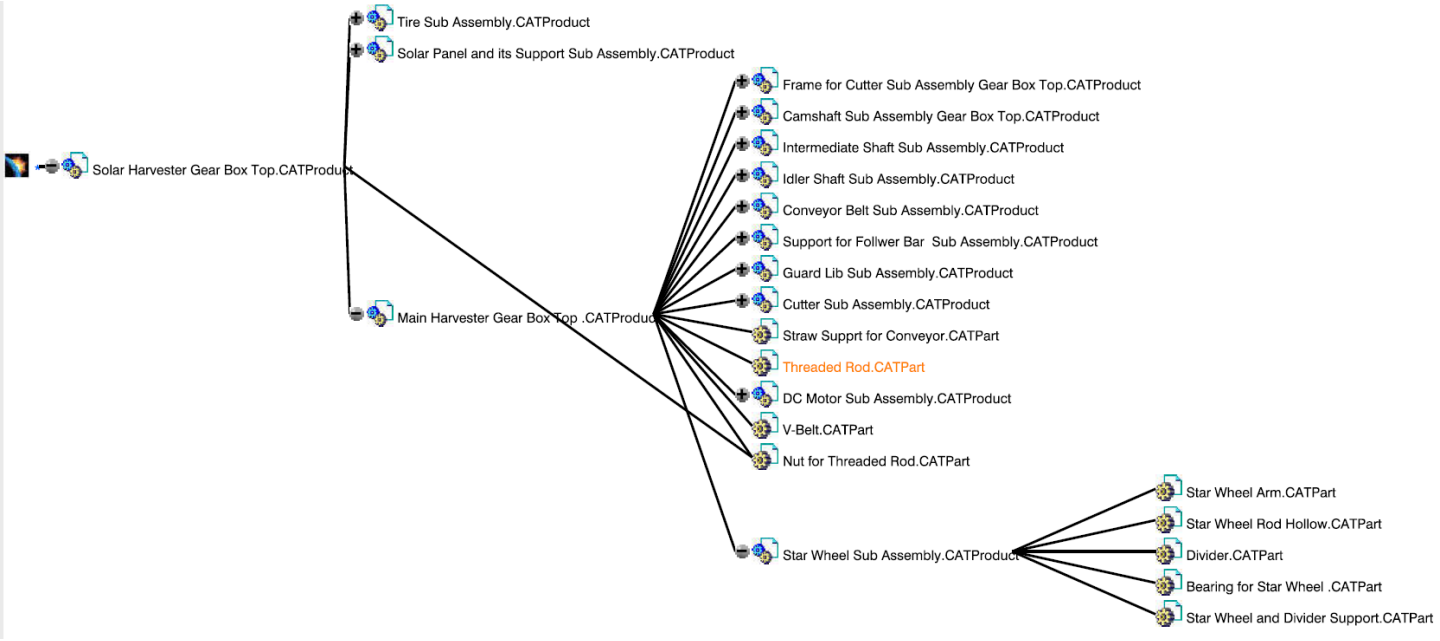

Assembly Tree 4-14 Components in Star Wheel Sub Assembly

The components in the top frame sub assembly are shown Assembly Tree 4-15. They are assembled as follows.

1. Weld gear box on the top cantilever beam
2. Weld intermediate shaft flat support on the top cantilever beam
3. Weld DC Motor support on the top cantilever beam
4. Weld stiffeners on the DC Motor supports
5. Weld thrust bearing seat for idler shaft

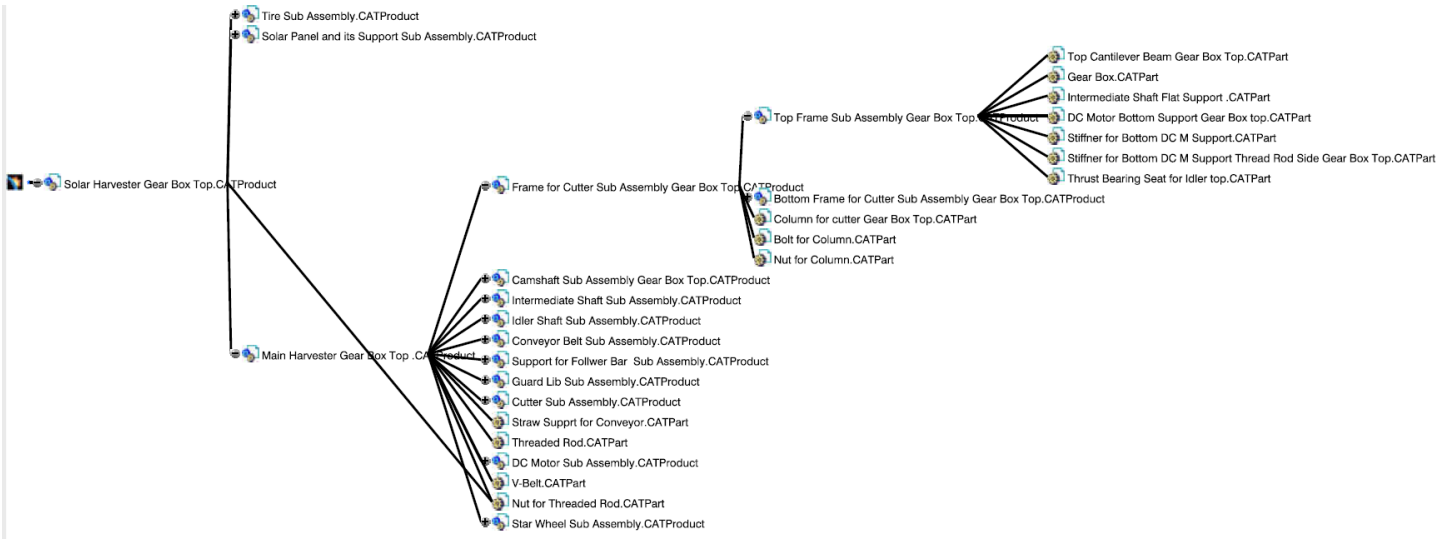

Assembly Tree 4-15 Components in Top Frame Sub Assembly

The components in the bottom frame for cutter sub assembly are shown **Assembly** Tree 4-16. They are assembled as follows.

1. Weld bearing seat for camshaft on the bottom cantilever beam
2. Weld fixed beam on bottom fixed beam
3. Weld bearing seat for idler shaft on idler shaft bottom support
4. Weld idler shaft bottom support on the bottom cantilever beam
5. Weld base for straw support holder on the bottom cantilever beam
6. Weld straw support holder on base for straw support holder

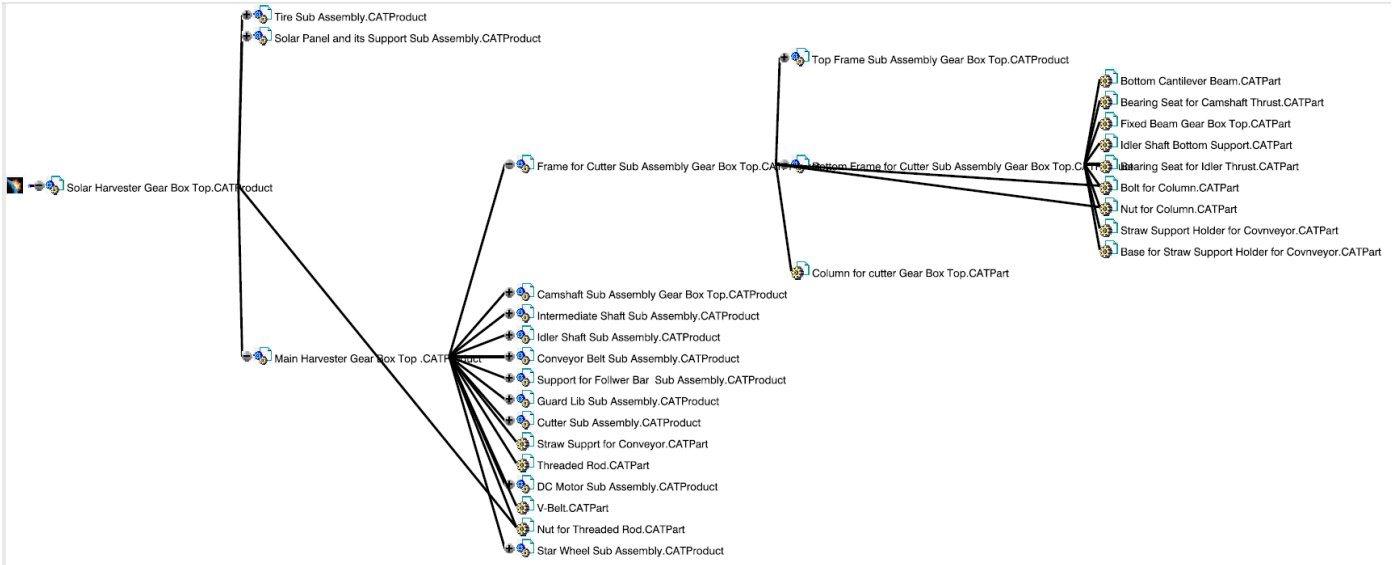

Assembly Tree 4-16 Components in Bottom Sub Assembly

Manufacturing Process and Cost Analysis

The manufacturing processes are recommended by considering the following assumption.

1. The workshop is well organized.
2. All the machineries are in good condition.
3. All the raw materials are available and placed nearer to the workshop.
4. All tools are on the hand of the machinist.
5. The machinist is full employee of 8495 monthly salary with rank of Chief Machinist II and 176 hours working times. The rate of payment for the machinist becomes **48.267** Birr per hour [**65**].
6. It is estimated by considering mass production otherwise it will be difficult to become competent throughout the world.
7. The finished products placed inside the workshop.

Manufacturing Process

Bevel Gear see Part Drawing 4-1

The bevel gears can be manufactured in five main operations; cutting, turning, boring, milling and facing. The first process is cutting on Hacksaw.

Machine	**Hacksaw**	**Main Operation**	**Cutting**
Activities	**Time Taken in Minutes**	**Sub Total Time**	**Remark**
Layout making	1	14	
Aligning & tightening work piece	1		
Cutting operation	10		
cleaning the machine, tools and work piece	2		

The send process is turning on lathe to make the taper.

Machine	**Lathe**	**Main Operation**	**Turning**
Activities	**Time Taken in Minutes**	**Sub Total Time**	**Remark**
Layout making	1	45.5	
Aligning & tightening work piece	5		
Changing& tightening tools	5		

Turning operation	30		
Untightening tools	1		
Untightening work piece	1		
cleaning the machine, tools and work piece	2.5		

The third process is boring to make the hole.

Machine	**Lathe**	**Main Operation**	**Boring**
Activities	**Time Taken in Minutes**	**Sub Total Time**	**Remark**
Layout making	1	23.5	
Aligning & tightening work piece	1		
Changing& tightening tools	5		
Boring operation	10		
Untightening tools	2		
Untightening work piece	2		
cleaning the machine, tools and work piece	2.5		

The fourth process is milling to make the teeth and key way.

Machine	**Milling**	**Main Operation**	**Milling**
Activities	**Time Taken in Minutes**	**Sub Total Time**	**Remark**
Layout making	10	83	
Aligning & tightening work piece	2		
Changing& tightening tools	2		
Milling operation	60		
Untightening tools	2		
Untightening work piece	2		
cleaning the machine, tools and work piece	5		

The last process is facing on ends.

Machine	**Lathe**	**Main Operation**	**Facing**
Activities	**Time Taken in Minutes**	**Sub Total Time**	**Remark**

Layout making	1	29.5	
Aligning & tightening work piece	2		
Changing& tightening tools	2		
Facing operation	20		
Untightening tools	1		
Untightening work piece	1		
cleaning the machine, tools and work piece	2.5		

Pinion Bevel Gears see Part Drawing 4-2

The bevel gears can be manufactured in five main operations; cutting, turning, boring, milling and facing. The first process is cutting on Hacksaw.

Machine	**Hacksaw**	**Main Operation**	**Cutting**
Activities	**Time Taken in Minutes**	**Sub Total Time**	**Remark**
Layout making	1	9	
Aligning & tightening work piece	1		
Cutting operation	5		
cleaning the machine, tools and work piece	2		

The send process is turning on lathe to make the taper.

Machine	**Lathe**	**Main Operation**	**Turning**
Activities	**Time Taken in Minutes**	**Sub Total Time**	**Remark**
Layout making	1	35.5	
Aligning & tightening work piece	5		
Changing& tightening tools	5		
Turning operation	20		
Untightening tools	1		
Untightening work piece	1		
cleaning the machine, tools and work piece	2.5		

The third process is boring to make the hole.

Machine	**Lathe**	**Main Operation**	**Boring**
Activities	**Time Taken in Minutes**	**Sub Total Time**	**Remark**
Layout making	1	23.5	
Aligning & tightening work piece	1		
Changing& tightening tools	5		
Boring operation	10		
Untightening tools	2		
Untightening work piece	2		
cleaning the machine, tools and work piece	2.5		

The fourth process is milling to make the teeth and key way.

Machine	**Milling**	**Main Operation**	**Milling**
Activities	**Time Taken in Minutes**	**Sub Total Time**	**Remark**
Layout making	10	63	
Aligning & tightening work piece	2		
Changing& tightening tools	2		
Milling operation	40		
Untightening tools	2		
Untightening work piece	2		
cleaning the machine, tools and work piece	5		

The last process is facing on ends.

Machine	**Lathe**	**Main Operation**	**Facing**
Activities	**Time Taken in Minutes**	**Sub Total Time**	**Remark**
Layout making	1	19.5	
Aligning & tightening work piece	2		
Changing& tightening tools	2		
Facing operation	10		
Untightening tools	1		

Untightening work piece	1		
cleaning the machine, tools and work piece	2.5		

Conveyor Pulley on Camshaft See Part Drawing 4-3

It can be manufactured in four main operations; turning, facing, drilling and milling.

The first process is turning on lathe to reduce the diameter from 145 to 135 mm over a length of 12 mm.

Machine	**Lathe**	**Main Operation**	**Turning**
Activities	**Time Taken in Minutes**	**Sub Total Time**	**Remark**
Layout making	1	30.5	
Aligning & tightening work piece	5		
Changing& tightening tools	5		
Turning operation	15		
Untightening tools	1		
Untightening work piece	1		
cleaning the machine, tools and work piece	2.5		

The second process is facing on both ends to get 38 mm length.

Machine	**Lathe**	**Main Operation**	**Facing**
Activities	**Time Taken in Minutes**	**Sub Total Time**	**Remark**
Layout making	1	35.5	
Aligning & tightening work piece	5		
Changing& tightening tools	5		
Facing operation	20		
Untightening tools	1		
Untightening work piece	1		
cleaning the machine, tools and work piece	2.5		

The third process is drilling to make the five holes.

Machine	Drilling	Main Operation	Drilling
Activities	**Time Taken in Minutes**	**Sub Total Time**	**Remark**
Layout making	5	87.5	
Aligning & tightening work piece	10		
Changing& tightening tools	5		
Drilling operation	50		
Untightening tools	5		
Untightening work piece	10		
cleaning the machine, tools and work piece	2.5		

The last process is milling to make key way.

Machine	Milling	Main Operation	Milling
Activities	**Time Taken in Minutes**	**Sub Total Time**	**Remark**
Layout making	1	36	
Aligning & tightening work piece	5		
Changing& tightening tools	5		
Milling operation	10		
Untightening tools	5		
Untightening work piece	5		
cleaning the machine, tools and work piece	5		

Conveyor Pulley on Idler Shaft See Part Drawing 4-4

It can be manufactured in three main operations; turning, facing, and drilling.

The first process is turning on lathe to reduce the diameter from 145 to 135 mm over a length of 12 mm.

Machine	Lathe	Main Operation	Turning
Activities	**Time Taken in Minutes**	**Sub Total Time**	**Remark**
Layout making	1	30.5	
Aligning & tightening work piece	5		

Changing& tightening tools	5		
Turning operation	15		
Untightening tools	1		
Untightening work piece	1		
cleaning the machine, tools and work piece	2.5		
	30.5		

The second process is facing on both ends to get 38 mm length.

Machine	**Lathe**	**Main Operation**	**Facing**
Activities	**Time Taken in Minutes**	**Sub Total Time**	**Remark**
Layout making	1	35.5	
Aligning & tightening work piece	5		
Changing& tightening tools	5		
Facing operation	20		
Untightening tools	1		
Untightening work piece	1		
cleaning the machine, tools and work piece	2.5		

The third process is drilling to make the five holes.

Machine	**Drilling**	**Main Operation**	**Drilling**
Activities	**Time Taken in Minutes**	**Sub Total Time**	**Remark**
Layout making	5	87.5	
Aligning & tightening work piece	10		
Changing& tightening tools	5		
Drilling operation	50		
Untightening tools	5		
Untightening work piece	10		
cleaning the machine, tools and work piece	2.5		

Flat Belt see Part Drawing 4-5

It can be manufactured in two main operations; cutting and drilling.

The first process is cutting using blade.

Machine	**Blade**	**Main Operation**	**Cutting**
Activities	**Time Taken in Minutes**	**Sub Total Time**	**Remark**
Layout making	1	2	
cutting operation	1		

The second process is drilling.

Machine	**Hand Drill**	**Main Operation**	**Drilling**
Activities	**Time Taken in Minutes**	**Sub Total Time**	**Remark**
Layout making	5	26	
Changing& tightening tools	1		
Drilling operation	8		
Untightening tools	1		
cleaning the machine, tools and work piece	1		

Lug See Part Drawing 4-6

It can be manufactured in three main operations; cutting, drilling and bending.

The first process is cutting on Shearing machine.

Machine	**Shearing machine**	**Main Operation**	**Cutting**
Activities	**Time Taken in Minutes**	**Sub Total Time**	**Remark**
Layout making	1	3.5	
Aligning & tightening work piece	1		
Cutting operation	0.5		
cleaning the machine, tools and work piece	1		

The second process is drilling.

Machine	**Hand Drill**	**Main Operation**	**Drilling**
Activities	**Time Taken in Minutes**	**Sub Total Time**	**Remark**
Layout making	1	8.5	
Changing& tightening tools	1		

Drilling operation	2		
Untightening tools	1		
Untightening work piece	1		
cleaning the machine, tools and work piece	2.5		

The third process is bending.

Machine	**Bending**	**Main Operation**	**Bending**
Activities	**Time Taken in Minutes**	**Sub Total Time**	**Remark**
Layout making	1	3.5	
Aligning & tightening work piece	1		
Bending operation	0.5		
Untightening work piece	1		

Cutter or blade see Part Drawing 4-7

It can be manufactured in three main operations; cutting, drilling and grinding.

The first process is cutting on Shearing machine.

Machine	**Shearing machine**	**Main Operation**	**Cutting**
Activities	**Time Taken in Minutes**	**Sub Total Time**	**Remark**
Layout making	5	9.5	
Aligning & tightening work piece	1		
Cutting operation	1.5		
cleaning the machine, tools and work piece	2		

The second process is drilling to make the two holes.

Machine	**Hand Drill**	**Main Operation**	**Drilling**
Activities	**Time Taken in Minutes**	**Sub Total Time**	**Remark**
Layout making	1	8.5	
Changing& tightening tools	1		
Drilling operation	2		
Untightening tools	1		
Untightening work piece	1		

cleaning the machine, tools and work piece	2.5		

The third process is grinding to make the knife edges.

Machine	**Grinding**	**Main Operation**	**Grinding**
Activities	**Time Taken in Minutes**	**Sub Total Time**	**Remark**
Layout making	5	22	
Aligning & tightening work piece	1		
Grinding operation	15		
Untightening work piece	1		

Cutter bar see Part Drawing 4-8

It can be manufactured in two main operations; cutting and drilling.

The first process is cutting on Hacksaw.

Machine	**Hacksaw**	**Main Operation**	**Cutting**
Activities	**Time Taken in Minutes**	**Sub Total Time**	**Remark**
Layout making	1	9	
Aligning & tightening work piece	1		
Cutting operation	5		
cleaning the machine, tools and work piece	2		

The second process is drilling to make the holes.

Machine	**Drilling**	**Main Operation**	**Drilling**
Activities	**Time Taken in Minutes**	**Sub Total Time**	**Remark**
Layout making	5	31.5	
Changing& tightening tools	1		
Aligning & tightening work piece	1		
Drilling operation	20		
Untightening tools	1		
Untightening work piece	1		
cleaning the machine, tools and work piece	2.5		

Finger or guard lip see Part Drawing 4-9

It can be manufactured in four main operations; cutting, drilling, bending and welding.

The first process is cutting on Shearing machine the three pieces.

Machine	**Shearing machine**	**Main Operation**	**Cutting**
Activities	**Time Taken in Minutes**	**Sub Total Time**	**Remark**
Layout making	3	23	
Aligning & tightening work piece	3		
Cutting operation	15		
cleaning the machine, tools and work piece	2		

The second process is drilling to make the holes on the bottom piece.

Machine	**Drilling**	**Main Operation**	**Drilling**
Activities	**Time Taken in Minutes**	**Sub Total Time**	**Remark**
Layout making	5	16.5	
Changing& tightening tools	1		
Aligning & tightening work piece	1		
Drilling operation	5		
Untightening tools	1		
Untightening work piece	1		
cleaning the machine, tools and work piece	2.5		

The third process is bending to make the flange of finger on the bottom piece.

Machine	**Bending**	**Main Operation**	**Bending**
Activities	**Time Taken in Minutes**	**Sub Total Time**	**Remark**
Layout making	1	6	
Aligning & tightening work piece	1		
Bending operation	0.5		
Untightening work piece	1		
cleaning the machine, tools and work piece	2.5		

The fourth process is welding to join the three-pieces using electrode welding machine.

Machine	Welding	Main Operation	Joining
Activities	**Time Taken in Minutes**	**Sub Total Time**	**Remark**
Layout making	2	14.5	
Changing& tightening tools	1		
Aligning & tightening work piece	1		
Welding operation	6		
Untightening tools	1		
Untightening work piece	1		
cleaning the machine, tools and work piece	2.5		

Guard lip bar see Part Drawing 4-10

It can be manufactured in two main operations; cutting and drilling.

The first process is cutting on Hacksaw.

Machine	Hacksaw	Main Operation	Cutting
Activities	**Time Taken in Minutes**	**Sub Total Time**	**Remark**
Layout making	1	9	
Aligning & tightening work piece	1		
Cutting operation	5		
cleaning the machine, tools and work piece	2		

The second process is drilling to make the holes.

Machine	Drilling	Main Operation	Drilling
Activities	**Time Taken in Minutes**	**Sub Total Time**	**Remark**
Layout making	5	36.5	
Changing& tightening tools	1		
Aligning & tightening work piece	1		
Drilling operation	25		
Untightening tools	1		
Untightening work piece	1		

cleaning the machine, tools and work piece	2.5		

Follower bar see Part Drawing 4-11

It can be manufactured in one main operation; cutting.

This process is cutting using Portable Chop Saw.

Machine	**Portable Chop Saw**	**Main Operation**	**Cutting**
Activities	**Time Taken in Minutes**	**Sub Total Time**	**Remark**
Layout making	3	9	
Aligning & tightening work piece	3		
Cutting operation	1		
cleaning the machine, tools and work piece	2		

Rectangular box for follower bar see Part Drawing 4-12

It can be manufactured in two main operation; cutting and drilling.

The first process is cutting using Portable Chop Saw.

Machine	**Portable Chop Saw**	**Main Operation**	**Cutting**
Activities	**Time Taken in Minutes**	**Sub Total Time**	**Remark**
Layout making	3	10	
Aligning & tightening work piece	3		
Cutting operation	2		
cleaning the machine, tools and work piece	2		

The second process is drilling to make the holes.

Machine	**Drilling**	**Main Operation**	**Drilling**
Activities	**Time Taken in Minutes**	**Sub Total Time**	**Remark**
Layout making	5	26.5	
Changing& tightening tools	1		
Aligning & tightening work piece	1		
Drilling operation	15		

Untightening tools	1		
Untightening work piece	1		
cleaning the machine, tools and work piece	2.5		

Follower Head see Part Drawing 4-13

It can be manufactured in one main operation; cutting.

This process is cutting using Portable Chop Saw.

Machine	**Portable Chop Saw**	**Main Operation**	**Cutting**
Activities	**Time Taken in Minutes**	**Sub Total Time**	**Remark**
Layout making	3	10	
Aligning & tightening work piece	3		
Cutting operation	2		
cleaning the machine, tools and work piece	2		

Idler Shaft see Part Drawing 4-14

It can be manufactured in three main operations; turning, facing and milling. The first process is turning on lathe to reduce the diameter from 8 to 6 and 7 mm over a length of 38 mm and 10 mm respectively.

Machine	**Lathe**	**Main Operation**	**Turning**
Activities	**Time Taken in Minutes**	**Sub Total Time**	**Remark**
Layout making	1	35.5	
Aligning & tightening work piece	5		
Changing& tightening tools	5		
Turning operation	20		
Untightening tools	1		
Untightening work piece	1		
cleaning the machine, tools and work piece	2.5		

The second process is facing on both ends to get 48 mm length.

Machine	**Lathe**	**Main Operation**	**Facing**

Activities	Time Taken in Minutes	Sub Total Time	Remark
Layout making	1	30.5	
Aligning & tightening work piece	5		
Changing& tightening tools	5		
Facing operation	15		
Untightening tools	1		
Untightening work piece	1		
cleaning the machine, tools and work piece	2.5		

The last process is milling to make key way.

Machine	Milling	Main Operation	Milling
Activities	**Time Taken in Minutes**	**Sub Total Time**	**Remark**
Layout making	1	36	
Aligning & tightening work piece	5		
Changing& tightening tools	5		
Milling operation	10		
Untightening tools	5		
Untightening work piece	5		
cleaning the machine, tools and work piece	5		

Camshaft see Part Drawing 4-16

It can be manufactured in three main operations; turning, facing and milling. The first process is turning on lathe.

Machine	Lathe	Main Operation	Turning
Activities	**Time Taken in Minutes**	**Sub Total Time**	**Remark**
Layout making	1	35.5	
Aligning & tightening work piece	5		
Changing& tightening tools	5		
Turning operation	20		
Untightening tools	1		

Untightening work piece	1		
cleaning the machine, tools and work piece	2.5		

The second process is facing on both ends to get the required length.

Machine	**Lathe**	**Main Operation**	**Facing**
Activities	**Time Taken in Minutes**	**Sub Total Time**	**Remark**
Layout making	1	30.5	
Aligning & tightening work piece	5		
Changing& tightening tools	5		
Facing operation	15		
Untightening tools	1		
Untightening work piece	1		
cleaning the machine, tools and work piece	2.5		

The last process is milling to make key way.

Machine	**Milling**	**Main Operation**	**Milling**
Activities	**Time Taken in Minutes**	**Sub Total Time**	**Remark**
Layout making	1	41	
Aligning & tightening work piece	5		
Changing& tightening tools	5		
Milling operation	15		
Untightening tools	5		
Untightening work piece	5		
cleaning the machine, tools and work piece	5		

Intermediate shaft see Part Drawing 4-22

It can be manufactured in three main operations; turning, facing and milling. The first process is turning on lathe to reduce the diameter from 8 to 6 and 7 mm over a length of 38 mm and 10 mm respectively.

Machine	**Lathe**	**Main Operation**	**Turning**
Activities	**Time Taken in Minutes**	**Sub Total Time**	**Remark**
Layout making	1	35.5	
Aligning & tightening work piece	5		
Changing& tightening tools	5		
Turning operation	20		
Untightening tools	1		
Untightening work piece	1		
cleaning the machine, tools and work piece	2.5		

The second process is facing on both ends to get 48 mm length.

Machine	**Lathe**	**Main Operation**	**Facing**
Activities	**Time Taken in Minutes**	**Sub Total Time**	**Remark**
Layout making	1	30.5	
Aligning & tightening work piece	5		
Changing& tightening tools	5		
Facing operation	15		
Untightening tools	1		
Untightening work piece	1		
cleaning the machine, tools and work piece	2.5		

The last process is milling to make key way.

Machine	**Milling**	**Main Operation**	**Milling**
Activities	**Time Taken in Minutes**	**Sub Total Time**	**Remark**
Layout making	1	36	
Aligning & tightening work piece	5		
Changing& tightening tools	5		
Milling operation	10		
Untightening tools	5		

Untightening work piece	5		
cleaning the machine, tools and work piece	5		

Eccentric cam see Part Drawing 4-15

It can be manufactured in three main operations; casting, drilling and milling. This process is casting using die casting.

Machine	**Die Casting**	**Main Operation**	**Casting**
Activities	**Time Taken in Minutes**	**Sub Total Time**	**Remark**
Material Preparation	5	42	
Aligning & tightening work piece	5		
Casting operation	30		
cleaning the machine, tools and work piece	2		

The second process is drilling to make the holes.

Machine	**Drilling**	**Main Operation**	**Drilling**
Activities	**Time Taken in Minutes**	**Sub Total Time**	**Remark**
Layout making	5	16.5	
Changing& tightening tools	1		
Aligning & tightening work piece	1		
Drilling operation	5		
Untightening tools	1		
Untightening work piece	1		
cleaning the machine, tools and work piece	2.5		

The last process is milling to make key way.

Machine	**Milling**	**Main Operation**	**Milling**
Activities	**Time Taken in Minutes**	**Sub Total Time**	**Remark**
Layout making	1	24	
Aligning & tightening work piece	1		

Changing& tightening tools	5		
Milling operation	10		
Untightening tools	1		
Untightening work piece	1		
cleaning the machine, tools and work piece	5		

Keys see Part Drawing 4-17, Part Drawing 4-18, Part Drawing 4-19, Part Drawing 4-23 and Part Drawing 4-24

It can be manufactured in two main operations; cutting and milling. This process is cutting using Portable Chop Saw.

Machine	**Portable Chop Saw**	**Main Operation**	**Cutting**
Activities	**Time Taken in Minutes**	**Sub Total Time**	**Remark**
Layout making	1	5	
Aligning & tightening work piece	1		
Cutting operation	1		
cleaning the machine, tools and work piece	2		

The second process is milling to make key way.

Machine	**Milling**	**Main Operation**	**Milling**
Activities	**Time Taken in Minutes**	**Sub Total Time**	**Remark**
Layout making	1	36	
Aligning & tightening work piece	5		
Changing& tightening tools	5		
Milling operation	10		
Untightening tools	5		
Untightening work piece	5		
cleaning the machine, tools and work piece	5		

V-Grooved Pulley on Motor Shaft see Part Drawing 4-20

It can be manufactured in four main operations; turning, facing, drilling and milling. The first process is turning on lathe to reduce the diameter from 64 to 40 mm over a length of 13 mm.

Machine	**Lathe**	**Main Operation**	**Turning**
Activities	**Time Taken in Minutes**	**Sub Total Time**	**Remark**
Layout making	1	35.5	
Aligning & tightening work piece	5		
Changing& tightening tools	5		
Turning operation	20		
Untightening tools	1		
Untightening work piece	1		
cleaning the machine, tools and work piece	2.5		

The second process is facing on both ends to get 38 mm length.

Machine	**Lathe**	**Main Operation**	**Facing**
Activities	**Time Taken in Minutes**	**Sub Total Time**	**Remark**
Layout making	1	25.5	
Aligning & tightening work piece	5		
Changing& tightening tools	5		
Facing operation	10		
Untightening tools	1		
Untightening work piece	1		
cleaning the machine, tools and work piece	2.5		

The third process is drilling to make the hole.

Machine	**Drilling**	**Main Operation**	**Drilling**
Activities	**Time Taken in Minutes**	**Sub Total Time**	**Remark**
Layout making	1	21.5	
Aligning & tightening work piece	2		
Changing& tightening tools	2		

Drilling operation	10		
Untightening tools	2		
Untightening work piece	2		
cleaning the machine, tools and work piece	2.5		

The last process is milling to make key way.

Machine	**Milling**	**Main Operation**	**Milling**
Activities	**Time Taken in Minutes**	**Sub Total Time**	**Remark**
Layout making	2	22.5	
Aligning & tightening work piece	2		
Changing& tightening tools	2		
Milling operation	10		
Untightening tools	2		
Untightening work piece	2		
cleaning the machine, tools and work piece	2.5		

V-Grooved Pulley on Motor Shaft see Part Drawing 4-21

It can be manufactured in four main operations; turning, facing, drilling and milling. The first process is turning on lathe to reduce the diameter from 152 to 128 mm over a length of 13 mm.

Machine	**Lathe**	**Main Operation**	**Turning**
Activities	**Time Taken in Minutes**	**Sub Total Time**	**Remark**
Layout making	1	40.5	
Aligning & tightening work piece	5		
Changing& tightening tools	5		
Turning operation	25		
Untightening tools	1		
Untightening work piece	1		
cleaning the machine, tools and work piece	2.5		

The second process is facing on both ends to get 38 mm length.

Machine	**Lathe**	**Main Operation**	**Facing**
Activities	**Time Taken in Minutes**	**Sub Total Time**	**Remark**
Layout making	1	30.5	
Aligning & tightening work piece	5		
Changing& tightening tools	5		
Facing operation	15		
Untightening tools	1		
Untightening work piece	1		
cleaning the machine, tools and work piece	2.5		

The third process is drilling to make the hole.

Machine	**Drilling**	**Main Operation**	**Drilling**
Activities	**Time Taken in Minutes**	**Sub Total Time**	**Remark**
Layout making	3	53	
Aligning & tightening work piece	5		
Changing& tightening tools	5		
Drilling operation	25		
Untightening tools	5		
Untightening work piece	5		
cleaning the machine, tools and work piece	5		

The last process is milling to make key way.

Machine	**Milling**	**Main Operation**	**Milling**
Activities	**Time Taken in Minutes**	**Sub Total Time**	**Remark**
Layout making	2	22.5	
Aligning & tightening work piece	2		
Changing& tightening tools	2		
Milling operation	10		
Untightening tools	2		

Untightening work piece	2		
cleaning the machine, tools and work piece	2.5		

Star wheel vertical rod see Part Drawing 4-25

It can be manufactured in three main operation; cutting, turning and bending. This first process is cutting using Portable Chop Saw.

Machine	**Portable Chop Saw**	**Main Operation**	**Cutting**
Activities	**Time Taken in Minutes**	**Sub Total Time**	**Remark**
Layout making	1	6	
Aligning & tightening work piece	1		
Cutting operation	2		
cleaning the machine, tools and work piece	2		

The second process is turning on lathe.

Machine	**Lathe**	**Main Operation**	**Turning**
Activities	**Time Taken in Minutes**	**Sub Total Time**	**Remark**
Layout making	1	14.5	
Aligning & tightening work piece	2		
Changing& tightening tools	2		
Turning operation	5		
Untightening tools	1		
Untightening work piece	1		
cleaning the machine, tools and work piece	2.5		

The last process is bending on bending machine.

Machine	**Bending**	**Main Operation**	**Bening**
Activities	**Time Taken in Minutes**	**Sub Total Time**	**Remark**
Layout making	1	7	
Aligning & tightening work piece	2		

Bending operation	2		
cleaning the machine, tools and work piece	2		

Bearing Seat for star wheel see Part Drawing 4-26

It can be manufactured in two main operation; cutting and boring. This first process is cutting using Portable Chop Saw.

Machine	**Portable Chop Saw**	**Main Operation**	**Cutting**
Activities	**Time Taken in Minutes**	**Sub Total Time**	**Remark**
Layout making	1	9	
Aligning & tightening work piece	1		
Cutting operation	5		
cleaning the machine, tools and work piece	2		

The second process is boring on lathe.

Machine	**Lathe**	**Main Operation**	**Boring**
Activities	**Time Taken in Minutes**	**Sub Total Time**	**Remark**
Layout making	1	24.5	
Aligning & tightening work piece	2		
Changing& tightening tools	2		
Boring operation	15		
Untightening tools	1		
Untightening work piece	1		
cleaning the machine, tools and work piece	2.5		

Star wheel arm assembly see Part Drawing 4-27

It can be manufactured in two main operation; cutting and welding. The first process is cutting using Portable Chop Saw.

Machine	**Portable Chop Saw**	**Main Operation**	**Cutting**
Activities	**Time Taken in Minutes**	**Sub Total Time**	**Remark**

Layout making	1	5	
Aligning & tightening work piece	1		
Cutting operation	2		
cleaning the machine, tools and work piece	2		

The second process is welding on electrode welding machine.

Machine	**Electrode Welding**	**Main Operation**	**Joining**
Activities	**Time Taken in Minutes**	**Sub Total Time**	**Remark**
Layout making	1	34.5	
Aligning & tightening work piece	2		
Changing& tightening tools	2		
Welding operation	25		
Untightening tools	1		
Untightening work piece	1		
cleaning the machine, tools and work piece	2.5		

Divider see Part Drawing 4-28

It can be manufactured in two main operations; cutting and drilling. The first process is cutting on Shearing machine.

Machine	**Shearing machine**	**Main Operation**	**Cutting**
Activities	**Time Taken in Minutes**	**Sub Total Time**	**Remark**
Layout making	3	8.5	
Aligning & tightening work piece	3		
Cutting operation	1.5		
cleaning the machine, tools and work piece	1		

The second process is drilling.

Machine	**Hand Drill**	**Main Operation**	**Drilling**
Activities	**Time Taken in Minutes**	**Sub Total Time**	**Remark**
Layout making	1	7.5	

Changing& tightening tools	1		
Drilling operation	1		
Untightening tools	1		
Untightening work piece	1		
cleaning the machine, tools and work piece	2.5		

Divider Support See Part Drawing 4-29

It can be manufactured in three main operation; cutting, turning and bending. This first process is cutting using Portable Chop Saw.

Machine	**Portable Chop Saw**	**Main Operation**	**Cutting**
Activities	**Time Taken in Minutes**	**Sub Total Time**	**Remark**
Layout making	1	6	
Aligning & tightening work piece	1		
Cutting operation	2		
cleaning the machine, tools and work piece	2		

The second process is bending on bending machine.

Machine	**Bending**	**Main Operation**	**Bening**
Activities	**Time Taken in Minutes**	**Sub Total Time**	**Remark**
Layout making	1	7	
Aligning & tightening work piece	2		
Bending operation	2		
cleaning the machine, tools and work piece	2		

Frame for solar panel support see Part Drawing 4-30

There are 12 components in solar panel support. It can be manufactured in two main operation; cutting and welding. The first process is cutting using Portable Chop Saw.

Machine	**Portable Chop Saw**	**Main Operation**	**Cutting**
Activities	**Time Taken in Minutes**	**Sub Total Time**	**Remark**

Layout making	12	38	
Aligning & tightening work piece	12		
Cutting operation	12		
cleaning the machine, tools and work piece	2		

The second process is welding on electrode welding machine.

Machine	**Electrode Welding**	**Main Operation**	**Joining**
Activities	**Time Taken in Minutes**	**Sub Total Time**	**Remark**
Layout making	12	125	
Aligning & tightening work piece	12		
Changing& tightening tools	12		
Welding operation	60		
Untightening tools	12		
Untightening work piece	12		
cleaning the machine, tools and work piece	5		

Gear Box see Part Drawing 4-31

It can be manufactured in two main operation; cutting and drilling. The first process is cutting using Portable Chop Saw.

Machine	**Portable Chop Saw**	**Main Operation**	**Cutting**
Activities	**Time Taken in Minutes**	**Sub Total Time**	**Remark**
Layout making	3	12	
Aligning & tightening work piece	3		
Cutting operation	4		
cleaning the machine, tools and work piece	2		

The second process is drilling to make the holes.

Machine	**Drilling**	**Main Operation**	**Drilling**
Activities	**Time Taken in Minutes**	**Sub Total Time**	**Remark**
Layout making	5	21.5	

Changing& tightening tools	1		
Aligning & tightening work piece	1		
Drilling operation	10		
Untightening tools	1		
Untightening work piece	1		
cleaning the machine, tools and work piece	2.5		

Frame for cutter see Part Drawing 4-32, Part Drawing 4-33, Part Drawing 4-34 and Figure 4-84

There are six components which comprise the frame for cutter assembly. It can be manufactured by using three main operations; cutting, drilling and welding. The first process is cutting using Portable Chop Saw.

Machine	**Portable Chop Saw**	**Main Operation**	**Cutting**
Activities	**Time Taken in Minutes**	**Sub Total Time**	**Remark**
Layout making	6	20	
Aligning & tightening work piece	6		
Cutting operation	6		
cleaning the machine, tools and work piece	2		

The second process is drilling to make the holes.

Machine	**Drilling**	**Main Operation**	**Drilling**
Activities	**Time Taken in Minutes**	**Sub Total Time**	**Remark**
Layout making	5	37	
Changing& tightening tools	3		
Aligning & tightening work piece	3		
Drilling operation	15		
Untightening tools	3		
Untightening work piece	3		
cleaning the machine, tools and work piece	5		

The last process is welding on electrode welding machine.

Machine	**Electrode Welding**	**Main Operation**	**Joining**
Activities	**Time Taken in Minutes**	**Sub Total Time**	**Remark**
Layout making	6	65	
Aligning & tightening work piece	6		
Changing& tightening tools	6		
Welding operation	30		
Untightening tools	6		
Untightening work piece	6		
cleaning the machine, tools and work piece	5		

Axel see Part Drawing 4-35

It can be manufactured by using three main operations; cutting, turning and threading. The first process is cutting using Portable Chop Saw.

Machine	**Portable Chop Saw**	**Main Operation**	**Cutting**
Activities	**Time Taken in Minutes**	**Sub Total Time**	**Remark**
Layout making	1	9	
Aligning & tightening work piece	1		
Cutting operation	5		
cleaning the machine, tools and work piece	2		

The second process is turning on lathe.

Machine	**Lathe**	**Main Operation**	**Turning**
Activities	**Time Taken in Minutes**	**Sub Total Time**	**Remark**
Layout making	1	19.5	
Aligning & tightening work piece	2		
Changing& tightening tools	2		
Turning operation	10		
Untightening tools	1		

Untightening work piece	1		
cleaning the machine, tools and work piece	2.5		

Column for Cutter Frame Part Drawing 4-34

It can be manufactured by using three main operations; cutting, drilling and welding. The first process is cutting using Portable Chop Saw.

Machine	**Portable Chop Saw**	**Main Operation**	**Cutting**
Activities	**Time Taken in Minutes**	**Sub Total Time**	**Remark**
Layout making	1	14	
Aligning & tightening work piece	1		
Cutting operation	10		
cleaning the machine, tools and work piece	2		

The second process is drilling to make the holes.

Machine	**Drilling**	**Main Operation**	**Drilling**
Activities	**Time Taken in Minutes**	**Sub Total Time**	**Remark**
Layout making	5	32	
Changing& tightening tools	3		
Aligning & tightening work piece	3		
Drilling operation	10		
Untightening tools	3		
Untightening work piece	3		
cleaning the machine, tools and work piece	5		

The last process is welding on electrode welding machine.

Machine	**Electrode Welding**	**Main Operation**	**Joining**
Activities	**Time Taken in Minutes**	**Sub Total Time**	**Remark**
Layout making	6	45	
Aligning & tightening work piece	6		

Changing& tightening tools	6		
Welding operation	10		
Untightening tools	6		
Untightening work piece	6		
cleaning the machine, tools and work piece	5		

Handle see Part Drawing 4-36

It can be manufactured by using two main operations; cutting and welding. The first process is cutting using Portable Chop Saw.

Machine	**Portable Chop Saw**	**Main Operation**	**Cutting**
Activities	**Time Taken in Minutes**	**Sub Total Time**	**Remark**
Layout making	1	10	
Aligning & tightening work piece	1		
Cutting operation	6		
cleaning the machine, tools and work piece	2		

The last process is welding on electrode welding machine.

Machine	**Electrode Welding**	**Main Operation**	**Joining**
Activities	**Time Taken in Minutes**	**Sub Total Time**	**Remark**
Layout making	1	12.5	
Aligning & tightening work piece	1		
Changing& tightening tools	1		
Welding operation	5		
Untightening tools	1		
Untightening work piece	1		
cleaning the machine, tools and work piece	2.5		

Threaded Rod see Part Drawing 4-37

It can be manufactured by using one main operation; cutting. This process is cutting using Portable Chop Saw.

Machine	Portable Chop Saw	Main Operation	Cutting
Activities	**Time Taken in Minutes**	**Sub Total Time**	**Remark**
Layout making	1	7	
Aligning & tightening work piece	1		
Cutting operation	3		
cleaning the machine, tools and work piece	2		

Cost Analysis

The cost of the machine was analyzed by considering manpower, machine rent, raw materials and standard part costs.

$$Man\ power\ cost = time\ taken\ in\ min \times rate\ of\ machinist\ \ Birr/min \text{---------- 4-111}$$

$$machine\ cost = time\ taken\ in\ min \times machine\ rent\ Birr/min \text{---------- 4-112}$$

$$Manufacturing\ Cost = Man\ power\ cost + machine\ cost \text{---------- 4-113}$$

$$Total\ Cost = Manufacturing\ Cost + standard\ part\ cost \text{---------- 4-114}$$

Table 4-18 Manufacturing Costs [66], [67] and Table 4-25 Machine Rate (Source: Vision International Consultants)Table 4-25

Part Name	Machine	Time Taken in min.	Machine Cost in Birr	Man Power Cost in Birr	Mass in Kg	Materials Cost Birr/Kg	Raw Materials Cost in Birr	Quantity	Sub Total Cost in Birr
Bevel Gear	Hacksaw	14.00	26.83	11.26	2.31	1.43	3.29	1	990.31
	Lathe	98.50	443.25	79.24					
	Milling	83.00	359.67	66.77					
Pinion Gear	Hacksaw	9.00	17.25	7.24	0.23	1.43	0.33	1	764.90
	Lathe	78.50	353.25	63.15					
	Milling	63.00	273.00	50.68					
Convey or Pulley I	Lathe	66.00	297.00	53.09	2.78	1.43	3.96	1	777.12
	Drilling	87.50	167.71	70.39					
	Milling	36.00	156.00	28.96					
Convey or Pulley I	Lathe	66.00	297.00	53.09	2.74	1.43	3.91	1	592.10
	Drilling	87.50	167.71	70.39					
Flat Belt	Blade	2.00	0.17	1.61	0.18	235.59	42.41	1	114.93
	drilling	26.00	49.83	20.92					
Lug	Shearing Machine	3.50	5.37	2.82	0.03	0.71	0.02	13	106.65
	Drilling	8.50	16.29	6.84					
	Bending	3.50	4.08	2.82					
Cutter	Shearing Machine	9.50	14.57	7.64	0.03	0.71	0.02	8	1179.13

	Drilling	8.50	16.29	6.84					
	Grinder	22.00	84.33	17.70					
Cutter Bar	Hacksaw	9.00	17.25	7.24	0.23	0.71	0.16	1	110.37
	Drilling	31.50	60.38	25.34					
Guard Lip	Shearing Machine	23.00	3.53	18.50	0.01	0.71	0.01	10	1218.42
	Drilling	16.50	31.63	13.27					
	Bending	6.00	7.00	4.83					
	Welding	14.50	31.42	11.66					
Guard Lip Bar	Hacksaw	9.00	17.25	7.24	0.14	0.71	0.10	1	123.91
	Drilling	36.50	69.96	29.36					
Follower Bar	Portable Chop Saw	9.00	16.50	7.24	0.10	0.71	0.07	1	23.81
Rectangular Box …	Portable Chop Saw	10.00	18.33	8.04	0.17	0.71	0.12	1	50.24
	Drilling	26.50	50.79	21.32					
Follower Head	Portable Chop Saw	10.00	18.33	8.04	0.13	0.71	0.09	2	52.94
Idler Shaft	Lathe	66.00	297.00	53.09	0.02	0.71	0.01	1	535.07
	Milling	36.00	156.00	28.96					
Camshaft	Lathe	66.00	297.00	53.09	0.70	0.71	0.50	1	561.24
	Milling	41.00	177.67	32.98					
Intermediate Shaft	Lathe	66.00	297.00	53.09	0.08	0.71	0.06	1	535.11
	Milling	36.00	156.00	28.96					
Eccentric Cam	Casting	42.00	178.50	33.79	0.52	0.71	0.37	1	380.86
	Drilling	16.50	31.63	13.27					
	Milling	24.00	104.00	19.31					
Keys	Portable Chop Saw	5.00	9.17	4.02	0.01	0.71	0.01	1	198.16
	Milling	36.00	156.00	28.96					
V-Pulley M	Lathe	61.00	274.50	49.07	0.42	1.43	0.60	1	720.27
	Drilling	21.50	41.21	17.30					
	Milling	22.50	319.50	18.10					
V-Pulley I	Lathe	71.00	319.50	57.12	1.83	1.43	2.61	1	639.04
	Drilling	53.00	101.58	42.64					
	Milling	22.50	97.50	18.10					
Star Wheel Rod	Portable Chop Saw	6.00	11.00	4.83	0.14	0.71	0.10	4	426.55
	lathe	14.50	65.25	11.66					
	Bending	7.00	8.17	5.63					
Seat for Star Wheel	Portable Chop Saw	9.00	44.92	7.24	0.03	0.71	0.02	4	305.55
	Lathe	24.50	4.50	19.71					
Star Wheel Arm	Portable Chop Saw	5.00	9.17	4.02	0.13	0.71	0.09	4	463.14
	Welding	34.50	74.75	27.75					
Divider	Shearing Machine	8.50	13.03	6.84	0.11	0.71	0.08	4	161.43
	Drilling	7.50	14.38	6.03					
	Portable Chop Saw	6.00	11.00	4.83	0.19	0.71	0.14	4.00	119.04

Divider Support	Bending	7.00	8.17	5.63					
Solar Panel Support	Portable Chop Saw	38.00	69.67	30.57	0.96	0.71	0.68	1	472.31
	Welding	125.00	270.83	100.56					
Gear Box	Portable Chop Saw	12.00	22.00	9.65	0.17	0.71	0.12	1	90.28
	Drilling	21.50	41.21	17.30					
Frame for Cutter	Portable Chop Saw	20.00	36.67	16.09	4.34	0.71	3.09	1	419.57
	Drilling	37.00	140.83	29.76					
	Welding	65.00	140.83	52.29					
Axel	Portable Chop Saw	9.00	16.50	7.24	1.46	0.71	1.04	1	128.22
	Lathe	19.50	87.75	15.69					
Column	Portable Chop Saw	14.00	25.67	11.26	0.17	0.71	0.12	1	257.83
	Drilling	32.00	61.33	25.74					
	Welding	45.00	97.50	36.20					
Handle	Portable Chop Saw	10.00	18.33	8.04	2.32	0.71	1.65	1	65.17
	Welding	12.50	27.08	10.06					
Threaded Rod	Portable Chop Saw	7.00	12.83	5.63	1.19	0.71	0.85	1	19.31
									12658.7

Table 4-19 Cost of Standard Parts Sources [68], [69], [70], [71], [72], [73], [74], [75], [76], [77][78], [79] and [80]

Part Name	**Materials**	**Dimension**	**Unit Price in Birr**	**Quantity**	**Sub Total in Birr**
DC Motor	Pc	1.5 hp	15493.18	1	15493.18
Solar Panel	Pc	400 W	1551.84	1	1551.84
Rivet	Al	ϕ4x7	0.323	26	8.398
Bolt	Steel	M4x11.5	0.647	16	10.352
Nut	Steel	M4x2.66	0.323	52	16.796
Bolt	Steel	M4x6.5	0.647	20	12.94
Bearing	Ball	ϕ16xϕ4x5	3.233	4	12.932
Bolt	Steel	M4x15	0.647	4	2.588
Bearing	Ball	ϕ9xϕ4x2.5	6.789	8	54.312
Bolt	Steel	M4x35	0.647	12	7.764
Bearing	Thrust	ϕ13xϕ6x5	3.556	1	3.556
Bearing	Thrust	ϕ14xϕ6x5	1.617	1	1.617
Bearing	Ball	ϕ24xϕ15x5	16.165	2	32.33
Bearing	Thrust	ϕ26xϕ12x9	16.165	1	16.165
Bearing	Thrust	ϕ28xϕ15x9	16.165	1	16.165

Bearing	Thrust	ϕ19xϕ8x7	1.617	4	6.468
Solid Tire	polyurethane	ϕ394.2xϕ19.1x86.5	549.61	2	1099.22
Nut	Steel	M20x15	0.485	6	2.91
Nut	Steel	M19x12	0.485	2	0.97
Nut	Steel	M9x6.75	0.323	4	1.292
Bolt	Steel	M4x18	0.647	4	2.588
Bolt	Steel	M4x45	0.647	4	2.588
Bolt	Steel	M9x32	0.647	4	2.588
Bolt	Steel	M4x65	0.647	4	2.588
Electrode	Pc	ϕ3.15	85	1	85
					18447.147

The total cost of the machine can be estimated by using **equation** 4-114.

Total Cost=12658.7+18447.147=31105.847 Birr

Conclusion and Recommendation

Conclusion

The small-scale solar powered harvester has been designed and prototyped by using materials which are purchased and collected from ASTU and old spare sellers. It incorporates power generation system, cutting system and vehicle system. The power is collected directly from sunray using solar panels 200 watt each. This power is transferred to the cutting system using Dc Motor with 1 Hp power rate.

The prototype needs 49.877 V to drive the whole system. However, it can be reduced by making the prototype as per the design. The amount of solar power was enough to drive the whole system which was proved during testing even if there are power losses at different stages. The harvester should be driven by using only two solar panel for those farmers who are under low economy level. However, it can be driven by using Li-ion solar battery for those farmers are capable of buying this battery. In general, the harvester is effective by using solar panels instead of batteries. Therefore, it is confidential to conclude that a small-scale solar harvest is feasible as one means of harvesting grains in order to improve the amount of grains collected during harvesting.

Recommendation

The effectiveness of solar grain harvester is promising. Hence, it is recommended to manufacture and supply to the users by improving some components. In order to do this, it is advisable to:

1. redesign and optimize the weight
2. manufacture the components as per the design.

The harvester will be used to collect grasses for animal feeds in addition to harvesting grains.

References

[1] M.L. Jat, S.R. Bhakar, S.K. Sharma, A.K. Kothari, "Dryland Technology", Scientific Publisher, 2016, 2nd Ed.

[2] Okoro, K., "Development of a locally Fabricated Engine Powered Lawn Mower", (Unpublished). Department of Agric/Environmental Engineering, RSUST, Port-Harcourt, Nigeria, 2010

[3] Jeremy (2005) solar charged lawn mower: https://www.appropedia.org/Solar_Charged_Lawnmower

[4] Victor, V.M., Verns, A, "Design and development of power operated rotary weeder for wetland paddy", Journal of Agricultural Mechanization in Asia, African and Latin America, 3(4), 27-29, 2003.

[5] Moheb M. A. El-Sharabasy, "CONSTRUCTION AND MANUFACTURE A SELF-PROPELLED MACHINE SUITS FOR CUTTING SOME GRAIN CROPS TO MINIMIZE LOSSES AND MAXIMIZE EFFICIENCY", Misr J. Ag. Eng., 23(3): 509- 531, 2006

[6] Prof. P.B. Chavan, Prof. D.K. Patil and Prof. D.S. Dhondge, "Design and Development of manually Operated Reaper", IOSR Journal of Mechanical and Civil Engineering (IOSR-JMCE), Volume 12, 2015

[7] M.J. O'Dogherty, J.A.Huber, J.Dyson and C.J.Marshall, " Physical and mechanical properties of Wheat Straw", Journal of Agricultural Engineering Research, ELSEVIER, 2002.

[8] Hamed Tavakoli, Seyed Saeid Mohtasebi and A. Jafari, "Physical and mechanical properties of wheat straw as influenced by moisture content", Int. Agrophysics,23,175-181 2009.

[9] Hamed Tavakoli, Seyed Saeid Mohtasebi, A. Jafari and Yalda Nazari, "Some Engineering Properties of Barley Straw",American Society of Agricultural and Biological Engineers, 2009

[10] H. Tavakoli, S.S. Mohtasebi, A. Jafari, "Effects of moisture content, internode position and loading rate on the bending characteristics of barley straw", RES. AGR. ENG., 55, 2009 (2): 45–51

[11] M. Tavakoli, H. Tavakoli, M.H. Azizi and G.H. Haghayegh, "Comparison of Mechanical Properties Between Two Varieties of Rice Straw", Advance Journal of Food Science and Technology 2(1): 50-54, 2010.

[12] R. Tabatabaee Koloo and A. Borgheie, "Measuring the Static and Dynamic Cutting

[13] Force of Stems for Iranian Rice Varieties", J. Agric. Sci. Techol. Vol. 8: 193-198, 2006.

[14] Ganesh C. Bora and Gunner K. Hansen, "low cost mechanical aid for rice harvesting", Journal of Applied Science 7 (23): 3815-3818, 2007

[15] Muhammad Nadeem, Anjum Munir and Manzoor Ahmad Choudhary, "Design and Evaluation of Self-Propelled Reaper for Harvesting Multi Crops", ASABE Annual International Meeting Paper, 2015

[16] Gozde Değer and et al, "STRENGTH OF WHEAT AND BARLEY STEMS AND DESIGN OF NEW BEAM/COLUMNS", Mathematical and Computational Applications, Vol. 15, No. 1, pp. 1-13, 2010.

[17] A. Celik, "Design and operating characteristics of a push type cutter bar mower", CANADIAN BIOSYSTEMS ENGINEERING, Volume 48, 2006.

[18] Tom Leblicq_, Simon Vanmaercke, Herman Ramon, Wouter Saeys, "Mechanical analysis of the bending behavior of plant Stems", 2014

[19] Joseph Edward Shigley, John Joseph Uicker, "Theory of Machines and Mechanism", McGraw-Hill Book Company, 1988

[20] Ivanov, K. Likhoyedenko, M. Reznichenko, G. Chernov, "Agricultural Machinery Part II", Printed in the Union of Soviet Socialist Republics

[21] Joseph E. Shigley and Charles R. Mischke, "Standard hand Book of Machine Design", Second Edition, *McGraw-Hill, New York, 1996*

[22] D.N. Sharma and S.Mukesh , "Farm Machinery Design Principles and Problems", Jain Brothers, NewDelhi, 2nd edition, 2010

[23] Michael M. Khonsari and E. Richard Booser, "Applied Tribology: Bearing Design and Lubrication", Jonh Wiley and Sons, Ltd, 2017, 3rd edition

[24] Dudley D. Fuller, "Coefficient of Friction", Columbia University

[25] R. C. HIBBELER, "STATICS AND DYNAMICS", Pearson Prentice Hall, Upper Saddle River, New Jersey 07458, 2010, 12th edition

[26] Devnani (1985) [23]

[27] Yuncai Hu; Zoltan Burucs; Urs Schmidhalter, "Short-Term Effect of Drought and Salinity on Growth and Mineral Elements in Wheat Seedlings", Journal of Plant Nutrition, 29:12, 2227 – 2243, 2006

[28] H. M. AUSTENSON and P. D. WALTON, “RELATIONSHIPS BETWEEN INITIAL SEED WEIGHT AND MATURE, PLANT CHAR.ACTERS IN SPRING WHEAT”, Can. J, Plant Sci. Vol. 50, 53-58, (Jan. 1970)

[29] S. Afzalinia1 and M. Roberge, “Physical and mechanical properties of selected forage materials”, CANADIAN BIOSYSTEMS ENGINEERING, Volume 49 2007

[30] Caihong Bai, Yinli Liang and Malcolm J. Hawkesford, “Identification of QTLs associated with seedling root traits and their correlation with plant height in wheat”, Journal of Experimental Botany, Vol. 64, No. 6, pp. 1745–1753, 2013

[31] Fa Cui and et al, “Conditional QTL mapping for plant height with respect to the length of the spike and internode in two mapping populations of wheat”, Springer, Theor Appl Genet 122:1517–1536, 26 February 2011

[32] R.S. KHURMI and J.K. GUPTA, “A TEXTBOOK OF Machine Design”, EURASIA PUBLISHING HOUSE (PVT.) LTD, RAM NAGAR, NEW DELHI-110 055, 2005

[33] DR. P.S. Bimbhra, “Electrical machinery”, KHANNA PUBLISHERS, 2009. 7th edition

[34] Robert L. Mott, “Machine Elements in Mechanical Design”, Pearson Prentice Hall, 2004, 4th edition

[35] Budynas Nisbett, “Shigley’s Mechanical Engineering Design”, McGraw−Hill, 2008, Eighth Edition

[36] Dr.-Ing. Daniel Kitaw (), “Materials Handling Equipment”, Addis Ababa University, page 162.

[37] V B Bhandari, “Machine Design Data Book”, McGraw Hill Education (India) PLtd, 2014

[38] S Bhattacharya, B Sarkar & R N Mukherjee, “Evaluation of a conveyor belt material based on multi-criteria decision making”, Indian Journal of Engineering & Materials Sciences Vol. 11, October 2004, pp. 401-405

[39] Bailling (1985) [23]

[40] Daniel Collins, “The relationship between voltage and DC motor output speed”, December 6, 2015

[41] NEMA 56C Frame, “Permanent Magnet DC Motors”, *OMPM-DC Series*

[42] Andrew Pytel, Jaan Kiusalaas, “Mechanics of Materials”, Cengage Learning, Second Edition, 2012

[43] R.L. Kushwaha, A.S. Vaishnav, and G.C. Koerb, “Shear Strength of Wheat Straw”, Can. Agric. Eng. 25: 163-166, 1983

[44] https://books.google.ae/books?id=R8yADQAAQBAJ&pg=PA104&lpg=PA104&dq=advantages+and+disadvantages+of+single+slider+crank+mechanism&source=bl&ots=CnaD9gjCgl&sig=srXm6Xxknin6GDr6tMJukWX8adg&hl=en&sa=X&redir_esc=y#v=onepage&q&f=true (November 30, 2016)

[45] https://www.ccohs.ca/oshanswers/ergonomics/push2.html March 1, 2017

[46] https://msis.jsc.nasa.gov/sections/section04.htm February, 2016

[47] *http://ecoursesonline.iasri.res.in/course/view.php?id=57*

[48] https://farmer.gov.in/dacdivision/Machinery1/chap5a.pdf

[49] https://www.google.com/url?sa=t&rct=j&q=&esrc=s&source=web&cd=2&cad=rja&uact=8&ved=2ahUKEwjct8DW_qDmAhXYwAIHHUlfBaUQFjABegQIAxAC&url=http%3A%2F%2Fwww.trodeks.com%2FDownload%2FOMPM-DC_Specs.pdf&usg=AOvVaw1jo0CfBr7Or5gM8Mmjnf9X (December, 2019)

[50] https://britishsteel.co.uk/media/272176/british-steel-interactive-stock-range-guide.pdf

[51] https://www.pkl.hr/download/lezajevi/3-GeneralCatalogue.pdf

[52] http://rfl.ie/products/square-hollow-section/

[53] https://www.pkl.hr/download/lezajevi/skf-thrust-bearings.pdf

[54] http://www.spahrmetric.com/pdf/Metric-Steel-Metal-Tubing.pdf

[55] WWW.CARLISLEBRANDTIRES.COM (CARLISLE SPECIALTY TIRE AND WHEEL CATALOG page 16 November 2, 2019)

[56] http://hpwizard.com/tire-friction-coefficient.html

[57] https://www.quora.com/How-much-distance-human-cover-in-single-foot-step-while-walking

[58] https://m.grainger.com/mobile/product/FABORY-Fully-Threaded-Rod-19NN16?breadcrumbCatId=1000848&fc=MWP2IDP2PCP

[59] https://www.irishaid.ie/media/irishaid/allwebsitemedia/10storiesofprogress/case-study-ethiopia-concern-ar2012-678x300.JPG

[60] https://www.idrc.ca/sites/default/files/idrc_article_images/Photo-2004-07-23a.jpg

[61] https://i.pinimg.com/originals/cd/d7/dd/cdd7dd717f41c69112c50ce0c39c6440.jpg

[62] https://farmech.dac.gov.in/FarmerGuide/BI/8.htm

[63] https://www.newworldencyclopedia.org/entry/Agricultural_technology

[64] https://www.alibaba.com/product-detail/Wheat-Reaper_124175586.html

[65] Professor Jang Gyu Lee (President), "THE ASTU POLICY ON APPOINTMENT, PROMOTION, AND DETERMINATION OF SALARY OF ACADEMIC AND RESEARCH ASSISTANT, October 2015

[66] http://www.metalary.com/scrap-metal-prices/

[67] https://www.ebay.ca/itm/1-25mm-BALATA-BELTING-5-5mm-FLAT-DRIVE-WOVEN-BELT-machine-stationary-lathe/131150488818?hash=item1e892da4f2:g:-P8AAOxyM89Sb9zu September 05 2019

[68] https://www.omega.com/en-us/motion-control/motors/ac-and-dc-motors/p/OMPM-DC March 5, 2020

[69] https://www.alibaba.com/product-detail/Rosen-400w-Solar-Panel-Mono-450w_60802686968.html?spm=a2700.wholesale.deiletai6.6.49677f85ikKor2 March 5, 2020

[70] https://www.alibaba.com/product-detail/Aluminum-pop-rivets-6-4-20_62040708157.html?spm=a2700.galleryofferlist.0.0.32746480Rjnx8i&s=p March 5, 2020

[71] https://www.alibaba.com/product-detail/304-Material-Full-Thread-Hex-Nuts_62264798972.html?spm=a2700.galleryofferlist.0.0.13854a04xf5hYV&s=p March 5, 2020

[72] https://www.alibaba.com/product-detail/High-quality-galvanized-carbon-steel-M3_62397710471.html?spm=a2700.galleryofferlist.0.0.5e5820ba7OznMv&s=p March 5, 2020

[73] https://www.alibaba.com/product-detail/Direct-price-custom-miniature-ball-bearings_60263707082.html?spm=a2700.galleryofferlist.0.0.2d4a1aaaq7Wiqp&s=p March 5, 2020

[74] https://www.alibaba.com/product-detail/Miniature-bearings-8mm-diameter-628zz-628_60767414859.html?spm=a2700.galleryofferlist.0.0.52394890aCFyid&s=p March 5, 2020

[75] https://www.alibaba.com/product-detail/BA3-BA4-BA5-BA6-BA7-BA8_60780844143.html?spm=a2700.galleryofferlist.0.0.6ffe545d3wCVM4 March 5, 2020

[76] https://www.alibaba.com/product-detail/NTN-61802-deep-groove-ball-bearing_62061235888.html?spm=a2700.galleryofferlist.0.0.4ea73004CSXoW6&s=p March 5, 2020

[77] https://www.alibaba.com/product-detail/khrd-mini-thrust-ball-bearing-51101_62225664681.html?spm=a2700.galleryofferlist.0.0.142f3b97Ue1x34&s=p March 5, 2020

[78] https://www.alibaba.com/product-detail/CheapThrust-Ball-Bearing-51102-for-15_62224872303.html?spm=a2700.galleryofferlist.0.0.71e9696bqMM74s&s=p March 5, 2020

[79] https://www.alibaba.com/product-detail/pu-foam-solid-tire-6-50_60476088177.html?spm=a2700.galleryofferlist.0.0.50137a20dCoIlg March 5, 2020

[80] https://www.indiamart.com/proddetail/3-15-mm-welding-electrodes-14814291291.html March 5, 2020

Appendix

Table 4-20 Comparison for Advantages and Disadvantages of the Mechanisms [44]

Mechanism	Advantage	Disadvantage
Single crank and double-rocker mechanism	Simple, high efficiency, light weight, easy miniaturization	Flapping action is not completely symmetrical, there is a phase difference
Double crank and double rocker mechanism	Structure and movement are completely symmetrical	Two motors are out of phase, and increases the weight of the bodies
Slider-crank mechanism	The structure is simple and easy to implement	Slide has big friction, efficiency is not high
The cam spring mechanism	The structure is simple and compact	Point, line contact, easy to wear, difficult to manufacture
Double crank and double rocker mechanism + passive rotation mechanism	The structure is simple and compact, completely symmetrical, easy small	

Table 4-21 Recommended Limits in the Selection of Hand and Powered Trucks and Carts [45]

Type of Truck or Cart	Maximum Load		Maximum Transport Distance		Maximum Frequency Units (per 8 hr - shift)	Minimum Aisle Width		Type of Transfer to and from Truck+
	kg	lb	m	ft		m	ft	
2-wheeled hand cart	114	250	16	50	200	1.0	3	Ma, P
3-wheeled hand cart	227	500	16	50	200	1.0	3	Ma, P
4-wheeled hand cart	227	500	33	100	200	1.3	4	Ma, P
Hand pallet truck	682	1500	33	100	200	1.3	4	Me, UL
Electric pallet truck	2273	5000	82	250	400	1.3	4	Me, UL
Electric hand-jack lift truck	2273	5000	33	100	400	1.3	4	Me, UL
Power low lift truck	2273	5000	328	1000	400	2.0	6	Me, P, UL
Electric handstacking truck	682	1500	82	250	400	1.3	4++	Me, UL
Power fork truck	2273	5000	164	500	400	2.0	6++	Me, UL

+ Ma = Manual; Me = Mechanical; P = Parts; UL = Unit Load

++ These trucks have tiering capability. In order to use it, ceiling must be more than 4 m (12 ft) high.

Adapted from: Ergonomic Design for People at Work: Vol. 2, by Eastman Kodak Company. Van Nostrand Reinhold, 1986.

Table 4-22 Force Application and Push-Off Velocity [46]

Time of Force Application and Push-Off Velocity
(95th percentile American male -- 99.3 kg (219 lb))

Force N(lb)	Time in sec. for 0.3 m (1 ft) push-off	Push-off velocity m/sec (ft/sec)	Time in sec. for 0.6 m (2 ft) push-off	Push-off velocity m/sec (ft/sec)
4.45 (1)	3.66	0.16 (0.52)	5.18	0.23 (0.75)
22.25 (5)	1.64	0.37 (1.21)	2.31	0.52 (1.71)
44.50 (10)	1.16	0.52 (1.71)	1.64	0.73 (2.40)
89.00 (20)	0.82	0.73 (2.40)	1.16	1.04 (3.41)

Time of Force Application and Push-Off Velocity
(72.6 kg (160 lb individual))

Force N(lb)	Time in sec. for 0.3 m (1 ft) push-off	Push-off velocity m/sec (ft/sec)	Time in sec. for 0.6 m (2 ft) push-off	Push-off velocity m/sec (ft/sec)
4.45 (1)	3.12	0.19 (0.63)	4.42	0.27 (0.89)
22.25 (5)	1.40	0.42 (1.41)	1.98	0.61 (2.00)
44.50 (10)	0.99	0.61 (2.00)	1.40	0.86 (2.82)
89.00 (20)	0.70	0.86 (2.82)	0.99	1.21 (3.97)

Time of Force Application and Push-Off Velocity
(5th percentile Japanese Female -- 40.3 kg (89 lb))

Force N(lb)	Time in sec. for 0.3 m (1 ft) push-off	Push-off velocity m/sec (ft/sec)	Time in sec. for 0.6 m (2 ft) push-off	Push-off velocity m/sec (ft/sec)
4.45 (1)	2.33	0.26 (0.85)	3.30	0.36 (1.18)
22.25 (5)	1.04	0.57 (1.87)	1.47	0.81 (2.66)
44.50 (10)	0.74	0.82 (2.69)	1.04	1.15 (3.77)
89.00 (20)	0.52	1.15 (3.77)	0.74	1.63 (5.35)

Note: Please be aware that all of the above data was gathered under 1-g conditions.

Table 4-23 Average Physical Properties of Common Metals: SI Units [42]

Metal	Density (kg/m³)	Temp. coeff. of linear expansion [μm/(m·°C)]	Proportional limit (MPa)[a] Tension	Proportional limit (MPa)[a] Shear	Ultimate strength (MPa) Tension	Ultimate strength (MPa) Comp.	Ultimate strength (MPa) Shear	Modulus of elasticity (GPa)[a] Tension, *E*	Modulus of elasticity (GPa)[a] Shear, *G*	Percentage of elongation (in 50 mm)
Steel, 0.2% carbon, hot rolled	7 850	Varies from 11.0 to 13.2 Average is 11.7	240	150	410	[b]	310	200	80	35
0.2% carbon, cold rolled	7 850		420	250	550	[b]	420	200	80	18
0.6% carbon, hot rolled	7 850		420	250	690	[b]	550	200	80	15
0.8% carbon, hot rolled	7 850		480	290	830	[b]	730	200	80	10
Gray cast iron	7 200	10.8	[c]	[d]	140	520	[d]	100	40	Slight
Malleable cast iron	7 200	11.9	250	160	370	[b]	330	170	90	18
Wrought iron	7 700	12.1	210	130	350	[b]	240	190	70	35
Aluminum, cast	2 650	23.1	60	—	90	[b]	70	70	30	20
Aluminum alloy 17ST	2 700	23.1	220	150	390	[b]	220	71	30	—
Brass, rolled (70% Cu, 30% Zn)	8 500	18.7	170	110	380	[b]	330	100	40	30
Bronze, cast	8 200	18.0	140	—	230	390	—	80	35	10
Copper, hard-drawn	8 800	16.8	260	160	380	[b]	—	120	40	4

[a] The proportional limit and modulus of elasticity for compression may be assumed equal to these values for tension except for cast iron where the proportional limit is approximately 180 MPa.
[b] The ultimate compressive strength for ductile materials may be taken as the yield point, which is slightly greater than the proportional limit in tension.
[c] Not well defined; approximately 40 MPa.
[d] Cast iron fails by diagonal tension.

Table 4-24 Properties of Commonly used gear Materials [32]

Material (1)	*Condition* (2)	*Brinell hardness number* (3)	*Minimum tensile strength (N/mm²)* (4)
Malleable cast iron			
(*a*) White heart castings, Grade B	—	217 max.	280
(*b*) Black heart castings, Grade B	—	149 max.	320
Cast iron			
(*a*) Grade 20	As cast	179 min.	200
(*b*) Grade 25	As cast	197 min.	250
(*c*) Grade 35	As cast	207 min.	250
(*d*) Grade 35	Heat treated	300 min.	350
Cast steel	—	145	550
Carbon steel			
(*a*) 0.3% carbon	Normalised	143	500
(*b*) 0.3% carbon	Hardened and tempered	152	600

Table 4-25 Machine Rate (Source: Vision International Consultants)

Machine Name	Rate in Birr/60 Min	Remark
Milling	260	
Lathe	270	
Hacksaw	115	
Drilling	115	
Grinding	230	
Shearing Machine	92	

Bending Machine	70	
Hand Drill	70	
Welding	130	
Portable Chop Saw	110	
Die Casting	255	

Table 4-26 Fit and Tolerances for Remaining Components

Part name		basic size	Dmax	Dmin	D	i	Fit	Fundamental Tolerance	α	β	γ	Fundamental Deviation	Upper Deviation	Lower Deviation	Upper Limit	Lower Limit
Bolt for Cutter	Shaft	4	6	3	4.243	0.001	k6	0.007	0	0.6	0.33	0.001	0.001	-0.006	4.001	3.994
	Hole	4	6	3	4.243	0.001	H7	0.012	0	0.6	0.33		0.014	-0.001	4.014	3.999
Cutter center distance	Shaft	56.2	80	50	63.246	0.002	k6	0.019	0	0.6	0.33	0.002	0.002	-0.016	56.202	56.184
	Hole	56.2	80	50	63.246	0.002	H7	0.030	0	0.6	0.33		0.035	-0.002	56.235	56.198
Cutter bar center distance	Shaft	20	30	18	23.238	0.001	k6	0.013	0	0.6	0.33	0.002	0.002	-0.011	20.002	19.989
	Hole	20	30	18	23.238	0.001	H7	0.021	0	0.6	0.33		0.024	-0.002	20.024	19.998
Guard Lip L1+t1	Shaft	53.63	80	50	63.246	0.002	k6	0.019	0	0.6	0.33	0.002	0.002	-0.016	53.632	53.614
	Hole	53.63	80	50	63.246	0.002	H7	0.030	0	0.6	0.33		0.035	-0.002	53.665	53.628
Bolt for Guard Lip	Shaft	4	6	3	4.243	0.001	k6	0.007	0	0.6	0.33	0.001	0.001	-0.006	4.001	3.994
	Hole	4	6	3	4.243	0.001	H7	0.012	0	0.6	0.33		0.014	-0.001	4.014	3.999
Guard Lip Bar	Shaft	13	30	18	23.238	0.001	k6	0.013	0	0.6	0.33	0.002	0.002	-0.011	13.002	12.989
	Hole	13	30	18	23.238	0.001	H7	0.021	0	0.6	0.33		0.024	-0.002	13.024	12.998
Bearing for Cutter bar	Shaft	16	18	10	13.416	0.001	k6	0.011	0	0.6	0.33	0.001	0.001	-0.009	16.001	15.991
	Hole	16	18	10	13.416	0.001	H7	0.017	0	0.6	0.33		0.020	-0.001	16.020	15.999
Bolt for Bearing Cutter Bar	Shaft	4	6	3	4.243	0.001	k6	0.007	0	0.6	0.33	0.001	0.001	-0.006	4.001	3.994
	Hole	4	6	3	4.243	0.001	H7	0.012	0	0.6	0.33		0.014	-0.001	4.014	3.999
Follower Bar	Shaft	8	10	6	7.746	0.001	k6	0.009	0	0.6	0.33	0.001	0.001	-0.008	8.001	7.992
	Hole	8	10	6	7.746	0.001	H7	0.014	0	0.6	0.33		0.017	-0.001	8.017	7.999
Roller for Follower Bar	Shaft	9	10	6	7.746	0.001	k6	0.009	0	0.6	0.33	0.001	0.001	-0.008	9.001	8.992
	Hole	9	10	6	7.746	0.001	H7	0.014	0	0.6	0.33		0.017	-0.001	9.017	8.999
Rectangular Box for Follower	Shaft	26	30	18	23.238	0.001	k6	0.013	0	0.6	0.33	0.002	0.002	-0.011	26.002	25.989
	Hole	26	30	18	23.238	0.001	H7	0.021	0	0.6	0.33		0.024	-0.002	26.024	25.998
Pin for Follower Support	Shaft	4	6	3	4.243	0.001	k6	0.007	0	0.6	0.33	0.001	0.001	-0.006	4.001	3.994
	Hole	4	6	3	4.243	0.001	H7	0.012	0	0.6	0.33		0.014	-0.001	4.014	3.999
Follower Head	Shaft	16	18	10	13.416	0.001	k6	0.011	0	0.6	0.33	0.001	0.001	-0.009	16.001	15.991
	Hole	16	18	10	13.416	0.001	H7	0.017	0	0.6	0.33		0.020	-0.001	16.020	15.999
Idler Shaft	Shaft	5	6	3	4.243	0.001	k6	0.007	0	0.6	0.33	0.001	0.001	-0.006	5.001	4.994
	Hole	5	6	3	4.243	0.001	H7	0.012	0	0.6	0.33		0.014	-0.001	5.014	4.999
Camshaft	Shaft	377.76	400	315	354.96	0.004	k6	0.035	0	0.6	0.33	0.004	0.004	-0.031	377.764	377.729
	Hole	377.76	400	315	354.96	0.004	H7	0.057	0	0.6	0.33		0.067	-0.004	377.827	377.756
	Shaft	5	6	3	4.243	0.001	k6	0.007	0	0.6	0.33	0.001	0.001	-0.006	5.001	4.994
	Hole	5	6	3	4.243	0.001	H7	0.012	0	0.6	0.33		0.014	-0.001	5.014	4.999
Ball Bearing for Camshaft	Shaft	15	18	10	13.416	0.001	k6	0.011	0	0.6	0.33	0.001	0.001	-0.009	15.001	14.991
	Hole	15	18	10	13.416	0.001	H7	0.017	0	0.6	0.33		0.020	-0.001	15.020	14.999
	Shaft	12	18	10	13.416	0.001	k6	0.011	0	0.6	0.33	0.001	0.001	-0.009	12.001	11.991

Thrust Bearing for Camshaft	Hole	12	18	10	13.416	0.001	H7	0.017	0	0.6	0.33		0.020	-0.001	12.020	11.999
	Shaft	9	10	6	7.746	0.001	k6	0.009	0	0.6	0.33	0.001	0.001	-0.008	9.001	8.992
	Hole	9	10	6	7.746	0.001	H7	0.014	0	0.6	0.33		0.017	-0.001	9.017	8.999
Cam	Shaft	38.1	50	30	38.730	0.002	k6	0.016	0	0.6	0.33	0.002	0.002	-0.014	38.102	38.086
	Hole	38.1	50	30	38.730	0.002	H7	0.025	0	0.6	0.33		0.029	-0.002	38.129	38.098
	Shaft	101.2	120	80	97.980	0.002	k6	0.022	0	0.6	0.33	0.003	0.003	-0.019	101.203	101.181
	Hole	101.2	120	80	97.980	0.002	H7	0.035	0	0.6	0.33		0.041	-0.003	101.241	101.197
Key on Camshaft for Gear	Shaft	3.31	6	3	4.243	0.001	k6	0.007	0	0.6	0.33	0.001	0.001	-0.006	3.311	3.304
	Hole	3.31	6	3	4.243	0.001	H7	0.012	0	0.6	0.33		0.014	-0.001	3.324	3.309
	Shaft	15	18	10	13.416	0.001	k6	0.011	0	0.6	0.33	0.001	0.001	-0.009	15.001	14.991
	Hole	15	18	10	13.416	0.001	H7	0.017	0	0.6	0.33		0.020	-0.001	15.020	14.999
Key on Camshaft for Pulley:	Shaft	3.88	6	3	4.243	0.001	k6	0.007	0	0.6	0.33	0.001	0.001	-0.006	3.881	3.874
	Hole	3.88	6	3	4.243	0.001	H7	0.012	0	0.6	0.33		0.014	-0.001	3.894	3.879
	Shaft	30	50	30	38.730	0.002	k6	0.016	0	0.6	0.33	0.002	0.002	-0.014	30.002	29.986
	Hole	30	50	30	38.730	0.002	H7	0.025	0	0.6	0.33		0.029	-0.002	30.029	29.998
Key on Camshaft for Cam:	Shaft	5.77	6	3	4.243	0.001	k6	0.007	0	0.6	0.33	0.001	0.001	-0.006	5.771	5.764
	Hole	5.77	6	3	4.243	0.001	H7	0.012	0	0.6	0.33		0.014	-0.001	5.784	5.769
	Shaft	5	6	3	4.243	0.001	k6	0.007	0	0.6	0.33	0.001	0.001	-0.006	5.001	4.994
	Hole	5	6	3	4.243	0.001	H7	0.012	0	0.6	0.33		0.014	-0.001	5.014	4.999
V-Grooved Pulley on Motor Shaft	Shaft	40	50	30	38.730	0.002	k6	0.016	0	0.6	0.33	0.002	0.002	-0.014	40.002	39.986
	Hole	40	50	30	38.730	0.002	H7	0.025	0	0.6	0.33		0.029	-0.002	40.029	39.998
	Shaft	32	50	30	38.730	0.002	k6	0.016	0	0.6	0.33	0.002	0.002	-0.014	32.002	31.986
	Hole	32	50	30	38.730	0.002	H7	0.016	0	0.6	0.33		0.029	-0.002	32.029	31.998
	Shaft	16	18	10	13.416	0.001	k6	0.011	0	0.6	0.33	0.001	0.001	-0.009	16.001	15.991
	Hole	16	18	10	13.416	0.001	H7	0.017	0	0.6	0.33		0.029	-0.002	16.029	15.998
V-Grooved Pulley on Intermediate Shaft	Shaft	128.12	120	80	97.980	0.002	k6	0.022	0	0.6	0.33	0.003	0.003	-0.019	128.123	128.101
	Hole	128.12	120	80	97.980	0.002	H7	0.035	0	0.6	0.33		0.041	-0.003	128.161	128.117
	Shaft	32	50	30	38.73	0.002	k6	0.016	0	0.6	0.33	0.002	0.002	-0.014	32.002	31.986
	Hole	32	50	30	38.73	0.002	H7	0.025	0	0.6	0.33		0.029	-0.002	32.029	31.998
	Shaft	15	18	10	13.42	0.001	k6	0.011	0	0.6	0.33	0.001	0.001	-0.009	15.001	14.991
	Hole	15	18	10	13.42	0.001	H7	0.011	0	0.6	0.33		0.020	-0.001	15.020	14.999
Intermediate Shaft	Shaft	26	30	18	23.24	0.001	k6	0.013	0	0.6	0.33	0.002	0.002	-0.011	26.002	25.989
	Hole	26	30	18	23.24	0.001	H7	0.021	0	0.6	0.33		0.024	-0.002	26.024	25.998
	Shaft	5	6	3	4.24	0.001	k6	0.007	0	0.6	0.33	0.001	0.001	-0.006	5.001	4.994
	Hole	5	6	3	4.24	0.001	H7	0.012	0	0.6	0.33		0.014	-0.001	5.014	4.999
Ball Bearings for Intermediate Shaft	Shaft	15	18	10	13.42	0.001	k6	0.011	0	0.6	0.33	0.001	0.001	-0.009	15.001	14.991
	Hole	15	18	10	13.42	0.001	H7	0.017	0	0.6	0.33		0.020	-0.001	15.020	14.999
	Shaft	24	30	18	23.24	0.001	k6	0.013	0	0.6	0.33	0.002	0.002	-0.011	24.002	23.989
	Hole	24	30	18	23.24	0.001	H7	0.013	0	0.6	0.33		0.024	-0.002	24.024	23.998
	Shaft	5	6	3	4.24	0.001	k6	0.007	0	0.6	0.33	0.001	0.001	-0.006	5.001	4.994
	Hole	5	6	3	4.24	0.001	H7	0.012	0	0.6	0.33		0.014	-0.001	5.014	4.999
Thrust Bearings for	Shaft	12	18	10	13.42	0.001	k6	0.011	0	0.6	0.33	0.001	0.001	-0.009	12.001	11.991
	Hole	12	18	10	13.42	0.001	H7	0.017	0	0.6	0.33		0.020	-0.001	12.020	11.999

Intermediate Shaft	Shaft	26	30	18	23.24	0.001	k6	0.013	0	0.6	0.33	0.002	0.002	-0.011	26.002	25.989
	Hole	26	30	18	23.24	0.001	H7	0.021	0	0.6	0.33		0.024	-0.002	26.024	25.998
	Shaft	9	10	6	7.75	0.001	k6	0.009	0	0.6	0.33	0.001	0.001	-0.008	9.001	8.992
	Hole	9	10	6	7.75	0.001	H7	0.009	0	0.6	0.33		0.017	-0.001	9.017	8.999
Key on Intermediate Shaft for Pulley & Gear	Shaft	3.1	6	3	4.24	0.001	k6	0.007	0	0.6	0.33	0.001	0.001	-0.006	3.101	3.094
	Hole	3.1	6	3	4.24	0.001	H7	0.012	0	0.6	0.33		0.014	-0.001	3.114	3.099
	Shaft	15.35	18	10	13.42	0.001	k6	0.011	0	0.6	0.33	0.001	0.001	-0.009	15.351	15.341
	Hole	15.35	18	10	13.42	0.001	H7	0.017	0	0.6	0.33		0.020	-0.001	15.370	15.349
Star Wheel vertical Rod	Shaft	399.26	400	315	354.96	0.004	k6	0.035	0	0.6	0.33	0.004	0.004	-0.031	399.264	399.229
	Hole	399.26	400	315	354.96	0.004	H7	0.057	0	0.6	0.33		0.067	-0.004	399.327	399.256
	Shaft	160	180	120	146.97	0.003	k6	0.025	0	0.6	0.33	0.003	0.003	-0.022	160.003	159.978
	Hole	160	180	120	146.97	0.003	H7	0.025	0	0.6	0.33		0.047	-0.003	160.047	159.997
Bearing Between Star Wheel Arm	Shaft	8	10	6	7.75	0.001	k6	0.009	0	0.6	0.33	0.001	0.001	-0.008	8.001	7.992
	Hole	8	10	6	7.75	0.001	H7	0.014	0	0.6	0.33		0.017	-0.001	8.017	7.999
	Shaft	19	30	18	23.24	0.001	k6	0.013	0	0.6	0.33	0.002	0.002	-0.011	19.002	18.989
	Hole	19	30	18	23.24	0.001	H7	0.021	0	0.6	0.33		0.024	-0.002	19.024	18.998
	Shaft	7	10	6	7.75	0.001	k6	0.009	0	0.6	0.33	0.001	0.001	-0.008	7.001	6.992
	Hole	7	10	6	7.75	0.001	H7	0.014	0	0.6	0.33		0.017	-0.001	7.017	6.999
Star Wheel Bearing Seat	Shaft	21.3	30	18	23.24	0.001	k6	0.013	0	0.6	0.33	0.002	0.002	-0.011	21.302	21.289
	Hole	21.3	30	18	23.24	0.001	H7	0.013	0	0.6	0.33		0.024	-0.002	21.324	21.298
	Shaft	19	30	18	23.24	0.001	k6	0.013	0	0.6	0.33	0.002	0.002	-0.011	19.002	18.989
	Hole	19	30	18	23.24	0.001	H7	0.021	0	0.6	0.33		0.024	-0.002	19.024	18.998
Star Wheel Arm	Shaft	76.13	80	50	63.25	0.002	k6	0.019	0	0.6	0.33	0.002	0.002	-0.016	76.132	76.114
	Hole	76.13	80	50	63.25	0.002	H7	0.030	0	0.6	0.33		0.035	-0.002	76.165	76.128
	Shaft	72	80	50	63.25	0.002	k6	0.019	0	0.6	0.33	0.002	0.002	-0.016	72.002	71.984
	Hole	72	80	50	63.25	0.002	H7	0.030	0	0.6	0.33		0.035	-0.002	72.035	71.998
Divider	Shaft	152.5	180	120	146.97	0.003	k6	0.025	0	0.6	0.33	0.003	0.003	-0.022	152.503	152.478
	Hole	152.5	180	120	146.97	0.003	H7	0.025	0	0.6	0.33		0.047	-0.003	152.547	152.497
	Shaft	200	250	180	212.13	0.003	k6	0.029	0	0.6	0.33	0.004	0.004	-0.025	200.004	199.975
	Hole	200	250	180	212.13	0.003	H7	0.046	0	0.6	0.33		0.054	-0.004	200.054	199.996
	Shaft	28	30	18	23.24	0.001	k6	0.013	0	0.6	0.33	0.002	0.002	-0.011	28.002	27.989
	Hole	28	30	18	23.24	0.001	H7	0.021	0	0.6	0.33		0.024	-0.002	28.024	27.998
	Shaft	20	30	18	23.24	0.001	k6	0.013	0	0.6	0.33	0.002	0.002	-0.011	20.002	19.989
	Hole	20	30	18	23.24	0.001	H7	0.021	0	0.6	0.33		0.024	-0.002	20.024	19.998
Star Wheel and Divider Support	Shaft	153.68	180	120	146.97	0.003	k6	0.025	0	0.6	0.33	0.003	0.003	-0.022	153.683	153.658
	Hole	153.68	180	120	146.97	0.003	H7	0.025	0	0.6	0.33		0.047	-0.003	153.727	153.677
	Shaft	80.4	120	80	97.98	0.002	k6	0.022	0	0.6	0.33	0.003	0.003	-0.019	80.403	80.381
	Hole	80.4	120	80	97.98	0.002	H7	0.035	0	0.6	0.33		0.041	-0.003	80.441	80.397
	Shaft	380.51	400	315	354.96	0.004	k6	0.035	0	0.6	0.33	0.004	0.004	-0.031	380.514	380.479
	Hole	380.51	400	315	354.96	0.004	H7	0.057	0	0.6	0.33		0.067	-0.004	380.577	380.506
Frame for Solar Panel Support	Shaft	1591.84	1600	1400	1496.66	0.007	k6	0.066	0	0.6	0.33	0.007	0.007	-0.060	1591.847	1591.780
	Hole	1591.84	1600	1400	1496.66	0.007	H7	0.106	0	0.6	0.33		0.126	-0.007	1591.966	1591.833
	Shaft	1588	1600	1400	1496.66	0.007	k6	0.066	0	0.6	0.33	0.007	0.007	-0.060	1588.007	1587.940

	Hole	1588	1600	1400	1496.66	0.007	H7	0.066	0	0.6	0.33		0.126	-0.007	1588.126	1587.993
	Shaft	1580	1600	1400	1496.66	0.007	k6	0.066	0	0.6	0.33	0.007	0.007	-0.060	1580.007	1579.940
	Hole	1580	1600	1400	1496.66	0.007	H7	0.106	0	0.6	0.33		0.126	-0.007	1580.126	1579.993
Gear Box	Shaft	147.4	180	120	146.97	0.003	k6	0.025	0	0.6	0.33	0.003	0.003	-0.022	147.403	147.378
	Hole	147.4	180	120	146.97	0.003	H7	0.040	0	0.6	0.33		0.047	-0.003	147.447	147.397
	Shaft	15	18	10	13.42	0.001	k6	0.011	0	0.6	0.33	0.001	0.001	-0.009	15.001	14.991
	Hole	15	18	10	13.42	0.001	H7	0.017	0	0.6	0.33		0.020	-0.001	15.020	14.999
Bottom & Top Cantilever Beam	Shaft	609.6	630	500	561.25	0.004	k6	0.043	0	0.6	0.33	0.005	0.005	-0.038	609.605	609.562
	Hole	609.6	630	500	561.25	0.004	H7	0.043	0	0.6	0.33		0.081	-0.005	609.681	609.595
	Shaft	106.9	120	80	97.98	0.002	k6	0.022	0	0.6	0.33	0.003	0.003	-0.019	106.903	106.881
	Hole	106.9	120	80	97.98	0.002	H7	0.035	0	0.6	0.33		0.041	-0.003	106.941	106.897
Column for Cutter	Shaft	555.76	630	500	561.25	0.004	k6	0.043	0	0.6	0.33	0.005	0.005	-0.038	555.765	555.722
	Hole	555.76	630	500	561.25	0.004	H7	0.068	0	0.6	0.33		0.081	-0.005	555.841	555.755
Axel	Shaft	409.6	500	400	447.21	0.004	k6	0.039	0	0.6	0.33	0.004	0.004	-0.034	409.604	409.566
	Hole	409.6	500	400	447.21	0.004	H7	0.062	0	0.6	0.33		0.073	-0.004	409.673	409.596
	Shaft	20	30	18	23.24	0.001	k6	0.013	0	0.6	0.33	0.002	0.002	-0.011	20.002	19.989
	Hole	20	30	18	23.24	0.001	H7	0.013	0	0.6	0.33		0.024	-0.002	20.024	19.998
	Shaft	19.07	30	18	23.24	0.001	k6	0.013	0	0.6	0.33	0.002	0.002	-0.011	19.072	19.059
	Hole	19.07	30	18	23.24	0.001	H7	0.021	0	0.6	0.33		0.024	-0.002	19.094	19.068
Tires	Shaft	394.165	400	315	354.96	0.004	k6	0.035	0	0.6	0.33	0.004	0.004	-0.031	394.169	394.134
	Hole	394.165	400	315	354.96	0.004	H7	0.057	0	0.6	0.33		0.067	-0.004	394.232	394.161

Photo 4-14 Photo during Field Test